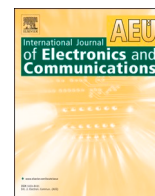


***3.5.1 Number of Collaborative activities for research,
Faculty exchange, Student exchange/ internship per year***

Research Collaboration



Regular paper

A small wideband inverted L-shaped flexible antenna for sub-6 GHz 5G applications

Neeta Kulkarni^{a,b,*}, Rajin M. Linus^c, Nilesh Bhaskarrao Bahadure^d

^a Department of Electronics Engineering, Sanjay Ghodawat University, Kolhapur, India

^b Department of Electronics & Telecommunication Engineering, SVERI's College of Engineering, Pandharpur, India

^c Department of Electrical & Electronics Engineering, Sanjay Ghodawat University, Kolhapur, India

^d Department of Computer Science & Engineering, Symbiosis Institute of Technology Nagpur, Constituent of Symbiosis International (Deemed University), Pune, India



ARTICLE INFO

Keywords:

Flexible antenna
Wideband
Gain
MIMO
5G

ABSTRACT

This manuscript carries out design and examination of flexible inverted L-shaped connected with a circular ring having plus-shaped geometry on the top left corner and a partial ground on the back. The antenna is realized on a flexible polyimide substrate which is fabricated for further investigation. The flexible resonator achieves a designed footprint of $20 \times 30 \times 0.2 \text{ mm}^3$. The antenna is analyzed in terms of $|S_{11}|$, 2D gain, radiation patterns, and efficiency under both normal and bend conditions. The antenna shows a decent match between experimental and software simulated data. To establish the use of the proposed design for 5G MIMO applications, an 8-port MIMO with the common ground is designed where the antenna shows satisfactory isolation $>15 \text{ dB}$ and ECC <0.01 which makes the flexible antenna an excellent choice for realizing the 5G MIMO antennas working at sub-6 GHz band.

1. Introduction

The advancements in technology have been helping to achieve the miniaturization of the devices that are used for various wireless applications. Such applications not only demand a compact antenna but also demands high gain, wideband and low-cost characteristics. The antennas having wide bandwidth are suitable for sub-6 GHz applications due to higher data rate, lower transmission power, and high multipath channel performance. The popularity of low-profile antennas is increasing in wireless communication devices due to their cost-effectiveness and miniaturized size. The antenna with flexibility can be very well suited for miniaturized devices. Various wideband flexible antennas for applications like ISM (Industrial, Scientific & Medical) band [1], WiMAX and Sub-6 GHz [2], biomedical diagnostics [3], Sub-6 GHz, and WLAN [4] are proposed in the literature. Flexible antennas are realized using various methods like inkjet printing [5,6], etching over flexible substrates [7,8], and patterning transparent flexible materials [9]. Etching of flexible substrates is much easier in terms of fabrication and it is more cost-effective. The higher data rates can be fulfilled by combining the MIMO (Multiple Input Multiple Output) technology that helps in enhancing the reliability while helping in extending the communication range for the given bandwidth. The flexible MIMO

antennas using 2 ports [10,11], and 4 ports [12–17] are proposed by the researchers. Higher ports can suffice more user requirements. The 8-port MIMO antenna proposed in [18,19] are not flexible so the flexible antenna for 8-ports MIMO is not yet studied in the literature

The proposed compact flexible 8-port MIMO antenna for sub-6 GHz 5G applications is presented here. The antenna displays a decent result under normal and bending situations. The MIMO results depict that isolation $>15 \text{ dB}$ with ECC <0.1 is achieved which makes the antenna useful for miniaturized devices where higher user demands need to be sufficed.

2. Design and analysis of proposed antenna

The inverted L-shaped antenna with a plus-shaped geometry housed inside a circular ring is patterned on the top while the bottom layer has a partial ground plane as shown in Fig. 1(a and b). Flexible polyimide having a thickness of 0.2 mm is used as a substrate ($\epsilon_r = 3.5$, $\tan \delta = 0.0027$). The flexible antenna achieves a low profile of $20 \text{ mm} \times 30 \text{ mm}$. Microstrip feeding is used which is optimized to work at 50Ω .

The antenna geometry selection is justified with the help of antenna evolution as shown in Fig. 2 (a). For all the designs, the ground plane is fixed as 9 mm in length. In step 1, in the proposed system, inverted L-

* Corresponding author at: Department of Electronics Engineering, Sanjay Ghodawat University, Kolhapur, India.

E-mail addresses: kulkarnineeta777@gmail.com (N. Kulkarni), rajin.linus@sanjayghodawatuniversity.ac.in (R.M. Linus), nbahadure@gmail.com (N.B. Bahadure).

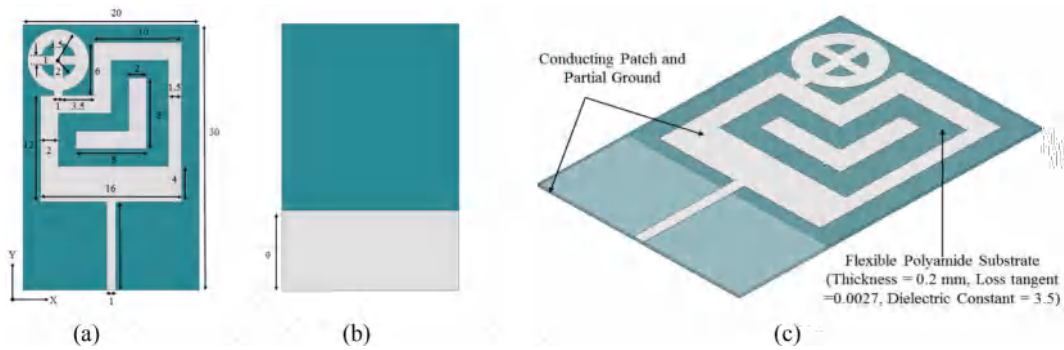


Fig. 1. Proposed antenna design (a) Front view. (b) Back view. (c) 3D View (All dimensions in mm).

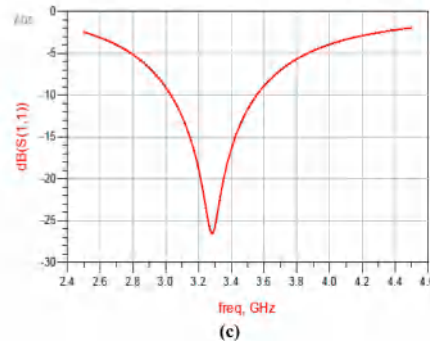
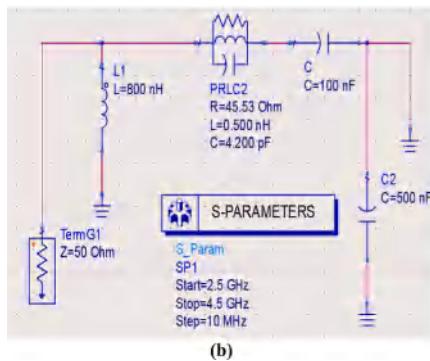
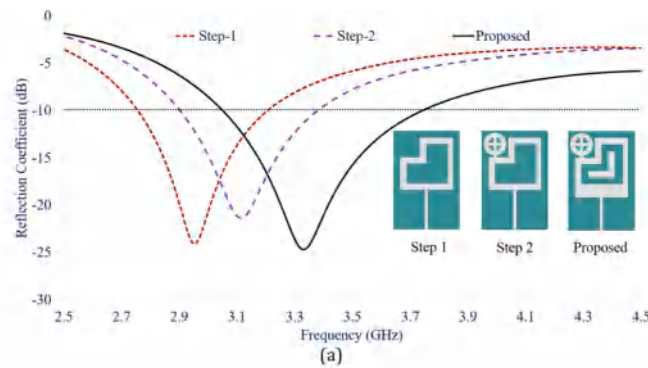


Fig. 2. (a) Flexible antenna evolution, (b) equivalent circuit model, (c) reflection coefficient (S_{11}) curve in dB.

shaped conductive arms connected with each other are selected to achieve compactness and to resonate at 3.3 GHz. The length and width are calculated from well-known mathematical equations and optimized using an electromagnetic full-wave CST microwave studio. As shown in Eqs. (1)–(4), W and L are denoted as the width and length of the interconnected inverted-L-shaped antenna, h is the thickness of flexible polyimide substrate, ϵ_{eff} , C , and f_r are the effective permittivity, speed of light (3×10^8 m/s), and resonating frequency respectively.

$$W = \frac{c}{4f_r \sqrt{\frac{\epsilon_r + 1}{2}}} \tag{1}$$

$$\epsilon_{eff} = \frac{\epsilon_r + 1}{2} + \frac{\epsilon_r - 1}{2} \left(\frac{1}{\sqrt{1 + 12 \frac{h}{W}}} \right) \tag{2}$$

$$L = \frac{c}{4f_r \sqrt{\epsilon_{eff}}} \tag{3}$$

The $|S_{11}|$ of the antenna is satisfactory however, the band of interest

(sub-6 GHz) is not achieved. Hence, to shift the frequency band, a plus-shaped geometry housed inside a circular ring is added to the top left corner (Step 2). It is observed that the frequency band is shifted to the higher side. The final tuning of the band is achieved by adding another inverted-L-shaped geometry in between the housing created in step 1. This inverted L-shape patch is not touching the other patch and leads to an effect similar to capacitive coupling (Proposed antenna). The reflection coefficient plot as shown in Fig. 2(a) emphasizes for the proposed design the antenna resonates between 3.05 and 3.74 GHz covering the sub-6 GHz band. The partial ground on the bottom plane helps in bandwidth enhancement. At 3.3 GHz, the antenna achieves a reflection coefficient of >24.69 dB. The optimized dimensions are shown in Fig. 1 (a). The final design is shown in Fig. 1(c).

To further justify the chosen geometry of the proposed antenna, an equivalent circuit model is designed by using Advanced Design System (ADS) software at resonating frequency 3.3 GHz and is shown below in Fig. 2(b) [20]. The parallel RLC circuit represents the interconnected two inverted-L antenna and plus sign radiator placed inside a circle. The single inductor and series combination of capacitors present the microstrip feed line and parasitic patch. It can be observed from Fig. 2(c)

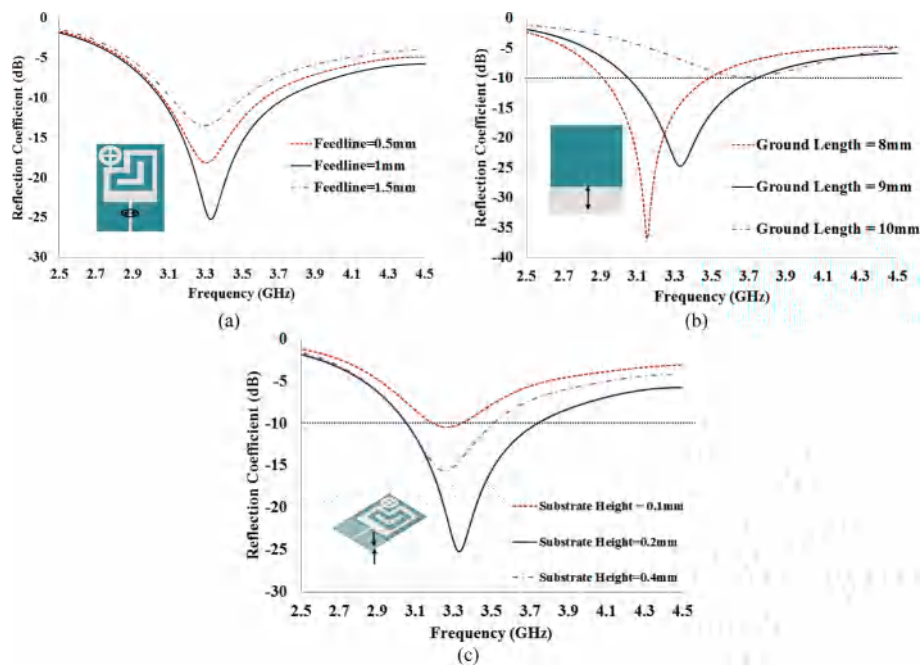


Fig. 3. . Parametric study (a) Feedline width. (b) Ground length. (c) Substrate height.

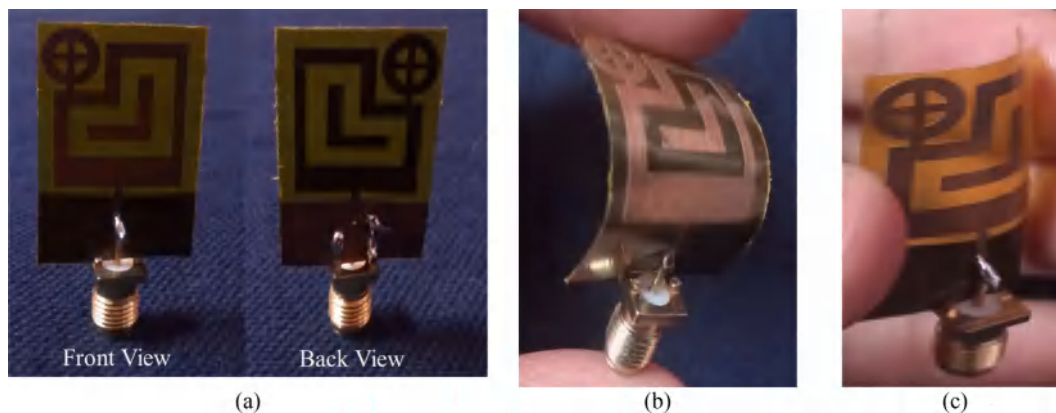


Fig. 4. . Fabricated Antenna (a) without bending, (b) X-axis bending, (c) Y-axis bending.

that the reflection coefficient curve lies in the frequency range of 3.20–3.59 GHz covering the required bandwidth of Sub-6 GHz 5G bands.

2.1. Parametric Analysis

The parametric analysis is carried out on various parameters of the antenna like the width of the feedline, length of the ground plane, the height of the substrate and its corresponding reflection coefficient is observed.

As shown in Fig. 3(a), the feed width variation directly affects the impedance matching of the antenna so the value of 1 mm is selected which gives the best impedance matching performance. Next, the effect of partial ground on bandwidth enhancement is analyzed by varying the length. It is observed that the impedance bandwidth greatly depends on the length of the ground plane. The value of 9 mm is selected for achieving maximum impedance bandwidth as displayed in Fig. 3(b). Lastly, the effect on the reflection coefficient by variation of substrate height is carried out which is illustrated in Fig. 3(c). The substrate height of 0.2 mm gives a decent performance.

3. Results and discussion

The optimized antenna using CST software is fabricated for verifying the results with the simulated one. The antenna prototype is displayed in Fig. 4(a–c) where three different conditions including normal, bending along the X axis, and bending along the Y axis are depicted. The reflection coefficients of antennas under these conditions are measured using Keysight VNA 99212A while an anechoic chamber is utilized for the measurement of radiation patterns.

Fig. 5 illustrates the reflection coefficient plots for all three conditions. It is observed that under normal conditions the antenna displayed an impedance bandwidth of 3.05–3.74 GHz with a center frequency of 3.3 GHz. After bending the antenna at a radius of 10 cm which is chosen based on the maximum bending angle along the X and Y axis, the reflection coefficient is not much deteriorated. The measured values coincide well.

The current distribution at resonating frequency 3.3 GHz without and with bending is shown in Fig. 6(a–c). From Fig. 6(a) it can be observed that the current is flowing through the outer inverted L-shaped arms which helps in generating the resonance at 3.3 GHz. The small current flowing through the plus-shaped geometry housed inside a

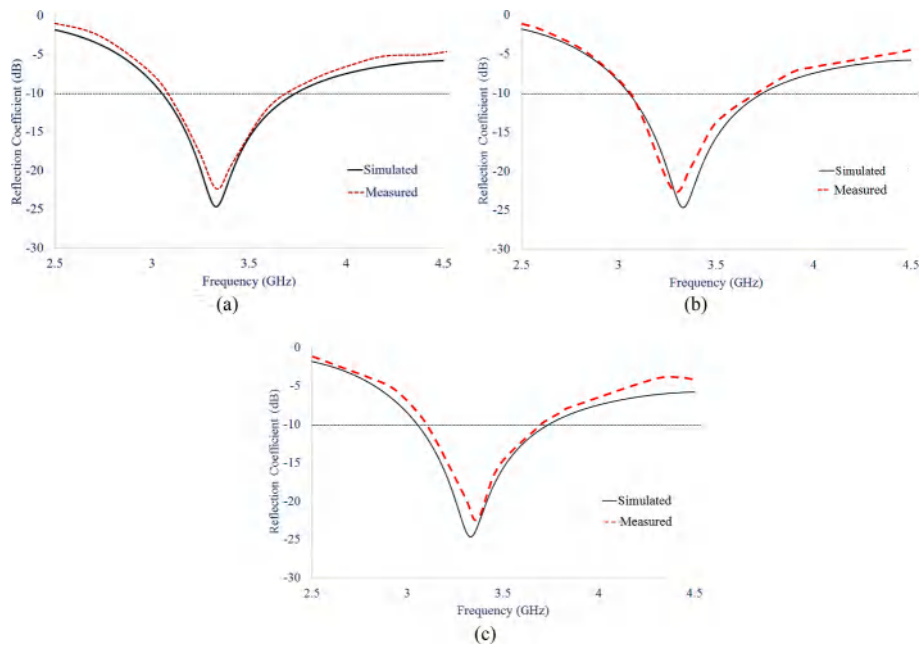


Fig. 5. . Reflection Coefficient (a) without bending, (b) X-axis bending, (c) Y-axis bending.

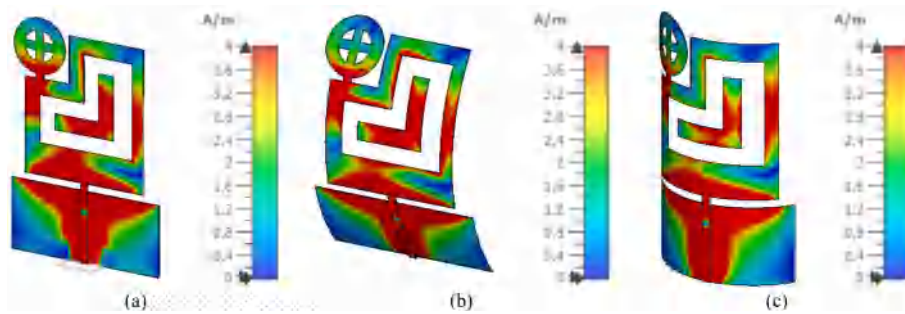


Fig. 6. . Current Distribution Pattern at 3.3 GHz (a) Without bending. (b) Bending along X. (c) Bending along Y.

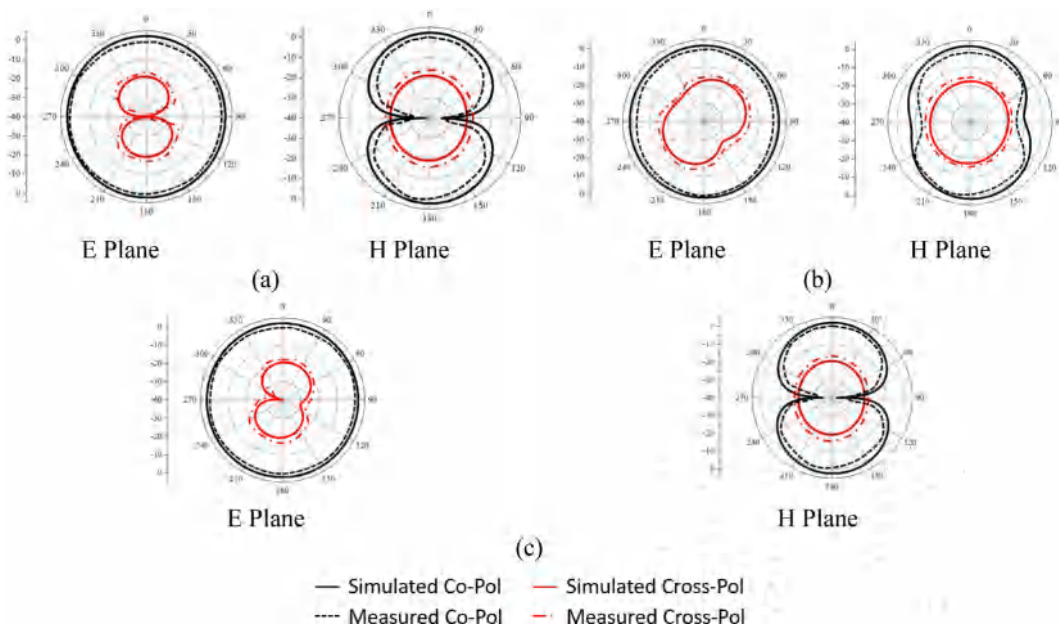


Fig. 7. . Co/Cross Pol patterns at 3.3 GHz along E and H Plane (a) without bending, (b) X-axis bending, (c) Y-axis bending.

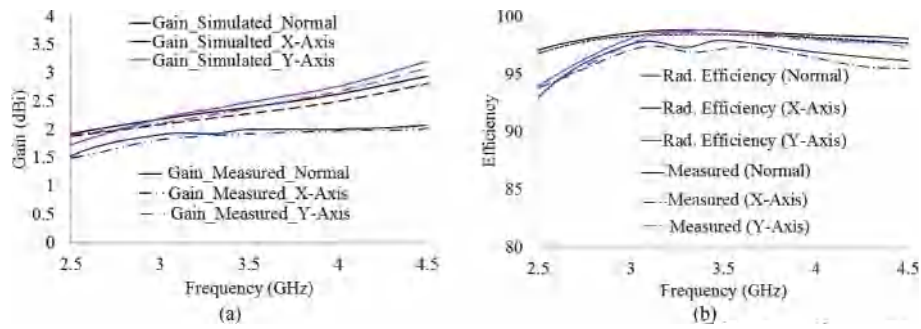


Fig. 8. Plot of the antenna with and without bending for (a) Gain, and (b) Efficiency.

circular ring indicates that it acts as a capacitive reactance and helps in shifting the resonance towards higher frequency. Finally, the current flowing through a middle inverted L-shaped arm indicates that it acts as a coupling element between the outer arms which helps in fine-tuning the resonant frequency band.

When the antenna is bent along the X and Y axis as shown in Fig. 6(b) and (c), the variation in current distribution on the arm just above the feedline as well as through the inverted L-shaped arm is observed while it remains almost similar to that of the antenna in normal conditions on the two side arms.

The co/cross-pol pattern is depicted in Fig. 7 at E and H planes, respectively. For normal and bending conditions, the isolation is better than 15 dB for measured and software-simulated data.

The gain and efficiency plot of the antenna is shown in Fig. 8. Under normal conditions the gain of the antenna is >2.2 dBi within the

resonant band which deteriorated to under 2 dBi when the antenna was bent along the X axis. The gain for Y-axis bending is almost similar to that of the normal antenna. The efficiency of the antenna for all conditions is well above 95 %. A reasonable correlation is observed between measured and simulated outcomes.

The antenna is tested in terms of ECC and S parameters for 8-port MIMO configuration as shown in Fig. 9. The antenna elements are deployed horizontally with an edge-to-edge distance of 9 mm whereas the same distance of 9 mm is maintained between vertical elements as well to form 8-port MIMO geometry. The reflection coefficient is well matched with the single antenna with isolation >15 dB and ECC <0.1. For brevity, only a few reflection co-efficient, as well as transmission coefficient curves, are shown.

The proposed flexible antenna is compared with other MIMO antennas (see Table 1) where it is observed that the antenna proposed in

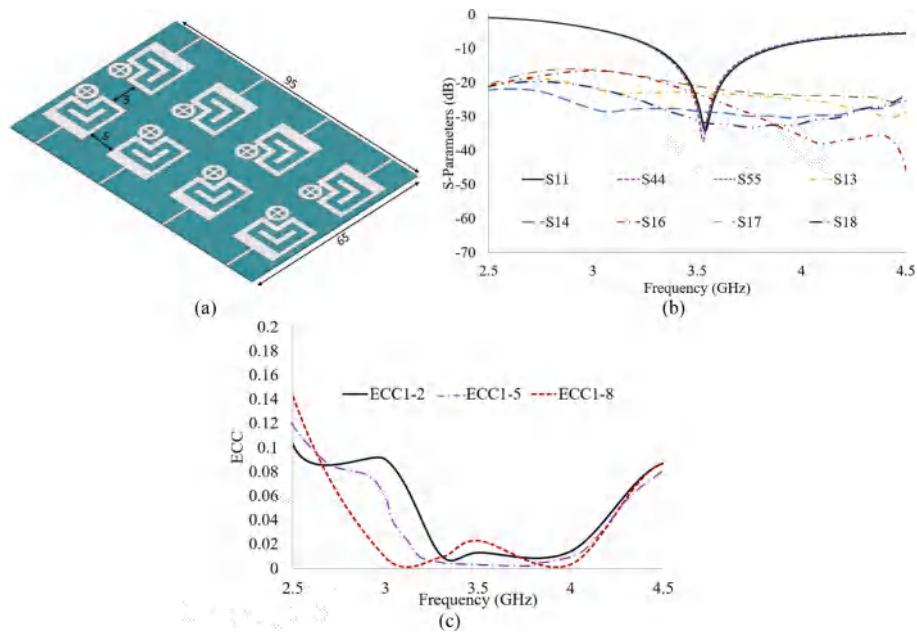


Fig. 9. . 8-Port MIMO antenna (a) Antenna prototype. (b) S-parameters. (c) ECC.

Table 1
Parameters comparison of the antennas.

Reference	Dimensions (mm ³)	Bandwidth (GHz)	Isolation (dB)	ECC	Flexible	No of ports
[14]	66 × 45 × 0.625	2.21–6	>15	<0.016	Yes	4
[15]	31.62 × 3.3 × 0.5	11.6 % (35 GHz center)	>40	<0.06	Yes	4
[16]	22 × 31 × 0.125	3.43–10.1	>15	<0.3	Yes	4
[17]	25.4 × 11 × 0.147	27.2–40	>20	<0.06	Yes	4
Proposed	95 × 65 × 0.2	3.05–3.74	>15	<0.1	Yes	8

[14,16] resonate at the band of interest however they both have higher volume. Antennas in [15,17] are proposed for higher frequency bands. Moreover, all the antennas are 4-port antennas.

4. Conclusion

The design of an inverted L-shaped flexible antenna with the partial ground is studied. The antenna is fabricated and tested under normal and bend conditions. The partial ground plane with an inverted L-shaped structure helped in achieving the required band. The fabricated flexible 8-port MIMO antenna achieves a dimension of $95 \times 65 \times 0.2 \text{ mm}^3$ that is appropriate for the integration with miniaturized circuits. The experimental data matches well with the software-simulated data. The flexible 8-port MIMO antenna presented here shows a low profile, an impedance bandwidth of 3.05–3.74 GHz covering the sub-6 GHz band with Isolation of >15 dB, ECC <0.1 with acceptable gain and efficiency values under normal and bend conditions.

Declaration of Competing Interest

The authors declare that they have no known competing financial interests or personal relationships that could have appeared to influence the work reported in this paper.

Data availability

Data will be made available on request.

References

- [1] Awan WA, Hussain N, Le TT. Ultra-thin flexible fractal antenna for 2.45 GHz application with wideband harmonic rejection. *AEU-Int J Electron Commun* 2019; 110:152851.
- [2] Faisal F, Amin Y, Cho Y, Yoo H. Compact and flexible novel wideband flower-shaped CPW-fed antennas for high data wireless applications. *IEEE Trans Antennas Propag* 2019;67(6):4184–8.
- [3] Alqadami ASM, Nguyen-Trong N, Stancombe AE, Bialkowski K, Abbosh A. Compact flexible wideband antenna for on-body electromagnetic medical diagnostic systems. *IEEE Trans Anten Propag* 2020;68(12):8180–5.
- [4] Kulkarni J, Alharbi AG, Sim C-Y-D, Anguera J. Compact, multiband, flexible decagon ring monopole antenna for GSM/LTE/5G/WLAN applications. In: 2022 16th European conference on antennas and propagation (EuCAP); 2022. p. 1–5.
- [5] Li Wen Tao, Hei Yong Qiang, Grubb Peter Mack, Shi Xiao-Wei, Chen Ray T. Inkjet printing of wideband stacked microstrip patch array antenna on ultrathin flexible substrates. *IEEE Trans. Compon. Packag. Manuf. Technol.* 2018;8(9):1695–701.
- [6] Castro AT, Sharma SK. Inkjet-printed wideband circularly polarized microstrip patch array antenna on a PET film flexible substrate material. *IEEE Anten Wirel Propag Lett* 2017;17(1):176–9.
- [7] Kantharia M, Desai A, Upadhyaya TK, Patel R, Mankodi P, Kantharia M. High gain flexible cpw fed fractal antenna for Bluetooth/WLAN/WPAN/WiMAX applications. *Prog Electromagn Res Lett* 2018;79:87–93.
- [8] Desai A, Jayshri Kulkarni MM, Kamruzzaman SH, Hsu H-T, Ibrahim AA. Interconnected CPW fed flexible 4-port MIMO antenna for UWB, X, and Ku band applications. *IEEE Access* 2022;10:57641–54.
- [9] Desai A, Upadhyaya T, Patel J, Patel R, Palandoken M. Flexible CPW fed transparent antenna for WLAN and sub-6 GHz 5G applications. *Microw Opt Technol Lett* 2020;62(5):2090–103.
- [10] Aliakbari H, Lau BK. Low-profile two-port MIMO terminal antenna for low LTE bands with wideband multimodal excitation. *IEEE Open J Anten Propag* 2020;1: 368–78.
- [11] Kulkarni J, Sim C-Y-D, Chitre A, Kulkarni N, Kulkarni S, Talware R. Design and analysis of compact 2D MIMO sub-6 GHz 5G flexible antenna. *IEEE Madras Sect Conf (MASCONE) 2021;2021:1–5.*
- [12] Kulkarni J, Alharbi AG, Desai A, Sim C-Y-D, Poddar A. Design and analysis of wideband flexible self-isolating MIMO antennas for sub-6 GHz 5G and WLAN smartphone terminals. *Electronics* 2021;10(23):3031.
- [13] Neeta P. Kulkarni, Nilesh Bhaskarrao Bahadure, P.D. Patil, Jayshri S. Kulkarni, Flexible interconnected 4-port MIMO antenna for sub-6 GHz 5G and X band applications, In: *AEU – international journal of electronics and communications*, vol. 152; 2022.
- [14] Desai A, Palandoken M, Kulkarni J, Byun G, Nguyen TK. Wideband flexible/transparent connected-ground MIMO antennas for sub-6 GHz 5G and WLAN applications. *IEEE Access* 2021;9:147003–15.
- [15] Q. Wang, N. Mu, L. Wang, S. Safavi-Naeini, J. Liu, 5G MIMO conformal microstrip antenna design. *Wireless Commun Mobile Comput* 2017; 2017: 7616825.
- [16] Li W, Hei Y, Grubb PM, Shi X, Chen RT. Compact inkjet printed flexible MIMO antenna for UWB applications. *IEEE Access* 2018;6. pp. 50290_50298.
- [17] Jilani SF, Rahimian A, Alfadhl Y, Alomainy A. Low-profile flexible frequency-reconfigurable millimetre-wave antenna for 5G applications. *Flex Printed Electron* 2018;3(3).
- [18] Addepalli, Tathababu, Arpan Desai, Issa Elfergani, N. Anveshkumar, Jayshri Kulkarni, Chemseddine Zebiri, Jonathan Rodriguez, Raed Abd-Alhameed. 8-Port semi-circular arc MIMO antenna with an inverted L-strip loaded connected ground for UWB applications. *Electronics* 2021; 10(12): 1476.
- [19] Kulkarni J, Chen J-Y, Zhang T-Y, Sim C-Y-D. A broadband 8-antenna array design for 5G MIMO smartphone applications. In: *International symposium on antennas and propagation (ISAP)*; 2021. p. 1–2.
- [20] Kulkarni J, Multiband S-Y. miniaturized, maze shaped antenna with an air-gap for wireless applications. *Int J RF Microw Comput Aided Eng* 2020:e22502.

A versatile methodology for preventing a parallel transmission system using impedance-based techniques

Mohan P. Thakre¹, Rakesh Shrivastava², Rahul G. Mapari³, Deepak Prakash Kadam⁴,
Sunil Somnath Kadlag⁵

¹Department of Electrical Engineering, SVERI's College of Engineering, Solapur, India

²Department of Electrical Engineering, Matoshri College of Engineering and Research Center, Nashik, India

³Department of Electronics and Telecommunication Engineering, Pimpri Chinchwad College of Engineering and Research, Ravet Pune, India

⁴Department of Electrical Engineering, MET Institute of Engineering, Nashik, India

⁵Department of Electrical Engineering, Amrutvahini College of Engineering, Sangamner, India

Article Info

Article history:

Received Sep 26, 2022

Revised Jan 4, 2023

Accepted Jan 29, 2023

Keywords:

Adaptive protection

Cross-sectional technique

Digital relaying

Impedance-based technique

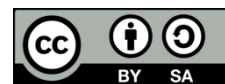
Mutual coupling effect

Parallel transmission line

ABSTRACT

The various configurations that exist for a compatible circuit depend on an object, such as operating conditions, the occurrence of an inter-circuit error and the result of the coupling of the transmission line. This feature makes the protection of the same transmission lines very difficult. This paper introduces a new algorithm based on a state diagram that contains location data collected on a passing bus. Combine the different separation processes and the impedance-based process is used. The classification process cannot detect internal errors and only compares with existing phases where the same regional error occurs in the 2D space and the impedance-based method used to cover the resulting error. The proposed algorithm incorporates impedance-based methodology and separation technology to provide the appropriate response under all operating conditions of the same circuits.

This is an open access article under the [CC BY-SA](https://creativecommons.org/licenses/by-sa/4.0/) license.



Corresponding Author:

Mohan P. Thakre

Department of Electrical Engineering, SVERI's College of Engineering

Pandharpur, Solapur, Maharashtra, India

Email: mohanthakre@gmail.com

1. INTRODUCTION

Parallel transmission lines are all now widely used in the electrical network and they're less expensive to develop than new designs. That alone ensures this same transmitting line's dependability and safety [1]. Because of their higher frequencies, parallel configuration power lines set up in the same towers are used on high-voltage transmission implementations. But the factors like the mutual coupling effect, inter-circuit faults, external faults, and the faults that occur due to different operating conditions of the parallel transmission line make the protection of a parallel transmission a challenging task [2]. The current differential protection scheme using a communication link between the ends of the transmission line could provide accurate protection of the parallel transmission line. But the reliability of the transmission line is directly proportional to the reliability of the communication links hence the protection system could use the algorithm which depends on the local information available at the relay point will help the protection system of the parallel transmission line for accurate fault detection and mitigation [3].

If a traditional distance relay is being used to protect a parallel transmission system, mutual inductance has an effect on the distance relay's performance [4]. When both line segments are operational, if the distance relay is established to secure 80% of the total of the transmission network, and besides based on mutual linkage, this only protects 50% of the line. In contrast, when one of the lines has been out of the system or grounded at both endpoints, the distance relay would provide 100% coverage [5], [6].

It is important to remember that the transmitting stage will be lowered due to the effect of the exchange between the same connection if the typical range has been carried out to defend the related sections. For a reliable transmission sequence, if the distance transmission configuration is set to 85% of the impedance line, then only half of the overhead lines will be covered. Today, a transmitter can have coverage of more than 100% if one of the identical circuits is dormant and deeply implanted at both ends [7]. Capacitive reactance, fault resistance, and the implications of mutual coupling all affect the performance of distance relays. It causes problems in the functioning of the distance relay. To ensure the distance relay functions accurately, various filtering methods are being implemented. They include wavelet filtering, rapid Fourier transform, and prony filtering. However, a distance relay's effectiveness is affected by several factors, including its capacitive reactance, fault resistance, and mutual coupling.

Innovative algorithms prevent this [8], [9]. One method safeguards the entire transmission line. Terminal-based functions include cross-differential. The cross-differential approach compares parallel circuit current phasor magnitudes. When two current phasors surpass the threshold value, it detects an inter-circuit fault [10], [11]. Cross differential protects the line from mutual coupling and responds faster than distance protection. Comparing parallel circuit phases' impedances is another option. One such approach is activated if both circuits appear active and disabled otherwise. Nonetheless, this method may be better at detecting transmission line end distant site defects [12]. A nonpilot-based parallel electrical transmission protection methodology describing distant circuit breaker (CB) operation has been utilized to find remote defects. Superimposed currents can detect remote CB openings [13]. During transmission line, and internal fault conditions, the distance relay's second zone operation has been sped up. However, such a technique must be tested for changing faults, where the problem expanded to other phases after a time delay [14]. An evolutionary defect may misunderstand the superimposed waveforms as a remote CB, causing the relay to operate improperly.

The article explains a method for safeguarding dual-circuit transmission lines using a state diagram. The proposed method combines the results of the impedance-based approach and the crossover method [15], [16] to deliver a protection system that is both faster and more reliable. To compare the phases of the currents in parallel circuits, a novel cross-differential approach is created. The complete range of operational states in a two-dimensional space has been partitioned into six parallel regions [17]–[19]. The frequency-division differential strategy is not always capable of spotting internal faults; hence an additional impedance-based method has been utilized to cover all possible mistakes. By simulating a parallel connection across a sliced-up two-dimensional domain, the impedance-based method effectively recreates the mutual coupling effect [20]–[22]. In certain operational situations, the residual current of the grounding circuit is to be expected when one of the parallel circuits breaks and both ends were mostly grounded. The suggested method identifies transmission line functionality in addition to including the end of the transmission line, and it is based on a state diagram that makes use of the transition sequence between distinct defined states to handle particular faults. Have made use of the CB that was cut out of the tree [23]–[26]. Section 2 outlines the system relay's traditional operating principle. Section 3 outlines the system state diagram based on state logic, and in section 4, we conclude that, compared in comparison to other algorithms, the suggested methodology appropriately as well as efficiently encompasses inter-circuit and evolving faults. Furthermore, this protects the transmission line's end by detecting the functioning of the remote-end CBs.

2. PROPOSED RELAY

The full circuit diagram of the double-circuit transmission network in use to evaluate the novel methodology is shown in Figure 1. A single-pole tripping operation is used by the CB. The given methodology is used to secure the system by opening the CB of all phases after discovering interior problems, even if the single-pole tripping functionalities are not usable.

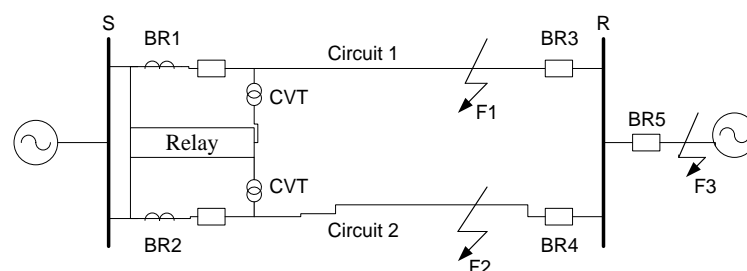


Figure 1. Transmission circuit layout with two circuits

2.1. Presented 2D space cross-differential method

The fundamental concept of the cross-differential method is based on comparing the current phases of a parallel transmission network. The current balanced relay's status is indicated by:

$$|I_1| - |I_2| > I_{op} \Rightarrow \text{Trip circuit 1} \quad (1)$$

$$|I_2| - |I_1| > I_{op} \Rightarrow \text{Trip circuit 2} \quad (2)$$

Where I_1 represents the current in phase circuit 1 and I_2 represents the current in phase circuit 2. Whenever the variation in magnitude between parallel circuit currents increases a top threshold, the relay sends a trip command to a CB. The highest imbalance identified during the non-faulty condition has been used to determine the threshold value. Meanwhile, whenever a remote fault happens on one of the circuits, the variation in the magnitude of the current of the parallel connection is much less than the prescribed level of threshold current, and the cross-differential methodology has been unable to cover the full length of the transmission network.

Since both phases of a double circuit line have become operational, the cross-differential method is well because it does have high sensitivity as well as fast fault clearing. Whether any of the lines is not operational, the characteristics also aren't met, and the cross-differential methodology could fail to prevent relay mal-operation. Also, as consequence, the suggested methodology could be incapable of resolving evolving flaws. In the case of SPT, the traditional cross differential relay wrongly trips this same healthy section after the SPT operation of the CB tries to open the fault occurs section. Figure 2 depicts the current waveforms of phase c on circuit 1 of the parallel transmission line, which is where the line to ground (LG) fault is generated. After the 20s, the issue on bus S is fixed by SPT. As soon as the issue is fixed, the phase C current in the unfaltering part of the circuit rises, while the current in the faulted part of the circuit begins to fall. As seen in Figure 3, this state of affairs persists until the breaker opens the faulty part, resulting in a false tripping of the healthy section.

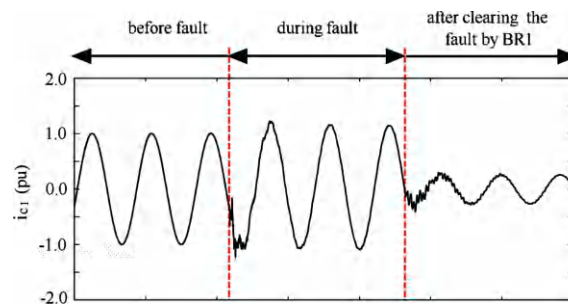


Figure 2. Current waveforms during LG fault of circuit 1

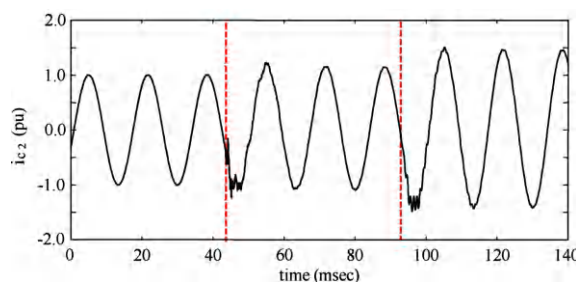


Figure 3. Current waveforms during LG fault of circuit 2

Inter-circuit failures between two different phases have the same issue. To prevent the asymmetric current from exceeding the threshold level in the healthy portion of parallel circuits during single faults, the threshold current value must be set appropriately. This technique lessens the need for relays to safeguard the parallel lines end from a cross differential. In Figure 4, we see the cross-differential method in action, segmenting a two-dimensional space. Using the potential scenarios of the power network under different circuit operating conditions, we can classify six sectors.

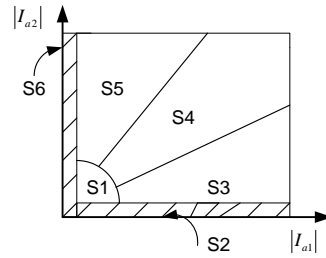


Figure 4. Illustrates the suggested cross-differential computation 2D space segmentation

There are a variety of power network conditions in each region, which are summarized in Table 1. The proposed method accommodates all possible operational states of parallel circuits, and it need not be disabled anytime one of the circuits is down. However, additional conditions are taken into account in particular regions (i.e., S1, S2, S4, and S6) to distinguish internal problems happening on the protected transmission network. This is because, as shown in Table 1, many alternate scenarios for the local electrical grid have become practicable in these areas.

Table 1. Feasible conditions corresponding to various regions of the suggested 2D cross-differential relay

Area	Transmission system condition.
S1	Normal load condition. Internal and external faults when the impedance of the source is very high.
S2	Circuit 2 is out for service, with Normal load conditions. An external fault on circuit 1 when circuit 2 is not in operation.
S3	A fault occurs on circuit 1 of a parallel transmission line.
S4	A remote fault occurs on both circuit 1 and circuit 2 when both are in operation.
S5	A fault occurred on circuit 2 of a parallel transmission line.
S6	An external fault occurs when circuit 1 is not in operation. Normal load condition.

2.2. Adjacent line zero-sequence current adaptive compensation

Incorrect distances relay functioning may occur as a result of the mutual coupling effect of a parallel transmission line on phase voltages. One of the parallel circuits failing to work properly and becoming grounded at both ends is the worst-case situation. Because of this, external faults that are far from the remote bus may be apparent within the first protective zone of the relay, even though the relay is designed to protect only against faults within its range. A compensating factor improves the accuracy of the measured impedance of a faulted circuit, but it also causes false tripping of a healthy circuit. A suggested two-dimensional cross-differential methodology includes an appropriate method for assessing if the impedance should have been determined even without mutual coupling compensation. If the current locus would be in the second or third quadrant, the impedance has been estimated with mutual coupling compensation in which compensation wasn't given to circuit 2.

However, if the current locus has been in a second or third quadrant, impedance has been determined with mutual coupling compensation, even if compensation wasn't presented to circuit 2. If the locus has been between the first and fourth regions, mutual coupling compensation has been applied to both parallel circuits. As shown in Figure 5, the current transformer has been assembled behind its CB, so that when the CB has been opened, the relay cannot connect directly to the current of the corresponding line. When one of the circuits is turned off and both ends are grounded, of that kind situations exist. By connecting additional CT the current will compensate but it is not practically possible. The suggested method solves this issue by using relay data to calculate an estimate of the zero-sequence current in the grounded circuit. For Figure 5(a) the formula for the current in the zero sequences when circuit 2 is off and both ends are grounded is (3):

$$I_{S02} = \frac{\alpha \cdot Z_{0m12} \cdot I_{S01} - (1-\alpha) \cdot Z_{0m12} \cdot I_{R01}}{Z_{12} + Z_{02}} \tag{3}$$

Mutual coupling impedance between circuits 1 and 2 is denoted as Z_{0m12} , where I_{S01} and I_{R01} represent the zero-sequence currents at the transmitting and receiving ends of circuit 1 respectively. The positive zero sequence impedance is denoted by Z_{01} , and the negative impedance is denoted by Z_{02} . The distance between the site of the failure and the relay, measured in power units, is denoted by. Relay-to-fault-point distance on a per-unit basis. The formula for the zero sequence current in a grounded circuit is (4):

$$I_{S02} = \frac{Z_{0m12} \cdot I_{S01}}{Z_{12} + Z_{02}} \quad (4)$$

Two scenarios of parallel circuit configuration is depicted in Figure 5, where only one circuit is functioning at a time. As can be seen in Figure 5(a), in the initial state, the zero-sequence current is flowing through the ground return. Figure 5(b), the zero-sequence current is absent in condition 2. Voltage readings are close to zero when the power-off circuit is grounded at both ends. When both ends of a circuit are disconnected, the induced voltage from the two parallel interconnects will cancel out, and the measured value will be the same as the open-circuit voltage. Thus, the proposed method always assumes that (3) is fulfilled for grounded sections and the zero-sequence current is zero for ungrounded sections.

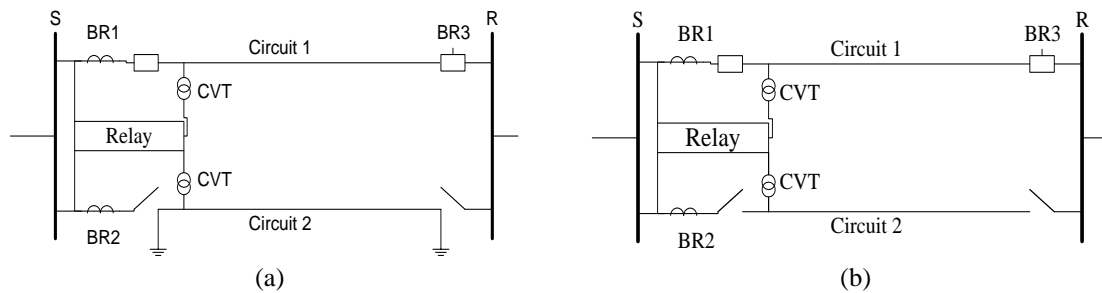


Figure 5. Parallel circuit configuration (a) power off circuit is grounded at both ends and (b) power-off circuits are open at both ends

3. STATE DIAGRAM-BASED DECISION-MAKING LOGIC PROPOSED

The whole work presented a state-diagram-based technique that combines impacts of opposite division with impedance-based techniques. Throughout this manner, a sequence of events distinct from the transfer system could be observed, facilitating the transition of quick and reliable judgments. It really should be mentioned that incorporating multiple transfer releases with the basic thing "OR" does not address the issues they could encounter in the same line of safety. For illustration, if the transmitted impedance has been used to prevent parallel lines from traveling differently, this could construct a faulty route to the positive line besides confronting the closest line.

In another instance, whenever one of the same lines seems to be closed, standard separation techniques must be deactivated needed to reduce false positives in the service line. As a third scenario, whenever a remote error occurs at the end of a portion of a transmission line, none of its most common orders to distinguish based on the discriminatory impedance error seems to be applicable. The suggested impedance methodology has been divided into two modules that are protected for circuits 1 and 2. Each impedance module has been composed of six components. Three of such essentially concerned only those errors in the sub-protection classification that have been involved in the error for each category (e.g., category A, G, -, and - the materials used). Whenever one of the following techniques has been satisfactory, the outcome of each item has seemed.

- The approximate impedance of the feature is found within the original protection zone.
- When an object's limiting impedance is detected inside the second safety zone, the associated countdown clock has run out. In contrast to conventional range transmission, the suggested approach finds multiphase faults using phase unit extraction. It is up to the class attributes in each unit category to decide if the fault involves a protected category or associated circuits. This method of testing the impedance modules' output with a cutting-edge classification algorithm guarantees that any faulty parts will be identified in the event of inter-circuit faults. Meanwhile, the state according to the same circuits in a different 2-D environment compensates for the effect of collaboration between the same circuits. For the sake of clarity, we received some notices all over the paper to demonstrate how we could make up for the reunion. Please continue with a description of the impedance modules that include the loop-loop errors estimated without accounting for the impact of cooperation between the same circuits.

It has also been demonstrated that the overall effect of these is compensated for using zero algebraic currents and that the loop-loop impedance has been calculated using zero sequences of the adjoining circuit. The six provinces have been described due to differing spatial conditions of the circular circuits in the 2-D spacing, as shown in Table 2. The graphic-based method developed by the government has been intended to conduct in-depth research and computation analyses under various conditions. Figure 6 illustrates the proposed method which is divided into three parts for clarity, so each category has been described separately.

Part I: the first section of the suggested method is depicted in Figure 6(a). So both circuits seem to be operational, this somehow encompasses internal inconsistencies by one of them. A fault in region 1 would cause the appropriate circuit cycle locations to shift from their usual state (say, Location S_1) to Location S_3 . In this instance, we have resolved an internal problem in region 1 and sent a trip order to the corresponding CB B_{R1} . If B_{R1} is released, the system will transition to state 6 and the current in the negative circuit's corresponding phase will decrease to zero. There may be local currents in the S_5 region before the end of the year. It's possible that the healthy region's twin region won't return to normal until the problem is fixed by opening the remote CB B_{R3} . A rise in output from the impedance module, indicating an increase in line impedance and an associated error, begins at time value 6.

Compensation for the outcome of the merger is explicitly excluded from this. This is done so that when proximity errors occur in one part of the world, they won't be mistaken for favorable results in a healthy part of the world. State 3 locus currents will transition to state 4 if the fault is not corrected and circuit 2 is reset to the same phase before B_{R1} is closed. Here, performance has been employed to identify a mutable node in circuit 2 and agitate the associated CB2 B_{R2} . When an error occurs in circuit 2, the S_5 region continues to experience the same circuit's current magnitude, and a dispatch signal is sent to the B_{R2} conductor of the associated circuit. The system enters condition 2 when the current in the associated phase drops to zero after B_{R2} has been opened. In region 2, the impedance module begins making line impedance estimates, and this estimation process is flawed regardless of the level of the output.

Table 2. Conditions of transmission lines under various states

State number	Description
1	The locus of the two circuit currents is inside area S1
2	The locus of the two circuit currents is inside area S2
3	The locus of the two circuit currents is inside area S3
4	The locus of the two circuit currents is inside area S4
5	The locus of the two circuit currents is inside area S5
6	The locus of the two circuit currents is inside area S6

Part II: Figure 6(b) shows the second part of the diagram of the proposed state algorithm. The rotating area of the same circuits may remain within the S_4 area under a variety of conditions (i.e., remote errors from the same line, inter-circuit errors covering the same sections in both regions, and external errors). Table 3 summarizes the possible sequence of state changes in various contexts. The suggested methodology employs cutting-edge switch sequences to detect remote inaccuracies just at the end of the line, which can be handled by basic separation transmission as well as impedance transmission. For example, a remote error in region 1 is quickly identified as a proximity error with a transmission attached to a remote bus. Therefore, long-term transmission can disable compatible CB B_{R3} .

If BR3 is open, the twin phase current in the functional circuit will increase (i.e., circuit 2). As the strain on the system lessens, as shown in Figure 6(b), the system changes from state 1 to state 2 or state 3 as appropriate. This particular scene involves a trip command being issued to CB BR1 after a remote malfunction on circuit 1 was detected. In a like fashion, if a remote fault is detected on circuit 2, the remote relay will trip CB BR4, which will then cause the system to transition to either state 5 or state 6 depending on the load. At all times, this scenario involves the establishment of a remote fault on circuit 2 and the subsequent imposition of a trip command on CB BR2. As a result of disturbances from the outside, the system transitions from state 1 to state 4. A fault remains in state 4 until the associated protective relay clears it. Once the outside cause of the problem has been fixed, the system will revert to state 1.

Next, impedance modules and secondary safeguards were added to the long-distance transmission system. Modules that do this measure currents in a zero-crossing and utilize that information to determine impedance, compensating for the effect of mutual coupling. CBs BR1 and BR2 will trip to disassociate the fault if the external fault is not rectified before the 2nd zone timings expire. The locus of parallel circuit currents may also be within region S4 in the event of inter-circuit failures involving phases shared by both interconnects. Such malfunctions are shielded by the impedance modules. In addition to rapid operating rates for faults in the first protective zone, the impedance modules also contain the line terminal end in the 2nd protective zone. It should have been noted that due to the configuration of three phases on the structural system, such inter-circuit faults take place infrequently in practice 3).

Part III: Figure 6(c) depicts the third part of the suggested technique. It can be used to prevent the transmission system whenever one of the parallel connections fails. In the last section, we discussed how the relay might not have had access to the zero-sequence current of the disconnected circuit because of the way the current transformers were set up. It changes to state 2 when the phase currents in circuit 2 are zero, which

happens when the circuit is shut off. If the line impedance output has grown significantly during state 2, this indicates a problem. In state 6, the mutual coupling effect is compensated for using the approximated zero-sequence current; this is achieved by preventing the distance relay first zone overreach, which would otherwise cause unnecessary tripping due to external faults far beyond the remote bus equally upon turning off circuit 1. When the transmission system is included throughout (state 6), the impedance module keeps a constant eye on the line impedance and shuts it down if necessary.

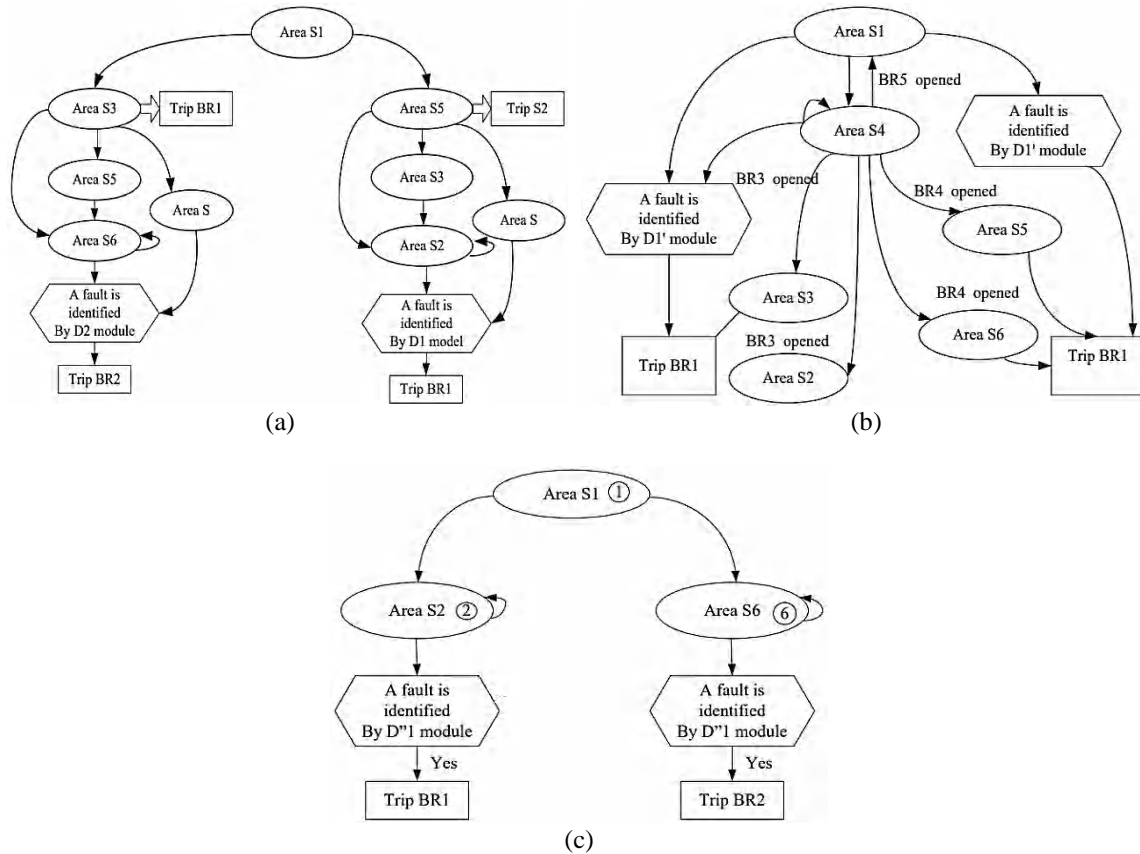


Figure 6. Proposed method (a) part I of the proposed algorithm, (b) part II of the proposed algorithms and (c) part III of the proposed algorithm

Table 3. The state transition for each circumstance in part II

Case	Events	State transition
1	External fault on the remote line, BR5 opened	1,4,1
2	A remote fault occurs on circuit 1, BR3 opened	1,4,3
3	A remote fault occurs on circuit 1, BR3 opened	1,,2
4	A remote fault occurs on circuit 2, BR opened	1,4,5
5	A remote fault occurs on circuit 2, BR4 opened	1,4,6
6	Inter circuit fault detected by relay D'1	1,4, D'1 output is high
7	External fault not detected by the associated relay, it can be identified by the 2 nd zone of D'1	1,4, D'2 output is high
	Inter circuit fault detected by relay D'2	
	External fault not detected by the associated relay, it can be identified by the 2 nd zone of D'2	

4. CONCLUSION

The mutual couple effect is affecting the operation of the relay. It causes the relay to underreach or overreach. This paper introduces a new algorithm to protect the parallel transmission line from the mutual coupling effect. The new algorithm used a two-dimensional space state diagram which used information at the remote location of the relay. An impedance-based technique and the cross-differential method both contribute to the final result, which is then integrated using a schematic. To evaluate the current in the parallel connection of the transmission system, the cross-differential method is used. While using parallel circuits, the traditional cross-differential method algorithm must be disabled. A cross-differential method monitors the impedance-based approach, which dynamically modifies the mutual interaction based on the state of the

parallel circuit currents in discrete regions of 2-dimensional space. So, if any of the parallel circuits was not around and has been grounded at both endpoints, the zero-sequence current of the ground circuit can be used to counteract the relay's overreach issue.




A state diagram technique requires the sequence transition between different zones to diagnose the issues, allowing the relay to have sent the correct trip command to the correct CB. When both circuits of a parallel transmission line have become operational, the suggested methodology responds to transient conditions or modifications in the process with less than a cycle. Because of the good precision of the cross-differential methodology, it provides a quick response during a change in operation, even during the fault-clearing technique. In comparison with other methodologies, the suggested methodology accurately and consistently encompasses inter-circuit as well as evolving faults. Furthermore, it protects the lines end by sensing the operation of the remote-end CBs.

REFERENCES




- [1] H. M. Ismail, "Effect of tower displacement of parallel transmission lines on the magnetic field distribution," in *IEEE Transactions on Power Delivery*, vol. 23, no. 4, pp. 1705-1712, 2008, doi: 10.1109/TPWRD.2008.919029.
- [2] A. Sharma, B. K. Saxena, and K. V. S. Rao, "Comparison of smart grid development in five developed countries with focus on smart grid implementations in India," in *2017 International Conference on Circuit, Power and Computing Technologies (ICCPCT)*, 2017, doi: 10.1109/iccpct.2017.8074195.
- [3] B. Li *et al.*, "Measurement and analysis of electromagnetic environment of ± 500 kV double-circuit DC transmission lines on the same tower," in *2020 IEEE Int. Conf. on High Voltage Engineering and Application*, 2020, doi: 10.1109/ichve49031.2020.9279618.
- [4] P. R. Khade and M. P. Thakre, "Advance approach to prevent the effect of mutual coupling and series capacitor for series compensated parallel transmission lines," in *2020 International Conference on Power, Energy, Control and Transmission Systems (ICPECTS)*, 2020, doi: 10.1109/icpepts49113.2020.9336982.
- [5] P. M. Anderson, C. Henville, R. Rifaat, B. Johnson, and S. Meliopoulos, "Reliability concepts in system protection," in *Power System Protection*, IEEE-Power System Protection, 2022, pp. 1197-1260, doi: 10.1002/9781119513100.ch28.
- [6] K. R. Pillay and B. S. Rigby, "Studying the impact of mutual coupling on distance protection relays using a real-time simulator," in *IEEE Africon '11*, 2011, doi: 10.1109/afcon.2011.6072015.
- [7] S. Dambhare, S. A. Soman, and M. C. Chandorkar, "Current differential protection of transmission line using the moving window averaging technique," *IEEE Transactions on Power Delivery*, vol. 25, no. 2, pp. 610-620, 2010, doi: 10.1109/tpwr.2009.2032324.
- [8] L. N. Tripathy, P. K. Dash, and S. R. Samantaray, "A new cross-differential protection scheme for parallel transmission lines including UPFC," *IEEE Transactions on Power Delivery*, vol. 29, no. 4, pp. 1822-1830, 2014, doi: 10.1109/tpwr.2013.2288780.
- [9] M. P. Thakre and V. S. Kale, "An adaptive approach for three zone operation of digital distance relay with Static Var Compensator using PMU," *International Journal of Electrical Power and Energy Systems*, vol. 77, pp. 327-336, 2016, doi: 10.1016/j.ijepes.2015.11.049.
- [10] A. Saber, H. H. Zeineldin, T. H. M. El-Fouly and A. Al-Durra, "Time-domain fault location algorithm for double-circuit transmission lines connected to large scale wind farms," in *IEEE Access*, vol. 9, pp. 11393-11404, 2021, doi: 10.1109/ACCESS.2021.3049484.
- [11] M. P. Thakre and A. Ahmad, "Interline Power Flow Controller (IPFC) deployment in long transmission lines and its effects on distance relay," *Journal of The Institution of Engineers (India): Series B*, vol. 103, no. 2, pp. 491-505, 2021, doi: 10.1007/s40031-021-00637-y.
- [12] H. Sonawane and M. Thakre, "Modified transmission line protection throughout static VAR compensator's present state," in *2021 Third International Conf. on Intelligent Communication Technologies and Virtual Mobile Networks*, 2021, doi: 10.1109/icicv50876.2021.9388613.
- [13] J. Ciufo and A. Cooperberg, "What is power system protection, why is it required and some basics?," in *Power System Protection: Fundamentals and Applications*, IEEE, 2022, pp. 1-12, doi: 10.1002/9781119847397.ch1.
- [14] Y. Hu, D. Novosel, M. M. Saha, and V. Leitloff, "An adaptive scheme for parallel-line distance protection," *IEEE Transactions on Power Delivery*, vol. 17, no. 1, pp. 105-110, 2002, doi: 10.1109/61.974195.
- [15] A. Sharafi, M. Sanaye-Pasand, and P. Jafarian, "Non-communication protection of parallel transmission lines using breakers open-switching travelling waves," *IET Generation, Transmission and Distribution*, vol. 6, no. 1, p. 88, 2012, doi: 10.1049/iet-gtd.2011.0398.
- [16] A. H. Osman and O. P. Malik, "Protection of parallel transmission lines using wavelet transform," *IEEE Transactions on Power Delivery*, vol. 19, no. 1, pp. 49-55, 2004, doi: 10.1109/tpwr.2003.820419.
- [17] N. A. Sundaravaran, R. Meyur, P. Rajaraman, B. Mallikarjuna, M. J. B. Reddy, and D. K. Mohanta, "A wavelet based novel technique for detection and classification of parallel transmission line faults," in *2016 International Conference on Signal Processing, Communication, Power and Embedded System (SCOPES)*, 2016, doi: 10.1109/scopes.2016.7955788.
- [18] M. M. Eissa and O. P. Malik, "Laboratory investigation of a distance-protection technique for double circuit lines," *IEEE Transactions on Power Delivery*, vol. 19, no. 4, pp. 1629-1635, 2004, doi: 10.1109/tpwr.2004.832399.
- [19] Z. Q. Bo, X. Z. Dong, B. R. J. Cauce, and R. Millar, "Adaptive noncommunication protection of double-circuit line systems," *IEEE Transactions on Power Delivery*, vol. 18, no. 1, pp. 43-49, 2003, doi: 10.1109/tpwr.2002.803748.
- [20] D. A. Tziouvaras *et al.*, "Mathematical models for current, voltage, and coupling capacitor voltage transformers," *IEEE Transactions on Power Delivery*, vol. 15, no. 1, pp. 62-72, 2000, doi: 10.1109/61.847230.
- [21] Y.-S. Cho, C.-K. Lee, G. Jang, and H. J. Lee, "An innovative decaying dc component estimation algorithm for digital relaying," *IEEE Transactions on Power Delivery*, vol. 24, no. 1, pp. 73-78, 2009, doi: 10.1109/tpwr.2008.2005682.
- [22] Q. Wang, X. Dong, Z. Bo, B. Bounce, A. Apostolov, and D. Tholomier, "Cross differential protection of double lines based on super-imposed current," in *18th International Conference and Exhibition on Electricity Distribution (CIRED 2005)*, 2005, doi: 10.1049/cp:20051196.
- [23] M. S-Pasand and P. Jafarian, "Adaptive protection of parallel transmission lines using combined cross-differential and impedance-based techniques," *IEEE Transactions on Power Delivery*, vol. 26, no. 3, pp. 1829-1840, 2011, doi: 10.1109/tpwr.2011.2142014.
- [24] M. R. Araújo and C. Pereira, "Distance protection algorithm for long parallel transmission lines with no common bus," in *IEEE Transactions on Power Delivery*, vol. 35, no. 2, pp. 1059-1061, April 2020, doi: 10.1109/TPWRD.2019.2903932.
- [25] P. S. Jagtap and M. P. Thakre, "Effect of infeed current and fault resistance on distance protection for tee-feed line," in *2020 IEEE First International Conference on Smart Technologies for Power, Energy and Control (STPEC)*, 2020, doi: 10.1109/stpec49749.2020.9297799.
- [26] A. Sharma and S. Gangolu, "Positive sequence impedance based fault discrimination technique in grid connected solar PV system," in *2021 2nd International Conference for Emerging Technology (INCET)*, May 2021, doi: 10.1109/incet51464.2021.9456143.

BIOGRAPHIES OF AUTHORS






Dr. Mohan P. Thakre    received the B.Tech. and M. Tech degrees in electrical power engineering from Dr. Babasaheb Ambedkar Technological University (Dr. BATU), Maharashtra, India, in 2009 and 2011 respectively, and the Ph.D. Degree in electrical engineering from Visvesvaraya National Institute of Technology (VNIT), Nagpur, Maharashtra, India in 2017. Currently, he is an Associate Professor at the Department of Electrical Engineering, SVERI's College of Engineering, Pandharpur, Maharashtra, India. His research interests include FACTS and power system protection. He can be contacted at email: mohanthakre@gmail.com.






Dr. Rakesh Shrivastava    obtained Ph.D. Degree in Electrical Engineering specializing in power electronics and drives from RTM Nagpur University, (India) in 2017. He occupied various positions to serve the engineering institutes for about 24 years. He is currently working as a Professor at Department of Electrical Engineering, Matoshri College of Engineering and Research Center, Nashik. His research interests include the analysis and control of electrical drives, particularly in hybrid and electric vehicle applications. He has several publications in national and international journals. He attended International and National conferences and also worked as a jury member. He is a member of professional bodies such as ISTE and IAENG. He can be contacted at email: rakesh_shrivastava@rediffmail.com.






Dr. Rahul G. Mapari    received the bachelor and master degree in Electronics Engineering from Savitribai Phule Pune University, India in 2004 and 2007 respectively and the PhD degree in Electronics and Telecommunication Engineering from Amravati University, India in 2016. From 2005 to 2015 he worked at Savitribai Phule Pune University involved in teaching and research in power converters. Since 2017, he has been in Department of Electronics and Telecommunication Engineering of Pimpri Chinchwad College of Engineering and Research and is currently working as Professor and Head of Department. His research interest is power converters and power electronics. He can be contacted at email: rahul.mapari@pccoer.in.



Dr. Deepak Prakash Kadam    received a B.E from the Government College of Engineering, Amaravati, and M.E degrees in electrical power systems from Walchand College of Engineering, Sangli, Maharashtra, India, in 1997 and 2005 respectively, and the Ph.D. degree in electrical engineering from Savitribai Phule Pune University, Pune Maharashtra, India in 2015. Currently, he is an Associate Professor at the Department of Electrical Engineering, Bhujbal Knowledge City, MET Institute of Engineering, Nashik, India. His research interests include renewable energy technology, power quality, and power system. His total teaching experience is around 23 years. He can be contacted at email: dpkadam@gmail.com.



Dr. Sunil Somnath Kadlag    received B.E in Electrical Engineering from Dr. Babasaheb. Ambedkar. Marathwada University, Aurangabad (Dr B.A.M.U) in 1997 and M.E in Electrical Engineering (Control System) from Government College of Engineering Pune (Pune University) in 2005 and Ph.D in Electrical Engineering from Suresh Gyan Vihar University Jaipur (Rajasthan) in 2021. His research area is electric vehicles. He is presently working as an Associate Professor and Head, of the Department of Electrical Engineering, Amrutvahini College of Engineering, Sangamner, Savitribai Phule Pune University, Pune, Maharashtra, India. He can be contacted at email: sunilkadlag5675@gmail.com.

Performance analysis of FOC space vector modulation DCMLI driven PMSM drive

Rakesh Shriwastava¹, Mohan P. Thakre², Jagdish Choudhari³, Sunil Somnath Kadlag⁴, Rahul Mapari⁵,
Deepak Prakash Kadam⁶, Shridhar Khule¹

¹Department of Electrical Engineering, Matoshri College of Engineering and Research Center, Nashik, India

²Department of Electrical Engineering, SVERI's College of Engineering, Solapur, India

³Department of Electrical Engineering, Nagpur Institute of Technology, Nagpur, India

⁴Department of Electrical Engineering, Amrutvahini College of Engineering, Sangamner, India

⁵Department of Electrical Engineering, Pimpri Chinchwad College of Engineering and Research, Ravet Pune, India

⁶Department of Electrical Engineering, MET Institute of Engineering, Nashik, India

Article Info

Article history:

Received Sep 12, 2022

Revised Nov 2, 2022

Accepted Mar 24, 2023

Keywords:

Automatic voltage regulator

Field oriented control

Permanent magnet synchronous motor

Space vector modulation

Total harmonic distortion

ABSTRACT

The effectiveness of a permanent magnet synchronous motor (PMSM) drive managed by an automatic voltage regulator (AVR) microcontroller using field oriented control (FOC) with space vector modulation (SVM) and a diode clamped multilevel inverter (DCMLI) is investigated. Due to its efficacy, FOC would be widely implemented for PMSM speed regulation. The primary drawbacks of a 3-phase classic bridge inverter appear to be reduced dv/dt stresses, lesser electromagnetic interference, and a relatively small rating, especially when compared to inverters. PMSMs have a better chance of being adopted in the automotive industry because of their compact size, high efficiency, and durability. The SVM idea states that an inverter's three driving signals are created simultaneously. Using MATLAB simulations, researchers looked into incorporating a DCMLI with a resistive load on an AVR microcontroller. Torque, current, and harmonic analysis were evaluated between the SVM and the inverter-driven PMSM drive in this research. In comparison to the prior art, the proposed PMSM drive has better speed and torque management, less output distortion, and less harmonic distortion.

This is an open access article under the [CC BY-SA](https://creativecommons.org/licenses/by-sa/4.0/) license.



Corresponding Author:

Rakesh Shriwastava

Department of Electrical Engineering, Matoshri College of Engineering and Research Center

Nashik, India

Email: rakesh_shriwastava@rediffmail.com

1. INTRODUCTION

The characteristics of permanent magnet synchronous motor (PMSM) are the low value of cogging torque, ruggedness, high efficiency, high power to weight ratio, and additional reluctance torque. In an electric vehicle application, the motor, run to different load and speed profiles; hence it is used application. In PMSM, due to the magnet in the rotor and constant air gap, it is not needed to supply magnetizing currents through the stator flux. When at high speed, it gives high current and fewer switching losses. If put into practice, it would allow for a range of speeds by rapidly switching between low switching frequencies for slow speeds and high switching frequencies for fast speeds [1], [2]. Vector control is the most useful method for field oriented control (FOC). The FOC approach has replaced the direct torque control (DTC) method in AC drives [3], [4] because of its superior performance. The good-current regulation, high torque response, and simple construction have the advantages of FOC. Some of the advantages of multilayer inverters include increased efficiency, lower voltage

distortion, lower harmonic content, and lower dv/dt at each switch. A pulse width modulation (PWM) controller multilayer inverter can switch to a lower frequency [5], [6]. The FOC is a vector control method based on the working principle of a separately excited d.c motor. This method can effectively control the motor torque and flux by controlling the stator reference currents, rotor angle, and torque of the alternating machine. In this paper, a novel space vector modulation (SVM) technique is designed for the FOC based diode clamped multilevel inverter (DCMLI) PMSM to drive for torque, speed, and stator current of PMSM [6].

The inverter switching vectors have been automatically constructed from the instantaneously sampled reference phase voltages [7], [8] without the need for lookup tables or difficult logical choices. In this study, we analyze DCMLI using a simulated SVM and then feed the results into a three-phase resistive load. It reduces switching losses and total harmonic distortion (THD). In this case, the automatic voltage regulator (AVR) microcontroller simulation results have been confirmed for use in actual projects. Pulses are generated by the atmega 8 and fed into the inverter.

FOC provides high-quality control capability in FOC SVM over the full range of torque and speed fluctuations [9]–[11]. There are d & q current modes in FOC. The q torque mode is run the desired torque from the PMSM. The d current mode is run with a zero to minimize the unwanted direct torque component [12]–[14]. To overcome this drawback in PWM, an SVM modulation technique is used. SVM selects vectors in a d - q stationary frame. Space vectors are based on induction machines magnetism. Three-phase amounts become two-phase [15], [16]. Space vectors can represent active and "0" switching [17]. V_1 - V_6 forms a symmetric hexagon to diversify sectors (1 to 6). Each sector is 60° apart. SPWM compares sine waves to triangular waves [18]–[20]. Switching points result from the triangular carrier wave of frequency f_c and the reference modulatory sine wave of frequency f_m . This research presents MATLAB simulation and hardware validation of three-level DCMLI-fed FOC-PMSM drives using SVM and AVR microcontroller [21]–[25]. This paper follows this format. Section 1 covers the overview, section 2 the analytical approach, section 3 the virtual world assessment and outcomes, and section 4 the hardware configuration. section 5 is the experimental outcome and the conclusion of this paper is in section 6.

2. METHODOLOGY

Mathematical model analysis of PMSM is a concern, the d -axis-induced voltage is:

$$u_d = R_d i_d + \frac{d\lambda_d}{dt} - \omega_r \lambda_q \quad (1)$$

The q -axis induced voltage is:

$$u_q = R_q i_q + \frac{d\lambda_q}{dt} - \omega_r \lambda_d \quad (2)$$

$$\lambda_d = L_d i_d + \lambda_m \quad (3)$$

$$\lambda_q = L_q i_q \quad (4)$$

$$L_d = L_q \quad (5)$$

The torque equation is:

$$T_e = \frac{3p}{2} (\lambda_d i_q - \lambda_q i_d) \quad (6)$$

Put in (7):

$$T_e = \frac{3p}{2} [(\lambda_d i_d + \lambda_m) i_q - L_q i_q i_d] \quad (7)$$

$$T_e = \frac{3p}{2} [(L_d - L_q) i_d i_q + \lambda_m i_q] \quad (8)$$

$$\text{Reluctancetorque} = \frac{3p}{2} (L_d - L_q) i_d i_q \quad (9)$$

$$\text{fieldtorque} = \frac{3p}{2} \lambda_m i_q \quad (10)$$

$$T_e = \frac{3p}{2} \lambda_m i_q \quad (11)$$

$$T_e = K_t i_q \quad (12)$$

$$K_t = \frac{3p}{2} \lambda_m \quad (13)$$

Therefore, electromagnetic torque is:

$$T_e = T_l + B_{\omega_m} + J \frac{d\omega_m}{dt} \quad (14)$$

The primary goal of FOC is the control of torque and currents along the stator axis (d and q). By regulating the motor's torque and flux based on information from the stator currents and the rotor angle, FOC can accomplish desirable results such as high output and reduced torque ripple. The system consists of a current regulator, a direct-axis component, a q-axis component, and a speed regulator. The FOC method is depicted in block format in Figure 1.

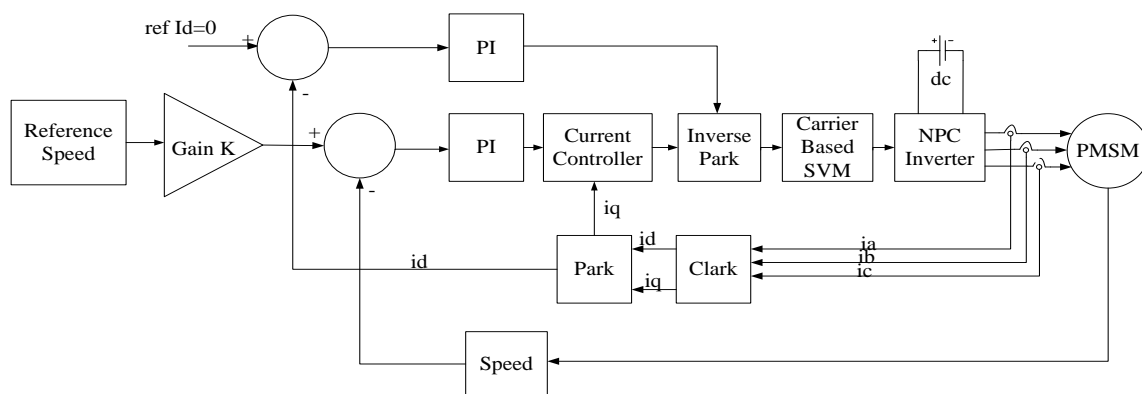


Figure 1. Schematic illustration of FOC

Design of converter:

- Design of diode bridge rectifier

Voltage (input)=290 V, frequency=50 Hz, filter output voltage (rectifier)=380 Vdc

- Design of three-level diode clamp inverter, while selecting MOSFET, $V_{dc} > 0.707 \times m_a \times V_{dc}$ [let $m_a = 1$ (max)] $> 0.707 \times 1 \times 380 > 268.66$ volts, $V_{gs} > 12$ volts, $I_d > I_{Lmax} > 2$ amps

Transition times should be minimized. IRFP460 is the MOSFET of choice, output voltage (inverter)=280 V, switching frequenc=2.5 KHz, inverter rating (KVA)=1.5 KVA

- Isolator drive and AVR microcontroller details

To regulate the output, there are twelve 7,812 ICs and twelve 4N35 optical couplers. The transformers have a rating of 230 volts to 12 volts and 500 milliamperes (12 No). The ATmega8 (28 Pin) is responsible for creating pulses, while the ATmega16 (40 Pin) is in charge of the control and monitoring circuit (40 Pin).

3. SIMULATION ANALYSIS AND DISCUSSION

The simulation diagram of FOC is shown in Figure 2. Design, simulation, and implementation of FOC SVM DCMLI-driven PMSM drive using an AVR microcontroller are investigated for the different speeds. It is shown in Figures 3-7. The frequency analysis of the inverter output and THD analysis are shown in Figures 8 and 9. The parameters of the motor and inverter have been listed in Tables 1 and 2. THD, torque, and current ripples of DCMLI are listed in Tables 3 and 4. Figures 3 and 4 shows inverter voltage and current respectively with less THD. Figures 5-7 show the performance of the PMSM drive using SVM.

The reference speed changed from 0 to 1,000 rpm for time $t=0.05$ s and speed are constant for the time of $t=0.05$ s to 0.3 s. Motor speed was 1,700 rpm for time $t=0.3$ s to 0.35 s. Speed reached the reference value for time $t=0.6$ s as shown in Figure 6. The value of load torque is 0.2 N.m for time $t=0$ s to 0.4 s. It is decreased for time $t=0.3$ s to 0.4 s shown in Figure 6. The initial current of the motor was 1.4 amp and it reduces up to 1.3 amp for time $t=0$ s to 0.1 s as shown in Figure 7.

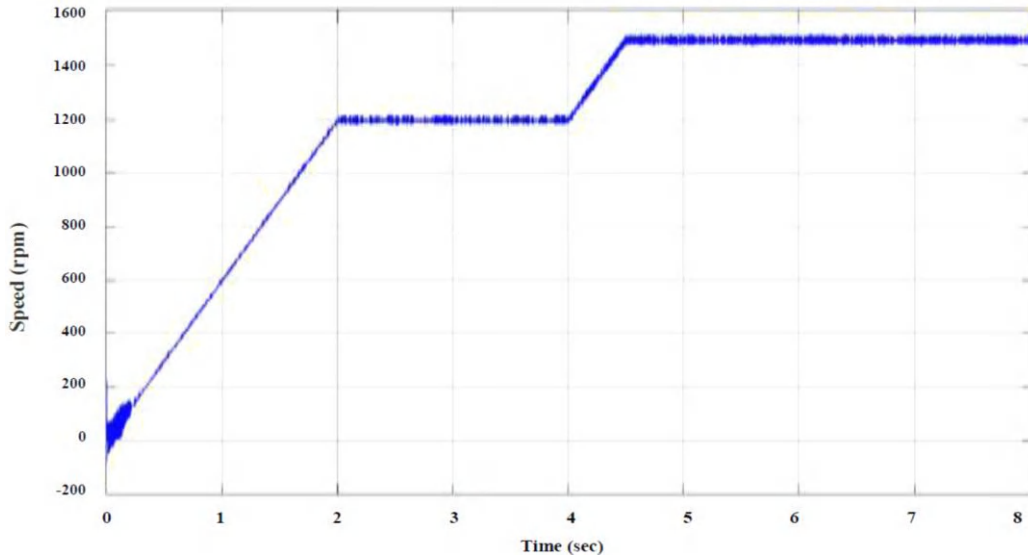


Figure 5. Output speed response of FOC-DCMLI

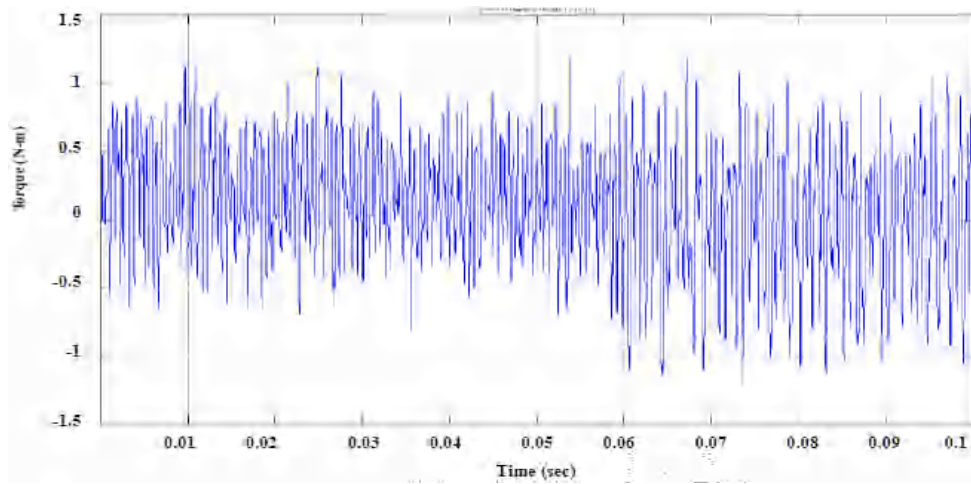


Figure 6. Output torque response of FOC-DCMLI

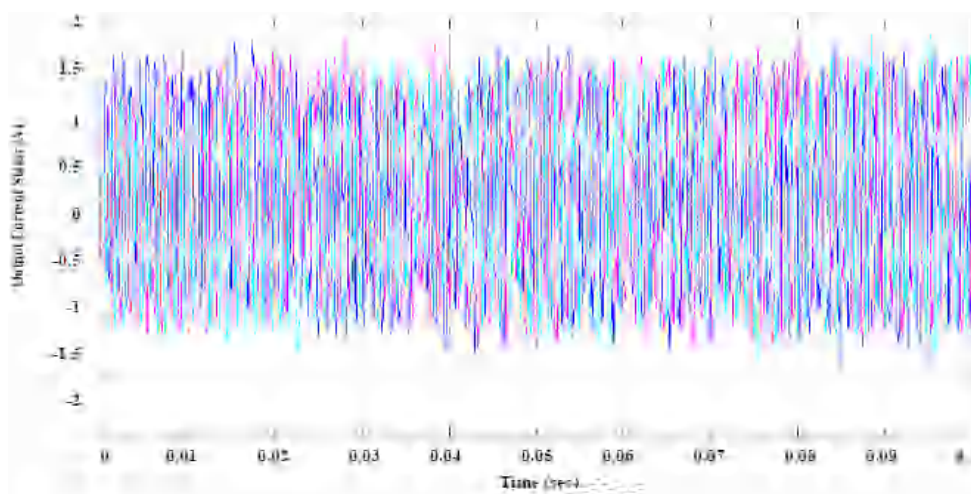


Figure 7. Output phase current FOC-DCMLI

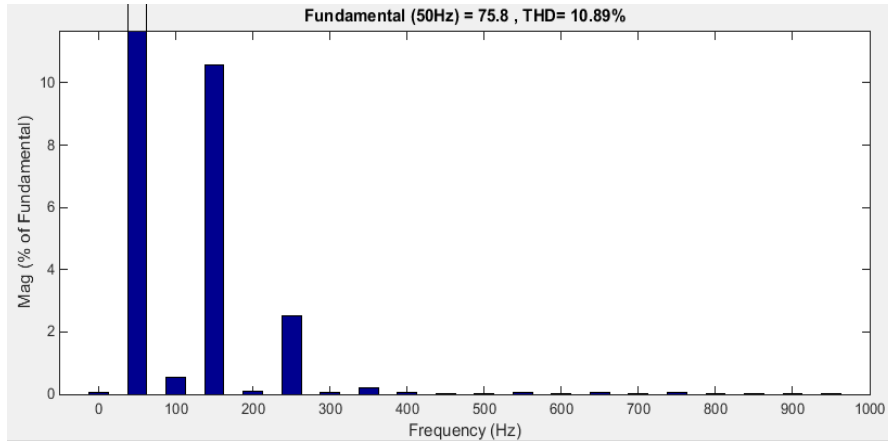


Figure 8. THD of the voltage of FOC-DCMLI

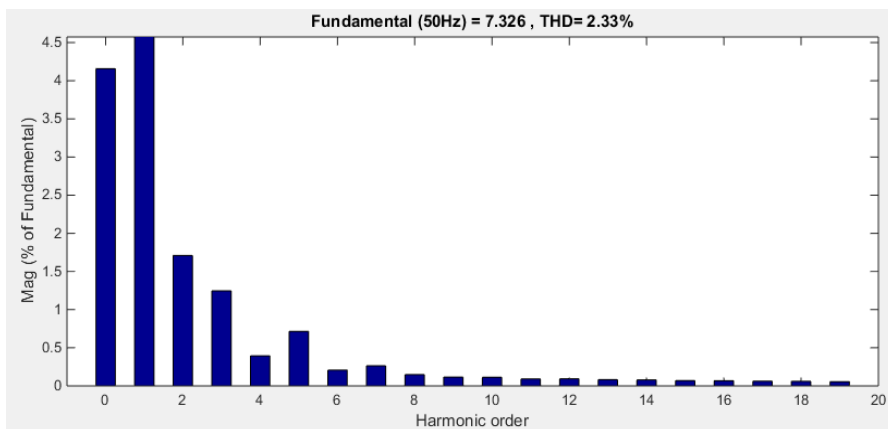


Figure 9. THD of current of FOC-DCMLI

Table 1. PMSM specification

Parameters	Values
Motor stator resistance (R_s)	4.865 Ω
Motor stator inductance (L_s)	0.0174 H
Motor torque (T_e)	0.544 N-m
Movement of inertia (J)	0.000114 Kg/m ²
Viscous coefficient (f)	0.0000447 Nms
Number of pole(P) pair	2
Inductive load	PMSM

Table 2. Inverter parameter

Parameters	Values
Input voltage	280 V (rms)
Output filter voltage	380 Vdc
Supply frequency	50 Hz
Inverter voltage	270V
Switching frequency	2.5 kHz
Inverter rating	1.5 KVA
Resistive load	200 Watts

Table 3. THD analysis

Parameter	THD (%)
Voltage	10.89
Current	2.33

Table 4. Torque and current ripples

	1100 rpm	1300 rpm	1600 rpm
Torque ripples	0.52 Nm	0.49 Nm	0.46 Nm
Current ripples	8.4 mA	7.8 mA	7.5 mA

4. HARDWARE ANALYSIS

The block diagram of the proposed AVR microcontroller-based three-level DCMLI with three-phase resistive load and real image for the experiment is shown in Figures 10 and 11 respectively. The three-level DCMLI is used to convert DC to three phases of AC. The generation of pulses using the SVM

technique by the AVR microcontroller is shown. For triggering the insulated gate bipolar transistors (IGBTs), DCMLI generates gate pulses.

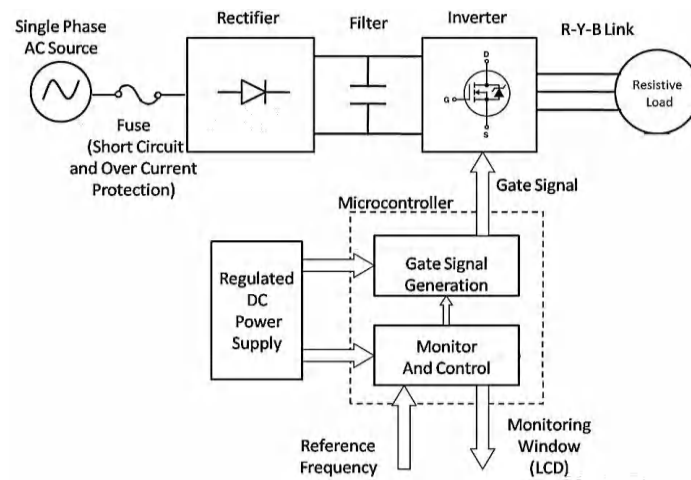


Figure 10. Block schematic of proposed FOC-DCMLI PMSM drive

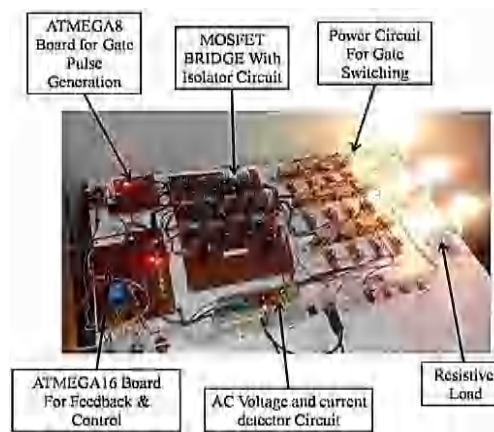


Figure 11. Real image for the experiment

5. EXPERIMENTAL OUTCOME

A proposed method has been established by using AVR microcontroller. An empirical investigation has been carried out with a view to the validity of the presented AVR microcontroller premised SVM. Methods of regulation have been presented, and their efficacy with a 3 Nm load has been demonstrated. It has been experimentally looked into how fast each approach can respond. Load-related variations in the motor speed at constant modulating frequencies of 40 Hz, 45 Hz, and 50 Hz. Figures 12(a)-(c) display DCMLI phase voltages at 40 Hz, 45 Hz, and 50 Hz, respectively.

To verify the reliability of the suggested SVM approach, a three-tiered DCMLI was devised and implemented. DC-modulated multi-level interleaved-switched voltage modulation is superior to PWM. Figures 13(a)-(c) display the DCMLI line voltages at 40 Hz, 45 Hz, and 50 Hz, respectively.

Observational data shows low levels of THD, ripple current (IR), and ripple torque (Tr). The evidence is in Tables 3 and 4. Tables 5 and 6 illustrate the load readings for 33 Hz and 59 Hz, respectively, at various motor speeds. Figure 14 shows waveforms of DCMLI current, speed-torque variation at 33 Hz and 59 Hz is seen in Figure 15.

There is no change in frequency or speed due to changes in load. Changing the inverter's frequency will also vary the motor's output. Power output vs torque is depicted in Figure 15(a) and load versus speed is depicted in Figure 15(b).

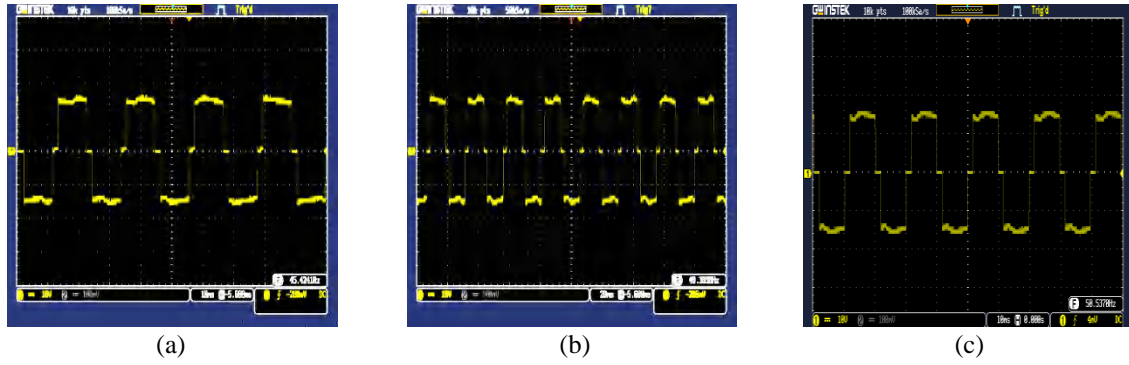


Figure 12. DCMLI phase voltages: (a) at 40 Hz, (b) at 45 Hz, and (c) at 50 Hz

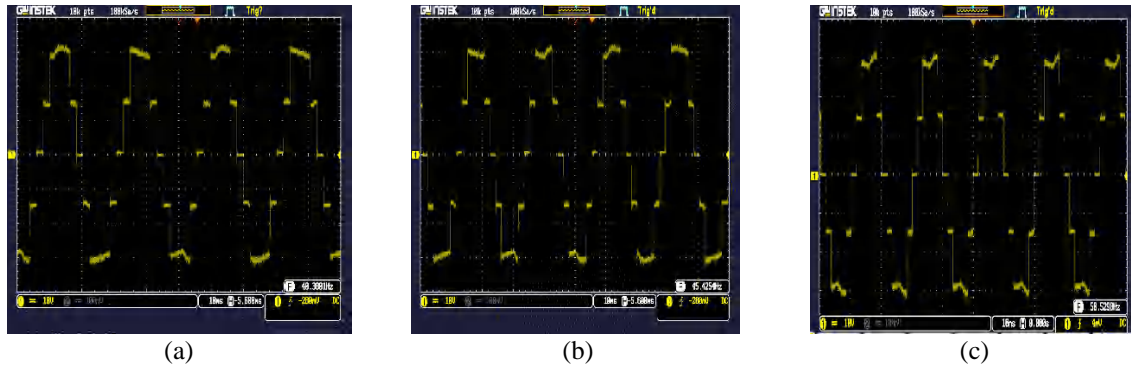


Figure 13. DCMLI line voltages: (a) at 40 Hz, (b) at 45 Hz, and (c) at 50 Hz

Table 5. Motor speed-load reading at 33 Hz

Sr. No.	Weight (gm)	Actual speed (rpm)	Calculated speed (rpm)	Voltage (volts)
1.	600	998	1011	272
2.	1100	998	1011	272
3.	1600	998	1011	272
4.	2100	998	1011	272
5.	2600	998	1011	272
6.	3200	998	1011	272

Table 6. Motor speed-load reading at 59 Hz

Sr. No.	Weight (gm)	Actual speed (rpm)	Calculated speed (rpm)	Voltage (volts)
1.	600	1770	1792	268
2.	1100	1770	1792	268
3.	1600	1770	1792	268
4.	2100	1770	1792	268
5.	2600	1770	1792	268
6.	3200	1770	1792	268

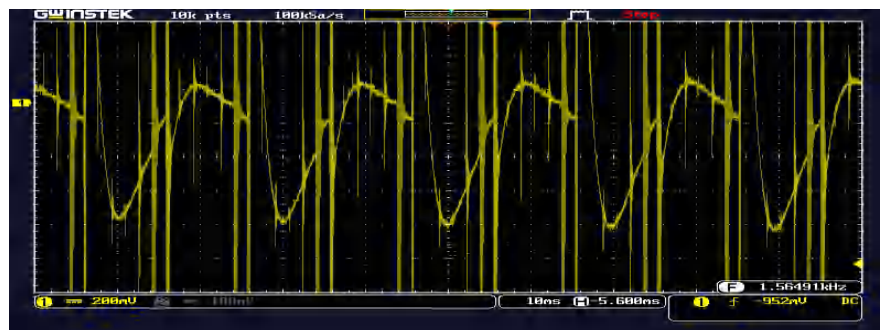


Figure 14. Waveforms of DCMLI current

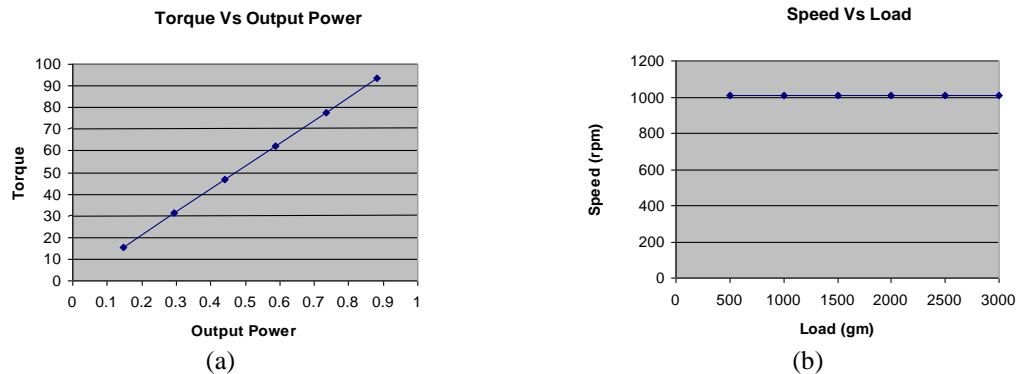


Figure 15. Speed-torque variation: (a) at 33 Hz and (b) at 59 Hz

6. CONCLUSION

In this study, we analyze the efficiency of a PMSM drive controlled by a FOC SVM DCMLI and driven by an AVR microcontroller. This evaluation is predicated on an AVR microcontroller-driven PMSM motor and is controlled by a DCMLI. The inverter-driven PMSM drive with SVM was compared in terms of torque, current, and harmonic analysis. Less harmonic distortion is achieved as a result of using DCMLI. Improved steering efficiency in terms of speed and torque response, in addition to better dynamic characteristics, less contorted output, and reduced costs are provided by the proposed AVR microcontroller-based DCMLI-driven PMSM drive. Since it can adapt to changes in speed quickly and has a lower load ripple than conventional inverters, it is well suited for use in the automotive industry.





REFERENCES

- [1] V. T. Ha, "Torque Ripple Reduction of the SRM Motor Using Nonlinear Controller for Electric Vehicles Application," in *2022 11th International Conference on Control, Automation and Information Sciences (ICCAIS)*, Nov. 2022, doi: 10.1109/iccais56082.2022.9990491.
- [2] Z. Alqarni, "Improved Control Strategy for 4 WD Electric Vehicle Using Direct Torque Control Technique with Space Vector Modulation," in *2022 IEEE 12th Annual Computing and Communication Workshop and Conference (CCWC)*, Jan. 2022, doi: 10.1109/ccwc54503.2022.9720858.
- [3] K.-B. Lee, J.-H. Song, I. Choy, and J.-Y. Yoo, "Torque ripple reduction in DTC of induction motor driven by three-level inverter with low switching frequency," *IEEE Transactions on Power Electronics*, vol. 17, no. 2, pp. 255–264, Mar. 2002, doi: 10.1109/63.988836.
- [4] L. Romeral, A. Arias, E. Aldabas, and M. G. Jayne, "Novel direct torque control (DTC) scheme with fuzzy adaptive torque-ripple reduction," *IEEE Transactions on Industrial Electronics*, vol. 50, no. 3, pp. 487–492, Jun. 2003, doi: 10.1109/tie.2003.812352.
- [5] R. G. Shrivastava, M. P. Thakare, K. V. Bhadane, M. S. Harne, and N. B. Wagh, "Performance enhancement of DCMLI fed DTC-PMSM drive in electric vehicle," *Bulletin of Electrical Engineering and Informatics*, vol. 11, no. 4, pp. 1867–1881, Aug. 2022, doi: 10.11591/eei.v11i4.3714.
- [6] M. S. Merzoug and F. Nacéri, "Comparison of Field-Oriented Control and Direct Torque Control for Permanent Magnet Synchronous Motor (PMSM)," *International Journal of Electrical and Computer Engineering*, vol. 2, no. 9, pp. 1797–1802, Sep. 2008, doi: 10.5281/zenodo.1330719.
- [7] Y. Li, W. Liu, Z. Fu, and D. Gerling, "The control of stator flux and torque in the surface permanent magnet synchronous motor direct torque control system," in *2009 4th IEEE Conference on Industrial Electronics and Applications*, May 2009, doi: 10.1109/iciea.2009.5138554.
- [8] R. G. Shrivastava, S. S. Hadpe, S. B. Patil, R. S. Kadam, and M. P. Thakre, "Voltage Flicker Control in EAF Using P-Q Power Compensation Through STATCOM," in *Advances in Intelligent Systems and Computing*, Springer Nature Singapore, 2022, pp. 601–615, doi: 10.1007/978-981-16-7330-6_46.
- [9] Y. Li, D. Gerling, J. Ma, J. Liu, and Q. Yu, "The Comparison of Control Strategies for the Interior PMSM Drive used in the Electric Vehicle," *World Electric Vehicle Journal*, vol. 4, no. 3, pp. 648–654, Sep. 2010, doi: 10.3390/wevj4030648.
- [10] Z. Zhang and J. Shu, "Matlab-based permanent magnet synchronous motor vector control simulation," in *2010 3rd International Conference on Computer Science and Information Technology*, Jul. 2010, doi: 10.1109/iccisit.2010.5563610.
- [11] K. Huang, W. Peng, C. Lai, and G. Feng, "Efficient Maximum Torque Per Ampere (MTPA) Control of Interior PMSM Using Sparse Bayesian Based Offline Data-Driven Model With Online Magnet Temperature Compensation," *IEEE Transactions on Power Electronics*, vol. 38, no. 4, pp. 5192–5203, Apr. 2023, doi: 10.1109/tpe.2022.3230052.
- [12] Y. Li, M. Jian, Y. Qiang, and L. Jiangyu, "A Novel Direct Torque Control Permanent Magnet Synchronous Motor Drive used in Electrical Vehicle," *International Journal of Power Electronics and Drive Systems (IJPEDS)*, vol. 1, no. 2, Nov. 2011, doi: 10.11591/ijped.v1i2.141.
- [13] L. Y. L. Yaohua, L. Jingyu, M. J. M. Jian, and Y. Q. Y. Qiang, "A Simplified Voltage Vector Selection Strategy for Direct Torque Control," *TELKOMNIKA (Telecommunication Computing Electronics and Control)*, vol. 9, no. 3, Dec. 2011, doi: 10.12928/telkomnika.v9i3.746.
- [14] L. M. Masisi, S. Williamson, and P. Pillay, "A comparison between A 2-level and 3-level inverter for a permanent magnet synchronous motor drive under different inverter switching frequencies," in *2012 IEEE International Conference on Power Electronics, Drives and Energy Systems (PEDES)*, Dec. 2012, doi: 10.1109/pedes.2012.6484370.





- [15] M. P. Thakre, J. A. Gangurde, R. Shrivastava, D. P. Kadam, S. S. Kadlag, and H. S. Sonawane, "Investigative uses of overmodulation techniques in modular multilevel cascaded converter," *Bulletin of Electrical Engineering and Informatics*, vol. 11, no. 6, pp. 3147–3156, Dec. 2022, doi: 10.11591/eei.v11i6.3958.
- [16] P. Ramana, B. S. Kumar, K. A. Mary, and M. S. Kalavathi, "Comparison of various pwm techniques for field oriented control vs fed pmsm drive," *International Journal of Advanced Research in Electrical, Electronics and Instrumentation Engineering*, vol. 2, Jul. 2013.
- [17] P. Yunhao, Y. Dejun, and H. Yansong, "The stator flux linkage adaptive SVM-DTC control strategy of permanent magnet synchronous motor," in *2021 6th Asia Conference on Power and Electrical Engineering (ACPEE)*, Apr. 2021, doi: 10.1109/acpee51499.2021.9437101.
- [18] R. G. Shrivastava, D. R. Bhise, and P. Nagrale, "Comparative Analysis of FOC Based Three Level DCMLI Driven PMSM Drive," in *2019 International Conference on Innovative Trends and Advances in Engineering and Technology (ICITAET)*, Dec. 2019, doi: 10.1109/icitaet47105.2019.9170242.
- [19] M. Haris, M. K. Pathak, and P. Agarwal, "Comparison of SPWM multilevel inverter fed PMSM drive with two level inverter fed drive," in *International Conference on Recent Advances and Innovations in Engineering (ICRAIE-2014)*, May 2014, doi: 10.1109/icraie.2014.6909123.
- [20] S. Devabhaktuni and R. G. "Performance analysis of three-phase and five-phase inverters with different PWM strategies," in *2019 Innovations in Power and Advanced Computing Technologies (i-PACT)*, 2019, doi: 10.1109/i-pact44901.2019.8960210.
- [21] S. D. Lakshmi and S. Dasan, "Analysis of Newly Developed Third Harmonic Injection Method with Ovpwm Method for a PV System Connected Through 3-Level Diode Clamped Inverter to an Induction Motor," in *2018 International Conference on Current Trends towards Converging Technologies (ICCTCT)*, Mar. 2018, doi: 10.1109/icctct.2018.8551049.
- [22] M. Saeedian, J. Adabi, and S. M. Hosseini, "Cascaded multilevel inverter based on symmetric–asymmetric DC sources with reduced number of components," *IET Power Electronics*, vol. 10, no. 12, pp. 1468–1478, 2017, doi: 10.1049/iet-pel.2017.0039.
- [23] A. Taghvaie, J. Adabi, and M. Rezaejad, "A Self-Balanced Step-Up Multilevel Inverter Based on Switched-Capacitor Structure," *IEEE Transactions on Power Electronics*, vol. 33, no. 1, pp. 199–209, Jan. 2018, doi: 10.1109/TPEL.2017.2669377.
- [24] K. K. Gupta, A. Ranjan, P. Bhatnagar, L. K. Sahu, and S. Jain, "Multilevel Inverter Topologies With Reduced Device Count: A Review," *IEEE Transactions on Power Electronics*, vol. 31, no. 1, pp. 135–151, Jan. 2016, doi: 10.1109/TPEL.2015.2405012.
- [25] Z. Du, B. Ozpineci, L. M. Tolbert, and J. N. Chiasson, "DC–AC Cascaded H-Bridge Multilevel Boost Inverter With No Inductors for Electric/Hybrid Electric Vehicle Applications," *IEEE Transactions on Industry Applications*, vol. 45, no. 3, pp. 963–970, May 2009, doi: 10.1109/TIA.2009.2018978.

BIOGRAPHIES OF AUTHORS




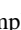


Dr. Rakesh Shrivastava     obtained Ph.D. Degree in Electrical Engineering specializing in Power Electronics and Drives from RTM Nagpur University, India in 2017. He occupied various positions to serve the Engineering Institutes for about 24 years. He is currently working as Professor at Department of Electrical Engineering, Matoshri College of Engineering and Research Center, Nashik. His research interests include the analysis and control of electrical drives, particularly in hybrid and electric vehicle applications. He has several publications in national and international journals. He attended International and National conferences and also worked as a jury member. He is a member of professional bodies such as ISTE and IAENG. He can be contacted at email: rakesh_shrivastava@rediffmail.com.






Dr. Mohan P. Thakre     received the B.Tech. and M. Tech degrees in Electrical Power Engineering from Dr. Babasaheb Ambedkar Technological University (Dr. BATU), Maharashtra, India, in 2009 and 2011 respectively, and the Ph.D. degree in Electrical Engineering from Visvesvaraya National Institute of Technology, (VNIT), Nagpur, Maharashtra, India in 2017. Currently, he is an Associate Professor at the Department of Electrical Engineering, SVERI's College of Engineering, Pandharpur, Maharashtra, India. His research interests include FACTS and power system protection. He can be contacted at email: mohanthakre@gmail.com.






Jagdish Choudhari     completed his Bachelor of Electrical Engineering and Master of Engineering in Electrical Power System from Government College of Engineering in 1999 and 2002 respectively. He has completed his Ph.D. in the area of Electrical Drives and Control in 2019 from Rashtrasant Tukadoji Maharaj Nagpur University. He has published 60 plus papers in National and International Journal and Conferences and granted 01 International and 01 National Patent. He is a member of LMISTE, MIE, QCFI and IAENG. He is working as Associate Professor and Head, Department of Electrical Engineering from June 2018 and Dean Academics from September 2022 at Nagpur Institute of Technology, Nagpur, Maharashtra (India). He can be contacted at email: jagdishchoudhari260878@gmail.com.






Dr. Sunil Somnath Kadlag    received B.E in Electrical Engineering from Dr. Babasaheb, Ambedkar, Marathwada University, Aurangabad (Dr B.A.M.U) in 1997 and M.E in Electrical Engineering (Control System) from Government College of Engineering Pune (Pune University) in 2005 and Ph.D. in Electrical Engineering from Suresh Gyan Vihar University Jaipur (Rajasthan) in 2021. His research area is electric vehicles. He is presently working as an Associate Professor and Head, of the Department of Electrical Engineering, Amrutvahini College of Engineering, Sangamner, Savitribai Phule Pune University, Pune, Maharashtra, India. He can be contacted at email: sunilkadlag5675@gmail.com.






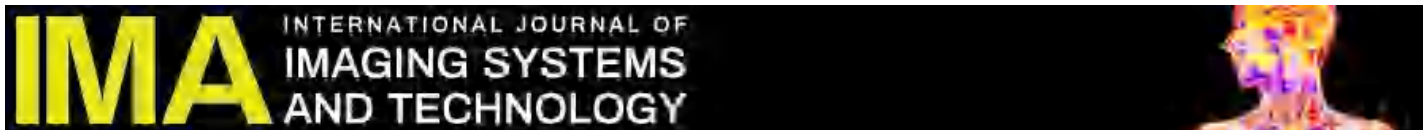
Dr. Rahul Mapari    received a bachelor's degree and master's degree in Electronics Engineering from Savitribai Phule Pune University, India, in 2004 and 2007 respectively, and a Ph.D. degree in Electronics and Telecommunication Engineering from Amravati University, India in 2016. He has a total of 17 years of experience in various reputed Technical Institutes. He is working as a Professor in the Department of Electronics and Telecommunication Engineering of Pimpri Chinchwad College of Engineering and Research, Pune since 2017. His research interests include power converters and power electronics. He can be contacted at email: rahul.mapari@pccoer.in.



Dr. Deepak Prakash Kadam    received a B.E from the Government College of Engineering, Amaravati, and M.E degrees in Electrical Power Systems from Walchand College of Engineering, Sangli, Maharashtra, India, in 1997 and 2005 respectively, and the Ph.D. degree in Electrical Engineering from Savitribai Phule Pune University, Pune Maharashtra, India in 2015. Currently, he is an Associate Professor at the Department of Electrical Engineering, Bhujbal Knowledge City, MET Institute of Engineering, Nashik, India. His research interests include renewable energy technology, power quality, and power system. His total teaching experience is around 23 years. He can be contacted at email: dpkadam@gmail.com.



Dr. Shridhar Khule    obtained Ph.D. Degree in Electrical Engineering specializing in power systems from Sant Gadge Baba Amravati University, Amravati, Maharashtra, India in 2021. He occupied various positions to serve engineering institutes for about 20 years. He is currently working as Professor in the Electrical Engineering Department of Matoshri College of Engineering and Research Center, Nashik. His research interests power system. He attended International and National conferences. He is a member of professional bodies such as ISTE and IET. He can be contacted at email: shridhar.khule@matoshri.edu.in.



RESEARCH ARTICLE

Multi-level deep learning based lung cancer classifier for classification based on tumour-node-metastasis approach

Swati P. Pawar , Sanjay N. Talbar

First published: 05 December 2022

<https://doi.org/10.1002/ima.22835>

 **Get access to the full version of this article. View access options below.**

Institutional Login



Access through your institution

Log in to Wiley Online Library

If you have previously obtained access with your personal account, please log in.

Log in

Purchase Instant Access

48-Hour online access | **\$12.00**
[Details](#) 

Online-only access | **\$20.00**
[Details](#) 

 **PDF download and online access**

\$49.00

[Details](#)



[Check out](#)

Abstract

Treatment of non-small cell lung cancer depends on detecting the cancer stage. The oncologist decides the cancer stage based on the tumour-node-metastasis (TNM) staging suggested by the American Joint Committee on Cancer (AJCC). This study simplifies the complicated problem of classifying computed tomography (CT) images into TNM-based classes using deep learning algorithms at various levels. In the first level, an optimised conditional generative adversarial network (c-GAN) network is developed for automatic lung segmentation, including nodules within the lung and juxtapleural nodules. Earlier studies used time-consuming manual identification of the region of interest patches from the lung CT image before applying the deep learning classification algorithm. At the next level, three different deep learning algorithms, along with three support vector machine classifiers, are used for the classification of Tumour, Node and Metastasis as per the AJCC staging nomenclature. The specially designed c-GAN network's performance is maximised using the Taguchi approach, which helps automatically preprocess CT images by removing unwanted background noises. Further, three different pre-trained Resnet50 networks are trained using transfer learning for extracting the deep features for finally applying to three different classifiers, resulting in three different classes. The comparative segmentation performance assessment in the form of the average dice similarity coefficient and Jaccard index indicates that the proposed c-GAN gives the best segmentation performance of the lung without losing the nodule compared to other segmentation algorithms. The proposed approach gives the classification performance for the Tumour as 91.94%–97.32%, the Nodule as 91.99%–100%, and the Metastasis as 99.25%–100.00%.

[Open Research](#)



DATA AVAILABILITY STATEMENT

The data that support the findings of this study are openly available in “The Cancer Imaging Archive (TCIA)” database at

<https://wiki.cancerimagingarchive.net/pages/viewpage.action?pageId=70224216> reference number.^{32, 33}

REFERENCES

1 Edge SB, Compton CC. The American joint committee on cancer: the 7th edition of the AJCC cancer staging manual and the future of TNM. *Ann Surg Oncol*. 2010; **17**: 1471-1474.

[PubMed](#) | [Web of Science®](#) | [Google Scholar](#)

2 Detterbeck FC. The eighth edition TNM stage classification for lung cancer: what does it mean on main street? *J Thorac Cardiovasc Surg*. 2018; **155**(1): 356-359.

[PubMed](#) | [Web of Science®](#) | [Google Scholar](#)

3 Rolke HB, Bakke PS, Gallefoss F. Delays in the diagnostic pathways for primary pulmonary carcinoma in southern Norway. *Respir Med*. 2007; **101**(6): 1251-1257.

[PubMed](#) | [Web of Science®](#) | [Google Scholar](#)

4 Byrne SC, Barrett B, Bhatia R. The impact of diagnostic imaging wait times on the prognosis of lung cancer. *Can Assoc Radiol J*. 2015; **66**(1): 53-57. Theme Issue: Thoracic and Cardiac Imaging.

[PubMed](#) | [Web of Science®](#) | [Google Scholar](#)

5 Naik A, Edla DR. Lung nodule classification on computed tomography images using deep learning. *Wirel Pers Commun*. 2021; **116**: 655-690.

[Web of Science®](#) | [Google Scholar](#)

6 Cheng JZ, Ni D, Chou YH, et al. Computer-aided diagnosis with deep learning architecture: applications to breast lesions in US images and pulmonary nodules in CT scans. *Sci Rep*. 2016; **6**: 24454.

[CAS](#) | [PubMed](#) | [Web of Science®](#) | [Google Scholar](#)

7 Liu K, Kang G. Multiview convolutional neural networks for lung nodule classification. *Int J Imaging Syst Technol.* 2017; **27**(1): 12-22.

[Web of Science®](#) | [Google Scholar](#)

8 da Silva GLF, da Silva NOP. Lung nodules diagnosis based on evolutionary convolutional neural network. *Multimed Tools Appl.* 2017; **76**: 19039-19055.

[Web of Science®](#) | [Google Scholar](#)

9 Dey R, Lu Z, Hong Y. Diagnostic classification of lung nodules using 3D neural networks. 2018 IEEE 15th International Symposium on Biomedical Imaging (ISBI 2018). 2018. 774–778.

[Google Scholar](#)

10 Zhao X, Liu L, Qi S, Teng Y, Li J, Qian W. Agile convolutional neural network for pulmonary nodule classification using CT images. *Int J CARS.* 2018; **13**: 585-595.

[Web of Science®](#) | [Google Scholar](#)

11 Xie Y, Zhang J, Xia Y, Fulham M, Zhang Y. Fusing texture, shape and deep model-learned information at decision level for automated classification of lung nodules on chest CT. *Inf Fusion.* 2018; **42**: 102-110.

[Web of Science®](#) | [Google Scholar](#)

12 Xie Y, Zhang J, Xia Y. Semi-supervised adversarial model for benign-malignant lung nodule classification on chest CT. *Med Image Anal.* 2019; **57**: 237-248.

[PubMed](#) | [Web of Science®](#) | [Google Scholar](#)

13 Shakeel PM, Burhanuddin MA, Desa MI. Lung cancer detection from CT image using improved profuse clustering and deep learning instantaneously trained neural networks. *Measurement.* 2019; **145**: 702-712.

[Web of Science®](#) | [Google Scholar](#)

14 Priya M, Jawhar D, Geisa D. Optimal deep belief network with opposition based pity beetle algorithm for lung cancer classification: A DBNOPBA approach. *Comput Methods Prog Biomed.* 2021;

199:105902.

[PubMed](#) | [Web of Science®](#) | [Google Scholar](#)

15 Kasinathan G, Jayakumar S, Gandomi AH, Ramachandran M, Fong SJ, Patan R. Automated 3-D lung tumor detection and classification by an active contour model and CNN classifier. *Expert Syst Appl.* 2019; **134**: 112-119.

[Web of Science®](#) | [Google Scholar](#)

16 Lakshmanaprabu SK, Mohanty SN, Shankar K, Arunkumar N, Ramirez G. Optimal deep learning model for classification of lung cancer on CT images. *Futur Gener Comput Syst.* 2019; **92**: 374-382.

[Web of Science®](#) | [Google Scholar](#)

17 Halder A, Chatterjee S, Dey D, Kole S, Munshi S. An adaptive morphology based segmentation technique for lung nodule detection in thoracic CT image. *Comput Methods Prog Biomed.* 2020; **197**:105720.

[PubMed](#) | [Web of Science®](#) | [Google Scholar](#)

18 Nanglia P, Kumar S, Mahajan AN, Singh P, Rathee D. A hybrid algorithm for lung cancer classification using SVM and neural networks. *ICT Express.* 2021; **7**: 335-341.

[Web of Science®](#) | [Google Scholar](#)

19 Tiwari L, Raja R, Awasthi V, et al. Detection of lung nodule and cancer using novelMask-3 FCM and TWEDLNN algorithms. *Measurement.* 2021; **172**:108882.

[Web of Science®](#) | [Google Scholar](#)

20 MohanaPriya R, Venkatesan P. An efficient image segmentation and classification of lung lesions in pet and CT image fusion using DTWT incorporated SVM. *Microprocess Microsyst.* 2021; **82**:103958.

[Web of Science®](#) | [Google Scholar](#)

21 Sünnetci KM, Alkan A. Lung cancer detection by using probabilistic majority voting and optimization techniques. *Int Nat J Imag Syst Technol.* 2022; **32**(6): 2049-2065.

[Web of Science®](#) | [Google Scholar](#)

22 Kirienko M, Sollini M, Silvestri G, et al. Convolutional neural networks promising in lung cancer T-parameter assessment on baseline FDG-PET/CT. *Contrast Media Mol Imaging*. 2018; **2018**:1382309.

[PubMed](#) | [Web of Science®](#) | [Google Scholar](#)

23 Zhao X, Wang X, Xia W, et al. A cross-modal 3D deep learning for accurate lymph node metastasis prediction in clinical stage T1 lung adenocarcinoma. *Lung Cancer*. 2020; **145**: 10-17.

[PubMed](#) | [Web of Science®](#) | [Google Scholar](#)

24 Moitra D, Mandal R. Classification of non-small cell lung cancer using one-dimensional convolutional neural network. *Expert Syst Appl*. 2020; **159**:113564.

[Web of Science®](#) | [Google Scholar](#)

25 Isola P, Zhu JY, Zhou T, Efros AA. Image-to-image translation with conditional adversarial networks. *2017 IEEE Conference on Computer Vision and Pattern Recognition (CVPR)*. IEEE; 2017: 5967-5976.

[Google Scholar](#)

26 Ulyanov D, Vedaldi A, Lempitsky VS. Instance Normalization: The Missing Ingredient for Fast Stylization. *2016 IEEE Conference on Computer Vision and Pattern Recognition (CVPR)*. 2016.

[Google Scholar](#)

27 Roy RK. *Design of Experiments Using the Taguchi Approach: 16 Steps to Product and Process Improvement*. Wiley; 2001.

[Google Scholar](#)

28 Dice LR. Measures of the amount of ecologic association between species. *Ecology*. 1945; **26**: 297-302.

[Web of Science®](#) | [Google Scholar](#)

29 Jaccard P. Distribution comparee de la flore alpine dans quelques regions des Alpes occidentales et orientales. *Bull Soc Vaud Sci Nat.* 1901; **37**: 241-272.

[Google Scholar](#)

30 He K, Zhang X, Ren S, Sun J. Deep Residual Learning for Image Recognition. 2016 IEEE Conference on Computer Vision and Pattern Recognition (CVPR). 2016. 770–778.

[Google Scholar](#)

31 Sethy PK, Barpanda NK, Rath AK, Behera SK. Deep feature based rice leaf disease identification using support vector machine. *Comput Electron Agric.* 2020; **175**:105527.

[Web of Science®](#) | [Google Scholar](#)

32 Li P, Wang S, Li T, Lu J, HuangFu Y, Wang D. A large-scale CT and PET/CT dataset for lung cancer diagnosis. *Cancer Imaging Arch.* 2017; **76**: 19039-19055.

[Google Scholar](#)

33 Clark K, Vendt B, Smith K, et al. The cancer imaging archive (TCIA): maintaining and operating a public information repository. *J Digit Imaging.* 2013; **26**(6): 1045-1057.

[PubMed](#) | [Web of Science®](#) | [Google Scholar](#)

34 Hosseini-Asl E, Zurada JM, Gimelfarb G, El-Baz A. 3-D lung segmentation by incremental constrained nonnegative matrix factorization. *IEEE Trans Biomed Eng.* 2016; **63**(5): 952-963.

[PubMed](#) | [Web of Science®](#) | [Google Scholar](#)

35 Ronneberger O, Fischer P, Brox T. U-net: convolutional networks for biomedical image segmentation. In: N Navab, J Hornegger, WM Wells, AF Frangi, eds. *Medical Image Computing and Computer-Assisted Intervention – MICCAI 2015*. Springer International Publishing; 2015: 234-241.

[Google Scholar](#)

36 Paing M, Choomchuay S. Classification of Margin Characteristics from 3D Pulmonary Nodules. Proceedings of the 2017 10th Biomedical Engineering International Conference Hokkaido, Japan. IEEE; 2017. 1–5.

[Google Scholar](#)

37 Ma J, Wang Q, Ren Y, Hu H, Zhao J. Automatic Lung Nodule Classification with Radiomics Approach. Proceedings of the Medical Imaging 2016: PACS and Imaging Informatics: Next Generation and Innovations. San Diego, CA, USA; 2016. 978906.

[Google Scholar](#)

[Download PDF](#)

ABOUT WILEY ONLINE LIBRARY

[Privacy Policy](#)
[Terms of Use](#)
[About Cookies](#)
[Manage Cookies](#)
[Accessibility](#)

[Wiley Research DE&I Statement and Publishing Policies](#)
[Developing World Access](#)

HELP & SUPPORT

[Contact Us](#)
[Training and Support](#)
[DMCA & Reporting Piracy](#)

OPPORTUNITIES

[Subscription Agents](#)
[Advertisers & Corporate Partners](#)

CONNECT WITH WILEY

[The Wiley Network](#)
[Wiley Press Room](#)

Copyright © 1999-2024 John Wiley & Sons, Inc or related companies. All rights reserved, including rights for text and data mining and training of artificial technologies or similar technologies.

[The Imaging Science Journal >](#)

Volume 70, 2022 - Issue 7

91 | 0

Views | CrossRef citations to date | Altmetric

0

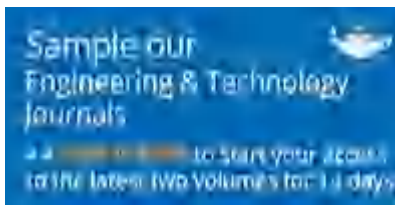
Research Articles

Maximization of lung segmentation of generative adversarial network for using taguchi approach

Swati P. Pawar & Sanjay N. Talbar

Pages 473-482 | Received 30 Dec 2020, Accepted 20 Jan 2023, Published online: 02 Feb 2023

Cite this article

<https://doi.org/10.1080/13682199.2023.2172525>

Full Article

Figures & data

References

Citations

Metrics

Reprints & Permissions

Read this article

ABSTRACT

Conditional generative adversarial network (c-GAN) is one of the best-performing convolutional neural networks (CNN) for the segmentation of lung computed tomography (CT). However, lung segmentation from CT images becomes complicated in the presence of various dense abnormalities. The performance in the presence of dense abnormalities can be improved by tuning the c-GAN architecture and parameters of the network. This study focuses on maximizing lung segmentation performance of a c-GAN segmentation algorithm by configuring and tuning the network using the Taguchi

[Home](#) ▶ [All Journals](#) ▶ [The Imaging Science Journal](#) ▶ [List of Issues](#) ▶ [Volume 70, Issue 7](#)

▶ [Maximization of lung segmentation of gen ...](#)

dataset for evaluating the performance of the proposed approach. The comparative performance analysis of the proposed algorithm shows that the proposed algorithms outperform the existing state-of-the-art methods, even in the presence of dense abnormalities in lung CT scans. Furthermore, the proposed approach has been demonstrated for lung segmentation in the presence of large nodules.

Q KEYWORDS: [Computer-aided diagnosis](#) [conditional generative adversarial network](#) [taguchi approach](#) [lung CT scan](#) [lung segmentation](#) [optimal design of CNN](#) [interstitial lung disease \(ILD\)](#) [lung nodule](#)

Disclosure statement

No potential conflict of interest was reported by the author(s).

[◀ Previous article](#)

[View issue table of contents](#)

[Next article ▶](#)

Log in via your institution

▶  [Access through your institution](#)

Log in to Taylor & Francis Online

▶ [Log in](#)

Restore content access

▶ [Restore content access for purchases made as guest](#)

Purchase options *

[Save for later](#)

[Home](#) ▶ [All Journals](#) ▶ [The Imaging Science Journal](#) ▶ [List of Issues](#) ▶ [Volume 70, Issue 7](#)

▶ [Maximization of lung segmentation of gen](#)

- 48 hours access to article PDF & online version
- Article PDF can be downloaded
- Article PDF can be printed

USD 61.00

 Add to cart

Issue Purchase

- 30 days online access to complete issue
- Article PDFs can be downloaded
- Article PDFs can be printed

USD 305.00

 Add to cart

* Local tax will be added as applicable

Related Research

Recommended articles

Cited by

[A corneal ulcer segmentation approach using U-Net and stepwise fine-tuning](#) >

Helano M. B. F. Portela et al.

Computer Methods in Biomechanics and Biomedical Engineering: Imaging & Visualization

Published online: 27 Aug 2023

[Left atrium MRI image segmentation using efficient Xception stochastic depth based generative adversarial network](#) >

Anupama Bhan et al.

International Journal of Healthcare Management

Published online: 21 Jan 2023

[Imbalanced medical disease dataset classification using enhanced generative adversarial network](#) >

[Home](#) ▶ [All Journals](#) ▶ [The Imaging Science Journal](#) ▶ [List of Issues](#) ▶ [Volume 70, Issue 7](#)
▶ [Maximization of lung segmentation of gen](#)

Computer Methods in Biomechanics and Biomedical Engineering

Published online: 2 Nov 2022

[View more](#)

[Home](#) ▶ [All Journals](#) ▶ [The Imaging Science Journal](#) ▶ [List of Issues](#) ▶ [Volume 70, Issue 7](#)
▶ [Maximization of lung segmentation of gen ...](#)

- [Authors](#)
- [R&D professionals](#)
- [Editors](#)
- [Librarians](#)
- [Societies](#)
- [Opportunities](#)
- [Reprints and e-prints](#)
- [Advertising solutions](#)
- [Accelerated publication](#)
- [Corporate access solutions](#)

- [Open Access](#)
- [Overview](#)
- [Open journals](#)
- [Open Select](#)
- [Dove Medical Press](#)
- [F1000Research](#)
- [Help and information](#)
- [Help and contact](#)
- [Newsroom](#)
- [All journals](#)
- [Books](#)

Keep up to date

Register to receive personalised research and resources by email

 [Sign me up](#)

Copyright © 2024 Informa UK Limited [Privacy policy](#) [Cookies](#) [Terms & conditions](#)


Taylor & Francis Group

[Accessibility](#)

Registered in England & Wales No. 3099067
5 Howick Place | London | SW1P 1WG



Contents lists available at ScienceDirect

Expert Systems With Applications

journal homepage: www.elsevier.com/locate/eswa

Securing trustworthy evidence for robust forensic cloud-blockchain environment for immigration management with improved ECC encryption

Sahadev Maruti Shinde^{a,1,*}, Venkateswara Rao Gurrala^b

^a Research Scholar, Department of Computer Science and Engineering, GITAM School of Technology, GITAM (Deemed to be University), Visakhapatnam, Andhra Pradesh, India and Assistant Professor, SVERI's College of Engineering, Pandharpur, MH, India

^b Professor, Department of Computer Science and Engineering, GITAM School of Technology, GITAM (Deemed to be University), Visakhapatnam, Andhra Pradesh, India

ARTICLE INFO

Keywords:

Cloud
Blockchain
Improved ECC
Public key
CAHSACM scheme

ABSTRACT

At present in this digitalized era, the passport is still a substantial thing. It is taken at every place together with other journey-related ID like Immigration stamps and VISA, which are also an element of a passport. In this research, a novel forensic method is developed for privacy-preserved management of migration in cloud-assisted blockchain networks. The decentralized model of blockchain made public ledger tampering a chief problem. The conservation of confidentiality is the main demand in legal forensics. The developed approach adapts appropriate techniques for conserving anonymity and confidentiality, which assured that no private data, is disclosed throughout the blockchain-based procedure derivation function. The technique integrated six stages, like "Initialization phase, Log File collection phase, Key generation and management, partial proof generation, certificate and file encryption, adding encryption proofs on public key infrastructure, proof verification by cloud forensic investigator". As a new thing, we choose the public keys optimally via Combined Archimedes and Hunger Games Search Algorithm with Cauchy's Mutation (CAHSACM). In addition, "improved Elliptical curve cryptography (IECC) based encryption" is done to authenticate the data. At last, the improvements of CAHSACM are proven using varied analyses.

1. Introduction

Nowadays, the procedure of receiving a VISA and passport is still mainly paper-oriented. The procedure to apply for a passport and other voyage ID like VISA has a lot of recurring processes and necessitates documents that require to be surrendered numerous times for confirmation. Actually, in numerous scenarios, applying for a diverse VISA to a similar nation also insists to pursue a similar procedure that was done for a previous VISA (Park et al., 2017; Dasaklis et al., 2020; Irfan et al., 2016). Throughout travel, citizens stand by in long queues to get their migration checks finished owing to the paper-oriented stamping procedure. At all times, there is a huge annoy concern if the ID is missed or the information in the passport is compromised or incorrect (Manoj & Bhaskari, 2016; Battistoni et al., 2016; Pourvahab & Ekbatanifard, 2019). In general, the troubles citizens face for their journey are the longer postponements in getting their voyage ID ready. The present procedure is ineffective, time-consuming and susceptible to errors as it

entails 3rd party and paper-oriented authentication made manually (Irfan et al., 2015; Zawoad et al., 2015; Kent et al., 2006) (see Fig. 1).

Owing to classy technology, an increase in the need for a cloud paradigm amid organizations, administration, and every conclusion resulted in safety concerns (Rama Krishna, 2021; Wang, 2021; Michael Mahesh, 2020). In the cloud, the receptive data of a person become vulnerable to attacks (Park et al., 2017; Patel et al., 2020). Cloud services are developing and had turned into an effectual case to resolve cloud forensics for averting illegitimate and suspicious tasks (Manoj & Bhaskari, 2016; Stelly & Roussev, 2017). An extraordinary group is implemented for determining these attacks in the cloud paradigm, known as cloud forensics (Jain, 2020; Pourvahab & Ekbatanifard, 2019; Dalezios et al., 2020; Stelly & Roussev, 2017). The tasks done by users in the cloud have to gather logs. The acts of users could be tracked by means of the action logs in the cloud. Therefore, the researcher relies on CSP to collect logs (Patel & Mistry, 2018; Duy et al., 2019; Santra et al., 2018; Dasaklis et al., 2020; Patel et al., 2020). The forensic approach is developed for SDN-aided IoT with blockchain (Irfan et al., 2016; Patel

* Corresponding author at: Department of Computer Science and Engineering, GITAM School of Technology, GITAM (Deemed to be University), Visakhapatnam, Andhra Pradesh, India.

E-mail address: sahadevmaruti@gmail.com (S.M. Shinde).

¹ ORCID: 0000-0003-2744-0164.

<https://doi.org/10.1016/j.eswa.2023.120478>

Received 13 July 2022; Received in revised form 2 March 2023; Accepted 3 March 2023

Available online 12 May 2023

0957-4174/© 2023 Elsevier Ltd. All rights reserved.

Nomenclature			
Abbreviation	Description	DHO	Deer Hunting Optimization
AOA	Archimedes Optimization Algorithm	FCS	Fuzzy-Based Smart Contracts
AES	Advanced Encryption Standard	HGC	Hunger Games Search
BlockSLaaS	Block Chain Assisted Secure Logging As- A-Service	HSO	Harmony Search Optimization
CAHSACM	Combined Archimedes and HGS Algorithm with Cauchy's Mutation	IECC	Improved Elliptical Curve Cryptography
CC	Cloud Computing	IoT	Internet Of Things
CSP	Cloud Service Provider	LGoE	Logical Graph Of Evidence
CA	Certificate Authority	LA	Lion Algorithm
CFI	Cloud Forensic Investigator	PRO	Poor Rich Optimization
CADF	Cloud Auditing Data Federation	RSA	Rivest-Shamir-Adleman
CSC	Cloud Service Customer	ROA	Rider Optimization
CS	Cloud Server	SA-DECC	Sensitivity Aware Deep ECC
DMTF	Distributed Management Task Force's	SSO	Shark Smell Optimization
		SDN	Software-Defined Networking
		SRVA	Secure Ring Verification-Based Authentication
		WT	Walsh Transform

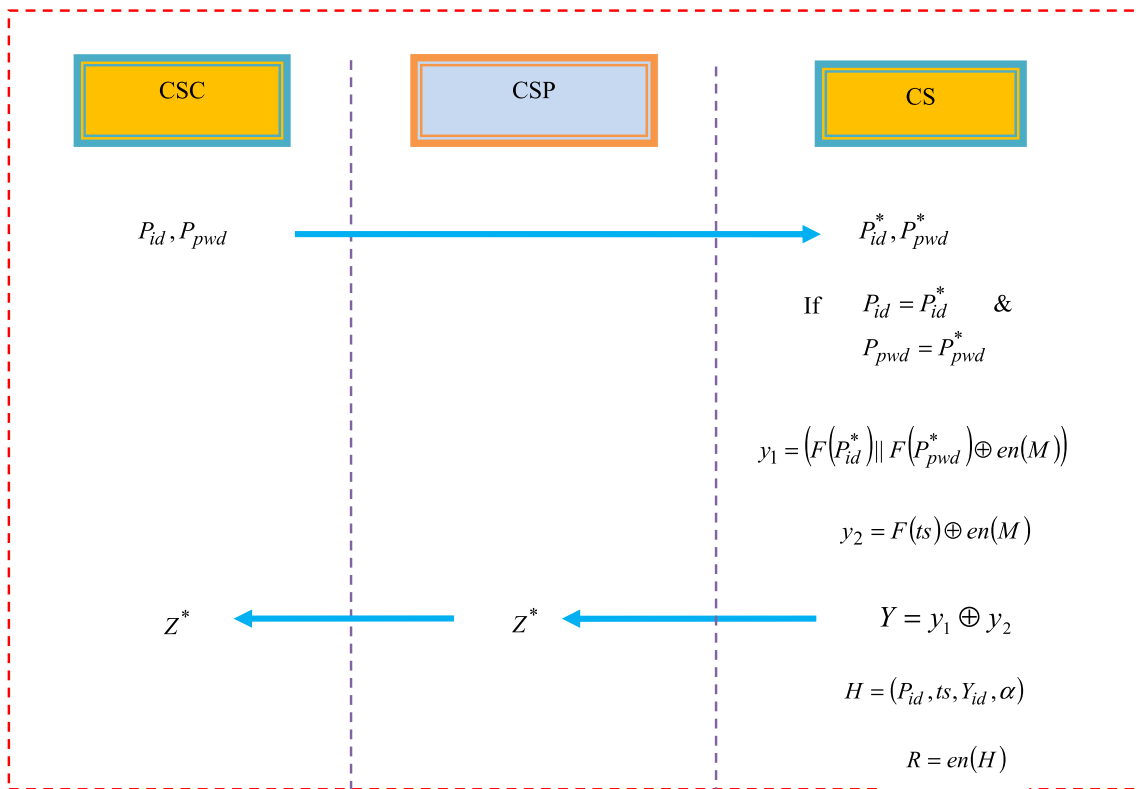


Fig. 1. Log file creation stage.

et al., 2020). Cloud forensics is a part of forensic science, which encompassed the investigation and recovery of materials determined in the cloud paradigm to assess misdeeds (Ma et al., 2019; Pasquale et al., 2016; Xia et al., 2017; Ashok Kumar & Vimala, 2020; Wang et al., 2018).

A variety of schemes to facilitate data reliability in which the blockchain, namely the ledger is developed as a system to facilitate reliability (Pasquale et al., 2016; Xia et al., 2017; Pourvahab & Ekbatanifard, 2019). NIST describes CC as cloud forensic, which entail technical standard and practices and portrays verified schemes to reconstruct previous CC events. The authorized process is done in “collection, identification, examination, preservation, interpretation, and reporting”. An emerging field of cloud computing and digital forensics is cloud forensics. Although it is a type of application in digital forensics, the environment is changing. But that creates a lot of

difficulties when conducting forensics in a cloud setting. The preservation and recreation of historical events are the ultimate goals (Patel & Mistry, 2018; Wang et al., 2018; Ma et al., 2019; Guo et al., 2019). The blockchain method (Ashok Kumar & Vimala, 2020; Wang et al., 2018) is used as a logging service for handling and accumulating logs whilst dealing with issues on numerous stakeholders, logs confidentiality, and integrity. The digital forensics procedure uses a blockchain technique to secure forensic data in terms of performance and transparency. As the blockchain keeps its data at multiple nodes throughout the world, the system would be decentralized. This system's data would be unchangeable because it is impossible to alter data that is contained in Blockchain. Most importantly, it would be seamless since there would be no single point of failure and data redundancy at every node, ensuring high availability of the data entered into the system. (Patel et al., 2020;

Maesa et al., 2019; Dagher et al., 2018; Lin et al., 2018; Abhay et al., 2020; Shahbazi & Byun, 2022).

In forensics, hash functions are employed to construct the digest and preserve the integrity of the data assets. However, the primary emphasis of applications connected to cloud forensics is on data validation and hard drive integrity. The experience of the investigators will determine the cloud forensic strategy. The cloud forensic system from (Abhay et al., 2020) keeps a record of immigrants by preserving a variety of relevant data in the form of immutable and exclusive recordings in Blockchain. The forensic integration of NLP techniques (Shahbazi & Byun, 2022) with blockchain secures the collected dataset with limited access to avoid hacking or attack. However, these conventional cloud forensic technique based on blockchain schemes faces problems in trustworthiness, integrity, improved provenance, scalability, and availability. By harnessing the benefits of Blockchain technology, this study intends to resolve these issues by providing a ledger system that can track each immigration and emigration that occurs in the nation. This study proposes a log integrity conservation model and optimal public key blockchain-based safeguarding the forensic evidence.

The contribution is as follows:

1. Employs phases including setup phase, logfile collection phase, key management phase, certifying and verifying phase, and proof of verification phase.
2. Develops a log integrity conservation model, where, optimal public keys are chosen using the CAHSACM method.
3. Deploys improved ECC for ensuring the encryption phase.

The paper is sorted as: Section 2 analyses the work. Section 3 explains the developed log integrity preservation method and section 4 described optimal key generation via the CAHSACM algorithm. Sections 5 and 6 depict results and conclusion.

2. Literature review

2.1. Related works

Panchamia and Byrappa (2017) devised a new technique with the idea of digitizing VISA, Passport, and migration ID. Digitizing VISA and Passports helped in simplifying and streamlining VISA and Passport validation, renewing, issuing, authentication, and revoking processes. For this procedure, a solution depending upon distributed ledger was proposed for retrieving and storing data. After implementation, this system helped with finding false VISA and passports, and repetitive and illegal data confirmation procedures. Blockchain-based execution solved numerous issues related to paper-based verification and improved effectiveness and lowered costs at every level.

Patel and Mistry (2018) proposed a system using the blockchain technique for creating scalable, secured, and decentralized immigration records of persons. Here, "Ethereum blockchain and proof of work were utilized as consensus algorithm". The process of illegal immigration was mitigated by keeping a unique and absolute record of migration state and individual information of a person to ensure their legitimacy. The anticipated scheme not only helped to ensure illegal migration but permitted to ensure that a person has productively arrived at the planned end.

Patel et al. (2020) proposed a system using the blockchain technique for creating scalable, secured, and decentralized arrival and departure records of travelers. A framework was provided by means of "Hyper ledger fabric", to maintain the inter port records of travellers exit and entry in a nation and to assist gateless entrance back to the travellers nation. The legal and privacy concerns over biometric data storage were mitigated on the blockchain. The prospect of modifying the extant kiosk was also explored with blockchain design at the back end; as a result, the travelers were not necessarily recognizable with a novel process.

Rane and Dixit (2019) devised forensic-based BlockSLaaS for

Table 1

The strength and weaknesses of the existing approaches.

Author	Strength	Weakness
Panchamia and Byrappa (2017)	<ul style="list-style-type: none"> Find repetitive and illegal data Improved effectiveness and lower costs 	<ul style="list-style-type: none"> Lack of interoperability Implementation cost is high
Patel and Mistry (2018)	<ul style="list-style-type: none"> Create scalable, secured, and decentralized immigration records 	<ul style="list-style-type: none"> Data Immutability Limited availability of technical talent
Patel et al. (2020)	<ul style="list-style-type: none"> The legal and privacy concerns over biometric data storage were mitigated 	<ul style="list-style-type: none"> Integration with legacy systems No transparency
Rane and Dixit, (2019)	<ul style="list-style-type: none"> Solve multi-stakeholder complicity problem Provide better integrity and confidentiality 	<ul style="list-style-type: none"> Need more standardization Available very limited technical talent
Jain, (2020)	<ul style="list-style-type: none"> Preserve reliability of log files Transform centralized storage systems into the decentralized storage system 	<ul style="list-style-type: none"> Cannot maximize CSP
Pourvhab and Ekbatanifard (2019)	<ul style="list-style-type: none"> Preserve the system from illegal users Strengthen cloud paradigm using private keys 	<ul style="list-style-type: none"> Struggling to authenticate when appropriate logs were provided by the CSP Utilize more energy
Dalezios et al., (2020)	<ul style="list-style-type: none"> Enhanced apache cloud stack platform to become forensic reverberation 	<ul style="list-style-type: none"> Time-consuming Proof of work demands works on the users' and their devices' parts.
Stelly and Roussev (2017)	<ul style="list-style-type: none"> Addresses the huge data volumes in the digital forensic study 	<ul style="list-style-type: none"> Issue in immutability Have privacy and security risk
Patil, et al., (2021)	<ul style="list-style-type: none"> Have secured forensic evidence system Enhanced integrity, traceability, and immutability improve the security of the evidence 	<ul style="list-style-type: none"> Lack of Regulatory Support
Shahbazi and Byun (2022)	<ul style="list-style-type: none"> Prevent network attacks and hacking 	<ul style="list-style-type: none"> Sustainability of centralized records in non-state entities

gradually processing and storing logs by dealing with the multi-stakeholder complicity problems and assisting integrity and confidentiality. The CFI was able for accessing logs to investigate forensics using BlockSLaaS, which secluded the confidentiality of logs. Nevertheless, the technique fails to authenticate if the CSP offered accurate logs.

Jain (2020) devised blockchain techniques to preserve the reliability of log files. The blockchain and IPFS technologies were united to transform centralized storage systems into decentralized storage systems. Here, the reliability of the log files was conserved by storing log files in the blockchain. In the blockchain, each one consisted hash of the original data and the previous block, and then created a hash for the subsequent block. A system was used to store massive log files with the least gas value and transactional cost. Nevertheless, the technique was unsuccessful in maximizing the expectation of CSP by reducing the dependency on CSPs.

Pourvhab and Ekbatanifard (2019) devised the SRVA system to preserve the system from illegal users. To strengthen the cloud paradigm, the private keys were created by using HSO optimally. Here, the information was encrypted by means of sensitivity in the server. To carry out encryption, the SA-DECC model was created. The technique allowed the user to trace data by using FCS. Eventually, studies of evidence were done by creating LGoE collected with blockchain.

Dalezios et al. (2020) devised DMTF with CADF model for cloud forensic. Accordingly, CADF event logging was deployed in "Open Stack and has enhanced the Apache Cloud Stack platform" to become forensic reverberation.

Stelly and Roussev (2017) devised a technique, i.e. automatic

container employment and orchestration platform to attain eminent performances in digital forensics. The outcomes exposed that distributed container-oriented technique has shown a possible infrastructural base to address the huge data volumes in the digital forensic study.

Patil et al. (2021) established a chain of skilled users responsible for forensic inquiry, and a secure forensic evidence system had been developed to accomplish optimization. Blockchain technology is created on the private Ethereum platform. Implementing forensic evidence on the Ethereum platform, which had great integrity, traceability and immutability improves the security of the evidence. To obtain criminological reports, this framework was used. Each hub's refreshes were visible to the director hub. Whenever a new report was added to the chain, an exceptional hash was generated using cryptographic principles. When a report was added to the first square, if the other hub tried to transfer it, the report applied to the entire chain.

Shahbazi and Byun (2022) investigated Natural language processing (NLP) methods and the blockchain framework for digital forensics. Data collection analysis, representations of each phase, the vectorization phase, feature selection, and classifier evaluation were the key uses of NLP in this procedure. This system's implementation of a blockchain approach encrypts the data information to prevent network attacks and hacking. Through the use of a real-world dataset, the system's potential was revealed. Table 1. depicts the strength and weaknesses of the existing approaches.

2.2. Problem gap

The most important related crisis with the existing technique of exit/entry is the centralized data nature, building it into a simple target of attacks and its exploitation may lead to partial or complete loss of data. With the massive amount of kiosks authenticating data and entering information into this central database, it would be devastating if safety errors are found in the network. Finally, the exit/entry records are forever susceptible to adaptation either by malevolent 3rd parties or owing to interior opinionated pressures, etc. This information should be indisputable. The inter-communication amid numerous ports of entry of a nation with a centralized database is moreover a severe reason for concern regarding scalability and security. Aside from safety concerns, a simpler lapse in recording/stamping of data may cause an individual to an unacceptable applicant into a nation with no entrance record and with no means of departing the country. This is particularly factual as a lot of countries rely on a passport stamp to authenticate arrival, occasionally vis-a-vis sustaining a centralized proof (Park et al., 2017).

The main drawbacks of the existing approaches include the inability to maximize CSP expectations by lowering CSP dependence, failure to authenticate if the CSP provided accurate logs, the feasibility of nations not sustaining centralized records, lacking trustworthiness and integrity, and more. Thus the implementation of the proposed approach avoids the above-mentioned drawbacks of extant models. The next section provides a detailed description of our proposed approach.

3. Developed log integrity preservation method

In the cloud, the usability of log files for digital forensics is discovered using the developed integrity conservation technique depending upon the infrastructure of the public key. The adopted scheme contained diverse entities and involved a variety of stages by means of safety functions, like "encryption, decryption, hashing, and Walsh transform". Certain units entailed in the forensic analysis procedure are depicted in the setup stage. At the log file creation stage, the server created the log file depending on the user ID, time stamp, CSP ID, and services presented to users. The 3rd stage is the key management stage, wherein, the shared data between CFI and CA is produced by CA, while the key deployed for sharing amid the CFI and server entity is created by the server. At the encryption and certification stage, the CA created the certificate by means of "polynomial factor, Walsh transform, and the file associated

Table 2

Symbol description of proposed multi-level and mutual log integrity preservation method.

Symbol	Description
Z	Shared key of CSP and CSC
P_{pwd}	User Password
P_{id}	User ID
F	Hashing
p_{uk}	Public key
Y_{id}	CSP ID
R	Stored log file
H	Log file
en	Encryption
U_{id}	CFI ID
Z_T	Shared key of CFI and CA
m	Random number
ts	Timestamp
de	Decryption
U_{pwd}	CFI password
B	Mutual verified message
A	Request message
Q	Encrypted certificate
D	Certificate
Z_S	Shared key of CSC and CFI
IP	Investigation process
\oplus	Ex-or operation
	Concatenation operator

with the header". The concluding stage of the developed scheme is the verification stage, wherein, decryption occurs. Table 2 symbolizes the symbol and their explanation of the developed scheme.

3.1. Set up phase

The aspects of the integrity conservation technique are described as follows:

CSC: It represents the users who make use of the computing service for managing, accessing, and storing the resource from everywhere at whatever time.

CS: The data in the server is accessed by the user only by transferring the requested consent to the server.

CSP: It managed the cloud to provide data storing services. Nevertheless, only the owner could encrypt the information and situate them in the cloud to distribute to cloud customers.

CFI: It represents the cloud's end user dealing with the examination procedure. Nevertheless, the digital forensic examination guarantees the conservation of verification integrity throughout approval.

CA: It helps in gathering data regarding the users and files and then the accessing policies are assigned to files that symbolize the users.

Log file: The storage logs offered data concerning storage utilization, while usage logs offered data concerning every request made by users.

Cloud network: It permits users, the right of entry to network sources via a centralized source.

3.2. Log file creation phase

Here, the user password P_{pwd} and user id P_{id} are created by the user and forwarded to the server that receives the credentials of the user and stores as P_{id}^* and P_{pwd}^* , correspondingly. Following the reception of user credentials by the server, the CS verify if $P_{id} = P_{id}^*$ and $P_{pwd} = P_{pwd}^*$, and if they match, the server-generated 2 key aspects as y_1 and y_2 for generating the shared key. Nevertheless, y_1 created by the server as shown in Eq. (1).

$$y_1 = \left(F(P_{id}^*) || F(P_{pwd}^*) \oplus en(M) \right) \quad (1)$$

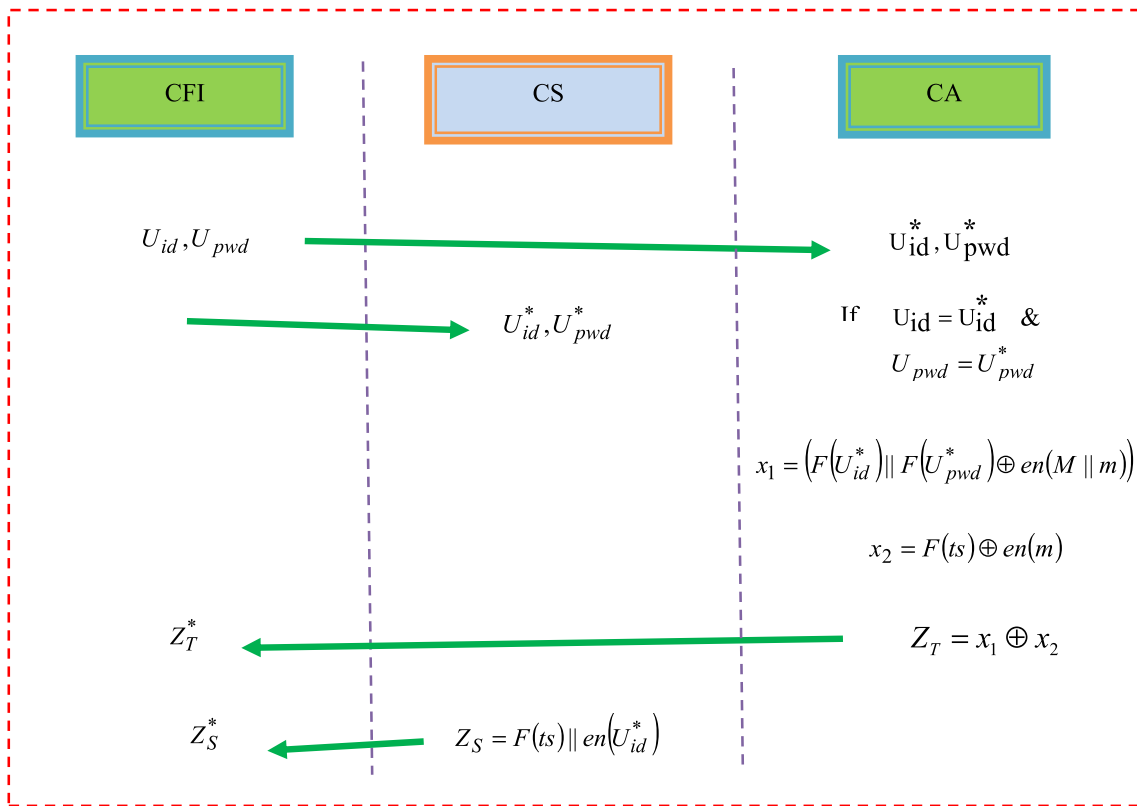


Fig. 2. Key management stage of the developed technique.

The P_{pwd} and P_{id} are applied individually to hashing operation and the resultant is permitted to do ex-or operation \oplus function with encrypted puk .

$$y_2 = F(t) \oplus en(M) \tag{2}$$

The timestamp is conveyed to hashing operation and the encryption operation is applied to the public key puk . The \oplus function is done with the hashed resultant of the timestamp and encrypted puk to create y_2 .

$$Z = y_1 \oplus y_2 \tag{3}$$

The shared key of CSC and CSP is created by doing the \oplus function using y_1 and y_2 . The key, which is shared among the CSP and CSC is are known as the shared key of CSC and CSP, in that order. The key produced by CS is transmitted to CSP and the user. While the key shared amid the CSC and CSP is harmonized, the user starts the communiqué-procedure with the server.

$$H = (P_{id}, ts, Y_{id}, \alpha) \tag{4}$$

The CS produces the log file by means of the constraints of ID of CSP, timestamp, user ID, and services presented to a user. The log file produced by CS is encrypted by means of an encryption operation and the encrypted log file is transmitted to the user. Fig.1 symbolizes this stage.

After the implementation of the log file formation stage, the key managing procedure starts by creating P_{pwd} and P_{id} of examiner by CFI. The CFI password U_{pwd} and CFI ID U_{id} created by CFI is transmitted to CA and server. The authority verifies if $U_{pwd} = U_{pwd}^*$ and $U_{id} = U_{id}^*$, if it matches, the CA generates the key factors x_1 and x_2 generates the shared key of CA and CFI. Nevertheless, x_1 is shown in Eq. (5).

$$x_1 = (F(U_{id}^*) || F(U_{pwd}^*) \oplus en(M || m)) \tag{5}$$

Here, the public keys are created using the CAHSACM model. The U_{pwd} and U_{id} are applied individually to hashing task and the puk is concatenated with an arbitrary integer such that the concatenated

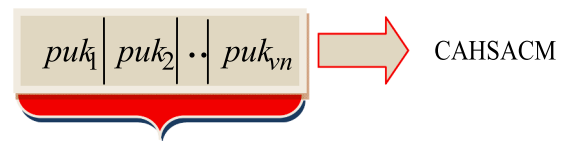


Fig. 3. Solution encoding.

product is applied to the encryption operation. The hashed product then performs the \oplus function with encrypted results for generating x_1 .

$$x_2 = F(ts) \oplus en(m). \tag{6}$$

The hashed ts is permitted to carry out the \oplus function with the encrypted arbitrary integer to create x_2 .

$$Z_T = x_1 \oplus x_2. \tag{7}$$

The shared key of CSC and CFI Z_S is created by CA with x_2 and x_1 , correspondingly. Both x_1 and x_2 are provided to \oplus function to produce the shared key of CFI and CA Z_T . In addition, Z_S is modeled in Eq. (8).

$$Z_S = F(ts) || en(U_{id}^*) \tag{8}$$

The hashing function is deployed to the timestamp t and hashed results are concatenated with an encrypted analyzer ID in CS. The shared key created by CS is transferred to CFI which receives the key from CS and accumulated in the analyzer database as Z_S^* . Fig. 2 shows the key management stage.

Solution Encoding: The public key (puk) is selected via the CAHSACM scheme optimally. Fig. 3 demonstrates the solution, in which $vn \rightarrow$ whole count of puk . The objective Obj is to increase the key breaking time (kbr) as exposed in Eq. (9).

$$Obj = \max(kbr). \tag{9}$$

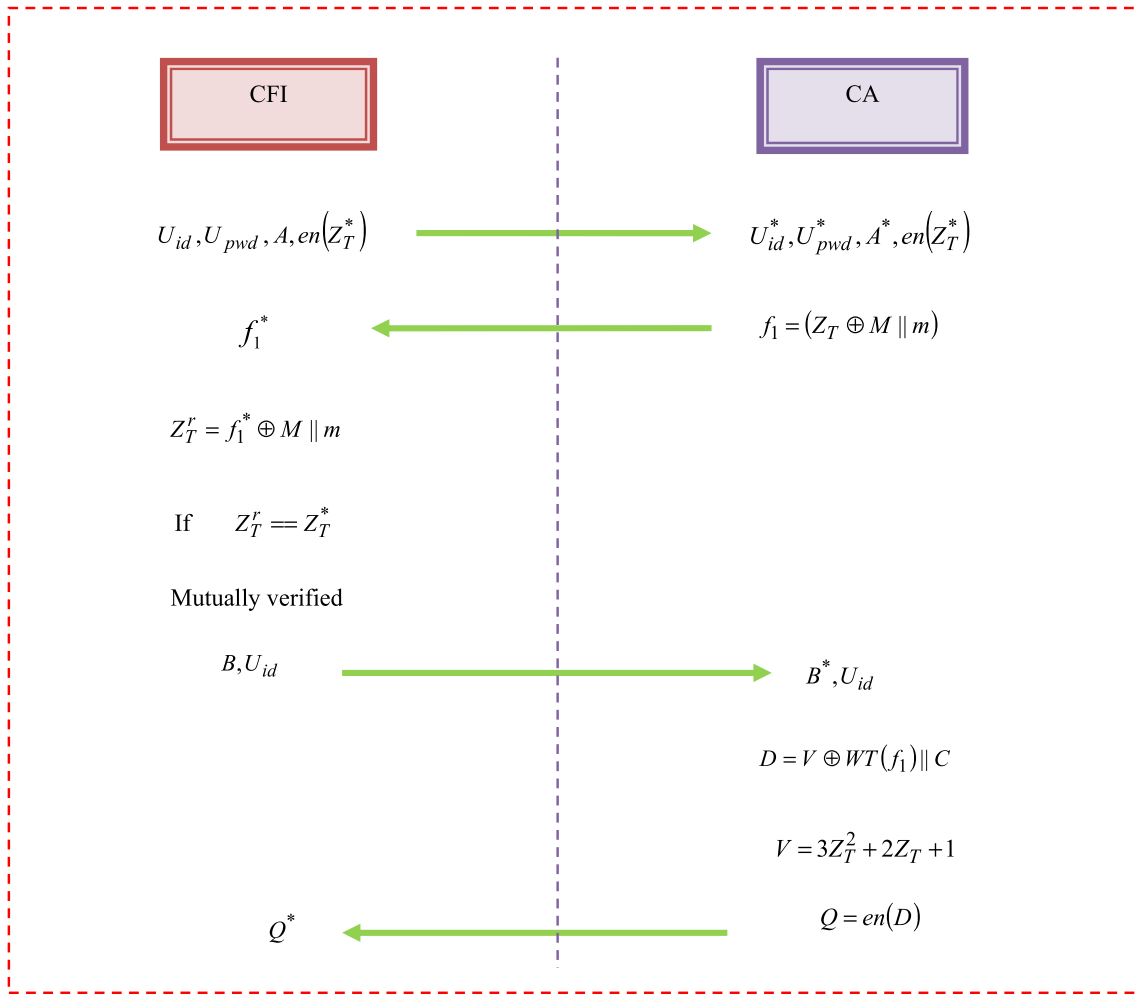


Fig. 4. Certification and verification stage.

3.3. Proposed CAHSACM

The existing AOA method (Hashim et al., 2021) exposed the best solutions; nonetheless, it suffered from lower precision. To overcome the inadequacy of AOA, the idea of HGS which has better performance (Yang et al., 2021) is incorporated with AOA known as CAHSACM. “Hybrid optimization models are proficient for specified searching issues” (Benou et al., 2014; Thomas & Rangachar, 2018; Devagnanam & Elango, 2020; Shareef & Rao, 2018):

The 2 principal phases of CAHSACM are “exploitation and exploration”.

Step 1- The N searching agents (populaces) are initialized.

Step 2- The positions of searching agents L^l and other constraints are assigned.

$$L^l = lb^l + rand^*(ub^l - lb^l) \tag{10}$$

Here, “ lb^l and ub^l denotes the lower and upper bounds of I^{th} search agent. In addition, the density Den^l as well as the volume Vo^l of each search agent is initialized randomly”. The acceleration J^l is shown in Eq. (11).

$$J^l = lb^l + rand^*(ub^l - lb^l). \tag{11}$$

The primary populace is assessed, and optimum fitness is chosen J_{best} ; Vo_{best} ; Den_{best} . For the ensuing position, the density Den_{it+1}^l and volume Vo_{it+1}^l are considered as in Eqs. (12) and (13), wherein, $rand \rightarrow$ arbitrary value.

$$Den_{it+1}^l = Den_{it}^l + rand^*(Den_{best} - Den_{it}^l) \tag{12}$$

$$Vo_{it+1}^l = Vo_{it}^l + rand^*(Vo_{best} - Vo_{it}^l) \tag{13}$$

Traditionally, the transfer operator TF is evaluated as in Eq. (14), in which, it and max^{it} signifies present and maximal iteration. As per CAHSACM, TF is evaluated as revealed in Eq. (15), which, κ implies constant value. In addition, Cauchy’s mutation is performed which resulted in a better rate of convergence.

$$TF = \exp\left(\frac{it - max^{it}}{max^{it}}\right) \tag{14}$$

$$TF = \left(1 - \frac{it}{max^{it}}\right)^{1/\kappa} \tag{15}$$

Step 3- Exploration Phase: If $TF \leq 0.5$, there is no collision amid the searching agent. The J^l for $it+1$ is calculated as in Eq. (16) J_{mr} , Vo_{mr} and Den_{mr} implies acceleration volume, and density of arbitrary searching agent.

$$Acc_{it+1}^l = \frac{Den_{mr} + Vo_{mr} + J_{mr}}{Den_{it+1}^l * Vo_{it+1}^l} \tag{16}$$

Step 4- Exploitation Phase: If $TF > 0.5$, there will not be a collision. The acceleration in this phase is evaluated as in Eq. (17).

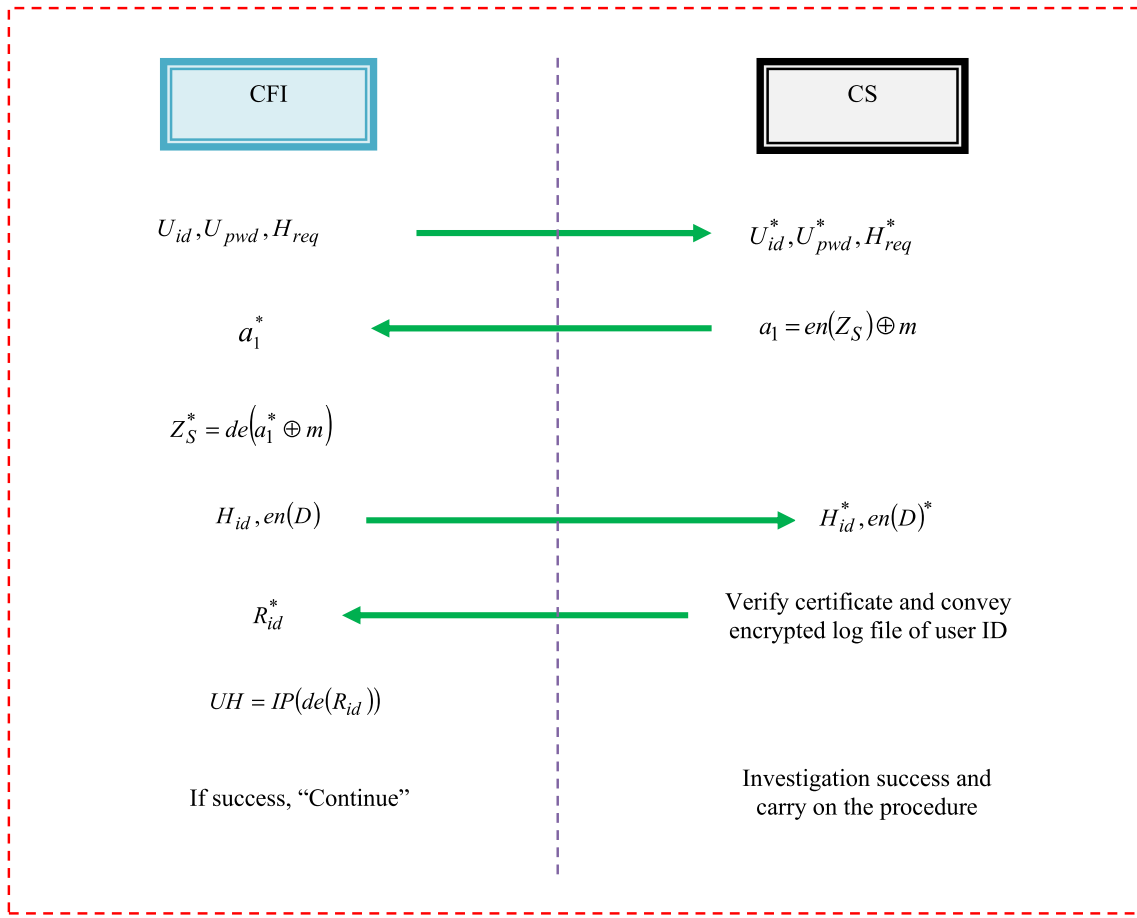


Fig. 5. Proof of Verification Stage.

$$Acc_{it+1}^I = \frac{Den_{best} + Vo_{best} + J_{best}}{Den_{it+1}^I * Vo_{it+1}^I} \quad (17)$$

As per CAHSACM, the position of the searching agent for the exploration phase is updated depending upon HGS as in Eq. (18), in which, “ r_1, r_2 denotes random integers amid 0 and 1, W lies between $[-a, a]$, w_1 and w_2 denotes weights, X_b denotes finest individual location, X_{it} denotes every individual location, $X_{it} * (1 + rand(1))$ represented how an agent can search for food hungrily and randomly at the current location”.

$$X_{it+1} = \begin{cases} game_1 : X_{it} * (1 + rand(1)), & r_1 < l \\ game_2 : w_1 * X_b + W.w_2 * |X_b - X_{it}|, & r_1 > l, r_2 > e \\ game_2 : w_1 * X_b - W.w_2 * |X_b - X_{it}|, & r_1 > l, r_2 < e \end{cases} \quad (18)$$

Throughout exploitation, the update of position is done as in Eq. (19).

$$X_{it+1}^I = X_{it}^I + fl * c2 * rand * J_{it+1}^{I-Norm} * d * (T * X^{best} - X_{it}^I) \quad (19)$$

$$d_{it+1} = \exp\left(\frac{\max^{it} - it}{\max^{it}}\right) - \left(\frac{it}{\max^{it}}\right) \quad (20)$$

In Eq. (19), “ J_{it+1}^{I-Norm} denotes normalized acceleration, $c1, c2$ are arbitrary constant X^{best} denotes best position particle and the fl is the flag that changes with respect to the direction”.

Step 5- Return optimum solution.

3.4. Certifying and verifying phase

Here, CFI produces U_{id} and U_{pwd} along with the request message A and shared encrypted key of CA and CFI are transmitted to authority. The CA obtains the constraints from the examiner and creates a message f_1 as in Eq. (21).

$$f_1 = (Z_T \oplus M || m) \quad (21)$$

The puk is concatenated with an arbitrary integer and the resultant is \oplus with the shared key of CA and CFI. The message created by CA has been transmitted to CFI receives the message and stores it in CFI as $f_1^* \cdot f_1^*$ is permitted to carry out the \oplus with puk and the results are concatenated with an arbitrary integer. The CFI ensures if $Z_T^r = Z_T^*$, and if it matches, then CFI generated the commonly confirmed message B and transmits it to authority together with U_{id} . The CA obtains the data and stores it in CA as B^* and U_{id} . Nevertheless, the CA produces certificates D via WT as in Eq. (22).

$$D = V \oplus WT(f_1) || C. \quad (22)$$

The WT is done with the message f_1 and the resulting factor is concatenated with the file related to a header. The polynomial factor \oplus functions with the concatenated resultant as shown in Eq. (23).

$$V = 3Z_T^2 + 2Z_T + 1 \quad (23)$$

The certificate is encrypted and saved as Q and transmitted to CFI that gets encrypted certificate and recorded as Q^* . Fig. 4 depicts this stage.

3.5. Proof of verification phase

Here U_{id}, U_{pwd} and log file requests H_{req} are transmitted to CS that receives and stores them in the server database as U_{id}^* , and H_{req}^* , in that order. After this, the server produces a message m_1 is modeled in U_{pwd}^* Eq. (24).

$$a_1 = en(Z_s) \oplus m. \tag{24}$$

The encryption operation is applied to the key shared among CFI and CS and encrypted results are permitted to carry out \oplus with arbitrary integers m . The CS transmits the message a_1 to CFI which receives the message and employs the message a_1^* to carry out \oplus with arbitrary integer and apply to decryption operation to produce Z_s^* . The CFI transmits the log file ID with an encrypted certificate to CS that receives the factor and saves it in the CS database as H_{id}^* , and $en(D)^*$. Nevertheless, the CS verifies the certificate and sends the encrypted log files regarding the user ID as R_{id}^* to CFI. The failure and success procedure is examined by deploying the examination procedure to the encrypted user log file ID R_{id} and if success is determined, subsequently CFI carries on the communiqué procedure. Fig. 5 depicts the verification stage.

IECC for encryption: The currently utilized Elliptical Curve Cryptography (ECC) is a public-key encryption process that relies on the elliptic curve concept that can generate cryptographic keys more quickly, more efficiently, and with fewer size requirements. As per the ECC strategy, an improved version of ECC is presented due to its features such as reduced CPU and memory requirements, faster encryption, the ability to use larger key sizes without significantly raising CPU or memory demands, and highly secure encryption for larger key sizes. The numerical model of IECC is shown in Eq. (25) - (31), in which, b and $a \rightarrow$ integers, x implies plain text.

$$x^2 = g^3 + bg + a. \tag{25}$$

3 kinds of keys are created in improved ECC.

- a. Private key, prk .
- b. Public key, puk .
- c. Secret key, srk .

Let B_s be the base point upon the curve. Further, choose a chaotic number that lies amid 0 and 1 via the tent map function as shown in Eq. (26), wherein, $g_k \in (0, 1)$.

$$g_{k+1} = \begin{cases} 2g_k; & 2(1 - g_k) \\ 2(1 - g_k); & g_k \geq 0.5 \end{cases} \tag{26}$$

The puk is evaluated in Eq. (27).

$$puk = prk + B_s. \tag{27}$$

Then srk is created by Eq. (28), wherein, w_e implies weight amongst 0 and 1. After the generation of the key, encryption is made.

$$srk = \sum (puk, prk, B_s) * w_e. \tag{28}$$

Encryption: While encrypting, the original data is encoded including 2 CTs as per Eqs. (29) and (30), in which, ct_1 and ct_2 implies CTs and $O_d \rightarrow$ original message and q_1 implies arbitrary integer.

$$ct_1 = q_1 \times B_s - srk. \tag{29}$$

$$ct_2 = O_d + (q_1 \times puk) - srk. \tag{30}$$

Decryption: At the receiver side, decryption is done as exposed in Eq. (31).

$$O_d = ((ct_2 - prk) * ct_1) + srk. \tag{31}$$

Table 3

Study on detection rate for CAHSACM over others for key size 64.

User count	100	200	300	400
Consensus approach (Panchamia & Byrappa, 2017)	0.71	0.45	0.63	0.73
AES	0.76	0.84	0.86	0.87
RSA	0.83	0.87	0.87	0.87
El-Gamal	0.83	0.88	0.88	0.89
Signcryption	0.85	0.89	0.88	0.92
WT (Tummalapalli & Chakravarthy, 2021)	0.94	0.95	0.95	0.95
SSO	0.95	0.95	0.95	0.95
LA	0.95	0.95	0.95	0.95
DHO	0.95	0.95	0.95	0.96
ROA	0.95	0.95	0.95	0.96
PRO	0.95	0.95	0.96	0.96
HGS	0.95	0.95	0.96	0.96
AOA	0.96	0.95	0.96	0.96
CAHSACM	0.98	0.98	0.98	0.99

Table 4

Study on detection rate for CAHSACM over others for key size 128.

User count	100	200	300	400
Consensus approach (Panchamia & Byrappa, 2017)	0.71	0.445	0.633	0.725
AES	0.76	0.84	0.88	0.88
RSA	0.85	0.89	0.88	0.88
El-Gamal	0.85	0.89	0.88	0.88
Signcryption	0.85	0.89	0.88	0.92
WT (Tummalapalli & Chakravarthy, 2021)	0.961	0.96	0.963	0.965
SSO	0.961	0.961	0.96	0.965
LA	0.962	0.962	0.965	0.966
DHO	0.963	0.964	0.967	0.969
ROA	0.963	0.965	0.967	0.971
PRO	0.96406	0.96862	0.968	0.9727
HGS	0.96852	0.96888	0.96937	0.97276
AOA	0.9688	0.96967	0.97044	0.97323
CAHSACM	0.98	0.98	0.9833	0.985

Table 5

Study on detection rate for CAHSACM over others for key size 256.

User count	100	200	300	400
Consensus approach (Panchamia & Byrappa, 2017)	0.71	0.7445	0.633333	0.725
AES	0.76	0.84	0.88	0.885
RSA	0.85	0.89	0.88	0.885
El-Gamal	0.85	0.89	0.88	0.885
Signcryption	0.85	0.89	0.88	0.92
WT (Tummalapalli & Chakravarthy, 2021)	0.961	0.962	0.964	0.965
SSO	0.964	0.962	0.965	0.969
LA	0.964	0.964	0.965	0.969
DHO	0.967	0.964	0.9662	0.9708
ROA	0.968	0.965	0.968	0.971
PRO	0.968	0.965	0.969	0.971
HGS	0.969	0.967	0.972	0.971
AOA	0.969	0.968	0.973	0.974
CAHSACM	0.98	0.98	0.983	0.985

4. Results and discussion

4.1. Simulation set up

The offered scheme for the log integrity conservation model was done in “JAVA tool with cloudsim”. The performance of the CAHSACM system was calculated over the Consensus approach (Panchamia & Byrappa, 2017), AES, RSA, El-Gamal, Signcryption, WT (Tummalapalli & Chakravarthy, 2021), SSO, LA, DHO, ROA, PRO, HGS and AOA on broader metrics lifetime, attack, etc. Here, scrutiny was made by varying key sizes from 64, 128, and 256 and user count from 100, 200, 300, and

Table 6
Study on memory bytes for CAHSACM over others for key size 64.

User count	100	200	300	400
Consensus approach (Panchamia & Byrappa, 2017)	595,009,392	499,321,960	513,209,656	595,125,672
AES	297,400,624	364,553,400	326,461,880	540,129,768
RSA	273,229,816	361,451,888	266,723,088	307,984,048
El-Gamal	225,644,592	219,573,856	229,113,008	244,802,200
Signcryption	217,169,912	145,753,632	138,847,792	243,311,296
WT (Tummalapalli & Chakravarthy, 2021)	167,244,424	113,145,000	118,115,464	225,501,536
SSO	137,876,264	104,361,248	86,301,328	208,977,088
LA	135,226,448	99,021,168	82,816,264	156,729,360
DHO	109,674,536	85,946,216	82,432,592	125,462,304
ROA	83,796,424	82,568,240	70,233,872	104,517,024
PRO	82,377,672	71,122,592	56,497,760	92,371,568
HGS	64,758,440	59,451,760	53,189,800	65,318,176
AOA	49,654,568	35,828,304	48,912,528	33,407,968
CAHSACM	2,072,312	6,619,232	1,636,112	4,144,128

400.

4.2. Analysis of detection rate

The detection rate of suggested CAHSACM is calculated over traditional schemes for varied key sizes of 64, 128, and 256. The assessment of the CAHSACM technique made over conservative models like the consensus approach (Panchamia & Byrappa, 2017), AES, RSA, El-Gamal, Signcryption, WT (Tummalapalli & Chakravarthy, 2021), SSO, LA,

Table 7
Study on memory bytes for CAHSACM over others for key size 128.

User count	100	200	300	400
Consensus approach (Panchamia & Byrappa, 2017)	840,323,000	885,920,072	930,411,952	1,077,725,288
AES	771,469,640	806,474,288	868,800,472	997,985,784
RSA	720,432,016	604,022,192	470,380,800	700,693,728
El-Gamal	378,098,976	583,155,768	365,407,520	620,654,224
Signcryption	375,987,720	231,124,648	242,355,488	475,036,992
WT (Tummalapalli & Chakravarthy, 2021)	213,711,544	223,719,744	169,774,528	328,084,960
SSO	138,818,920	206,853,000	127,846,376	302,869,424
LA	67,006,944	172,500,440	125,207,720	198,426,704
DHO	42,831,760	95,243,920	116,116,744	97,592,088
ROA	36,490,576	59,797,592	84,625,200	75,854,464
PRO	32,647,912	47,378,064	43,130,264	40,930,104
HGS	8,429,512	4,640,192	11,359,808	4,729,088
AOA	3,074,280	3,067,488	6,728,792	3,629,928
CAHSACM	2080	2080	1985	3,627,872

Table 8
Study on memory bytes for CAHSACM over others for key size 256.

User count	100	200	300	400
Consensus approach (Panchamia & Byrappa, 2017)	1,012,376,528	1,083,131,872	943,574,496	1,216,700,048
AES	976,371,760	539,174,512	786,618,424	846,758,280
RSA	600,098,696	528,755,656	687,820,488	759,673,544
El-Gamal	599,304,440	489,692,128	668,521,472	600,547,568
Signcryption	325,905,528	300,139,688	275,433,208	550,936,416
WT (Tummalapalli & Chakravarthy, 2021)	190,896,248	210,311,136	224,368,296	133,837,640
SSO	166,446,648	157,642,456	171,578,928	123,443,968
LA	150,934,608	155,593,304	147,860,264	95,839,184
DHO	132,872,328	100,501,544	59,664,296	89,157,096
ROA	102,606,128	84,435,784	56,601,168	59,363,776
PRO	49,754,272	54,770,784	52,666,496	49,914,256
HGS	5,738,720	7,481,784	19,959,528	5,377,976
AOA	4,920,976	4,924,384	5,986,344	4,920,976
CAHSACM	1,142,840	1,037,360	2,071,128	1,865,728

DHO, ROA, PRO, HGS, and AOA are exposed in Tables 3–5 for a varied count of users from, 100, 200, 300 and 400. Here, the presented CAHSACM offered a better detection rate over the Consensus approach (Panchamia and Byrappa, 2017), AES, RSA, El-Gamal, Signcryption, WT (Tummalapalli & Chakravarthy, 2021), SSO, LA, DHO, ROA, PRO, HGS, and AOA. In Table 3, the detection rate for CAHSACM is high when the user count is 400 than at other user counts when the key size is 64. At the 400th user count, the Consensus approach (Panchamia and Byrappa, 2017) has got comparatively less detection rate than other models. In Table 4, a high detection rate is found at the 400th user count. Particularly, it is noted that a higher detection rate is observed at the 400th user count for proposed and compared models than at other user count. This enhancement is due to the integrated IECC concept and optimal key creation. Thus, the advantage of CAHSACM is recognized over the Consensus approach (Panchamia and Byrappa, 2017), AES, RSA, El-Gamal, Signcryption, WT (Tummalapalli & Chakravarthy, 2021), SSO, LA, DHO, ROA, PRO, HGS, and AOA. Thus, from the obtained findings it is clear that the proposed CAHSACM method for choosing optimal public keys is the main reason for these improved results on detection.

4.3. Analysis of memory bytes

Tables 6–8 highlight the study on memory consumption accomplished using CAHSACM over conventional models (Consensus approach (Panchamia and Byrappa, 2017), AES, RSA, El-Gamal, Signcryption, WT (Tummalapalli & Chakravarthy, 2021), SSO, LA, DHO, ROA, PRO, HGS, and AOA). Tables 6–8 shows the analysis using key size 64, 128, and 256 respectively. Lesser memory consumption of 1,636,112 is achieved using CAHSACM for 300 user count for a key size of 64, while (Consensus approach (Panchamia and Byrappa, 2017), AES, RSA, El-Gamal, Signcryption, WT (Tummalapalli & Chakravarthy, 2021), SSO,

Table 9
Study on time (ms) for CAHSACM over others for key size 64.

User count	100	200	300	400
Consensus approach (Panchamia & Byrappa, 2017)	47,570	46,048	47,929	55,085
AES	47,489	45,935	47,783	55,001
RSA	47,339	45,766	47,586	54,873
El-Gamal	46,846	45,364	46,544	53,961
Signcryption	46,641	45,136	46,295	53,779
WT (Tummalapalli & Chakravarthy, 2021)	46,289	44,756	45,881	53,416
SSO	6362	6654	6587	15,943
LA	5655	5923	5827	15,201
DHO	4922	5177	5010	14,420
ROA	4192	4441	4268	13,667
PRO	3513	3528	3567	12,942
HGS	2785	2717	2835	12,136
AOA	2092	2032	2139	11,356
CAHSACM	1376	1346	1413	7158

Table 10
Study on time (ms) for CAHSACM over others for key size 128.

User count	100	200	300	400
Consensus approach (Panchamia & Byrappa, 2017)	119,816	120,504	122,482	130,017
AES	119,674	120,268	122,169	129,876
RSA	119,486	120,006	121,841	129,703
El-Gamal	64,611	67,259	67,172	71,208
Signcryption	59,785	62,027	61,812	65,985
WT (Tummalapalli & Chakravarthy, 2021)	58,879	60,918	60,618	65,023
SSO	12,732	14,778	12,488	14,298
LA	11,534	13,371	11,011	12,855
DHO	10,096	11,634	9607	11,140
ROA	8887	10,345	8507	9633
PRO	7692	9088	7438	8284
HGS	6413	7797	6339	6862
AOA	5153	6656	5237	5511
CAHSACM	2667	2596	2630	2470

Table 11
Study on time (ms) for CAHSACM over others for key size 256.

User count	100	200	300	400
Consensus approach (Panchamia & Byrappa, 2017)	92,686	90,907	94,167	96,296
AES	92,623	90,793	94,011	96,233
RSA	92,514	90,662	93,839	96,139
El-Gamal	56,590	56,236	56,680	58,134
Signcryption	48,563	48,023	48,117	49,950
WT (Tummalapalli & Chakravarthy, 2021)	48,028	47,440	47,483	49,465
SSO	8982	8828	8725	11,763
LA	8252	8111	7936	10,991
DHO	6649	6535	6382	9354
ROA	5956	5803	5668	8606
PRO	5287	5123	4996	7891
HGS	4568	4345	4235	7058
AOA	3864	3584	3517	6265
CAHSACM	2514	2459	2480	4879

LA, DHO, ROA, PRO, HGS, and AOA achieved high memory consumption. A much lesser memory is consumed for key size 128 for user counts of 100, 200, and 300. From Table 7, the consensus approach consumed the highest memory (840323000, at key size 128 and in the 100th user count) and the proposed model required lower memory of 2080 at the 100th user count and when the key size is 128. These developments are owing to the included IECC concept and optimal key creation in developed work.

Table 12
Study on encryption time (ms) for CAHSACM over others for key size 64.

User count	100	200	300	400
Consensus approach (Panchamia & Byrappa, 2017)	4,756,291	4,349,839	4,839,284	5,985,704
AES	2,781,939	3,692,131	4,183,849	4,304,053
RSA	2,602,068	2,740,129	2,705,423	2,477,915
El-Gamal	1,578,289	1,781,450	2,357,311	1,521,511
Signcryption	1,366,826	1,774,562	1,423,408	1,511,788
WT (Tummalapalli & Chakravarthy, 2021)	1,289,017	1,390,324	1,387,774	1,502,370
SSO	1,270,040	1,299,615	1,350,859	1,467,005
LA	1,254,055	1,293,688	1,301,793	1,426,327
DHO	1,238,391	1,287,193	1,284,582	1,414,174
ROA	1,193,010	1,211,350	1,265,826	1,377,944
PRO	1,063,343	952,565	1,025,589	846,192
HGS	603,955	593,539	575,531	667,099
AOA	298,061	283,212	324,375	329,744
CAHSACM	205,693	125,620	136,770	218,576

Table 13
Study on encryption time (ms) over for CAHSACM others for key size 128.

User count	100	200	300	400
Consensus approach (Panchamia & Byrappa, 2017)	9,740,796	1.04E+07	1.04E+07	1.06E+07
AES	3,296,276	3,589,038	3,277,840	4,961,081
RSA	2,597,410	2,935,563	2,384,487	2,473,254
El-Gamal	1,388,380	2,456,235	1,608,872	1,778,535
Signcryption	1,373,069	1,727,973	1,558,412	1,336,999
WT (Tummalapalli & Chakravarthy, 2021)	1,345,553	1,688,325	1,492,273	1,280,719
SSO	1,335,284	1,569,977	1,429,531	1,181,482
LA	1,304,719	1,563,573	1,391,004	1,163,848
DHO	1,279,556	1,549,119	1,362,025	1,160,456
ROA	1,260,494	1,340,558	1,345,453	1,153,710
PRO	908,456	977,797	1,021,147	926,532
HGS	680,684	602,428	705,875	634,221
AOA	291,668	331,719	343,195	332,305
CAHSACM	136,098	185,782	175,413	170,133

Table 14
Study on encryption time (ms) over for CAHSACM others for key size 256.

User count	100	200	300	400
Consensus approach (Panchamia & Byrappa, 2017)	1,906,536	1,995,624	2,016,894	2,445,512
AES	1,815,842	1,797,376	1,723,876	2,146,555
RSA	1,517,344	1,630,041	1,573,484	1,753,448
El-Gamal	1,457,645	913,984	1,499,264	1,608,800
Signcryption	986,985	894,509	924,772	1,003,342
WT (Tummalapalli & Chakravarthy, 2021)	965,005	869,256	892,941	921,396
SSO	964,071	866,515	864,690	908,099
LA	895,787	841,482	848,688	886,533
DHO	889,608	827,059	845,599	865,386
ROA	886,736	812,723	831,092	850,994
PRO	673,450	720,128	749,677	843,831
HGS	508,402	407,814	394,831	390,950
AOA	173,376	166,220	172,119	171,720
CAHSACM	129,175	106,628	70,230	89,959

4.4. Time analysis

Tables 9–11 demonstrate the time utilization for key sizes of 64, 128, and 256. Here, time is indicated in milliseconds (ms). The analysis is done for user counts of 100, 200, 300, and 400. In tables, it can be noticed that, as the user count increases, the time utilization increases. However, CAHSACM has acquired lesser time duration than compared

Table 15
Study on decryption time (ms) for CAHSACM over others for key size 64.

User count	100	200	300	400
Consensus approach (Panchamia & Byrappa, 2017)	51,166,912	51,438,432	53,744,421	55,531,440
AES	51,038,977	51,312,331	53,610,042	55,392,607
RSA	50,911,042	51,186,230	53,475,663	55,253,774
El-Gamal	50,783,107	51,060,129	53,341,284	55,114,941
Signcryption	50,655,172	50,934,028	53,206,905	54,976,108
WT (Tummalapalli & Chakravarthy, 2021)	50,527,237	50,807,927	53,072,526	54,837,275
SSO	50,399,302	50,681,826	52,938,147	54,698,442
LA	50,271,367	50,555,725	52,803,768	54,559,609
DHO	50,143,432	50,429,624	52,669,389	54,420,776
ROA	50,015,497	50,303,523	52,535,010	54,281,943
PRO	49,887,562	50,177,422	52,400,631	54,143,110
HGS	49,759,627	49,951,321	52,266,252	54,004,277
AOA	49,631,692	49,825,220	52,131,873	53,865,444
CAHSACM	49,503,757	49,799,119	51,997,494	53,726,611

Table 16
Study on decryption time (ms) over for CAHSACM others for key size 128.

User count	100	200	300	400
Consensus approach (Panchamia and Byrappa, 2017)	50,493,976	50,724,013	51,272,020	55,194,654
AES	50,367,728	50,597,192	51,143,818	55,056,651
RSA	50,241,480	50,470,371	51,015,616	54,918,648
El-Gamal	50,115,232	50,343,550	50,887,414	54,780,645
Signcryption	49,988,984	50,216,729	50,759,212	54,642,642
WT (Tummalapalli & Chakravarthy, 2021)	49,862,736	50,089,908	50,631,010	54,504,639
SSO	49,736,488	49,963,087	50,502,808	54,366,636
LA	49,610,240	49,836,266	50,374,606	54,228,633
DHO	49,483,992	49,709,445	50,246,404	54,090,630
ROA	49,357,744	49,582,624	50,118,202	53,952,627
PRO	49,231,496	49,455,803	49,990,000	53,814,624
HGS	49,105,248	49,328,982	49,861,798	53,676,621
AOA	48,979,000	49,202,161	49,733,596	53,538,618
CAHSACM	48,852,752	49,075,340	49,605,394	53,400,615

Table 17
Study on decryption time (ms) over for CAHSACM others for key size 256.

User count	100	200	300	400
Consensus approach (Panchamia and Byrappa, 2017)	39,140,240	38,656,030	39,668,728	40,857,425
AES	39,042,378	38,559,388	39,569,538	40,755,279
RSA	38,944,516	38,462,746	39,470,348	40,653,133
El-Gamal	38,846,654	38,366,104	39,371,158	40,550,987
Signcryption	38,748,792	38,269,462	39,271,968	40,448,841
WT (Tummalapalli & Chakravarthy, 2021)	38,650,930	38,172,820	39,172,778	40,346,695
SSO	38,553,068	38,076,178	39,073,588	40,244,549
LA	38,455,206	37,979,536	38,974,398	40,142,403
DHO	38,357,344	37,882,894	38,875,208	40,040,257
ROA	38,259,482	37,786,252	38,776,018	39,938,111
PRO	38,161,620	37,689,610	38,676,828	39,835,965
HGS	38,063,758	37,592,968	38,577,638	39,733,819
AOA	37,965,896	37,496,326	38,478,448	39,631,673
CAHSACM	37,868,034	37,399,684	38,379,258	39,529,527

(Consensus approach (Panchamia and Byrappa, 2017), AES, RSA, El-Gamal, Signcryption, WT (Tummalapalli & Chakravarthy, 2021), SSO, LA, DHO, ROA, PRO, HGS, and AOA models. Predominantly, the conventional RSA attained 47339 ms time, while the count of the user is 100 whereas our proposed model attain considerably a lower time 1376 ms at 100 user count. These improved outcomes are because of the IECC concept and optimal key creation.

4.5. Analysis of encryption and decryption time

Tables 12–14 shows the encryption time analysis using key sizes of 64, 128, and 256. Tables 15–17 shows the decryption time analysis using key sizes of 64, 128, and 256. The analysis is done for user counts of 100, 200, 300, and 400. The time to encrypt the data should be lower, which is accomplished by the CAHSACM scheme. For all key sizes, the CAHSACM scheme has acquired less encryption time. Especially, for user counts of 300 and 400, the encryption time is lesser for a key size of 256. In the case of decryption time, the outcome is lesser for key size of 256 than for key sizes of 64 and 128. Thus, minimal decryption and encryption time are revealed by the CAHSACM scheme over the Consensus approach (Panchamia and Byrappa, 2017), AES, RSA, El-Gamal, Signcryption, WT (Tummalapalli & Chakravarthy, 2021), SSO, LA, DHO, ROA, PRO, HGS and AOA. The improved ECC provides effective encryption and decryption, especially at a lower time.

4.6. Convergence analysis

Fig. 6 demonstrates the convergence for deployed CAHSACM schemes over conventional models (SSO, LA, DHO, ROA, PRO, HGS, and AOA). In Fig. 6, CAHSACM has exposed enhanced results by getting high key break time. At certain iterations, AOA has gained high key break time than SSO, LA, DHO, ROA, PRO, HGS, and AOA. However, this deviation can be considered negligible, as other metrics are satisfied by the CAHSACM scheme. Here, ROA has exposed the worst results by gaining less key break time. A high key break time of 442,000 is obtained by CAHSACM at the 50th iteration. Thus, the objective is fulfilled as in Eq. (20).

4.7. Attack analysis

The analysis of varied attacks such as brute force attacks and cipher text attacks is shown in Tables 18 and 19. The attack analysis of suggested CAHSACM is calculated over traditional schemes for varied key sizes of 128, 192, and 256. The estimation of the CAHSACM technique made over conservative models like the consensus approach (Panchamia and Byrappa, 2017), AES, RSA, El-Gamal, Signcryption, WT (Tummalapalli Chakravarthy, 2021), SSO, LA, DHO, ROA, PRO, HGS, and AOA is exposed for a varied count of users from, 100, 200, 300 and 400. The key breakage time by brute force and cipher text attacks are portrayed here. As per this statement, the suggested CAHSACM has exposed high key break time when prone to brute force and cipher text attacks. This development is due to improved IECC and optimal key creation concepts.

4.8. Analysis of ablation study

The analysis of the ablation study for varied attacks such as brute force attacks and cipher text attacks is shown in Table 20. The suggested CAHSACM is evaluated over the proposed method without including optimization for different key sizes of 128, 192, and 256. Predominantly, for brute force attack, the suggested method has an improved value of approximately 442,000 than the developed model without optimization. Furthermore, for Cipher text Attacks, the adopted CAHSACM technique has achieved a higher value of almost 442,000, while the proposed model without implementing optimization attained considerably a lower value of 512,237 which proves that the projected method has exhibited higher key break time under attacks employing cipher text and brute force, than the proposed method with using optimization.

5. Conclusion

This work developed a novel immigration management model with phases like, “initialization phase, log file collection phase, key

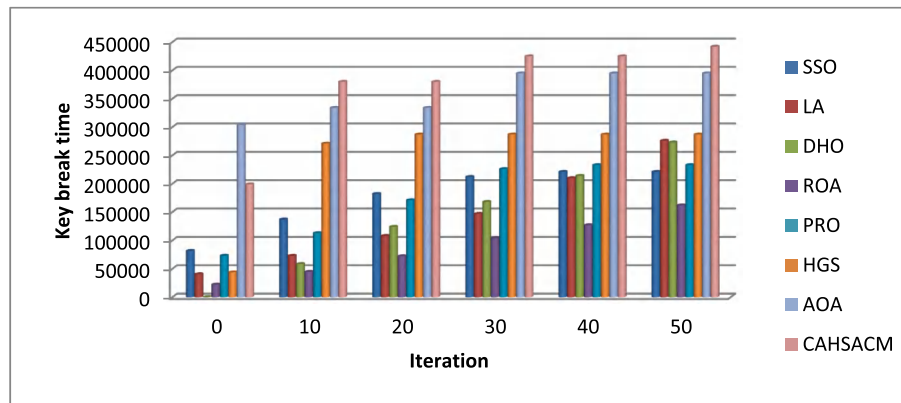


Fig. 6. Convergence analysis of CAHSACM over other schemes.

Table 18

Brute force attack of CAHSACM over others.

Key size(bits)	128	192	256
Consensus approach (Panchama and byrappa,2017)	30,605	26,821	31,200
AES	31,905	28,121	3.25E+04
RSA	35,905	32,121	3.65E+04
EL-Gamal	42,605	38,821	4.32E+04
Signcryption	48,205	44,421	4.88E+04
WT(Tummalapalli & Chakravarthy, 2021)	48,805	45,021	4.94E+04
SSO	181,405	177,621	1.82E+05
LA	220,405	216,621	2.21E+05
DHO	232,405	228,621	2.33E+05
ROA	281,405	277,621	2.82E+05
PRO	296,405	292,621	2.97E+05
HGS	356,405	352,621	3.57E+05
AOA	394,405	390,621	3.95E+05
CAHSACM	441,405	437,621	4.42E+05

Table 19

Cipher textAttack of CAHSACM over others.

Key size(bits)	128	192	256
Consensus approach (Panchama and byrappa,2017)	130,133	126,349	130,728
AES	131,433	127,649	1.32E+05
RSA	135,433	131,649	1.36E+05
EL-Gamal	142,133	138,349	1.43E+05
Signcryption	147,733	143,949	1.48E+05
WT(Tummalapalli & Chakravarthy, 2021)	148,333	144,549	1.49E+05
SSO	280,933	277,149	2.82E+05
LA	319,933	316,149	3.21E+05
DHO	331,933	328,149	3.33E+05
ROA	380,933	377,149	3.82E+05
PRO	395,933	392,149	3.97E+05
HGS	455,933	452,149	4.57E+05
AOA	493,933	490,149	4.95E+05
CAHSACM	540,933	537,149	5.42E+05

Table 20

Analysis of ablation study for both Brute Force and Cipher text Attack.

Brute Force Attack			
Key size (bits)	128	192	256
Proposed method without optimization	399,426	416,712	422,643
CAHSACM	441,405	437,621	4.42E+05
Cipher text Attack			
Key size(bits)	128	192	256
Proposed method without optimization	527,546	501,213	512,237
CAHSACM	540,933	537,149	42E+05

generation, and management, partial proof generation, certificate and file encryption, adding encryption proofs on public key infrastructure, proof verification by cloud forensic investigator". As a new thing, the public keys were chosen optimally via CAHSACM. In addition, IECC-based encryption was done to authenticate the data. Especially, the estimation of the CAHSACM technique made over conservative models like the consensus approach, AES, RSA, El-Gamal, Signcryption, WT, SSO, LA, DHO, ROA, PRO, HGS, and AOA was exposed for varied counts of users from, 100, 200, 300 and 400. The impact of the attack has to be lesser for better communication. As per this statement, the suggested CAHSACM has exposed less impact on both brute force attacks and cipher text attacks. In the future, varied types of attacks may be analyzed. The collision problem is not addressed in this research which can be resolved in future research.

Funding information

None.

CRedit authorship contribution statement

Sahadev Maruti Shinde: Conceptualization, Methodology, Formal analysis, Investigation. Venkateswara Rao Gurralla: Resources, Data curation.

Declaration of Competing Interest

The authors declare that they have no known competing financial interests or personal relationships that could have appeared to influence the work reported in this paper.

Data availability

The authors do not have permission to share data.

References

Abhay, G., Sharma, A., Gupta, D., & Khanna, A. (2020). Immigration control and management system using blockchain. *Proceedings of the international conference on innovative computing & communications (ICICC)*.

Ashok Kumar, C., & Vimala, R. (2020). Load balancing in cloud environment exploiting hybridization of chicken swarm and enhanced raven roosting optimization algorithm. *Multimedia Research*, 3(1), 45–55.

Battistoni, R., Di Pietro, R., & Lombardi, F. (2016). CURE—Towards enforcing a reliable timeline for cloud forensics: Model, architecture, and experiments. *Computer Communications*, 91, 29–43.

Beno, M. M., Valarmathi, I. R., Swamy, S. M., & Rajakumar, B. R. (2014). Threshold prediction for segmenting tumour from brain MRI scans. *International Journal of Imaging Systems and Technology*, 24(2), 129–137.

Dagher, G. G., Mohler, J., Milojkovic, M., & Marella, P. B. (2018). Ancile: Privacy-preserving framework for access control and interoperability of electronic health records using blockchain technology. *Sustainable Cities and Society*, 39, 283–297.

- Dalezios, N., Shiaeles, S., Kolokotronis, N., & Ghita, B. (2020). Digital forensics cloud log unification: Implementing CADF in Apache CloudStack. *Journal of Information Security and Applications*, 54, Article 102555.
- Dasaklis, T. K., Casino, F., & Patsakis, C. (2020). Sok: Blockchain solutions for forensics. In *Technology development for security practitioners* (pp. 21–40). Cham: Springer.
- Devagnanam, J., & Elango, N. M. (2020). Optimal resource allocation of cluster using hybrid grey wolf and cuckoo search algorithm in cloud computing. *Journal of Networking and Communication Systems*, 3(1), 31–40.
- Duy, P. T., Do Hoang, H., Khanh, N. B., & Pham, V. H. (2019). Sdnlog-foren: Ensuring the integrity and tamper resistance of log files for sdn forensics using blockchain. In *2019 6th NAFOSTED Conference on Information and Computer Science (NICS)* (pp. 416–421). IEEE.
- Guo, H., Li, W., Nejad, M., & Shen, C. C. (2019). Access control for electronic health records with hybrid blockchain-edge architecture. In *2019 IEEE international conference on blockchain (Blockchain)* (pp. 44–51). IEEE.
- Hashim, F. A., Hussain, K., Houssein, E. H., Mabrouk, M. S., & Al-Atabany, W. (2021). Archimedes optimization algorithm: A new metaheuristic algorithm for solving optimization problems. *Applied Intelligence*, 51(3), 1531–1551.
- Irfan, M., Abbas, H., & Iqbal, W. (2015). Feasibility analysis for incorporating/deploying SIEM for forensics evidence collection in cloud environment. In *In 2015 IEEE/ACIS 14th international conference on computer and information science (ICIS)* (pp. 15–21). IEEE.
- Irfan, M., Abbas, H., Sun, Y., Sajid, A., & Pasha, M. (2016). A framework for cloud forensics evidence collection and analysis using security information and event management. *Security and Communication Networks*, 9(16), 3790–3807.
- Jain, P. (2020). Decentralize log file storage and integrity preservation using blockchain. *International Journal of Computer Science and Information Technologies*, 11(2), 21–30.
- Kent, K., Chevalier, S., & Grance, T. (2006). Guide to integrating forensic techniques into incident. *Technical Reports*, 800–886.
- Lin, C., He, D., Huang, X., Choo, K. K. R., & Vasilakos, A. V. (2018). BSEIn: A blockchain-based secure mutual authentication with fine-grained access control system for industry 4.0. *Journal of Network and Computer Applications*, 116, 42–52.
- Ma, M., Shi, G., & Li, F. (2019). Privacy-oriented blockchain-based distributed key management architecture for hierarchical access control in the IoT scenario. *IEEE Access*, 7, 34045–34059.
- Maesa, D. D. F., Mori, P., & Ricci, L. (2019). A blockchain based approach for the definition of auditable access control systems. *Computers & Security*, 84, 93–119.
- Manoj, S. K. A., & Bhaskari, D. L. (2016). Cloud forensics-a framework for investigating cyber attacks in cloud environment. *Procedia Computer Science*, 85, 149–154.
- Michael Mahesh, K. (2020). Workflow scheduling using improved moth swarm optimization algorithm in cloud computing. *Multimedia Research*, 3(3), 36–43.
- Panchamia, S., & Byrappa, D. K. (2017). Passport, VISA and immigration management using blockchain. In *2017 23rd annual international conference in advanced computing and communications (ADCOM)* (pp. 8–17). IEEE.
- Park, J. H., Park, J. Y., & Huh, E. N. (2017). *Block chain based data logging and integrity management system for cloud forensics* (p. 149). Computer Science & Information Technology.
- Pasquale, L., Hanvey, S., Mcgloin, M., & Nuseibeh, B. (2016). Adaptive evidence collection in the cloud using attack scenarios. *Computers & Security*, 59, 236–254.
- Patel, D., Balakarthykeyan, & Mistry, V. (2020). *Border control and immigration on blockchain*. Springer.
- Patel, D., & Mistry, V. (2018). Border control and immigration on blockchain. In *International conference on blockchain* (pp. 166–179). Cham: Springer.
- Patil, S., Kadam, S., & Katti, J. (2021). Security enhancement of forensic evidences using blockchain. In *2021 Third International Conference on Intelligent Communication Technologies and Virtual Mobile Networks (ICICV)* (pp. 263–268). IEEE.
- Pourvahab, M., & Ekbatanifard, G. (2019a). An efficient forensics architecture in software-defined networking-IoT using blockchain technology. *IEEE Access*, 7, 99573–99588.
- Pourvahab, M., & Ekbatanifard, G. (2019b). Digital forensics architecture for evidence collection and provenance preservation in iaas cloud environment using sdn and blockchain technology. *IEEE Access*, 7, 153349–153364.
- Rama Krishna, M. (2021). Hybrid grasshopper optimization and bat algorithm based DBN for intrusion detection in cloud. *Multimedia Research*, 4(4), 31–38.
- Rane, S., & Dixit, A. (2019). BlockSLaaS: Blockchain assisted secure logging-as-a-service for cloud forensics. In *International conference on security & privacy* (pp. 77–88). Singapore: Springer.
- Santra, P., Roy, P., Hazra, D., & Mahata, P. (2018). Fuzzy data mining-based framework for forensic analysis and evidence generation in cloud environment. In *Ambient communications and computer systems* (pp. 119–129). Singapore: Springer.
- Shahbazi, Z., & Byun, Y. C. (2022). NLP-based digital forensic analysis for online social network based on system security. *International Journal of Environmental Research and Public Health*, 19(12), 7027.
- Shareef, S. M., & Rao, D. R. S. (2018). A hybrid learning algorithm for optimal reactive power dispatch under unbalanced conditions. *Journal of Computational Mechanics, Power System and Control (JCMPS)*, 1(1).
- Stelly, C., & Roussev, V. (2017). SCARF: A container-based approach to cloud-scale digital forensic processing. *Digital Investigation*, 22, S39–S47.
- Thomas, R., & Rangachar, M. J. S. (2018). Hybrid optimization based DBN for face recognition using low-resolution images. *Multimedia Research*, 1(1), 33–43.
- Tummalapalli, S. R. K., & Chakravarthy, A. S. N. (2021). Multi-level and mutual log integrity preservation approach for cloud forensics using public key infrastructure. *Int. J. Sci. Res. in Network Security and Communication*, 9(1).
- Wang, J. (2021). Grey wolf optimization and crow search algorithm for resource allocation scheme in cloud computing: Grey wolf optimization and crow search algorithm in cloud computing. *Multimedia Research*, 4(3).
- Wang, S., Zhang, Y., & Zhang, Y. (2018). A blockchain-based framework for data sharing with fine-grained access control in decentralized storage systems. *IEEE Access*, 6, 38437–38450.
- Xia, Q. I., Sifah, E. B., Asamoah, K. O., Gao, J., Du, X., & Guizani, M. (2017). MeDShare: Trust-less medical data sharing among cloud service providers via blockchain. *IEEE Access*, 5, 14757–14767.
- Yang, Y., Chen, H., Heidari, A. A., & Gandomi, A. H. (2021). Hunger games search: Visions, conception, implementation, deep analysis, perspectives, and towards performance shifts. *Expert Systems with Applications*, 177, Article 114864.
- Zawoad, S., Dutta, A. K., & Hasan, R. (2015). Towards building forensics enabled cloud through secure logging-as-a-service. *IEEE Transactions on Dependable and Secure Computing*, 13(2), 148–162.

Preserving Integrity of Evidence with Blockchain Technology in Cloud Forensics for Immigration Management

Sahadev Maruti Shinde and Venkateswara Rao Gurralla

GITAM School of Engineering, Visakhapatnam, Andhra Pradesh, India

<https://doi.org/10.26636/jtit.2023.164522>

Abstract — As the popularity of cloud computing increases, safety concerns are growing as well. Cloud forensics (CF) is a smart adaptation of the digital forensics model that is used for fighting the related offenses. This paper proposes a new forensic method relying on a blockchain network. Here, the log files are accumulated and preserved in the blockchain using different peers. In order to protect the system against illegitimate users, an improved blowfish method is applied. In this particular instance, the system is made up of five distinct components: hypervisor (VMM), IPFS file storage, log ledger, node controller, and smart contract. The suggested approach includes six phases: creation of the log file, key setup and exchange, evidence setup and control, integrity assurance, agreement validation and confidential file release, as well as blockchain-based communication. To ensure efficient exchange of data exchange between the cloud provider and the client, the methodology comprises IPFS. The SSA (FOI-SSA) model, integrated with forensic operations, is used to select the keys in the best possible way. Finally, an analysis is conducted to prove the effectiveness of the proposed FOI-SSA technique.

Keywords — cloud computing, cloud forensics, FOI-SSA model, improved blowfish

1	2
HSO	Harmony search optimization
ECC	Elliptical curve cryptography
IPFS	Interplanetary file system
LGoE	Logical graph of evidence
LA	Lion algorithm
RSA	Rivest-Shamir-Adleman
SRVA	Secure ring verification based authentication
SIEM	Security data information and event management
SA-DECC	Sensitivity aware deep ECC
SSA	Sparrow search algorithm
SSO	Salp swarm optimization
SRVA	Secure ring verification based authentication
TPS	Transaction per second

Tab. 1. Abbreviations and terms used in this paper.

Abbreviation	Description
1	2
AES	Advanced encryption standard
BlockSLaaS	Blockchain assisted secure logging as-a-service
BES	Bald eagle search
CF	Cloud forensics
CC	Cloud computing
CSP	Cloud service provider
CFI	Cloud forensic investigator
CADF	Cloud auditing data federation
DMTF	Distributed management task force
DBO	Dynamic butterfly optimization
EB	Ethereum blockchain
FCS	Fuzzy based smart contracts
FIO	Forensic investigation optimization

1. Introduction

When individuals leave their countries and move to other states, we are dealing with migration [1]–[5]. Such persons go through immigration-related processes in order to become permanent residents of their new country. Usually, the procedure is very complicated. The applicant needs to get a visa [1] and then apply for a permanent residency permit which may later be converted into citizenship [6]–[11]. This process becomes easier if the applicant is backed by a company or if their family member is already a resident of the country concerned [12]–[14]. Due to the strict immigration laws in effect in some countries, people revert to illegal practices and attempt to infiltrate states without permission [15], [16]. This leads to illegal immigration [17]–[19] – an issue faced by almost every other country in the world [20]–[22].

The proposed work keeps track of immigrants by storing several relevant pieces of information in the form of immutable [6] and unique blockchain records [23], [24]. When a person is suspected of illegal immigration, their official documents are

compared with the record stored using blockchain [25]–[27], i.e. a distributed ledger [28], [29].

Blockchain is a network of fault-tolerant and distributed servers that contain shared, duplicated, and distinct content [30]. The management of a blockchain is cheap and quick, since it is immutable and cannot contain false or duplicate information [31]–[33]. Blockchain can process fingerprints, facial recognition, and retinal scanning biometric data [17], [18]. Blockchain-based reactive data can be secured using protective confidentiality encryption, limiting its use to authorized entities only [34].

The novelty of this work lies in the fact that a novel blockchain-based CF scheme is proposed, where an improved blowfish mechanism is deployed for encryption purposes, and in exploiting the FOI-SSA algorithm for creating an optimal key. The paper is set up as follows. After the related works review given in Section 2, in Section 3 the project is presented and the model created is described. The FOI-SSA model recommended for generating the best key is described in Section 4. Section 5 presents the conclusions.

2. Literature Review

This section surveys the eight existing blockchain-dependent evidence integrity preservation methods used in CF. Rane and *et al.* [1] proposed the forensic-aware BlockSLaaS model to steadily process and store logs by addressing multi-stakeholder collusion issues and facilitating confidentiality and integrity. CFI was capable of accessing logs for forensic purposes, using BlockSLaaS to protect the logs' privacy. However, the method failed to validate whether the service provider guaranteed precise logs. Jain *et al.* [2] presented a blockchain method for preserving the integrity of log files. IPFS and the blockchain technology were combined to transform a centralized storage system into a decentralized one. The integrity of log files was preserved by storing log files in blockchain. Thanks to such an approach, the system was used for storing huge log files at a minimal cost. However, the method failed to maximize CSP trust by minimizing CSP dependencies.

Pourvhab *et al.* [3] presented an SRVA scheme for protecting the system against unauthorized users. To ensure even better protection of the cloud platform, the secret keys were optimally produced by utilizing the HSO technique. In this case, the server stored the data after they had been encrypted with the use of the SA-DECC algorithm. By modifying FCS, such a strategy allowed the user to track down data and LGoE collected with the use of blockchain enabled the evidence to be studied. However, the proposed method failed to improve the digital forensics model. Dalezios *et al.* [4] proposed the DMTF with CADF standard for CF. The authors improved the Apache Cloud Stack platform by employing CADF activity tracking adopted in an Open Stack and made it more forensically reverberant. Stelly *et al.* [5] developed a method relying on automated container deployment and orchestration platforms to attain improved performance in digital forensics.

The results showed that the distributed container-based approach offered a workable technical foundation for addressing the increased data volumes in digital forensic investigations.

Park *et al.* in [6] presented a permission blockchain-based data integrity management system for CFs. Such a method was capable of certifying the integrity of data while processing more transactions. However, there is an issue that the evaluation of performance cannot be made on anticipated data dimension. However, the model can be utilized as one of the methods for addressing security-related issues in cloud platforms. It failed, however, to accumulate network data by performing simulations concerned with computing precise TPS. Dasaklis *et al.* [7] described a CF method relying on the available blockchain-based technologies. The approach provided a detailed review of the various advantages and shortcomings of the mutually beneficial relationship between blockchain technology and the current digital forensics approach. Unfortunately, the method failed to identify different research issues in digital forensics. Irfan *et al.* [8] presented a model using SIEM to address the problem of effective evidence collection in CFs. The method shared evidence with cloud users, whenever needed. The proposed method helped perform detailed CF by adapting evidence, but failed to improve the performance of the solution by applying advanced optimization techniques.

3. Blockchain-based Protocol Developed for Maintaining Integrity in CF

Anti-tampering and privacy protection are two critical security requirements in cloud computing environments. Figure 1 shows the outline of the proposed architecture. In judicial forensics, maintaining privacy is a top priority. The suggested technique adopts an appropriate mechanism for maintaining confidentiality and anonymity, ensuring that no private data is released during the derivation function of a blockchain-based process. The system incorporates eight elements, including hypervisor, virtual machine, node controller, log ledger, IPFS file storage, blockchain network, CFI, and smart contract.

3.1. Initialization Step

The start-up phase involves launching virtual machines, hypervisors, node controllers, IPFS cloud storage, smart contracts, blockchain networks, CFI, and log ledgers. The following is a more detailed depiction of each entity. A virtual machine (VM) is a computational source that runs programs using software, rather than a real computer. The hypervisor is software that creates and operates a collection of virtual machines, allowing one host to handle several guest VMs, by sharing resources virtually. The nodes controller gathers logs from all virtual platform sources via log libraries and creates log entries for each log. IPFS cloud storage is a file transfer mechanism depending on cryptography hashes, that can be readily stored on the blockchain and regulated to effectively store and transfer large files, while smart contract acts as a set

of applications that are kept on the blockchain and continue to run when specific conditions are satisfied.

The blockchain network, in turn, offers ledger and smart contract functions to varied apps, and if questionable actions on the cloud take place, the CFI is tasked with gathering and reviewing evidence. The last resource component is the log ledger which contains a set of recorded results with a timestamp. Therefore, it serves as a helpful proof for initiating legal action against a suspect. The ledger aids in the preservation of the chronology of created logs.

Table 1 contains all acronyms and abbreviations used in this paper, while Tab. 2 summarizes the symbols used.

Tab. 2. Symbols used in of proposed evidence integrity preservation mechanism.

Symbol	Description
$M_{P\text{PWD}}$	Password of node controller
M_{ID}	User ID of node controller
K_M	Key of node controller
T	Time stamp
Hd	Host ID
L	Log file
P	Node controller program to record log file
pk	Public key
\otimes	Interpolation
\oplus	Ex-or operation
R_{Hd}	Requested ID
$\text{en}(\cdot)$	ECC encryption
S_M	Service name
$K(\cdot)$	Kernel transform
r	Random number
REQ	Integrity assurance request message
$h(\cdot)$	Hashing
S_{PWD}	Session password
K_L	Hypervisor key
A	Acknowledgement message
Q_{PWD}	CFI Password
Q_{Hd}	CFI ID
IA	Integrity assurance

3.2. Creation of Log File

At this stage, the user password M_{Hd} and user ID $M_{P\text{PWD}}$ are formed by the user, which accumulating logs from every each resource of the virtual podium. M_{Hd} and $M_{P\text{PWD}}$ are saved in the hypervisor as M_{Hd}^* and $M_{P\text{PWD}}^*$. The node controller key is produced after obtaining the user’s credentials. The key is created by XOR-ing the public key and the modulus of a random key. After combining the resulting product with the encrypted user ID, the modulus is used to generate the node controller key as:

$$K_M = |\text{en}(M_{Hd}^*) \bmod (r) \oplus pk|. \quad (1)$$

The Log L is formed in the hypervisor with the requested ID of user R_D , time stamp T , and service name S_M for Hd , as:

$$L = \langle Hd, T, R_D, S_M \rangle. \quad (2)$$

Similarly, the node controller key K_M , L , and encoded node controller programmes for recording the log files are provided to the node controller as:

$$K_M, L, \text{en}(P). \quad (3)$$

Thus, the node controller key is saved as K_M^* and the node controller program is set to trace the log file.

3.3. Key Setup and Exchange Process

Once the log file generation procedure is has been completed, three entities: the node controller, hypervisor, and log ledger, are used to start the key setup and exchange process. The stored node controller keys are given to the hypervisor and saved as K_M^{*R} . The hypervisor key is created by adding the encrypted node controllers programs and the kernel transformation of an arbitrary integer with the stored key. The final hypervisor key is generated by XOR-ing the acquired result with the hash timestamp Ts , which is modelled as:

$$K_L = h(Ts) \oplus \text{en}(p) || K(r). \quad (4)$$

The hash of the finalized hypervisor key is proceeded here to generate the session password S_{PWD} , which is then supplied to the node controller and saved as S_{PWD}^* . As a result, the session password is:

$$S_{\text{PWD}} = h(K_L). \quad (5)$$

Next, the acquired hypervisor key is saved as K_L^* in the log ledger. The hash of the stored hypervisor key is saved in M_1 and passed to the node controller, where it is saved as M_1^* :

$$M_1 = h(K_L^*). \quad (6)$$

If $M_1^* = S_{\text{PWD}}$, the ledger is confirmed and the confirmation occurs in the node controller.

3.4. Evidence and Contract Phase

For the sake of achieving privacy, the CFI and smart contract are used. The CFI ID Q_{Hd} and password Q_{PWD} are created during this phase and the credentials are passed into a the smart contract that is saved as Q_{Hd}^* and Q_{PWD}^* . Furthermore, the acknowledgment packet containing an encoded node control program, an the encoded ID, the cloud hashing forensic researcher ID, and the header are given to CFI and saved as A^* :

$$A = \langle \text{en}(P), \text{en}(R), h(Q_{Hd}), \text{Header} \rangle. \quad (7)$$

The evidence is formed by XOR-ing the hash message and secure CFI ID, which is kept in the smart contract as EP^* and modelled as:

$$EP = h(A^*) \oplus \text{en}(Q, D). \quad (8)$$

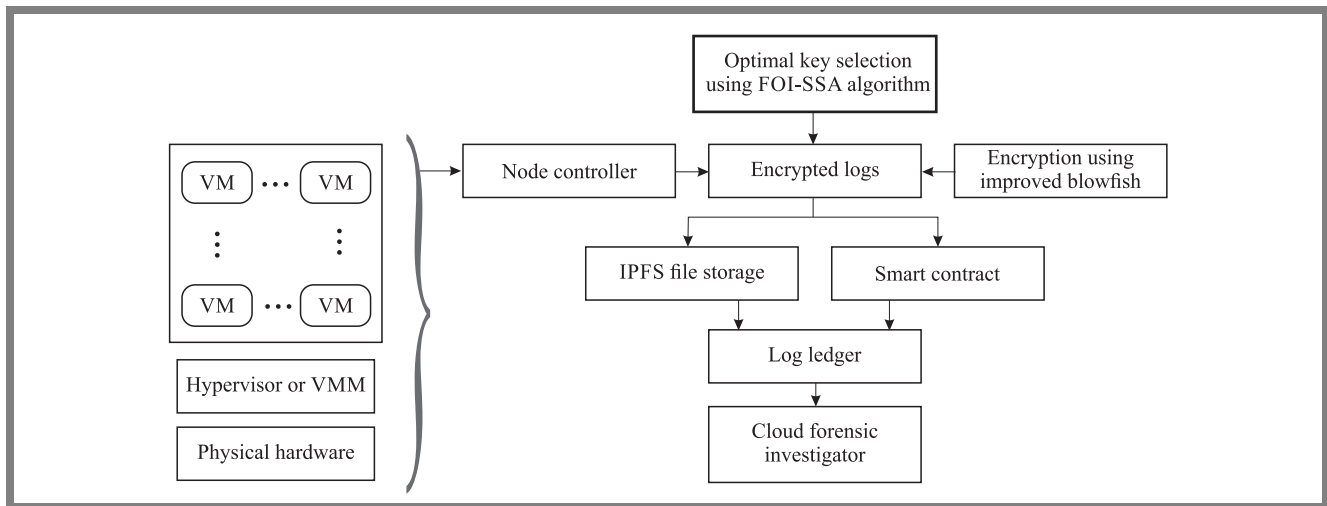


Fig. 1. Overall system model block diagram for evidence integrity preservation for cloud forensics.

The confirmation message is created by XOR-ing the saved evidence with the hashed message that is written as:

$$V = EP^* \oplus h(A). \tag{9}$$

If $V = en(Q_{Hd})$, then the validation was is considered accomplished and the information was is sent to CFI.

3.5. Integrity Assurance

Three entities are involved in this process: node controller, hypervisor, and CFI. The user ID, the request message and the stored key of the node controller are initially verified by the hypervisor that is expressed as:

$$M_{Hd}, REQ, K_M^*. \tag{10}$$

The user ID and the saved node controller key are verified by the hypervisor. Then, the message is created by XOR-ing the hash node controller key, the encoded shared key, and the hash hypervisor key, such as:

$$M_1 = h(K_N^*) \oplus en(pk) \oplus h(K_L). \tag{11}$$

The login password is formed by XOR-ing the hashed times-tamp with the encoded public key as:

$$S_{PWD} = h(Ts) \oplus en(pk). \tag{12}$$

The resultant message and session passcode are given into the CFI, which performs integrity assurance operations by XOR-ing the message and session passwords and storing the result in the hypervisor as:

$$IA = (M_1^* \oplus S_{PWD}). \tag{13}$$

Level 2 verification is calculated based on integrity security operations, using the saved integrity assurance and the saved message as:

$$V_2 = I_A^* \oplus M_1^*. \tag{14}$$

If $V_2 = S_{pwd}$, the guaranty is permitted. The required message and the CF ID are then sent to the node controller where the CF ID is saved.

3.6. Agreement and Confidential File Release

For agreement and private file release, the node controller, the CFI, and the blockchain network are considered. The CF ID and the request message are supplied to the node controller in this phase. Validation of the CF ID is carried out here in order to determine which one is genuine. Furthermore, two messages are produced, the first being formed by XOR-ing the encoded log and the encoded public key as:

$$R = en(log) \oplus en(pk). \tag{15}$$

The other message is created by combining the public key with a value, and then combining the result with the hash Req message as:

$$R_G^* = H(IREQ) || (pk) \Theta r. \tag{16}$$

The last message is created by XOR-ing the first and second messages, and then feeding them to the CFI and storing them as M_1^* , as shown in:

$$R^R = M_1^* \oplus R_G^Q. \tag{17}$$

The CFI creates two messages, the first of which is created by XOR-ing the last message with the second message. The second message is created by combining the public key with a randomized value, and then combining the result with the hash Req packet as:

$$R_G^Q = H(IREQ) || (pk) \Theta r. \tag{18}$$

By XOR-ing the initial message with the encoded public key, the log is created. If $\langle S, P \rangle = I(log)$, then it is found to be satisfactory and is sent again, and then a contact between the CFI and the blockchain network is created.

3.7. Improved Blowfish Algorithm

The blowfish scheme is highly efficient and is suitable for hardware implementation and related modeling [35]. However, to enhance the key management mechanism, a modified version of blowfish is introduced, as follows:

- the input includes 64 bit data,

- it includes 64-bit block ciphers with irregular key lengths,
- it includes four 32-bit S arrays and P boxes. The S array has 18 of 32-bit subkeys, while each P box comprising 256 entries,
- it comprises two elements: a key-expansion part and a data-encryption part.

The F operation employs four substitution boxes, each consisting 256 32-bit entries [36]. Conventionally, if block XL is divided to 8-bit blocks a, b, c, d , then the operation $F(XL)$ is shown as in Eq. (19). As per the modified blowfish model, $F(XL)$ is modelled as in Eq. (20):

$$F(XL) = [(P_{1,a} + P_{2,b} 2^{32}) \oplus P_{3,c}] + P_{4,d} 2^{32}, \quad (19)$$

$$F(XL) = [(P_{1,a} \oplus P_{3,c}) + (P_{2,b} \oplus P_{4,d}) 2^{32}]. \quad (20)$$

3.8. Blockchain-based Communication Phase

The blockchain-oriented communication stage is used to securely store and process logs, allowing for effective control of access to CFI and log integrity checking. An attack on the cloud can be carried out by a malevolent employee or an outside attacker. The functions that take place on the cloud platform generate logs for each VM operation, such as network interaction and VM setup logs. These logs are not power-independent, which means that if the VM is turned off, the data stored therein are lost. The suggested technique retrieves logs from Internet platforms and stores them in secondary memory storage to ensure data security and integrity.

The keys denoted by pk are optimally chosen via the FOI-SSA model. Figure 2 shows solutions in which nn indicates the overall count of keys. The objective Obj is to raise the key breaking time kbr as:

$$Obj = \max(kbr). \quad (21)$$

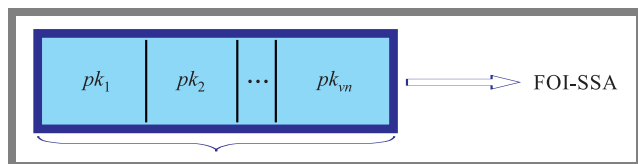


Fig. 2. Solution encoding scheme.

3.9. Proposed FOI-SSA Model for Optimal Key Generation

To achieve better convergence, FIO [37] is combined with the SSA model [38] to form FOI-SSA. Self-improvement of the optimization schemes results in better accuracy [39]– [42]. The behavior of the sparrows and formulated corresponding rules are described as:

- 1) The producers are typically highly energized. Assessment of each person’s fitness values generates information about their energy reserves;
- 2) As individual sparrows start to chirp, the producers are required to direct all scavengers to the safe area when the alert value exceeds the safety level;
- 3) Every sparrow proceeds to production in accordance with how often it seeks out larger food sources, but the ratio of

scavengers to producers becomes higher across the board. The producers would act as he sparrows with maximum energy levels. Numerous starving scavengers are inclined to fly towards different locations in search for food, to gain energy;

- 4) Scroungers look for food by emulating a farmer who actually produces the healthiest food. To increase their predation rate, certain scavengers may keep a tight eye on the producers and engage in food wars;
- 5) Sparrows in the center of the group haphazardly walk to be close to others when the sparrows at the group’s periphery are aware of danger and quickly go into the safe area to take a better position.

As per FOI-SSA, the chaotic-based OBL is performed to generate opposite solutions that ensure a good convergence rate.

The location of the sparrows is represented by:

$$Y = \begin{bmatrix} Y_{1,1} & Y_{1,2} & \dots & Y_{1,a} \\ Y_{2,1} & Y_{2,2} & \dots & Y_{2,a} \\ \vdots & \vdots & \vdots & \vdots \\ Y_{s,1} & Y_{s,2} & \dots & Y_{s,a} \end{bmatrix}. \quad (22)$$

This implies the sparrow count and the size of the optimized variable. The fitness of the sparrow is defined by Eq. (23), which also addresses the fitness of the individuals.

$$F_Y = \begin{bmatrix} f [(Y_{1,1} \ Y_{1,2} \ \dots \ Y_{1,a})] \\ f [(Y_{2,1} \ Y_{2,2} \ \dots \ Y_{2,a})] \\ \vdots \\ f [(Y_{s,1} \ Y_{s,2} \ \dots \ Y_{s,a})] \end{bmatrix}. \quad (23)$$

The locations of producers are updated as per rules 1–2 and:

$$Y_{c,d}^{r+1} = \begin{cases} Y_{c,d}^r e^{\frac{-c}{\alpha \cdot it_{\max}}} & \text{if } C_2 < st \\ Y_{c,d}^r + P \cdot M & \text{if } C_2 \geq st \end{cases}. \quad (24)$$

In Eq. (24), r represents the iteration, \max implies the maximum iteration, α is an arbitrary integer, st and C_2 are the safety threshold and the alarm value, and P is an arbitrary integer. M denotes a matrix of $1 \times d$ with element 1.

The scroungers follow rules 4–5. As stated earlier, various scroungers track producers. In FOI-SSA, the scrounger’s position is updated using FIO as:

$$Y(i)_{\text{new}} = Y_{B_{ij}} + ra_{10}^*(Y_{B_{ij}} - Y_{B_{rj}}) + ra_{11}^*(Y_{\text{best}} - Y_{B_{ij}}), \quad (25)$$

where ra_{10} and ra_{11} are arbitrary integers (0 and 1), Y_{best} implies the best position, B_i denotes the agent. In addition, in FOI-SSA, Cauchy’s mutation is performed as:

$$Y(i)_{\text{new}} = Y_{\text{best}} + Y_i^* \text{cauchy}(0, 1). \quad (26)$$

In addition, the model as per rule (6) is:

$$Y_{c,d}^{r+1} = \begin{cases} Y_{\text{best}}^r + \gamma \cdot |Y_{c,d}^r - Y_{\text{best}}^r| & \text{if } f_c < f_u \\ Y_{c,d}^r + Z \cdot \left(\frac{|Y_{c,d}^r - Y_{\text{worst}}^r|}{(f_c - f_w) + \varepsilon} \right) & \text{if } f_c = f_u \end{cases}, \quad (27)$$

where γ indicates the step size control parameter with a variance of 1 and a mean value of 0, R_{host} denotes the current global optimal location, $Z \in [-1, 1]$ denotes the route of the sparrow, f_c stands for the fitness value of the current sparrow, f_w and f_u are the worst fitness value and the current global best, ε is a small constant for avoiding the zero-division-error, and Y_{host} denotes the position at the center of the population.

4. Results and Discussion

The proposed CF integrity management plan has been created using Java and CloudSim. The performance of the FOI-SSA system was computed over EB [2], AES, ECC, RSA, El-Gamal, Signcryption, ECC + IPFS [43], DBO, BES, SSO, FIO, and SSA, taking into consideration such metrics as memory, detection rate, etc. In this case, the assessment was performed by altering the key size from 64 to 128 and the user count from 200 to 400.

4.1. Detection Rate Analysis

The detection accuracy of the proposed FOI-SSA algorithm is evaluated in comparison with traditional methods, for various key sizes of 64 and 128. Estimates concerning the FOI-SSA scheme, made over EB [2], AES, ECC, RSA, El-Gamal, Signcryption, ECC + IPFS [34], DBO, BES, SSO, FIO and SSA approaches are presented in Figs. 3 and 4 for user counts of 100, 200, 300 and 400. Here, the proposed FOI-SSA model showed an enhanced detection rate over EB, AES, ECC, RSA, El-Gamal, Signcryption, ECC + IPFS, DBO, BES, SSO, FIO and SSA. In Fig. 3, a higher detection rate is observed for

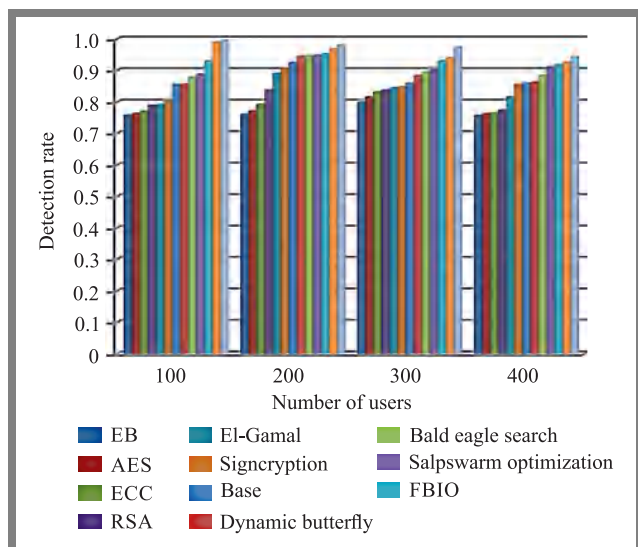


Fig. 3. Detection rate of FOI-SSA vs. other approaches, for a key size of 64.

FOI-SSA, with the user count of 100 for a key size of 64. With an increase in user count, the detection rates for FOI-SSA decreased for a key size of 64. This progression is the result of the enhanced blowfish concept and the integrated optimal key creation. Thus, the benefit of FOI-SSA is recognized over EB, AES, ECC, RSA, El-Gamal, Signcryption, ECC + IPFS, DBO, BES, SSO, FIO, and SSA.

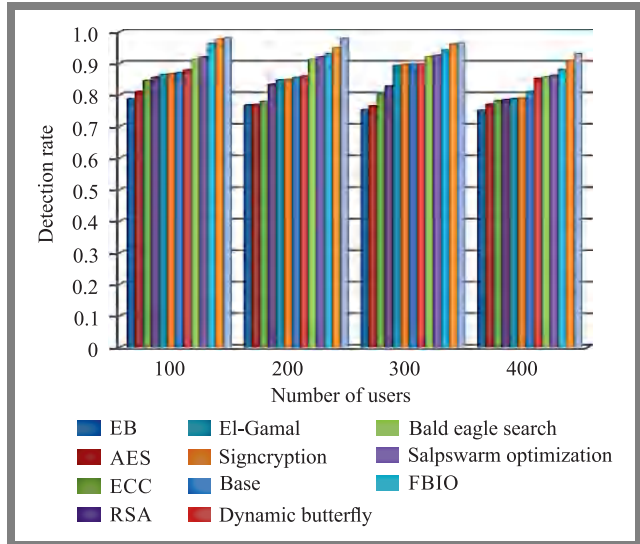


Fig. 4. Detection rate of FOI-SSA vs. other approaches, for a key size of 128.

4.2. Memory Usage Analysis

Figures 5–6 show an analysis of memory usage for FOI-SSA and other algorithms, for 128 and 64 key sizes. 8.5 MB of memory are used FOI-SSA for 100 users and a 64 key size, while other algorithms achieved higher utilization rates. Memory usage grows along with an increase in user count. These data help choose the optimal key and improve the blowfish concept.

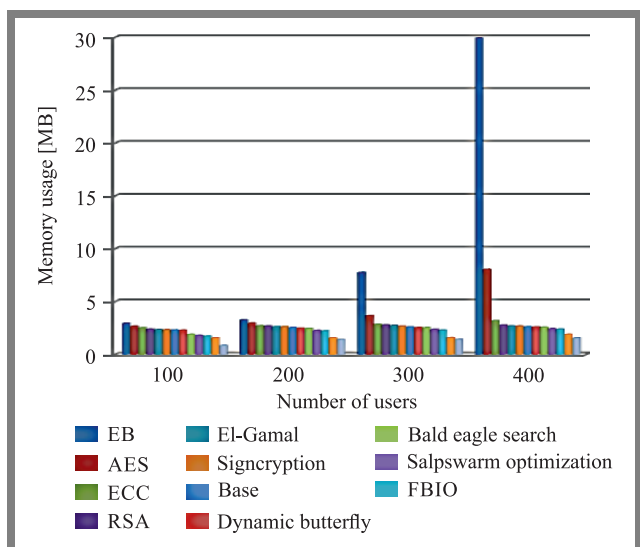


Fig. 5. Memory usage analysis of FOI-SSA vs. other approaches, for a key size of 64.

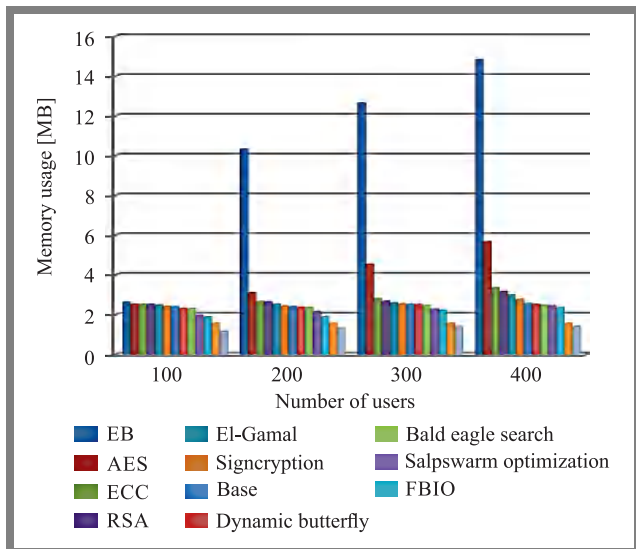


Fig. 6. Memory usage analysis of FOI-SSA vs. other approaches, for a key size of 128.

4.3. Time Analysis

Tables 3 and 4 show computational times for 128 and 64-bit keys. The analysis was performed for various user counts. For all key sizes, the time increases along with the user count. For 100 users, the computational time is shorter, but when the user count reaches 400, the time is longer for all other methods. However, FOI-SSA achieved a shorter time interval than its competitors. These advances are the result of using the blowfish concept and creating the optimal key.

4.4. Encryption and Decryption Time Analysis

The encryption time for various key sizes is summarized in Tables 5–6, while Tables 7–8 show the decoding time. For FOI-SSA, the encryption time is shorter for each key size. For user counts of 100 and 200, the decryption time is shorter with a 64-bit key which also requires less computational time for encryption. Thus, FOI-SSA achieves the shortest decryption and encryption times compared with its competitors, as shown in the tables.

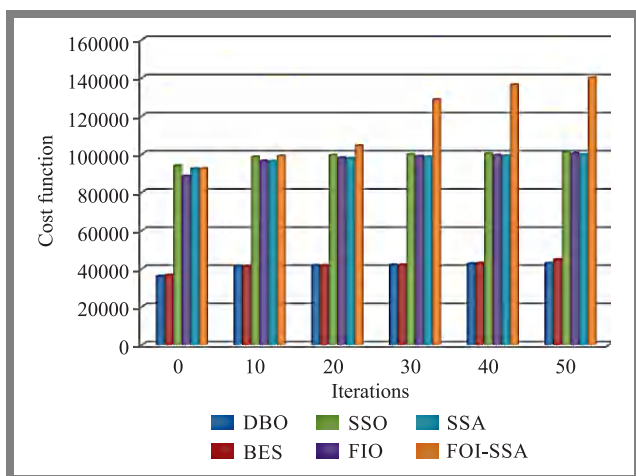


Fig. 7. Convergence analysis: FOI-SSA vs. other schemes.

4.5. Convergence Analysis

Convergence analysis of the proposed FOI-SSA system and the comparison of its performance with former models is shown in Fig. 7. FOI-SSA offers enhanced outcomes – the key break time at the 50-th iteration is 140004, meaning that it is higher than in the case of DBO, BES, SSO, FIO, and SSA. DBO’s poor results were disclosed by obtaining a reduced key break time. Therefore, the goal is achieved, as shown in Eq. (21).

4.6. Attack Analysis

Figures 8 and 9 show the outcomes of research on various attack types, including inside and password spoofing attacks, for various key sizes and for varied user counts. Figure 8 shows the average key breakage time for inside and password spoofing attacks. While vulnerable to insider and password spoofing attacks, the proposed FOI-SSA approach has revealed a higher key break time. This is achieved due to a better blowfish concept and optimal key creation in FOI-SSA.

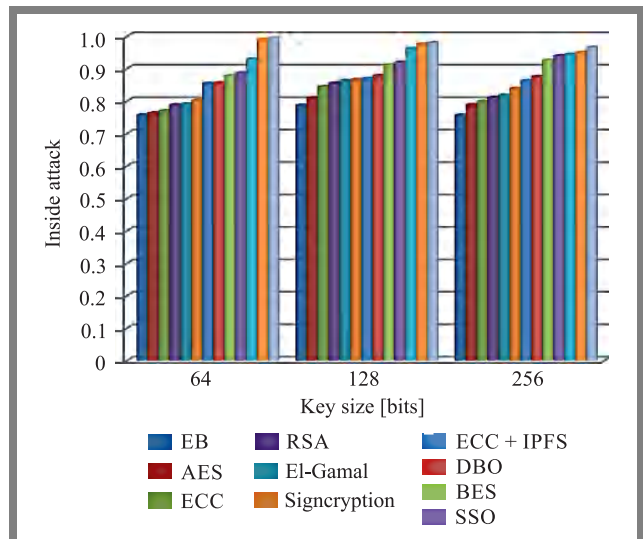


Fig. 8. Inside attack: FOI-SSA vs. other schemes.

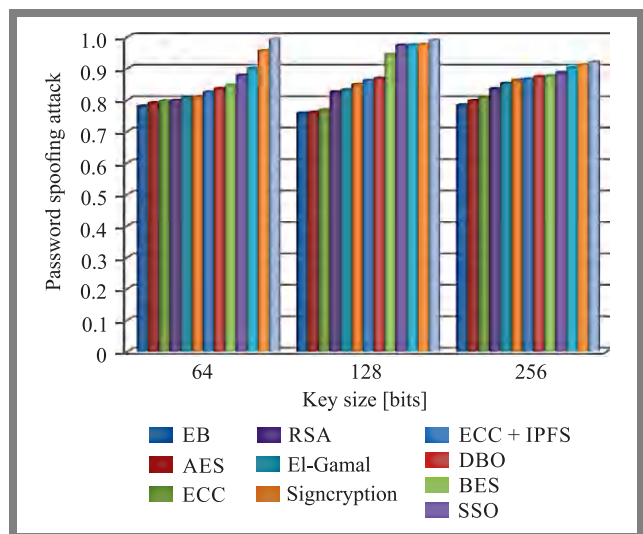


Fig. 9. Password spoofing attack: FOI-SSA vs. competitors.

Tab. 3. Time analysis using FOI-SSA over others algorithms for a key size of 64 [s].

User count	EB	AES	ECC	RSA	El-Gamal	Signcryption	ECC + IPFS	DBO	BES	SSO	FIO	SSA	FOI-SSA
100	505	504	503	402	351	324	327	221	184	146	110	74	35
200	506	505	505	403	351	324	323	222	185	147	110	74	36
300	509	509	508	405	352	325	324	222	185	147	110	74	36
400	712	709	707	504	453	426	425	223	186	149	110	73	36

Tab. 4. Time analysis using FOI-SSA over others algorithms for a key size of 128 [s].

User count	EB	AES	ECC	RSA	El-Gamal	Signcryption	ECC + IPFS	DBO	BES	SSO	FIO	SSA	FOI-SSA
100	613	612	612	407	355	327	326	217	181	145	109	73	35
200	643	642	641	472	414	377	375	223	187	149	110	73	35
300	702	701	701	487	420	393	391	224	187	149	112	73	37
400	790	789	787	598	546	519	518	226	188	150	113	74	37

Tab. 5. Encryption time for FOI-SSA vs. others algorithms for a key size of 64 [s].

User count	EB	AES	ECC	RSA	El-Gamal	Signcryption	ECC + IPFS	DBO	BES	SSO	FIO	SSA	FOI-SSA
100	25	25	17	16	16	16	16	16	28	0.8	0.7	0.3	0.3
200	25	25	17	17	16	16	16	16	28	0.8	0.7	0.4	0.3
300	25	25	17	17	17	16	16	16	29	0.8	0.7	0.4	0.3
400	27	26	17	17	17	17	16	16	29	1	0.8	0.4	0.3

Tab. 6. Encryption time for FOI-SSA vs. others algorithms for a key size of 128 [s].

User count	EB	AES	ECC	RSA	El-Gamal	Signcryption	ECC + IPFS	DBO	BES	SSO	FIO	SSA	FOI-SSA
100	25	25	16	16	16	17	16	16	3	0.8	0.6	0.4	0.3
200	25	25	17	17	17	17	16	16	3	0.9	0.8	0.4	0.3
300	35	26	17	17	17	17	16	16	3	0.9	0.8	0.5	0.5
400	55	27	18	17	17	17	17	16	4	1	1	0.8	0.7

Tab. 7. Decryption time for FOI-SSA vs. others algorithms for a key size of 64 [s].

User count	EB	AES	ECC	RSA	El-Gamal	Signcryption	ECC + IPFS	DBO	BES	SSO	FIO	SSA	FOI-SSA
100	76	75	48	17	16	16	16	16	16	0.6	0.194	0.2	0.1
200	76	75	48	17	17	16	16	16	16	0.7	0.241	0.2	0.1
300	77	76	49	17	17	16	16	16	16	0.7	0.241	0.2	0.1
400	177	177	50	17	17	17	16	16	16	0.7	0.265	0.2	0.1

Tab. 8. Decryption time for FOI-SSA vs. others algorithms for a key size of [s].

User count	EB	AES	ECC	RSA	El-Gamal	Signcryption	ECC + IPFS	DBO	BES	SSO	FIO	SSA	FOI-SSA
100	124	75	49	16	17	16	16	16	15	0.6	0.2	0.2	0.1
200	179	77	49	17	16	16	16	16	16	0.7	0.3	0.2	0.1
300	259	117	49	17	17	16	16	16	16	0.7	0.4	0.3	0.1
400	275	142	68	17	17	17	17	16	16	1	0.5	0.3	0.2

5. Conclusion

This paper proposes a novel forensic method relying on a blockchain network. In order to protect the system against illegitimate users, an improved blowfish method is used. The system is made up of five distinct elements: hypervisor, node controller, log logger, IPFS file storage, and smart contract.

The suggested method entails six phases, including determination of the log file concept, key arrangement and exchange process, setup and control of evidence, assurance of integrity, agreement validation, release of the confidential file, and the blockchain-based communication phase. The proposed FOI-SSA approach offers an enhanced detection rate compared with EB, AES, ECC, RSA, El-Gamal, Signcryption,

ECC+IPFS, DBO, BES, SSO, FIO, and SSA algorithms. A higher detection rate was observed for FOI-SSA for a user count of 100 and a key size of 64. As the user count increases, the detection rate of FOI-SSA decreases for a key size of 64.

References

- [1] S. Rane and A. Dixit, "BlockSLaaS: Blockchain assisted secure logging-as-a-service for cloud forensics", *Proceedings of International Conference on Security & Privacy*, pp. 77–88, 2019 (https://doi.org/10.1007/978-981-13-7561-3_6).
- [2] P. Jain, "Decentralize log file storage and integrity preservation using blockchain", *International Journal of Computer Science and Information Technologies*, vol. 11, no. 2, pp. 21–30, 2020 (<https://ijcsit.com/docs/Volume%2011/vol11issue02/ijcsit2020110202.pdf>).
- [3] M. Pourvahab and G. Ekbatanifard, "Digital forensics architecture for evidence collection and provenance preservation in IaaS cloud environment using SDN and blockchain technology", *IEEE Access*, vol. 7, pp. 153349–153364, 2019 (<https://doi.org/10.1109/ACCESS.2019.2946978>).
- [4] N. Dalezios, S. Shiaeles, N. Kolokotronis, and B. Ghita, "Digital forensics cloud log unification: Implementing CADF in Apache CloudStack", *Journal of Information Security and Applications*, vol. 54, pp. 102555, 2020 (<https://doi.org/10.1016/j.jisa.2020.102555>).
- [5] C. Stelly and V. Roussev, "SCARF: A container-based approach to cloud-scale digital forensic processing", *Digital Investigation*, vol. 22, pp. S39–S47, 2017 (<https://doi.org/10.1016/j.diin.2017.06.008>).
- [6] J.H. Park, J.Y. Park, and E.N. Huh, "Blockchain based data logging and integrity management system for cloud forensics", *Computer Science & Information Technology*, vol. 149, 2017 (<https://doi.org/10.5121/csit.2017.71112>).
- [7] T.K. Dasaklis, F. Casino, and C. Patsakis, "SoK: Blockchain solutions for forensics", in *Technology Development for Security Practitioners*, B. Akhgar, D. Kavallieros, and E. Sdongos, Eds. Springer Cham, 2021, pp. 21–40 (https://doi.org/10.1007/978-3-030-69460-9_2).
- [8] M. Irfan, H. Abbas, Y. Sun, A. Sajid, and M. Pasha, "A framework for cloud forensics evidence collection and analysis using security information and event management", *Security and Communication Networks*, vol. 9, no. 16, pp. 3790–3807, 2016 (<https://doi.org/10.1002/sec.1538>).
- [9] A.C. Kumar and R. Vimala, "Load balancing in cloud environment exploiting hybridization of chicken swarm and enhanced raven roosting optimization algorithm", *Multimedia Research*, vol. 3, no. 1, pp. 45–55, 2020 (<https://doi.org/10.46253/j.mr.v3i1.a5>).
- [10] R. Battistoni, R. Di Pietro, and F. Lombardi, "CURE-Towards enforcing a reliable timeline for cloud forensics: Model, architecture, and experiments", *Computer Communications*, vol. 91, pp. 29–43, 2016 (<https://doi.org/10.46253/j.mr.v3i1.a5>).
- [11] H. Mahdi, et al., "Vehicular Networks Performance Evaluation Based on Downlink Scheduling Algorithms for High-Speed Long Term Evolution-Vehicle", *International Journal of Interactive Mobile Technologies*, vol. 15, no. 21, 2021 (<https://doi.org/10.3991/ijim.v15i21.22475>).
- [12] Chao Lina, et al., "BSEn: A blockchain-based secure mutual authentication with fine-grained access control system for Industry 4.0", *Journal of Network and Computer Applications*, vol. 116, pp. 42–52, 2018 (<https://doi.org/10.1016/j.jnca.2018.05.005>).
- [13] D.F. Maesa, P. Mori, and L. Ricci, "A blockchain based approach for the definition of auditable access control systems", *Computers and Security*, vol. 84, pp. 93–119, 2019 (<https://doi.org/10.1016/j.cose.2019.03.016>).
- [14] P.T. Duy, H. Do Hoang, N.B. Khanh, and V.H. Pham, "Sdnlog-foren: Ensuring the integrity and tamper resistance of log files for SDN forensics using blockchain", *Proceedings of 2019 6th NAFOSTED Conference on Information and Computer Science (NICS)*, pp. 416–421, 2019 (<https://doi.org/10.1109/NICS48868.2019.9023852>).
- [15] G.G. Dagher, J. Mohler, M. Milojkovic, and P.B. Marell, "Ancile: Privacy-preserving framework for access control and interoperability of electronic health records using blockchain technology", *Sustainable Cities and Society*, vol. 39, pp. 283–297, 2018 (<https://doi.org/10.1016/j.scs.2018.02.014>).
- [16] Hao Gu, L. Wanxin, Mark Nejad, and Chien-Chung Shen, "Access Control for Electronic Health Records with Hybrid Blockchain-Edge Architecture", *2019 IEEE International Conference on Blockchain*, 2019 (<https://doi.org/10.1109/Blockchain.2019.00015>).
- [17] B. Prasanalakshmi, A. Kannammal, and R. Sridevi, "Multimodal biometric cryptosystem involving face, fingerprint and palm vein", *International Journal of Computer Science Issues (IJCSI)*, vol. 8, no. 4, pp. 604, 2011 (URL: <http://ijcsi.org/papers/IJCSI-8-4-1-604-610.pdf>).
- [18] S. Kokilavani, M.D. Vignesh, E. Surya, A. Narendran, and B. Prasanalakshmi, "Enhanced biometric smart key scheme for smart card authentication", *2014 International Conference on Communication and Signal Processing*, pp. 1589–1592. IEEE, 2014 (<https://doi.org/10.1109/ICCSP.2014.6950116>).
- [19] V. Rupapara, F. Rustam, H.F. Shahzadehmood, A. Ashraf, and G.S. Choi, "Impact of SMOTE on imbalanced text features for toxic comments classification using RVVC model", *IEEE Access*, vol. 9, pp. 78621–78634 (<https://doi.org/10.1109/ACCESS.2021.3083638>).
- [20] M. Irfan, H. Abbas, and W. Iqbal, "Feasibility analysis for incorporating/deploying SIEM for forensics evidence collection in cloud environment", *Proceedings of 2015 IEEE/ACIS 14th International Conference on Computer and Information Science (ICIS)*, pp. 15–21, 2015 (<https://doi.org/10.1109/ICIS.2015.7166563>).
- [21] K. Kent, S. Chevalier, T. Grance, and H. Dang, "Guide to integrating forensic techniques into incident response", *NIST Special Publication*, vol. 10, no. 14, pp. 800–806, 2006 (<https://nvlpubs.nist.gov/nistpubs/Legacy/SP/nistspecialpublication800-86.pdf>).
- [22] S.K. Manoj and D.L. Bhaskari, "Cloud forensics – a framework for investigating cyber attacks in cloud environment", *Procedia Computer Science*, vol. 85, pp. 149–154, 2016 (<https://doi.org/10.1016/j.procs.2016.05.202>).
- [23] M. Ma, G. Shi, and F. Li, "Privacy-Oriented Blockchain-based Distributed Key Management Architecture for Hierarchical Access Control in the IoT Scenario", *IEEE Access*, vol. 7, pp. 34045–34059, 2019 (<https://doi.org/10.1109/ACCESS.2019.2904042>).
- [24] L. Pasquale, S. Hanvey, M. Mcgloin, and B. Nuseibeh, "Adaptive evidence collection in the cloud using attack scenarios", *Computers and Security*, vol. 59, pp. 236–54, 2016 (<https://doi.org/10.1016/j.cose.2016.03.001>).
- [25] V.K. Netajihole and G.P. Bhole, "Optimal Container Resource Allocation Using Hybrid SA-MFO Algorithm in Cloud Architecture", *Multimedia Research*, vol. 3, no. 1, pp. 11–20, 2020 (<https://doi.org/10.46253/j.mr.v3i1.a2>).
- [26] A.C. Kumar and R. Vimala, "Load Balancing in Cloud Environment Exploiting Hybridization of Chicken Swarm and Enhanced Raven Roosting Optimization Algorithm", *Multimedia Research*, vol. 3, no. 1, pp. 45–55, 2020 (<https://doi.org/10.46253/j.mr.v3i1.a5>).
- [27] M.K. Mahesh, "Workflow scheduling using Improved Moth Swarm Optimization Algorithm in Cloud Computing", *Multimedia Research*, vol. 3, no. 3, 2020 (<https://doi.org/10.46253/j.mr.v3i3.a5>).
- [28] M. Pourvahab and G. Ekbatanifard, "An efficient forensics architecture in software-defined networking-IoT using blockchain technology", *IEEE Access*, vol. 7, pp. 99573–99588, 2019 (DOI: 10.1109/ACCESS.2019.2930345).
- [29] P. Santra, P. Roy, D. Hazra, and P. Mahata, "Fuzzy data mining-based framework for forensic analysis and evidence generation in cloud environment", *Ambient Communications and Computer Systems*, pp. 119–129, 2018 (https://doi.org/10.1007/978-981-10-7386-1_10).

- [30] S. Aishwarya, R.S. Selvi, and R. Ilakkiya, "Secure public Auditing With Code-Regeneration In Multi Storage Cloud Architecture", 2006 (<https://ijartet.com/1370/v3s15ranganathancseit/conference>).
- [31] S. Wang, Y. Zhang, and Y. Zhang, "A blockchain-based framework for data sharing with fine-grained access control in decentralized storage systems", *IEEE Access*, vol. 6, pp. 38437–38450, 2018 (<https://doi.org/10.1109/ACCESS.2018.2851611>).
- [32] X. Qi, E.B. Sifah, K.O. Asamoah, J. Gao, X. Du, and M. Guizani, "MeDShare: Trust-less medical data sharing among cloud service providers via blockchain", *IEEE Access*, vol. 5, pp. 14757–14767, 2017 (<https://doi.org/10.1109/ACCESS.2017.2730843>).
- [33] S. Zawoad, A.K. Dutta, and R. Hasan, "Towards building forensics enabled cloud through secure logging-as-a-service", *IEEE Transactions on Dependable and Secure Computing*, vol. 13, no. 2, pp. 148–62, 2015 (<https://doi.org/10.1109/TDSC.2015.2482484>).
- [34] P.P. Srivastava, S. Goyal, and A. Kumar, "Analysis of various NoSql database", *2015 International Conference on Green Computing and Internet of Things (ICGCIoT)*, pp. 539–544, 2015 (<https://doi.org/10.1109/ICGCIoT.2015.7380523>).
- [35] M. Agrawal and P. Mishra, "A Modified Approach for Symmetric Key Cryptography Based on Blowfish Algorithm", *International Journal of Engineering and Advanced Technology (IJEAT)*, vol. 1, no. 6, 2012 (<https://www.ijeat.org/wp-content/uploads/papers/v1i6/F0610071612.pdf>).
- [36] R.K. Meyers and A.H. Desoky, "An Implementation of the Blowfish Cryptosystem", *2008 IEEE International Symposium on Signal Processing and Information Technology*, 2008 (<https://doi.org/10.1109/ISSPIT.2008.4775664>).
- [37] J-S. Chou and N-M. Nguyen, "FBI inspired meta-optimization", *Applied Soft Computing*, vol. 93, 2020 (<https://doi.org/10.1016/j.asoc.2020.106339>).
- [38] J. Xue and B. Shen, "A novel swarm intelligence optimization approach: sparrow search algorithm", *Systems Science & Control Engineering*, vol. 8, no. 1, pp. 22–34, 2020 (<https://doi.org/10.1080/21642583.2019.1708830>).
- [39] M.M. Beno, I.R. Valarmathi, S.M. Swamy, and B.R. Rajakumar, "Threshold prediction for segmenting tumour from brain MRI scans", *International Journal of Imaging Systems and Technology*, vol. 24, no. 2, pp. 129–137, 2014 (<https://doi.org/10.1002/ima.22087>).
- [40] T. Renjith and M.J.S. Rangachar, "Hybrid Optimization based DBN for Face Recognition using Low-Resolution Images", *Multimedia Research*, vol. 1, no. 1, pp. 33–43, 2018 (<https://doi.org/10.46253/j.mr.v1i1.a5>).
- [41] J. Devagnanam, N.M. Elango, "Optimal Resource Allocation of Cluster using Hybrid Grey Wolf and Cuckoo Search Algorithm in Cloud Computing", *Journal of Networking and Communication Systems*, vol. 3, no. 1, pp. 31–40, 2020 (<https://doi.org/10.46253/jnacs.v3i1.a4>).
- [42] S.K.M. Shareef and R.S. Rao, "A Hybrid Learning Algorithm for Optimal Reactive Power Dispatch under Unbalanced Conditions", *Journal of Computational Mechanics Power System and Control*, vol. 1, no. 1, pp. 26–33, 2018 (<https://doi.org/10.46253/j.mr.v1i1.a5>).
- [43] P. Purnaye and V. Kulkarni, "BiSHM: Evidence detection and preservation model for cloud forensics", *Open Computer Science*, vol. 12, no. 1, 2022, pp. 154–170 (<https://doi.org/10.1515/comp-2022-0241>).

Sahadev Maruti Shinde

E-mail: sahadevmaruti@gmail.com

GITAM School of Engineering, Visakhapatnam, Andhra Pradesh, India

Venkateswara Rao Gurralla

Professor in Department of Computer Science and Engineering

GITAM School of Engineering, Visakhapatnam, Andhra Pradesh, India



Numerical analysis of encased granular pile with vertical hollow steel pipe

Ravikant S. Sathe¹ · Jitendra Kumar Sharma¹

Received: 18 April 2023 / Accepted: 1 July 2023
© The Author(s), under exclusive licence to Springer Nature Switzerland AG 2023

Abstract

Stone column/granular pile (GP) system has been utilized for supportive adaptable structures built on soft ground. However, in the instance of soft soil, granular piles experience excessive settlement due to inadequate lateral resistance presented by the soft soil in contradiction of bulging. Bulging might be minimized by fortifying the GPs either by encasing them with geosynthetic or by placing geosynthetic disks inside the GPs at an even interval. In the current study, vertical hollow steel pipe is used as an alternative to the above for confinement and increasing the overall stiffness. The encasement effect of vertical hollow steel pipe in granular piles on the load–displacement response is analyzed by a numerical method. The principle target of this investigation is to predict and quantify the effectiveness of the encasement of vertical hollow steel pipe in a single floating granular pile. This investigation focuses on the load–displacement response for different lengths of encasement of hollow pipe and the length to diameter (L/D) ratio of GP. The results show that the load–displacement response of encased GPs improved for the better with the increasing length of encased hollow steel pipe.

Keywords Vertical hollow steel pipe (VHSP) · Granular pile · L/D ratio · Finite element analysis (FEM)

List of symbols

γ_t	Total unit weight	L_e	Length of encasement
γ_s	Saturated unit weight	VHSP	Vertical hollow steel pipe
E	Deformation modulus	FEM	Finite element method
ν	Poisson's ratio	OGP	Unreinforced granular pile
c	Cohesion	EGP	Encased granular pile with VHSP
Φ	Angle of shearing resistance	dia.	Diameter
ψ	Angle of dilatancy	I_r	Inner radius of VHSP
		O_r	Outer radius of VHSP
		IF	Improvement factor
		GESC	Geosynthetic encasement stone columns

Abbreviations

GP	Granular pile
L/D	Length to diameter ratio of pile
L_p	Length of pile
D_p	Diameter of pile

✉ Ravikant S. Sathe
rssathe.phd17@rtu.ac.in

Jitendra Kumar Sharma
jksharma@rtu.ac.in

¹ Department of Civil Engineering, Rajasthan Technical University, Kota, India

1 Introduction

In order to undertake any developmental activities, it is crucial to improve the soft soil deposits that often suffer from excessive settlement and low bearing capacity. Several ground improvement methods have been suggested to achieve this, including dewatering, compaction, dynamic compaction, deep blending, deep densification, jet grouting, compaction grouting, and soil reinforcement. Among these methods, granular piles have emerged as a popular choice for improving the weak ground. This approach involves

Numerical analysis on load-settlement response of reinforced granular blanket over ordinary stone column

Himanshu Gupta^{1*}, Ravikant S. Sathe¹, Jitendra Kumar Sharma²

¹ Research Scholar, Department of Civil Engineering, Rajasthan Technical University, Kota., India.

² Professor, Department of Civil Engineering, Rajasthan Technical University, Kota., India.

ABSTRACT

Stone columns are a more economical and efficient method to enhance the strength of expansive soils. Using a granular blanket over the top of the ordinary stone columns (OSC) improves the drainage and distribution of the applied stress impending from the superstructure. The present study studied the effect of geogrid layers in a granular blanket (GB) over the top of the OSC numerically using 'PLAXIS 2D'. 'Mohr-Coulomb failure criterion was deliberated for the stone column, granular blanket, expansive soil, and elastoplastic behavior is considered for geogrid layers as reinforcement. Present review results are validated with the experimental results and agree greatly. Numerical results show that the construction of a GB with a geogrid layer over the stone column increases stress transformation to the depth of OSC. Thus 'stress concentration' is decreased in the higher zone of the OSC. Likewise, assessing the impact of geogrid layers in a granular blanket on the 'bearing capacity and settlement of OSC, it was observed that it reduces the lateral bulging, settlement and increases the ground's bearing capacity.

Keywords: Geogrid layers, Granular blanket, Stone column, Settlement, Bulging.

OPEN ACCESS 

Received: March 15, 2022


Revised: May 28, 2022

Accepted: July 12, 2022

Corresponding Author:

Himanshu Gupta

him_kota@yahoo.com

 **Copyright:** The Author(s).

This is an open access article distributed under the terms of the [Creative Commons Attribution License \(CC BY 4.0\)](https://creativecommons.org/licenses/by/4.0/), which permits unrestricted distribution provided the original author and source are cited.

Publisher:

[Chaoyang University of Technology](https://www.ijase.in/)

ISSN: 1727-2394 (Print)

ISSN: 1727-7841 (Online)

1. INTRODUCTION

Soft soil deposits cover a lot of regions all over the world, often located in important cities along rivers and seas. The lower shear strength and higher compressibility properties of deposits pose a significant problem to geotechnical engineers. Due to the construction of structures on soft soil, many challenges are expected to occur related to the soft clay layer, such as excessive settlement, significantly if this layer extends to a deep level below the foundation level. A few strategies are accessible to further develop ground conditions, like lime stabilization, granular piles, grouting, compaction, preloading and so on prior to utilizing any of these techniques; it is needed to realize the nearby ground conditions exhaustively. Despite the fact that processes are expensive, tedious, and should be done to choose the most appropriate and applicable ground improvement technique. Improving the ground by stone columns technique overcomes these difficulties by improving soil strength parameters as bearing capacity and decreasing vertical and lateral displacement.

Today, because of the development on unsatisfactory grounds and never-ending suburbia, feel the requirement for further developed strategies for soil like never before. Today, due to the construction on unsuitable lands and urban sprawl, feel the need for improved methods of soil more than ever. In-ground improvement methods, economic justification, effectiveness, and the necessary equipment have been presented all the time. Stone columns are appropriate ground improvement techniques that have been perceived as economical and harmless to the ecosystem techniques. They are called thick columnar components made of granular material in soft soil that various



Forecasting river basin yield using information of large-scale coupled atmospheric–oceanic circulation and local outgoing longwave radiation

Satyawan D. Jagdale, Satishkumar S. Kashid & Ajay U. Chavadekar

To cite this article: Satyawan D. Jagdale, Satishkumar S. Kashid & Ajay U. Chavadekar (2021): Forecasting river basin yield using information of large-scale coupled atmospheric–oceanic circulation and local outgoing longwave radiation, ISH Journal of Hydraulic Engineering, DOI: [10.1080/09715010.2021.1990143](https://doi.org/10.1080/09715010.2021.1990143)

To link to this article: <https://doi.org/10.1080/09715010.2021.1990143>



Published online: 27 Oct 2021.



Submit your article to this journal [↗](#)



View related articles [↗](#)



View Crossmark data [↗](#)



Forecasting river basin yield using information of large-scale coupled atmospheric–oceanic circulation and local outgoing longwave radiation

Satyawan D. Jagdale, Satishkumar S. Kashid and Ajay U. Chavadekar

Department of Civil Engineering, Walchand Institute of Technology, Solapur, India

ABSTRACT

Global and local climate parameters influence the distribution of precipitation over continents. The spatio-temporal distribution of rainfall and the depth of rainfall over a river basin influence the river basin yield. This study deals with the prediction of the river basin scale yield of the 'Upper Bhima River basin' from the Maharashtra State of India. The information on large-scale circulation patterns El Niño-Southern Oscillation (ENSO), Equatorial Indian Ocean Oscillation (EQUINOO) index, Multivariate ENSO Index (MEI), and local meteorological input viz. Outgoing longwave radiation (OLR) has been used to predict the river basin scale yield. The Artificial Intelligence (AI) tool – Genetic Programming (GP) – is used for developing prediction models. Ten different combinations of input variables are attempted for the development of monthly river basin yield models to arrive at the best input variable combination for the best predictions with varying lead times. Also, three combinations of input variables were tested for the prediction of 'Seasonal Yield'. The findings of this research work indicate that GP-derived monthly River Basin Scale Yield forecasting models are successful in the prediction of yield with a correlation coefficient of 0.83. The seasonal yields could be predicted with a correlation coefficient of 0.75.

ARTICLE HISTORY

Received 24 January 2021
Accepted 3 October 2021

KEYWORDS

River basin-scale yield; ENSO; EQUINOO; MEI; OLR; genetic programming

1. Introduction

A reliable prediction of river basin yield in advance helps in improving the management of water resource systems in the rural and urban environment (Chiew et al. 2003). The performance of streamflow prediction models enhances with the use of large-scale atmospheric circulation information and OLR as a local meteorological input along with streamflow at previous time steps (Maity and Kashid 2009).

The yield from a river basin primarily depends upon the rainfall depth, spatial distribution of rainfall over the catchment, the characteristics of the catchment, and losses due to infiltration, seepage, and evapotranspiration. The temporal pattern of basin yield depends upon the volume of water trapped in various dams and reservoirs in a river basin, water used for various purposes from dams, canals, and rivers, return flows of irrigation and releases from reservoirs in a river for ecology and maintaining minimum streamflow in the river.

The association between large-scale climate circulation patterns and hydrologic variables like rainfall and streamflow is termed as 'Hydroclimatic Teleconnection' (Chiew et al. 1998). Indian hydrometeorology is prominently influenced by two large-scale atmospheric circulation patterns viz. 'El Niño-Southern Oscillation (ENSO) from the tropical Pacific Ocean and the 'Equatorial Indian Ocean Oscillation' (EQUINOO) from the Indian Ocean.

El Niño Southern Oscillation is the coupled ocean-atmosphere mode of the tropical Pacific Ocean (Cane 1992). El Niño represents the warming of the Pacific Ocean, while La Niña represents the opposite cooling of the oceans in the same area. This oscillation observed over the Pacific Ocean gives rise to periodic shifts in the interacting winds and sea-surface exchanges. Both El Niño and La Niña

are accompanied by changes in atmospheric pressures between the eastern and western Pacific Ocean, known collectively as ENSO (El Niño Southern Oscillation).

The variation of streamflow with ENSO has been assessed for Indian hydroclimatology (Ashok et al. 2001; Maity and Kashid 2009). The Indian Summer Monsoon Rainfall (ISMR) mainly depends upon ENSO and EQUINOO observed over the tropical Indian Ocean (Gadgil et al. 2004). Murgulet et al. (2017) state that streamflow offers a significant response to the sea surface temperature anomalies. Douglas et al. (2001) had shown a significant relationship between natural variability of the annual flow of river Ganges and ENSO.

Another 'Hydroclimatic teleconnection' influencing 'Indian Summer Monsoon Rainfall' and Streamflows on the Indian Subcontinent is 'Equatorial Indian Ocean Oscillation' (EQUINOO) from the Indian Ocean. It is the atmospheric component of the 'Indian Dipole Mode' (Gadgil et al. 2004). The pattern of internal climate variability with anomalously low sea surface temperatures (SST) off Sumatra and high sea surface temperatures in the western part of the Indian Ocean is known as Indian Ocean Dipole (IOD) mode. IOD mode always occurs with wind and precipitation anomalies (Saji et al. 1999). This mode shows typical characteristics, e.g. significant changes in equatorial zonal wind field (70° E – 90° E, 5° S – 5° N) and seasonal phase locking. Strong empirical evidence of coupling between SST and the wind field through the precipitation field is the characteristics of IOD mode (Saji et al. 1999). EQUINOO can be treated as the atmospheric component of the IOD mode (Gadgil et al. 2004). The convection over the Eastern part of the Equatorial Indian ocean (EEIO) (90° E – 110° E, 10° S – 0°) is negatively correlated with the convection over the Western part of the Equatorial Indian Ocean (WEIO), (50° E – 70° E,

10° S – 10° N) during the Indian summer monsoon season (June to September). The oscillation between these two states is called the EQUINOO (Gadgil et al. 2004). EQWIN, the negative of zonal wind anomaly over the equatorial Indian Ocean region (60–90°E, 2.5° S–2.5° N) is used as the ‘EQUINOO index’ (Gadgil et al. 2004).

MEI is a single index, which is a combination of six different climate parameters such as sea-level pressure (P), zonal wind (U), meridional (V) components of the surface wind, surface air temperature (A), sea surface temperature (S), and total cloudiness fraction of the sky (C) (Wolter and Timlin 1993). MEI is developed and used for monitoring the ENSO index. Gutierrez and Dracup (2001) state that MEI is the best indicator of ENSO with the other indicators in the prediction of streamflow of Colombian river. MEI holds a strong relation in the prediction of the effect of ENSO on rainfall/ runoff than various other ENSO methods and indices for the Williams River catchment, New South Wales, Australia (Kiem and Franks 2001).

Summer rainfall in the tropics is usually associated with organized convective clouds, and these clouds modulate the Outgoing Longwave Radiation observed from satellite sensors. The OLR is electromagnetic radiation of wavelengths ranging between 3 and 100 μm , leaving the earth in the form of thermal radiation. The deep clouds in these largely cumulus convection-dominated regions correspond to more intense precipitation. Hence, OLR is used as a proxy for cumulus activity and precipitation over the river basin under consideration for this study.

OLR Patterns were studied by Gadgil et al. (2004) for studying the extremes of the Indian summer monsoon rainfall. Maity and Kashid (2009) used information of Large-Scale Coupled Atmospheric–Oceanic Circulation (ENSO and EQUINOO) and Local OLR for Short-Term Basin-Scale Streamflow Forecasting. Thus, it is established that the ISMR and the streamflow in the rivers and river basin yield are notably correlated with the ENSO and EQUINOO, through oceanic-atmospheric teleconnection, as well as the local meteorologic input OLR.

The aim of this paper is to investigate the influence of large-scale atmospheric circulation patterns and local meteorological inputs on the ‘River basin yield’. The likely improvement in prediction performance of ‘Monthly basin-scale yield’ supported by local climate input viz. ‘Outgoing Longwave Radiation’ will also be investigated in this work. ‘Basin-scale yield’ models for Monthly and Seasonal predictions are to be developed by adopting the ‘Genetic Programming’ approach.

2. Materials and methods

2.1. Study area-Upper Bhima river basin

The Upper Bhima river basin, which is a sub-basin of the Bhima river basin (Figure 1) of India, is selected for this study. River Bhima is a major tributary of river Krishna. It originates from the ‘Bhima Shankar’ hills of the Western ghats of India, which is 945 meters above the mean sea level. The coordinates of the Upper Bhima basin extend over 17.18° N to 19.24° N Latitudes and 73.20° E to 76.15° E Longitudes. The area of the Upper Bhima river basin is around 45,335 square kilometres.

The climate of the Upper Bhima is spatially and temporally variable. The average rainfall over the basin is 872 mm/year. The Maharashtra state of India has constructed 26 major dams along with 39 medium dams and 480 Minor projects in the Upper Bhima River basin. Figure 1 shows the locations of major reservoirs in the Bhima Basin.

2.1.1. River basin yield

River basin scale yield of water depends upon the rainfall and its distribution over the river basin along with various losses such as infiltration, etc. As explained in Section 1, the use of the El Nino-Southern Oscillation (ENSO) index, along with the Equatorial Indian Ocean Oscillation (EQUINOO) index, potentially improve the performance of river basin-scale streamflow prediction, and it helps in the proper management of water resources (Maity and Nagesh Kumar 2008). The

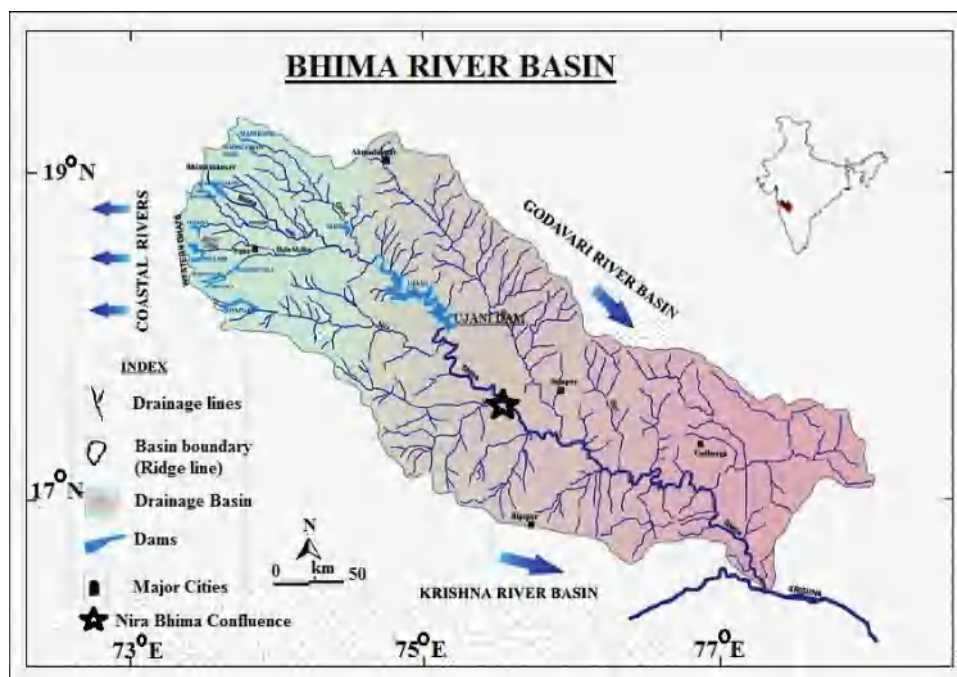


Figure 1. Upper Bhima River Basin with the Location of Major Reservoirs. (Note: Upper Bhima Basin is up to Nira Bhima Confluence indicated by * in the map)

performance of streamflow prediction models enhances with the addition of local meteorological input OLR as it is taken as a proxy to the rainfall (Maity and Kashid 2009). Murgulet et al. (2017) state that streamflow offers a significant response to the sea surface temperature anomalies. The MEI is used in place of ENSO in some combinations as Gutierrez and Dracup (2001) state that MEI is the best indicator of ENSO.

In the Upper Bhima river basin, the reservoirs are formed across various tributaries of river Bhima at suitable sites to meet the varying patterns of water demand for various uses viz. irrigation, drinking water, industry, etc., throughout the year by constructing dams.

There is interdependency in the system of reservoir filling pattern. After filling reservoirs located in the head reaches of the river basin, the water is released in the form of a spill. This water forms 'inflow' to the next adjacent reservoir on the downstream side and so on. To avoid the additional entry as inflow by this spill, we have separated the spill from all the reservoirs lying upstream of the end reservoir. This addition is carried out till the end reservoir lying over a tributary of Bhima. So, the net yield from a basin is calculated as the summation of inflow due to runoff in all the reservoirs, loss of surface water due to evaporation from all the reservoirs, use of water for different purposes from all the reservoirs, and spill from the last reservoir of the basin. After the cross-check and cautious scrutiny of all data, the basin yield values for month, season, and water year are confirmed.

The average monthly yield of the basin for the period of 1972 to 2014 varies from 472 MCM, to 2144 MCM. The river basin yield of June through October is considered as a 'Seasonal Yield' in this study. The variation of seasonal yield for the aforesaid period is from 1323 MCM to 14,707 MCM, indicating a very wide range of variation in yield over a period of time. The average annual yield of the catchment for the same period is about 10,496 MCM.

2.2. Data

- ENSO index data of 'anomaly sea surface temperature (SST)' from the Niño 3.4 region (120°-W to 170°-W and 5°-S to 5°-N) for the period January 1972 to December 2014 are used. The data are obtained from the website of 'National Weather Service', Climate Prediction Centre of 'National Oceanic and Atmospheric Administration' (NOAA). (<http://www.cpc.noaa.gov/data/indices/>)
- EQWIN, NCEP reanalysis data of surface wind are obtained from the 'National Centre for Environmental Prediction' from website <http://www.cdc.noaa.gov/Datasets>. For 'EQUINOO index', Monthly negative of zonal wind anomaly over the equatorial Indian Ocean region (60° - E to 90° - E and 2.5° - S to 2.5° -N) is used.
- Monthly OLR data are taken from the website of NOAA (<http://www.cdc.noaa.gov>) for the region (15° N to 20° N and 72.5° E to 77.5° E) from the year 1979 to 2014.
- Monthly MEI data are obtained from the Earth Science Research Laboratory (ESRI), Physical Science division (<https://www.esri.noaa.gov/psd/enso/mei/>) for the region (30°S-30°N and 100°E-70° W) from the year 1972–2014

- The data required to compute the water yield of Upper Bhima Basin are obtained from the Office Executive Director, Maharashtra Krishna Valley Development Corporation, Govt. of Maharashtra, Pune.

2.3. Methodology

It is scientifically and mathematically challenging to use climate signals for the prediction of basin-scale hydrologic variables because the climatic systems are very complex, and the physics of many systems are still not very clearly understood. The difficulties in modelling such complex systems are considerably reduced by the recent artificial intelligence tools like Artificial Neural Networks (ANN), Genetic Algorithm (GA)-based evolutionary optimizer and Genetic Programming (GP). Hence, such AI tools are tried nowadays for modelling complex systems like basin-scale streamflow forecasting using the information of large-scale atmospheric circulation phenomena.

Genetic Programming (GP) is a member of the evolutionary computing family. GP works on the population of computer programs iteratively and breeds a new generation of programs by applying analogs of naturally happening genetic operations. It is based on Darwinian principles of natural selection and biologically inspired processes (Koza 1992).

The implementation of GP in this work is done using software tools viz. 'Discipulus' (Francone 1998) that is based on an extension of the originally envisaged GP called Linear Genetic Programming (LGP). The LGP evolves sequences of instructions from an imperative programming language or machine language. The LGP expresses instructions in a line-by-line mode. The term 'linear' in Linear Genetic Programming refers to the structure of the (imperative) program representation. It does not stand for functional genetic programs that are restricted to a linear list of nodes only. Genetic programs normally represent highly non-linear solutions in this meaning. (Brameier 2004).

In Hydrology and water resources engineering, GP has been used for drought prediction (Maity and Chanda 2015; Chavadekar and Kashid 2019). GP is also used for rainfall-runoff modeling (Babovic and Keijzer 2002), streamflow forecasting on a monthly scale (Mehr et al. 2014).

2.3.1. Preparatory steps in genetic programming

GP evolves a functional relationship between input information and output information, which is of the form

$$Y^m = f(X^n), \quad (1)$$

where Y^m and X^n are the m-dimensional output vector and n-dimensional input vector, respectively.

In this study, the input vector consists of the Historical Average of net basin yield (monthly/seasonal) ENSO indices, EQUINOO indices, MEI indices, and OLR.

The output consists of river basin yield for the particular month/season. The flow chart of the GP methodology given by Hong and Bhamidimarri (2003) is shown in Figure 2.

2.3.2. Monthly basin yield prediction with one month lead time

‘Monthly River basin scale yield’ is a value of yield during a particular month, which is predicted with one month lead time. For example, the yield of the upcoming month of July is predicted at the end of the Month of June, using the specified inputs.

The river basin yield of a particular month is predicted based on the Historical Average of the Monthly Yield of the particular month (HAM Y), in combinations with Monthly ENSO indices, EQUINOO indices, MEI indices, and monthly OLR values of maximum three previous months as shown in typical Equation 2,

$$Y_t = f \left\{ \begin{matrix} HAM Y_t, (EN_{t-1}, EN_{t-2}, EN_{t-3}), (EQ_{t-1}, EQ_{t-2}, EQ_{t-3}), \\ (MEI_{t-1}, MEI_{t-2}, MEI_{t-3}), (OLR_{t-1}, OLR_{t-2}, OLR_{t-3}) \end{matrix} \right\} \quad (2)$$

For example,

$$Y_{June} = f \left\{ \begin{matrix} HAM Y_{June}, (EN_{May}, EN_{April}, EN_{March}), (EQ_{May}, EQ_{April}, EQ_{March}) \\ (MEI_{May}, MEI_{April}, MEI_{March}), (OLR_{May}, OLR_{April}, OLR_{March}) \end{matrix} \right\} \quad (3)$$

Likewise, ten models are developed as listed in Table 1 and tested for monthly river basin yield prediction.

For the training phase of GP models, the data from 1979 through 1996 (18 years) were used, for ‘validation’, data from 1997 through 2005 (9 years) were used and for testing, data from 2006 through 2014 (9 years) were used.

2.3.3. Prediction of seasonal river basin yield at the May end

The ‘Seasonal Yield’ of the river basin is a single value of yield, expected in the upcoming season from 1st June to 30th October of the particular water year. It is predicted as a ‘single value’ at the end of the Month of May for

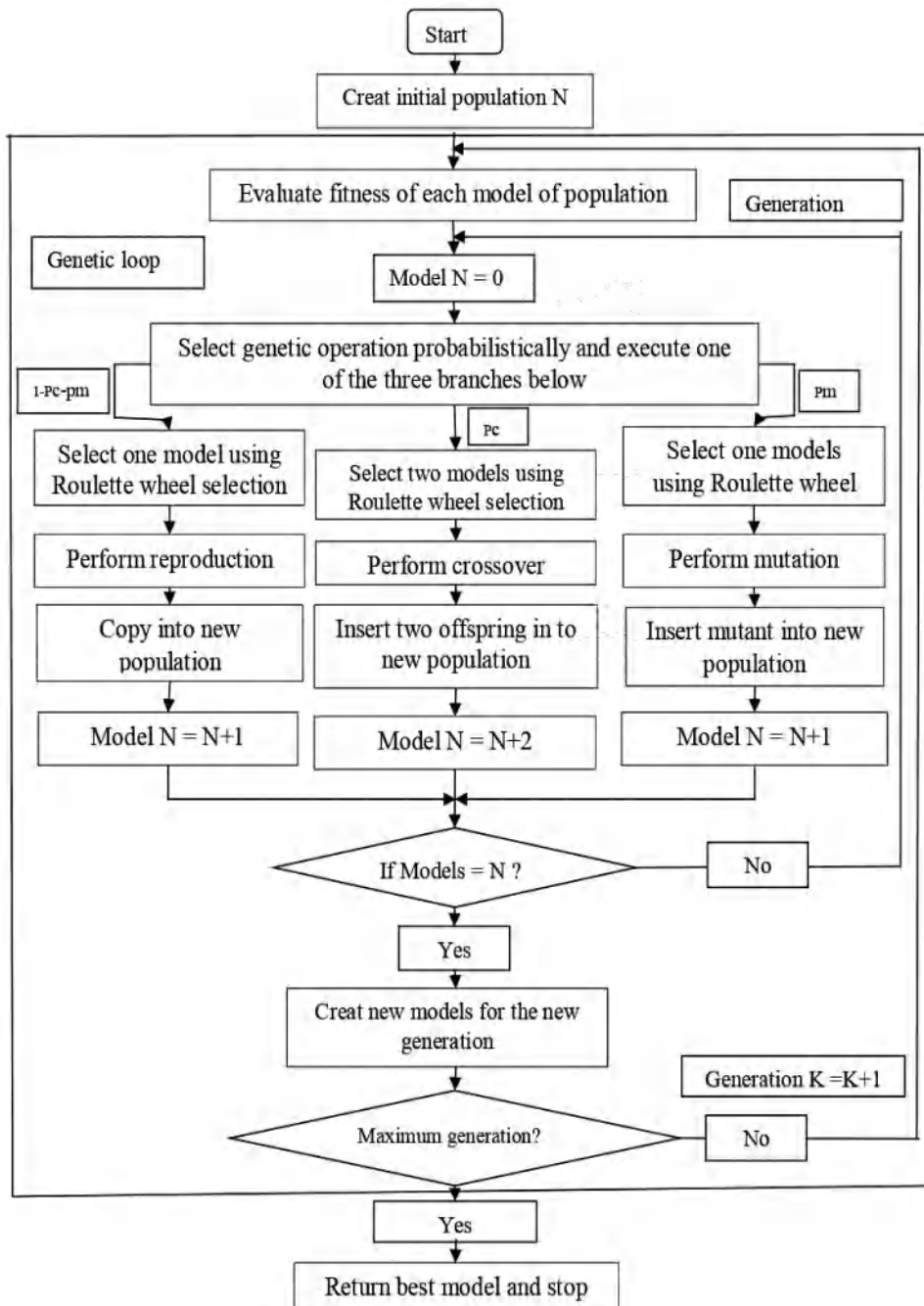


Figure 2. Flow chart of Genetic Programming (Hong and Bhamidimarri 2003).

Table 1. Different variable combinations attempted for the prediction of monthly basin yield and values of the Coefficient of determination (r^2), Pearson's C. C. (r), NSE, and RMSE.

Sr. No.	Variable Name	Input Variable Combinations									
		C-1	C-2	C-3	C-4	C-5	C-6	C-7	C-8	C-9	C-10
1	HAMY	✓	✓	✓	✓	✓	✓	✓	✓	✓	✓
2	EN (t-1)	✓	✓	✓					✓	✓	✓
3	EN (t-2)	✓	✓	✓					✓	✓	✓
4	EN (t-3)	✓	✓						✓	✓	✓
5	EQ (t-1)	✓	✓	✓	✓	✓	✓	✓	✓	✓	✓
6	EQ (t-2)	✓	✓	✓	✓	✓	✓	✓	✓	✓	✓
7	EQ (t-3)	✓	✓		✓	✓		✓			
8	OLR (t-1)	✓			✓	✓	✓			✓	✓
9	OLR (t-2)	✓			✓	✓	✓				
10	OLR(t-3)	✓			✓	✓					
11	MEI (t-1)				✓			✓			
12	MEI(t-2)				✓			✓			
13	MEI(t-3)				✓			✓			
r^2 (Training)		0.52	0.46	0.66	0.62	0.59	0.61	0.77	0.55	0.71	0.52
r^2 (Testing)		0.34	0.44	0.56	0.31	0.21	0.32	0.29	0.58	0.69	0.38
r (Training)		0.72	0.68	0.81	0.79	0.77	0.78	0.88	0.74	0.84	0.72
r (Testing)		0.58	0.66	0.75	0.56	0.46	0.57	0.54	0.76	0.83	0.62
NSE (Training)		0.66	0.57	0.75	0.74	0.71	0.73	0.61	0.53	0.76	0.26
NSE(Testing)		0.21	0.39	0.55	0.17	0.13	0.17	0.29	0.41	0.77	0.21
RMSE (Training)		850	851	649	799	621	720	681	866	589	959
RMSE (Testing)		1121	1189	1019	1146	1250	1147	1282	1172	1000	1150

a particular season (June through October of that year) to get the overall idea of expected basin-scale yield during the upcoming season.

The prediction is based on the Historical Average of Seasonal Yield (HASY) and monthly ENSO and EQUINOO indices of the maximum three previous months viz. May, April, and March using Equation (4) as follows.

$$Y_{season} = f\{HASY_{season}, (EN_{May}, EN_{March}, EN_{April}), (EQ_{May}, EQ_{March}, EQ_{April})\} \dots (4)$$

Three models with different variable combinations were developed and tested for seasonal analysis as listed in Table 3.

3. Results and discussion

The different variable combinations for prediction of 'Monthly river basin yield as well as 'Seasonal river basin yield' and their prediction performance are discussed in the following subsections.

3.1. Prediction of monthly river basin yield with one month lead time

'Monthly River basin scale yield' is a value of yield during a particular month. It is predicted with one month 'lead time' in this section. For example, the yield of the upcoming month of July is predicted at the end of the Month of June, using the specified inputs.

It is customary to plan and manage the water resources at a monthly time scale, as a month is the optimum time period for planning, management and utilization of water resources at river basin scale. That is why 'Monthly River Basin Yields' are predicted with One Month Lead Time in this case.

3.1.1. Variable combinations for one month lead time predictions

The different variable combinations are formed by changing input variables (Table 1), varying the number of inputs in a particular combination, and also changing the number of time steps to arrive at the best combination of inputs and the optimum number of time steps (Table 1). The choice is based

on the physical insight into the problem, the 'priori knowledge' of casual variables, and the 'input impacts' obtained by the GP Tool. The input impact frequencies on output values for the variables of monthly prediction are tabulated in Table 2.

3.1.1.1. Combination C-1. For this combination, the input variables are used with a reasonably long number of lags for every input variable. It includes the HAMY of the particular month, ENSO Indices, EQUINOO indices, and OLR of three previous monthly time steps.

The analysis of GP models in the training phase shows that this combination is able to capture variability in the observed yield and predicted yield up to 52% ($r^2 = 0.52$) and 34% ($r^2 = 0.34$) while testing the GP models. Pearson's coefficient of correlation between Observed yield and Predicted yield works out to be 0.72 ($r = 0.72$) while training and 0.58 ($r = 0.58$) in the testing phase.

From Table 2, it is observed that the highest impact (1.00) is given by HAMY of the particular month, which is quite obvious as it is the climatological value of that period. EN (t-2), EQ (t-1) and OLR (t-1) also show higher impacts, whereas OLR (t-2) and OLR (t-3) show comparatively much lower impacts.

Table 2. Input impact frequencies of variables given by GP for monthly basin yield prediction.

Variable Name	Input Variable Combination									
	C-1	C-2	C-3	C-4	C-5	C-6	C-7	C-8	C-9	C-10
HAMY	1.0	1.00	1.00	1.00	1.0	1.00	1.00	1.0	1.00	
EN (t-1)	0.70	0.63	0.67	-	-	-	-	0.83	0.83	0.73
EN (t-2)	1.00	0.90	0.80	-	-	-	-	1.00	0.97	0.83
EN (t-3)	0.77	0.81	-	-	-	-	-	0.80	0.93	0.70
EQ (t-1)	0.97	0.83	1.00	0.87	0.83	1.00	0.80	1.00	1.00	1.00
EQ (t-2)	0.53	0.40	0.63	0.70	0.87	0.87	0.73	0.77	0.73	0.60
EQ (t-3)	0.50	0.83	-	0.63	0.63	-	0.63	-	-	-
OLR (t-1)	1.00	-	-	0.87	1.00	0.97	-	-	0.83	1.00
OLR (t-2)	0.87	-	-	0.83	0.80	0.83	-	-	-	-
OLR(t-3)	0.67	-	-	0.70	0.69	-	-	-	-	-
MEI (t-1)	-	-	-	0.90	-	-	0.63	-	-	-
MEI(t-2)	-	-	-	0.70	-	-	0.77	-	-	-
MEI(t-3)	-	-	-	0.63	-	-	0.63	-	-	-

Table 3. Different variable combinations attempted for the prediction of Seasonal basin yield and values of the Coefficient of determination (r^2), Pearson's C. C. (r), NSE , and $RMSE$.

Variable No.	Variable	Variable combinations		
		S-1	S-2	S-3
1	HASY	√	√	√
2	EN (May)	√	√	√
3	EN (April)	√	√	√
4	EN (March)	√	√	√
5	EQ (May)	√	√	√
6	EQ (April)	√	√	√
7	EQ (March)	√	-	-
r^2 (Training)		0.79	0.81	0.72
r^2 (Testing)		0.46	0.49	0.56
r (Training)		0.89	0.90	0.85
r (Testing)		0.68	0.70	0.75
NSE (Training)		0.98	0.90	0.93
NSE (Testing)		0.76	0.74	0.86
$RMSE$ (Training)		2243	2122	1814
$RMSE$ (Testing)		3884	3971	2938

3.1.1.2. Combination C-2. In this combination, the information OLR is intentionally avoided to assess the efficacy of the ENSO and EQUINOO pair for basin yield prediction. This combination explains variability in predicted yield up to 44% ($r^2 = 0.44$) while testing and also yields a slightly better value of correlation coefficient ($r = 0.66$) while testing as compared to C-1.

3.1.1.3. Combination C-3. In this combination, the ENSO & EQUINOO for only two previous time steps are considered with the HAMMY. The third time step data are excluded by considering its impact in the previous combination C-2. The results obtained in this combination (Table 1) in the testing phase in terms of correlation coefficient ' r ' (0.75) and Nash–Sutcliffe model efficiency coefficient ($NSE = 0.55$) are slightly better than combinations C-1 and C-2 along with the smaller value of $RMSE$ (1019). It indicates that information of only two previous time steps of EQUINOO may be sufficient for the prediction of the basin yield.

3.1.1.4. Combination C-4. Some researchers have used MEI in place of the ENSO index in their studies (Ganguli and Reddy 2013). Hence, in his combination, MEI, EQUINOO, and OLR of three previous time steps with HAMMY are used. Here also, the results of the analysis while testing are slightly inferior to combination C-1, as indicated by 31% of variability explained ($r^2 = 0.31$) as compared to $r^2 = 0.34$ in variable combination C-1. It also indicates that the use of MEI indices in place of ENSO indices gives slightly inferior predictions of basin-scale yield.

3.1.1.5. Combination C-5. This variable combination attempts to use HAMMY with EQUINOO and OLR of three time steps and excludes ENSO and MEI totally. It is observed that this variable combination explained just 21% variability ($r^2 = 0.21$) in the testing phase. Hence, it can be emphasized that the influence of ENSO on ISMR and the river basin yields is substantial and cannot be neglected.

3.1.1.6. Combination C-6. Here, the OLR and EQUINOO indices of just two previous time steps are considered with HAMMY. The ENSO is purposely avoided to assess the efficacy of EQUINOO and OLR pair with just two previous time steps (instead of three in combination C-5). It is observed that although the time steps of EQUINOO and OLR are

reduced to 2 from 3, the variability explained is improved while testing from 21% to 32% ($r^2 = 0.32$). This indicates that the reduction of the number of time steps for EQUINOO as well as OLR may be advantageous to reduce noise in the data and arrive at better predictions.

3.1.1.7. Combination C-7. Here, EQUINOO and MEI indices of the previous three time steps along with HAMMY are used. This is an attempt to assess the applicability of MEI in place of ENSO. From the results, it is found that the variability of predicted data is not that satisfactorily. The correlation between observed and predicted basin yields came out to be 0.54, which is less than 0.75 in combination C-3. This clearly indicates that the combination of ENSO and EQUINOO is the best for basin-scale yield prediction.

3.1.1.8. Combination C-8. Here, the information of HAMMY, three previous time steps of ENSO, and two previous time steps of EQUINOO is used for checking the performance of combination to arrive at the best combination of input variables. The performance of the model is better than that of combination C-2, which considers three time steps each for ENSO and EQUINOO. It is also better than C-3, which considers two time steps each for ENSO and EQUINOO (Table 1).

3.1.1.9. Combination C-9. Here, the information of three previous time steps of ENSO, two previous time steps of EQUINOO, and one time step of OLR is used. From results, it is found that the performance of the model is the best amongst all the models C-1 through C-8, giving the highest value of $r = 0.84$ in training and 0.83 while testing, explaining variability up to 69% while testing.

It may be noted that the combination C-9 performs better than all other combinations because it uses inputs vis. ENSO indices of three previous time steps, EQUINOO indices of two previous time steps and OLR of just one previous time step. It matches with the logic of the evolution of ENSO over the Pacific ocean being more influential over three previous months, EQUINOO indices from the Indian Ocean more influential for two previous months and OLR more influential for one previous month as it is a local input. The influence of these selected inputs is also supported by 'Input Impact Values' calculated by the Genetic Programming tool. 'Input impact' calculated by the tool is based on the percentage of the best thirty programs from the project that contained the referenced input variable.

The monthly Observed and Predicted Yield of Upper Bhima river basin for combination C-9 while training and testing are shown in Figure 3(a,b) respectively.

Figure 3(a) Monthly observed and predicted Yield of Upper Bhima river basin for combination C-9 for the training period (1979–1996). (b) Monthly observed and predicted yield of Upper Bhima river basin for combination C-9 for the testing period (2006–2014). (c) Anomaly in observed and predicted Monthly yield for combination C-9 for the training period (1979–1996). (d) Anomaly in observed and predicted Monthly yields for combination C-9 for the testing period (2006–2014).

Figure 3(a) shows that the high yields, as well as low yields, are nicely captured by this combination. Also, from figure (b), it seems that for the testing period, GP nicely predicted the highest yield of August 2006. Also, the low yields in 2012 and 2014 were also nicely captured.

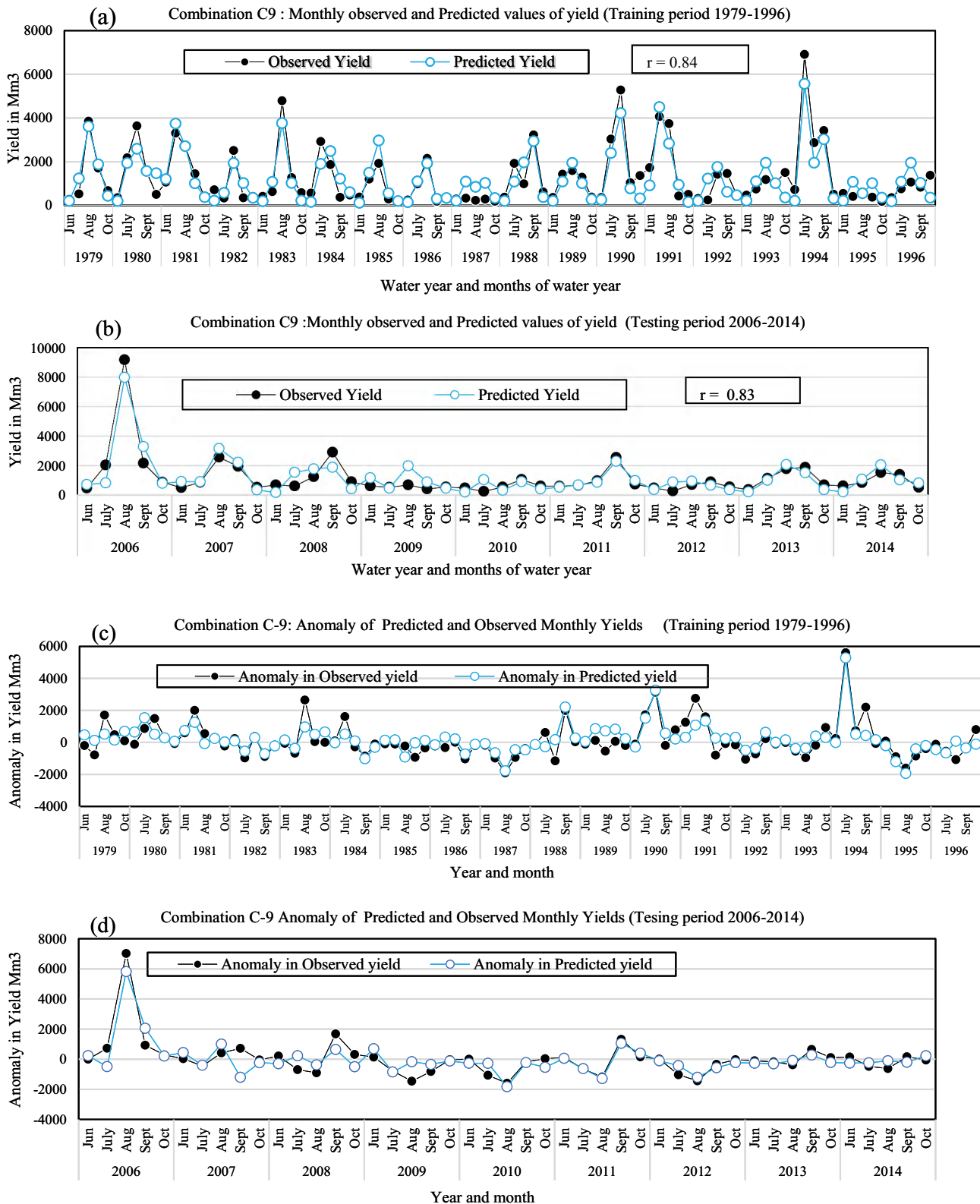


Figure 3. (a) Monthly observed and predicted Yield of Upper Bhima river basin for combination C-9 for the training period (1979–1996). (b) Monthly observed and predicted yield of Upper Bhima river basin for combination C-9 for the testing period (2006–2014). (c) Anomaly in observed and predicted monthly yield for combination C-9 for the training period (1979–1996). (d) Anomaly in observed and predicted monthly yield for combination C-9 for the testing period (2006–2014).

The plots of observed and predicted monthly yield in anomaly form for the combination C-9 are shown in Figure 3(c,d) for the training testing phase, respectively.

3.1.1.10. Combination C-10 (excluding HAMU from the best combination C-9). A unique variable combination is attempted to check the appropriateness of the model

in the absence of a practically long data set of ‘Historical basin yield’. It is observed that 38% ($r^2 = 0.38$) of the variability is explained by considering these inputs (Table 1) with a correlation coefficient = 0.62 while testing. Thus, the exclusion of HAMU leads to poorer performance. However, this combination is not completely useless.

3.1.2. Gradually evolving combinations and observations

It may be noted that the performances of the input variable combination C-9 is the best amongst all the combination of all possible influencing factors assessed simultaneously. The historical average yield provides information about the existing 'seasonality'; the large-scale atmospheric circulation information provides the information of global forcing on the local hydrologic processes, and the OLR considers the convective activity over the basin.

It may also be sensible to check whether the inclusion of historical average yield for a particular month (climatological value) as an input variable adds some artificial skill to the model. As indicated in the results of combination C-9, 69% of the variability is explained ($r = 0.83$) by this input variable combination. Now, the explained variance between historical monthly average basin yield values and observed monthly yield values is also calculated. The coefficient of determination was calculated and found to be 0.2048. This indicates that only 21% of the variance is explained by the climatological values and the remaining 48% of the variance is explained by the remaining inputs of the full model. It underlines the importance of global and local climate inputs in the prediction of river basin scale yield.

3.2. Seasonal river basin yield prediction at the end of May

The 'Seasonal Yield' of the river basin is a single value of yield, expected in the upcoming season from 1st June to 30th October of the particular water year. It is predicted at the end of the Month of May for a particular season (June through October of that year). It gives an overall idea of expected basin-scale yield during the upcoming season.

The seasonal prediction of basin-scale yield has a different aspect from monthly prediction. About 80% of rainfall in this region is observed during the Monsoon months of June through September. Hence, the major portion of the streamflow is observed during the months of June through October, giving a fair idea of the likely availability of water resources in the river basin in the ongoing water year (June of the current calendar year through May of next calendar year). Thus seasonal prediction at May end also has its significance.

In the seasonal analysis, three variable combinations with only the ENSO and EQUINOO indices are considered along with the Historical Average of Seasonal Yield (HASY) for the modelling. The information of OLR is not used for this model as OLR is used as a proxy for rainfall activity, and this period of rainfall is negligible in this basin. Each time step value is a different input variable in this analysis (Like EN(May), EN(April), EN(March), etc.). But the inputs in the particular variable combination are used as a group of variables. The tick mark(✓) in front of the variable indicates the inclusion of a particular variable in the particular variable combination.

The results of all the combinations are shown in Table 3.

The results of this combination during training and testing are shown in Figure 4(a) and figure (b), respectively.

Figure 4(a) Seasonal observed and predicted Yields of Upper Bhima river basin for combination S-3 during the training period (1972–1994). (b) Seasonal observed and pre-

dicted Yields of Upper Bhima river basin for combination S-3 during the testing period (2005–2014). (c) Anomaly in observed and predicted seasonal yields for combination S-3 for the testing period (2005–2014).

From Figure 4(b), it is observed that the GP has captured the seasonal variation of yield with sufficient accuracy. It is observed that GP has fairly captured the high yields during the years 2005 and 2006. Also, the low yields during 2009, 2010, and 2012 are satisfactorily captured in the testing period. The anomalies of observed and predicted seasonal yields during the testing phase are shown in Figure4(c).

It may be noted that Causal models are mathematical models representing causal relationships within an individual system facilitating inferences about causal relationships from data, whereas, 'Time series forecasting is the use of a model to predict future values based on previously observed values. However, the models developed in this study are deterministic models in which the output of the model is fully determined by the parameter values. The climatic systems causing the rainfall are roughly similar over the monsoon season. Hence, the models are assumed to be of homogeneous and deterministic type.

It might be essential to compare the GP with the traditional approaches, like autoregressive (AR) models and Artificial Neural Network (ANN) approaches. ANNs do have many smart features, but they suffer from a few limitations. The difficulties in choosing the optimal network architecture and the 'black-box nature' of the NN approach are the issues of concern. In an AR model, only the endogenous properties of the time series are used. To incorporate the external forcing, an option of an AR model with exogenous inputs (ARX) may be selected. However, if there are more exogenous inputs, computational complexity becomes a vital issue. In addition, it is linear in nature, which may not be suitable for many applications related to hydroclimatological systems (Maity and Kashid 2009).

4. Conclusion

This study attempts to predict monthly and seasonal river basin yield of the Upper Bhima River basin using global climate indices ENSO, EQUINOO, MEI, and local climate input OLR as predictors. The OLR is used as a proxy to rainfall activity over the river basin, and it is proved to give better predictions when used in association with large-scale climate inputs.

The information of only historical basin-scale yield records or only the large-scale circulation information or only the local scale OLR information cannot help to give good basin-scale yield predictions. Rather the simultaneous use of these inputs is found to give better predictions of basin-scale yield. The AI tool GP is employed for establishing a correlation between predictors and predictand. From the analysis, it is found that GP can develop good prediction models for river basin yield prediction. The inter-relations between climate inputs and basin yield as output are captured satisfactorily, although the phenomena are quite complex.

The correlation coefficient between observed and predicted yields while testing for monthly prediction with one month lead time could reach up to 0.83. The C.C. for the Seasonal prediction at May end could reach up to 0.75, which is quite alluring. Thus, it can be concluded that river basin yields can be predicted with reasonable accuracy based on

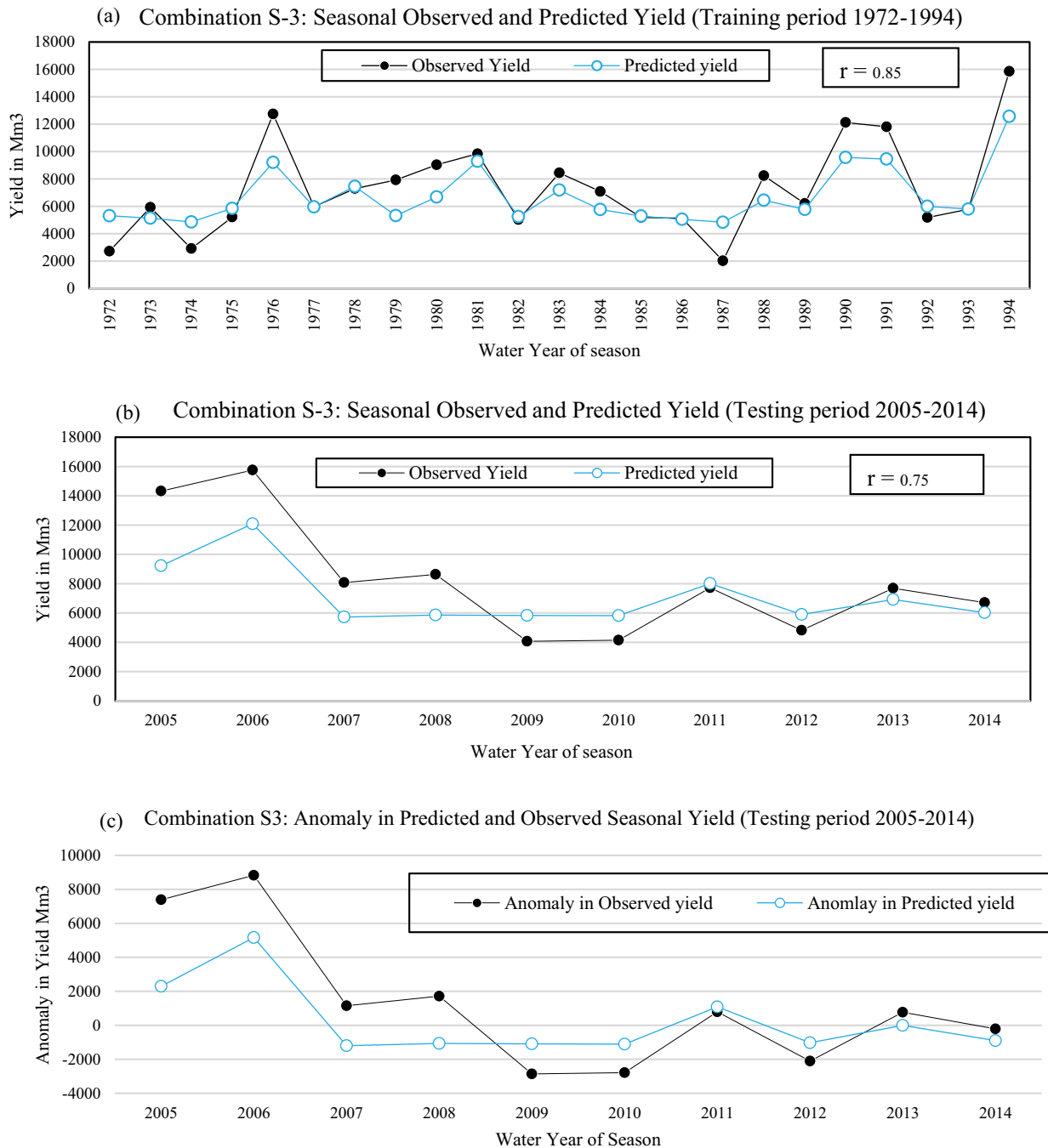


Figure 4. (a) Seasonal observed and predicted Yield of Upper Bhima river basin for combination S-3 during the training period (1972–1994). (b) Seasonal observed and predicted Yield of Upper Bhima river basin for combination S-3 during the testing period (2005–2014). (c) Anomaly in observed and predicted seasonal yield for combination S-3 for the testing period (2005–2014).

climate indices by using the novel tool GP. Such information of river basin yield can be advantageously used for planning reservoir operation over a season and a water year. However, it may be noted that the approach does not consider the effect of climate change on basin-scale yield over the analysis period, which may be taken as a limitation of this study. It is possible to develop similar models for other river basins; however, the climate inputs will be different for different regions influencing rainfall patterns for the particular region.

Disclosure statement

No potential conflict of interest was reported by the author(s).

References

- Ashok, K., Guan, Z., and Yamagata, T. (2001). "Impact of the Indian Ocean dipole on the relationship between the Indian monsoon rainfall and ENSO". *Geophys. Res. Lett.* 28(23), 4499–4502. doi:10.1029/2001GL013294
- Babovic, V., and Keijzer, M. (2002). "Rainfall runoff modelling based on genetic programming". *Hydrol. Res.* 33(5), 331–346. doi:10.2166/nh.2002.0012
- Brameier, M. (2004). "On Linear Genetic Programming." PhD thesis, Fachbereich Informatik, University at Dortmund, Germany.
- Cane, M.A. (1992). "Tropical Pacific ENSO models: ENSO as a mode of the coupled system". *Climate System Modeling*, K. Trenberth, Ed., Cambridge University Press, 583–616.
- Chavadekar, A.U., and Kashid, S.S. (2019). "Meteorological drought prediction of marathwada subdivision based on hydro-climatic inputs

- using genetic programming". *ISH J. Hydraul. Eng.* 1–13. doi:10.1080/09715010.2019.1620647
- Chiew, F.H., Piechota, T.C., Dracup, J.A., and McMahon, T.A. (1998). "El Niño/Southern Oscillation and Australian rainfall, streamflow and drought: Links and potential for forecasting". *J. Hydrol.* 204(1–4), 138–149. doi:10.1016/S0022-1694(97)00121-2
- Chiew, F.H.S., Zhou, S.L., and McMahon, T.A. (2003). "Use of seasonal streamflow forecasts in water resources management". *J. Hydrol.* 270 (1–2), 135–144. doi:10.1016/S0022-1694(02)00292-5
- Douglas, W.W., Wasimi, S.A., and Islam, S. (2001). "The El Niño Southern oscillation and long-range forecasting of flows in Ganges". *Int. J. Climatol.* 21(1), 77–87. doi:10.1002/joc.583
- Francone, F.D. (1998). *Discipulus owner's manual*, Machine Learning Technologies, Inc., Littleton, Colorado
- Gadgil, S., Vinayachandran, P.N., Francis, P.A., and Gadgil, S. (2004). "Extremes of the Indian summer monsoon rainfall, ENSO and equatorial Indian Ocean oscillation". *Geophys. Res. Lett.* 31(12), 12. doi:10.1029/2004GL019733
- Ganguli, P., and Reddy, M.J. (2013). "Analysis of ENSO-based climate variability in modulating drought risks over western Rajasthan in India". *J. Earth Syst. Sci.* 122(1), 253–269. doi:10.1007/s12040-012-0247-x
- Gutierrez, F., and Dracup, J.A. (2001). "An analysis of the feasibility of long range streamflow forecasting for Columbia using El Niño-Southern Oscillation indicators". *J. Hydrol.* 246, 181–196. doi:10.1016/S0022-1694(01)00373-0
- Hong, Y.S., and Bhamidimarri, R. (2003). "Evolutionary self-organising modelling of a municipal wastewater treatment plant". *Water Res.* 37 (6), 1199–1212. doi:10.1016/S0043-1354(02)00493-1
- Kiem, A.S., and Franks, S.W. (2001). "On the identification of ENSO-induced rainfall and runoff variability: A comparison of methods and indices". *Hydrol. Sci. J.* 46(5), 715–727. doi:10.1080/02626660109492866
- Koza, J.R. (1992). *Genetic programming: On the programming of computers by means of natural selection*, Vol. 1,
- Maity, R., and Chanda, K. (2015). "Potential of genetic programming in hydroclimatic prediction of droughts: An Indian perspective". *Handbook of genetic programming applications*, Springer, Cham, 381–398
- Maity, R., and Kashid, S.S. (2009). "Short-term basin-scale streamflow forecasting using large-scale coupled atmospheric–oceanic circulation and local outgoing longwave radiation". *J. Hydrometeorol.* 11(2), 370–387. doi:10.1175/2009JHM1171.1
- Maity, R., and Nagesh Kumar, D. (2008). "Basin-scale streamflow forecasting using the information of largescale atmospheric circulation phenomena". *Hydrol. Processes Int. J.* 22(5), 643–650. doi:10.1002/hyp.6630
- Mehr, A.D., Kahya, E., and Yerdelen, C. (2014). "Linear genetic programming application for successive-station monthly streamflow prediction". *Comput. Geosci.* 70, 63–72. doi:10.1016/j.cageo.2014.04.015
- Murgulet, D., Valeriu, M., Hay, R.R., Tissot, P., and Mestas-Nunez, A.M. (2017). "Relationships between sea surface temperature anomalies in the Pacific and Atlantic Oceans and South Texas precipitation and streamflow variability". *J. Hydrol.* 550, 726–739. doi:10.1016/j.jhydrol.2017.05.041
- Saji, N.H., Goswami, B.N., Vinayachandran, P.N., and Yamagata, T. (1999). "A dipole mode in the tropical Indian Ocean". *Nature.* 401(6751), 360–363. doi:10.1038/43854
- Wolter, K., and Timlin, M.S. (1993). "Monitoring ENSO in COADS with a Seasonally Adjusted Principal." In Proc. of the 17th Climate Diagnostics Workshop, Norman, OK, NOAA/NMC/CAC, NSSL, Oklahoma Clim. Survey, CIMMS and the School of Meteor., Univ. of Oklahoma, 52 (Vol. 57).

Faculty Industry Training

Industrial Training Certificate

TO WHOMEVER IT MAY CONCERN

This is to certify that **Mrs. Prajakta Abhishek Satarkar** working as Assistant Professor in Computer Science and Engineering Department, SVERI's College of Engineering has undergone training on Web development with various software tools at our training center from **22nd February 2023 to 21st March 2023**.

During the training session she was zealous, industrious and was learning with a good studious attitude.

With best wishes,

Thank you.



For Montcrest Software Pvt. Ltd.,
Amol Karanje
Human Resource

Montcrest Software Pvt. Ltd.

5-4-2023

To,
The Principal,
SVERI COEP.

Sub:- Report of 1 month industrial training.

Respected Sir,

I, the undersigned, am working as Asst. Professor in CSE dept from last 15 years. With reference to above subject, I would like to sincerely thank to management and my department for providing me this opportunity to learn beyond the theory.

In this training period I learnt new technologies new platforms for web development using HTML, CSS XML & JavaScript. The industry Montcrest software, Pune has provided hands on experience with all these technologies.

I have gained a good knowledge about website development & to some extent database in background. The environment in industry was nice & I had a great learning over there.

I have undergone the training from 22-2-2023 to 21-3-2023 in Montcrest software, Baner Pune. I will give presentation on the same so that my colleague will get benefitted from the same.

I am really thankful to you & organisation for providing me this opportunity.

Thanking you.

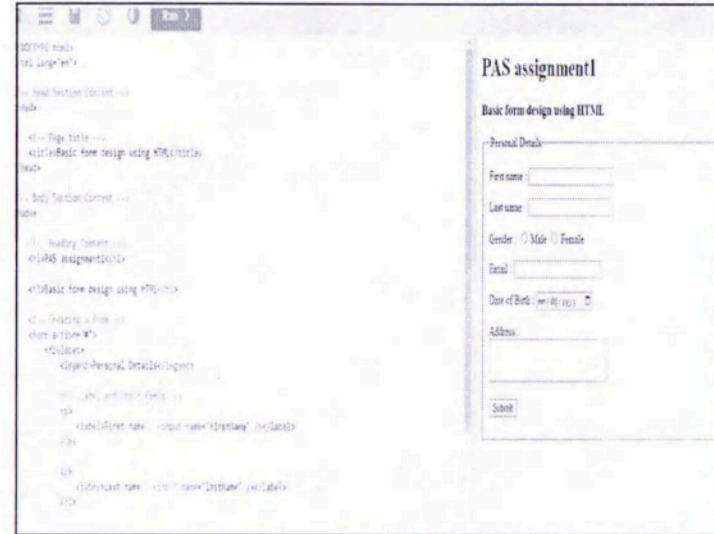
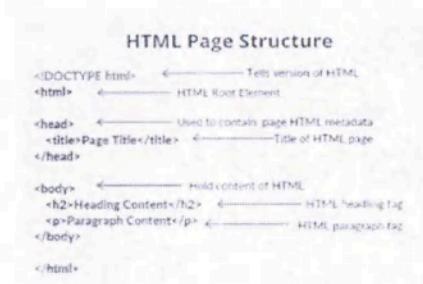
Yours sincerely,



[Satarkar P.A.]
CSE dept.

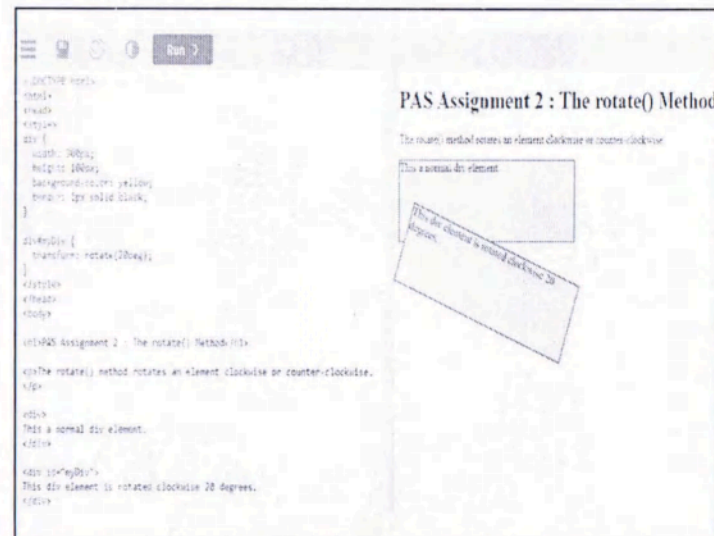
HTML

- Hypertext defines the link between the web pages and markup language defines the text document within the tag that define the structure of web pages.



CSS

- CSS is the language we use to style an HTML document
- CSS Syntax: Selector, Declaration, Property, Value
- Three Ways to Insert CSS : External, Internal, Inline
- Margin, borders, colors, navigation: vertical and horizontal
- Math functions, table, lists etc.
- Shadow effect, 2D transformations



JavaScript

- World's most popular programming language for web
- Syntax, declaration of variables, operators, functions, data type.
- Looping constructs: If-else, while, for
- Introduction to JS versions, objects, classes, functions, Graphics and JSON

PAS assignment 3
JavaScript can change HTML attribute values
In this case JavaScript changes the value of the src (source) attribute of an image

Turn on the light Turn off the light

```

<script>
  // Turn on the light
  function turnOnLight() {
    document.getElementById("light").src = "light.png";
  }

  // Turn off the light
  function turnOffLight() {
    document.getElementById("light").src = "light-off.png";
  }
</script>

```

PAS assignment 3
JavaScript can change HTML attribute values
In this case JavaScript changes the value of the src (source) attribute of an image

Turn on the light Turn off the light

Thank You!!



M-matic Automation Solutions

Regd. Office : Sr. No. 16/29, Sanskruti Building, Flat No. 501, Vishal Nagar, Pimple Nilakh, Pune - 411 027.

Date: 03 August 2023

INTERSHIP CERTIFICATE

This is to certify that Prof. Ms. Nirmala.T.Pujari of SVERI's College of Engineering, Pandharpur has successfully completed the Internship course of HMI & SCADA, which is conducted between 03rd July 2023 to 03rd August 2023 at M-Matic Automation Solutions Pune.

She has learn and worked on Schneider Vijeo Designer Basic Software of HMI and Schneider Plant SCADA for SCADA.

We wish her all the best.


Best regards,

For M-Matic Automation Solutions

Manijaa Waader
Proprietor

M-matic Automation Solutions

Manijaa Waader
Proprietor

 Bagal
Narsale &
Malape Developers

+91-9096258085 / +91-9860882811 / +91-9822831999

bnandmdevelopers@gmail.com

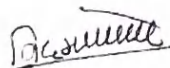
Date: 12/08/2023

To whom so ever it may concern

This is certifying that **Mr. Ravikiran Pandurang Jadhav** has worked in our organization as a Trainee Structural Engineer W.E.F July 10th, 2023 to August 10th, 2023. He is well conversant with all kind of structural design and analysis work with the help of software such as STAAD. Pro & E-tab related to residential and commercial buildings.

During service, we found **Mr. Ravikiran Pandurang Jadhav (M. Tech-Structure)** honest, obedient, and hard-working person. We wish him all success in life & are proud to say that where ever he works, he will be in an invaluable asset to his organization.

Thanking You.



BAGAL NARSALE AND MALAPE DEVEL (PVT) LTD

Managing Partner

(Mr. Nikhil H. Bagal)

Bagal Narsale and Malape Developers

ADDRESS:

Gat no 10, Isbavi, Pandharpur, Solapur 413304

REPORT ON INDUSTRIAL TRAINING OF "CONSTRUCTION PRACTICES IN CIVIL ENGINEERING"

Structural Component	Age
Footings	1 day
Sides of beams, columns, lintels, wall	2 days
Underside of beams spanning less than 6m	14 days
Underside of beams spanning over 6m	21 days
Underside of slabs spanning less than 4m	7 days
Underside of slabs spanning more than 4m	14 days
Flat slab bottom	21 days

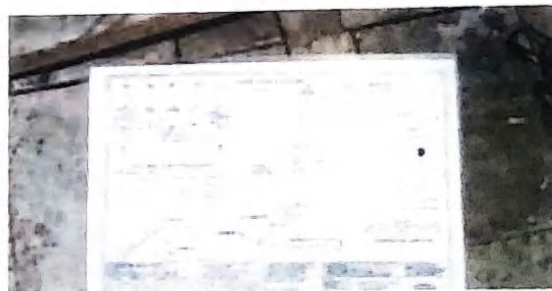


Fig:7 Slab Casting and RCC Plan

Mr. Ravikiran P. Jadhav
*(Assistant Professor
 Civil Engineering Department)*

Dr. P. M. Pawar
*(Dean Academics &
 Head of Department
 Civil Engineering Department)*

Dr. B. P. Ronge
*(Principal
 SVERI's College of Engineering
 Pandharpur)*

Date: - 29/09/23

Place: - Pandharpur

Some of photographs are attached below:







TO WHOMSOEVER IT MAY CONCERN

This is to certify that **Dr. Manik Deshmukh** Faculty in Civil Dept of **SVERI College** has undergone Internship in our organization. The topic is Cement and Manufacturing System, Unit Rajasahree Cement Works. He has done his program during the period **July 10, 2023 to August 10th, 2023**.

We wish him success in his future endeavors.

Thanking You.

For UltraTech Cement Limited

A handwritten signature in blue ink, appearing to read 'Gautam Sharma', with a long horizontal line extending to the right.

Gautam Sharma
Zonal Head Human Resource

UltraTech
CEMENT
The Engineer's Choice

UltraTech Cement Limited
(Central Marketing Office)
Ahura Centre, A-Wing, 1st Floor,
Mahakali Caves Road,
Andheri (E), Mumbai - 400093.

Tel. +91 22 66917360
Fax +91 22 66917361
Website www.ultratechcement.com
CIN NO. L26940MH2000LC128420

Regd. Office:
Ahura Centre, B-Wing, 2nd Floor,
Mahakali Caves Road,
Andheri (E), Mumbai - 400093.

Sponsored Project



ShriVithal Education & Research Institute's
COLLEGE OF ENGINEERING, PANDHARPUR



ISO 9001:2015

www.tuv.com
ID 1105048190



P.B. No. 54, Gopalpur - Ranjani Road, Gopalpur, **Tal.:** Pandharpur- 413304, **Dist.:** Solapur (MH)
Contact No.: 9545553888, 9545553757, **E-mail:** coe@svri.ac.in, **Website:** www.svri.ac.in
Approved by **A.I.C.T.E.**, New Delhi and affiliated to PunyashlokAhilyadeviHolkar Solapur University, Solapur. **NBA** Accredited all Eligible UG Programmes, **NAAC A+** Accredited Institute, ISO 9001-2015 Certified Institute. Accredited by Institution of Engineers (India) and TCS.

Date: 2/5/2023

NOTICE

All the students of TY C.S.E are hereby informed to note that, our department is organizing a online workshop on the topic “**Application of Artificial Intelligence for Product Development and Research**”.under the guidance of Dr. Anand S. Rao (Global Artificial Intelligence Leader, PWC). Session will be conducted in concerned classes.

Note: Attendance is mandatory for all the TY CSE students.

(Prof. M. Y. Shaikh)

Cordinator

(Dr. Mrs. S. P. Pawar)

HOD CSE

HOD,

Department of Computer Science & Engg
SVRI's C.O.E. Pandharpur



Shri Vithal Education & Research Institute's
COLLEGE OF ENGINEERING, PANDHARPUR



ISO 9001:2015



www.tuv.com
ID 9105049195

P.B. No. 54, Gopalpur - Ranjani Road, Gopalpur, Tal.: Pandharpur- 413304, Dist.: Solapur (MH)
Contact No.: 9545553888, 9545553757, **E-mail :** coe@sveri.ac.in, **Website:** www.sveri.ac.in
Approved by A.I.C.T.E., New Delhi and affiliated to Punyashlok Ahilyadevi Holkar Solapur University, Solapur
NBA Accredited all Eligible UG Programmes, NAAC A+ Accredited Institute, ISO 9001-2015 Certified Institute.
Accredited by Institution of Engineers (India) and TCS.

REF NO: COEPR/2022-23/CSE/

08-05-2023

To,
Dr. Anand S. Rao
Global Artificial Intelligence Leader
for PwC

Subject: Invitation as the Resource Person for a Session on a workshop "Application of Artificial Intelligence for Product and Research"

Respected Sir,

Shri Vithal Education and Research Institute (SVERI) is a charitable trust founded in Pandharpur (known as 'South Kashi' of India) by a group of technocrats. Today, around 4800 students are studying in this campus and around 1800 boys and 1500 girls are living in the separate hostels. The institute is moving ahead on the path of success with Excellent Academic Results, Excellent Placements, Excellent R & D, Excellent Infrastructure and Excellent Accreditations. After the establishment of the institution, various colleges have been started by this trust.

1. **SVERI's College of Engineering (UG & PG), Pandharpur (Year:1998)**
(NAAC A+ with 3.46/4.00 CGPA and All eligible UG Programs have been accredited by NBA)
2. **SVERI's College of Pharmacy (UG, PG & Diploma), Pandharpur (Year: 2006) (UG Program accredited by NBA)**
3. **SVERI's College of Pharmacy (Poly.), Pandharpur (Year: 2006)**
(Procedure for NBA is in progress)
4. **SVERI's College of Engineering (Poly.), Pandharpur (Year: 2008) (All eligible programs have been accredited by NBA)**

Sir, since inception, SVERI has been working for the betterment of society. The Rural Human Resource Development Facility (RHRDF) has been established at SVERI through MoU with Bhabha Atomic Research Center, Mumbai for deployment of the technologies of BARC in rural area. Around Rs. 2 Cr. CSR grant has been received from NPCIL, Tarapur for empowering villagers in Tarapur (Mumbai) region through propagation of BARC technologies. In addition, Rs. 5 Cr. grant has been approved by NITI Aayog for establishment of Atal Community Innovation Center (ACIC), in 2022. Recently, RGSTC has sanctioned research fund of Rs. 33.73 Cr. for the collaborative project of IIT Mumbai, VJTI, Mumbai and SVERI, Pandharpur on Drone Technology. The institute provides 'Earn & Learn' scheme to the needy students for bringing them in the flow of education by sparing budget around Rs. 1 Cr. every year and making expenditure accordingly.

Sir, we have organized a workshop on "Application of Artificial Intelligence for Product Development and Research" From 9th May 2023 for our Third year Students from Department of Electronics and Telecommunication Engineering and Department of Computer Science Engineering. We are pleased to invite you to take a session on "Application of Artificial Intelligence for Product Development and Research" on 9th, 10th and 18th May 2023 at 4pm (IST) in the institute.

We believe that your presence and words of wisdom will take us (students, faculty members and all other stakeholders of this institute) to a different energy level which will help us achieve new heights of success in our future journey.

Sir, we are very much eager to welcome you. We are waiting for your positive response.

Thank you.

Yourstruly,

S. P. Pawar
(Dr. Mrs. S. P. Pawar)
HOD CSE

HOD,
Department of Computer Science & Engg
SVERI's C.O.E. Pandharpur.



ShriVithal Education & Research Institute's
COLLEGE OF ENGINEERING, PANDHARPUR



ISO 9001:2015



www.tuv.com
ID: 8105048196

P.B. No. 54, Gopalpur - Ranjani Road, Gopalpur, Tal.: Pandharpur- 413304, Dist.: Solapur (MH)
Contact No.: 9545553888, 9545553757, E-mail: coe@sveri.ac.in, Website: www.sveri.ac.in
Approved by A.I.C.T.E., New Delhi and affiliated to Punyashlok Ahilyadevi Holkar Solapur University, Solapur
NBA Accredited all Eligible UG Programmes, NAAC A+ Accredited Institute, ISO 9001-2015 Certified Institute.
Accredited by Institution of Engineers (India) and TCS.

REF NO: COEPR/2022-23/CSE/

18-05-2023

To,
Dr. Anand S. Rao
Global Artificial Intelligence Leader
for PwC

Respected Sir,

We express our heartfelt gratitude towards you for accepting our invitation as the Resource Person for the Session in workshop on "Application of Artificial Intelligence for Product Development and Research" arranged at ShriVithal Education & Research Institute (SVERI) College of Engineering, Pandharpur from 8th May, 2023 onwards. We are sure that your presence and words of wisdom have taken our students and faculty members to a different energy level which will help all to achieve new heights of success in their future journey.

Your vision and insights in the area of Artificial Intelligence for Product Development and Research have certainly boosted the confidence of our students and faculty members. It is the matter of pride and delight for us that you have spared your valuable time and enlightened all through your scholarly address.

We request same kind of cooperation and guidance in future also.
Thank you once again.

Yours faithfully,

S. P. Pawar
(Dr. Mrs. S. P. Pawar)
HOD, CSE

HOD,
Department of Computer Science & Engg
SVERI's C.O.E. Pandharpur.



SVERI's College of Engineering, Pandharpur

An Exclusive workshop for SVERI

Speaker



'Application of Artificial Intelligence for Product Development & Research'

Dr. Anand S. Rao

Global Artificial Intelligence Lead at PWC,
Trusted Advisor, Innovator, Author, Educator

Organized by



IIC, AICTE, IEEE & Department of E&TC Engineering

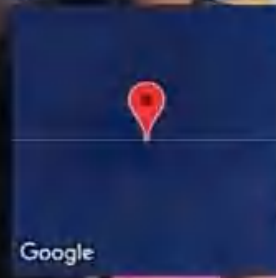
Venue

E&TC and CSE Department,
SVERI's College of Engineering, Pandharpur



DATA SCIENCE SERIES
A course of data science and its applications
Machine learning, deep learning and statistics
Python, statistics, data science, and reproducible data science
Dr. Anand...

SVERIS COE, Pandharpur, Maharashtra



Longitude Latitude
795.0° E 1.0E-4° N



0° C

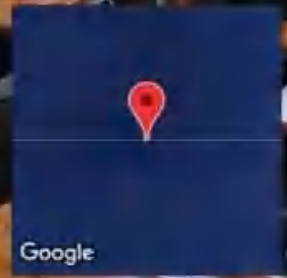
Tuesday, 09, May, 2023

04:20 PM



DATA SCIENCE SERIES
Introduction to Data Science
Data Science: Applications and Challenges
Data Science: Applications and Challenges

SVERIS COE, Pandharpur, Maharashtra



Google

Longitude Latitude
795.0° E 1.0E-4° N




0° C

Tuesday, 09, May, 2023

04:20 PM

DECISION TREE: DEFINITION

DEFINITION: A decision tree is a supervised machine learning algorithm that is used for classification and regression tasks. It is a model that is built from a set of data points and is used to predict the class of a new data point.



Understanding the data for a decision tree is the first step in building a model.

SVERIS COE, Pandharpur, Maharashtra



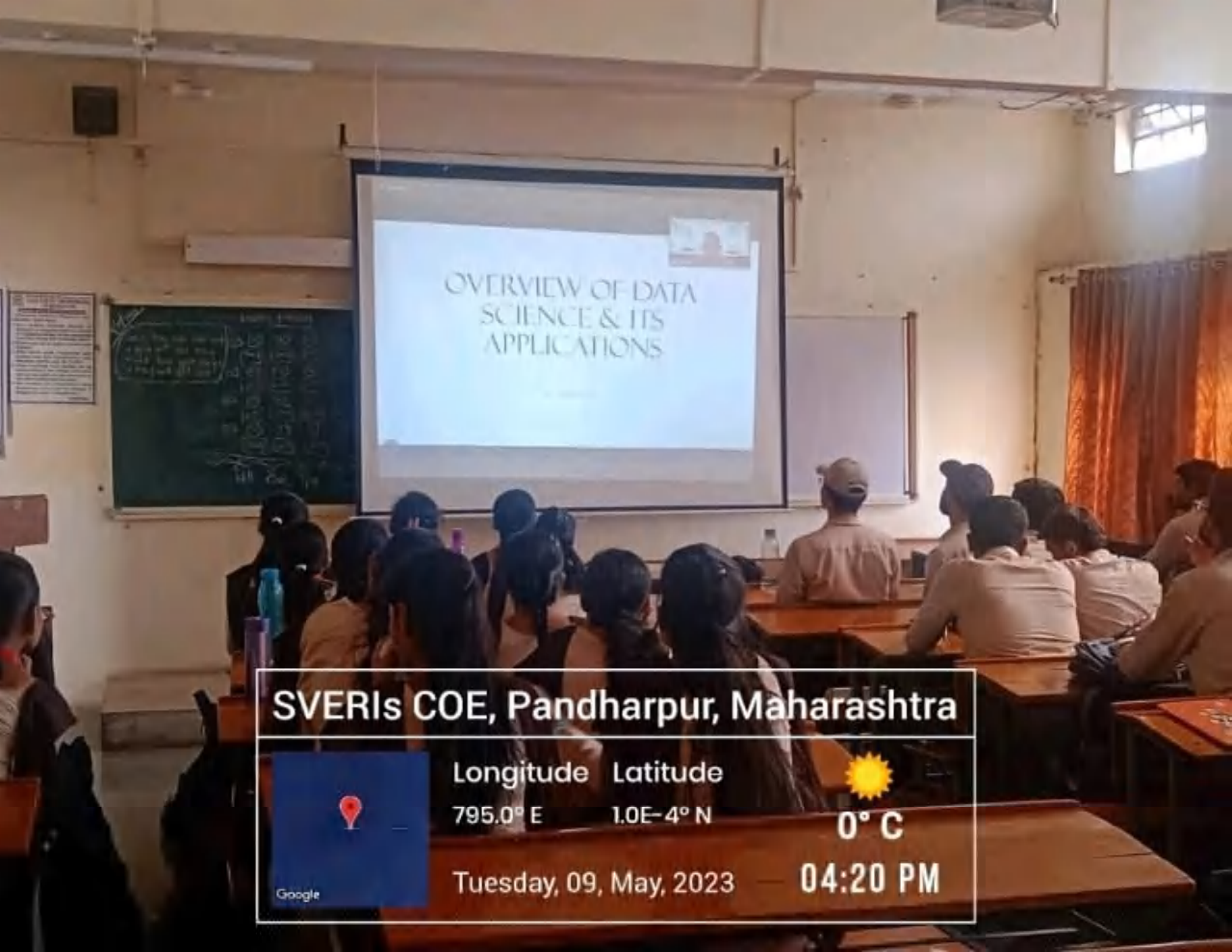
Longitude Latitude
795.0° E 1.0E-4° N



0° C

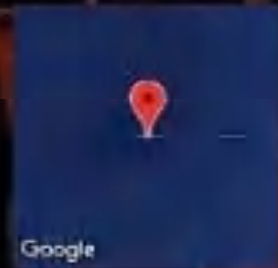
Wednesday, 10, May, 20...

04:57 PM



OVERVIEW OF DATA
SCIENCE & ITS
APPLICATIONS

SVERIS COE, Pandharpur, Maharashtra



Longitude Latitude

795.0° E 1.0E-4° N



0° C

Tuesday, 09, May, 2023

04:20 PM



**SHRI VITHAL EDUCATION & RESEARCH INSTITUTE'S
COLLEGE OF ENGINEERING, PANDHARPUR.**



ISO 9001:2015



ISO 9001-2015 Certified Institute & Accredited by Institute of Engineers, India,
NAAC and NBA Accredited.
Gopalpur-Ranjani Road, Gopalpur, P.B. No. 54, Tal-Pandharpur-413 304 Dist. Solapur
(Maharashtra) Ph.: (02186)225083, Fax: (02186)225082
(Approved by AICTE, New Delhi and affiliated to Solapur University, Solapur) E-mail :-
coe_pan@rediffmail.com

Date: 18-05-2023

Department of Computer Science and Engineering

To,
The Principal,
SVERI's COE,
Pandharpur.

Subject: Report Regarding Session in workshop

Respected Sir,

I, the undersigned Mr. M. Y. Shaikh (Asst. Prof.) working in CSE Department, submitting following report of session in workshop conducted.

Name of the Guest Faculty :Dr. Anand S. Rao(Anand S. Rao, for PwC)

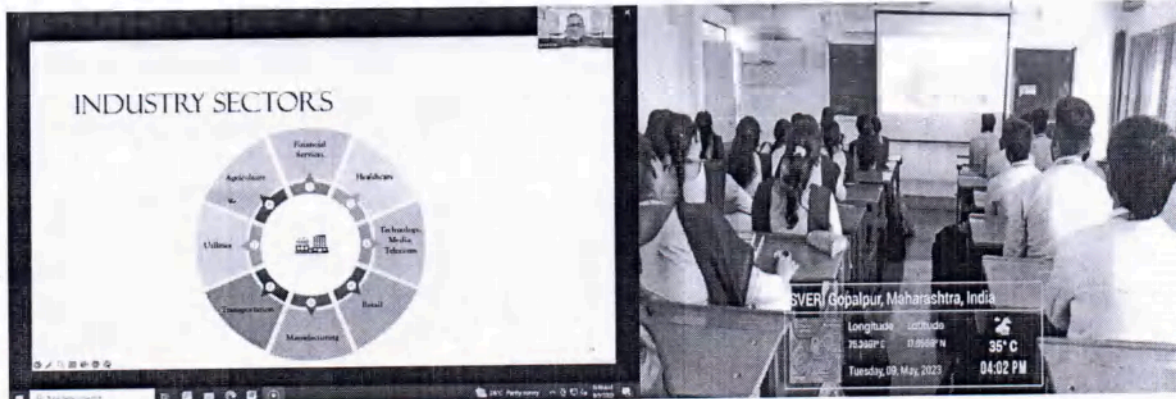
Class : TY CSE.

Topic of Guest Lecture :Application of Artificial Intelligence for Product Development and Research.

Total No. of Students : 150

Date of Guest Lecture Conducted : 9th, 10th, 18th May 2023.

Snaps of Session:



Thanking You,
Subject Teacher.

S. P. Pawar
(Dr. Mrs. S. P. Pawar)
HOD CSE

HOD,
Department of Computer Science & Engg
SVERI's C.O.E. Pandharpur.



**Shri Vithal Education & Research Institute's
College of Engineering, Pandharpur
Department of Computer Science and Engineering**



**In collaboration with
Global Indian Scientists and Technocrats(GIST)**

Organized a workshop on

“Application of Artificial Intelligence for Product Development & Research”

Certificate of Participation

This is to Certify that Mr/Ms. **Bahirwade Pooja Rajendra** COLLEGE OF ENGINEERING, PANDHARPUR has successfully attended a Workshop on **“Application of Artificial Intelligence for Product Development & Research”** from 8 May 2023 to 18 May 2023.

Dr. Mrs. V. S. Kshirsagar
IIC President

Dr. Mrs. S. P. Pawar
Head of Department

Mr. M. Y. Shaikh
IIC Coordinator

Dr. B. P. Ronge
Principal

Dr. Anand S. Rao
Global Artificial Intelligence
Lead in PwC



**Shri Vithal Education & Research Institute's
College of Engineering, Pandharpur**
Department of Computer Science and Engineering



In collaboration with
Global Indian Scientists and Technocrats(GIST)

Organized a workshop on

“Application of Artificial Intelligence for Product Development & Research”

Certificate of Participation

This is to Certify that Mr/Ms. **Birajdar Shraddha Siddharam** COLLEGE OF ENGINEERING, PANDHARPUR has successfully attended a Workshop on **“Application of Artificial Intelligence for Product Development & Research”** from 8 May 2023 to 18 May 2023.

Dr. Mrs. V. S. Kshirsagar
IIC President

Dr. Mrs. S. P. Pawar
Head of Department

Mr. M. Y. Shaikh
IIC Coordinator

Dr. B. P. Ronge
Principal

Dr. Anand S. Rao
*Global Artificial Intelligence
Lead in PwC*



**Shri Vithal Education & Research Institute's
College of Engineering, Pandharpur
Department of Computer Science and Engineering**



**In collaboration with
Global Indian Scientists and Technocrats(GIST)**

Organized a workshop on

“Application of Artificial Intelligence for Product Development & Research”

Certificate of Participation

This is to Certify that Mr/Ms. **Dalave Snehal Sanjay** COLLEGE OF ENGINEERING, PANDHARPUR has successfully attended a Workshop on **“Application of Artificial Intelligence for Product Development & Research”** from 8 May 2023 to 18 May 2023.

Dr. Mrs. V. S. Kshirsagar
IIC President

Dr. Mrs. S. P. Pawar
Head of Department

Mr. M. Y. Shaikh
IIC Coordinator

Dr. B. P. Ronge
Principal

Dr. Anand S. Rao
Global Artificial Intelligence
Lead in PwC



**Shri Vitthal Education & Research Institute's
College of Engineering, Pandharpur**
Department of Computer Science and Engineering



In collaboration with
Global Indian Scientists and Technocrats(GIST)

Organized a workshop on

“Application of Artificial Intelligence for Product Development & Research”

Certificate of Participation

This is to Certify that Mr/Ms. **Dhembare Monali Bandu** COLLEGE OF ENGINEERING, PANDHARPUR has successfully attended a Workshop on **“Application of Artificial Intelligence for Product Development & Research”** from 8 May 2023 to 18 May 2023.

Dr. Mrs. V. S. Kshirsagar
IIC President

Dr. Mrs. S. P. Pawar
Head of Department

Mr. M. Y. Shaikh
IIC Coordinator

Dr. B. P. Ronge
Principal

Dr. Anand S. Rao
*Global Artificial Intelligence
Lead in PwC*



**Shri Vithal Education & Research Institute's
College of Engineering, Pandharpur**
Department of Computer Science and Engineering



In collaboration with
Global Indian Scientists and Technocrats(GIST)

Organized a workshop on

“Application of Artificial Intelligence for Product Development & Research”

Certificate of Participation

This is to Certify that Mr/Ms. **Dhotre Khushi Avinash** COLLEGE OF ENGINEERING, PANDHARPUR has successfully attended a Workshop on **“Application of Artificial Intelligence for Product Development & Research”** from 8 May 2023 to 18 May 2023.

Dr. Mrs. V. S. Kshirsagar
IIC President

Dr. Mrs. S. P. Pawar
Head of Department

Mr. M. Y. Shaikh
IIC Coordinator

Dr. B. P. Ronge
Principal

Dr. Anand S. Rao
*Global Artificial Intelligence
Lead in PwC*



SHRI VITHAL EDUCATION & RESEARCH INSTITUTE'S

COLLEGE OF ENGINEERING, PANDHARPUR



P.B. No. 54, Gopalpur -Ranjani Road, Gopalpur, Tal.- Pandharpur- 413 304,Dist.- Solapur (Maharashtra)

Tel.: 02186-216063, 9503103757, E-mail : coe@sveri.ac.in, Website: www.sveri.ac.in

(Approved by A.I.C.T.E., New Delhi and affiliated to Solapur University, Solapur)

NBA Accredited all Eligible UG Programmes and , NAAC, Accredited Institute,

Accredited by The Institution of Engineers (India), Kolkata and TCS, Pune ISO 9001-2015 Certified Institute

Department of Computer Science & Engineering

RefNo: COE/CSE/2022-23/

Date: 05/04/2023

NOTICE

All the LY BTech Students of CSE Department are hereby informed that CSE Department has scheduled an interactive session/Expert talk. Details are as follows

Mentor Name:	Mr. Ramesh Adavi
Designation	Member
Institute Name	Multinational groups
Session Date & Time	11/04/2021 at 9:30 am
Session Topic	Product development
Venue/Mode	Offline Mode
Target Audience	Last Year B.Tech A Class

Your intellect participation is expected throughout entire session without fail and absenteeism will charged by fine.

(Mr. M. Y. Shaikh)
IIC Coordinator

(Dr. S. P. Pawar)
HOD CSE

Last Year B.Tech- A

HOD,
Department of Computer Science & Engg
SVERI's C.O.E. Pandharpur



SHRI VITHAL EDUCATION & RESEARCH INSTITUTE'S

COLLEGE OF ENGINEERING, PANDHARPUR



P.B. No. 54, Gopalpur -Ranjani Road, Gopalpur, Tal.- Pandharpur- 413 304, Dist.- Solapur (Maharashtra)

Tel.: 02186-216063, 9503103757, E-mail : coe@sveri.ac.in, Website: www.sveri.ac.in

(Approved by A.I.C.T.E., New Delhi and affiliated to Solapur University, Solapur)

NBA Accredited all Eligible UG Programmes and , NAAC, Accredited Institute,

Accredited by The Institution of Engineers (India), Kolkata and TCS, Pune ISO 9001-2015 Certified Institute

Department of Computer Science & Engineering

Ref No: COE/CSE/2022-23/

Date: 8/4/2023

To,
Mr. Ramesh Adavi.
Member,
Multinational groups.

Subject: Invitation for Expert Talk

Respected Sir,

Wishing you greetings for the day!!!

We, on behalf of CSE Department take privilege to invite you as resource person for mentoring our students, on topic "**Product development**" subject arranged for Last Year B. Tech A Class Computer Science and Engineering students on 11/04/2021.

We are hopefully waiting for your presence & valuable time with us.

Thanking You.

Yours faithfully,

(Dr. S. P. Pawar)

HoD CSE Dept. SVERI's CoE, Pandharpur.

HOD,
Department of Computer Science & Engg
SVERI's C.O.E. Pandharpur

Received
Ramesh Adavi
11/4/2023



SHRI VITHAL EDUCATION & RESEARCH INSTITUTE'S

COLLEGE OF ENGINEERING, PANDHARPUR



P.B. No. 54, Gopalpur -Ranjani Road, Gopalpur, Tal.- Pandharpur- 413 304, Dist.- Solapur (Maharashtra)
Tel.: 02186-216063, 9503103757, E-mail : coe@sveri.ac.in, Website: www.sveri.ac.in

(Approved by A.I.C.T.E., New Delhi and affiliated to Solapur University, Solapur)

NBA Accredited all Eligible UG Programmes and , NAAC, Accredited Institute,

Accredited by The Institution of Engineers (India), Kolkata and TCS, Pune ISO 9001-2015 Certified Institute

Department of Computer Science & Engineering

Ref No: COE/CSE/2022-23/

Date: 11/04/2023

Thanks letter

To,
Mr. Ramesh Adavi.
Member.
Multinational groups.

Respected Sir,

This is expressing our heartfelt gratitude towards you for accepting our invitation and gave us expert talk on "**Product development**".

It was really very valuable and useful session for our students.

We expect same kind of cooperation in future also.

Thanking You.

Yours faithfully,

S. Pawar
(Dr. S. P. Pawar)
HoD CSE Dept. SVERI's CoE, Pandharpur.

S. Pawar
HOD,
Department of Computer Science & Engineering
SVERI's C.O.E. Pandharpur

Received
R. Adavi
[RAMESH ADAVI]
11/4/2023



**SHRI VITHAL EDUCATION & RESEARCH INSTITUTE'S
COLLEGE OF ENGINEERING, PANDHARPUR.**

ISO 9001-2015 Certified Institute & Accredited by Institute of Engineers, India,
NAAC and NBA Accredited.

Gopalpur-Ranjani Road, Gopalpur, P.B. No. 54, Tal-Pandharpur-413 304

Dist. Solapur (Maharashtra) Ph.: (02186)225083, Fax: (02186)225082

(Approved by AICTE, New Delhi and affiliated to Solapur University, Solapur)

E-mail :- coe_pan@rediffmail.com

Date: 11/04/2023

Department of Computer Science and Engineering

To,
The Principal,
SVERI's COE,
Pandharpur

Subject: Report Regarding Guest Lecture

Respected Sir,

I, the undersigned Ms. S. A. Hajare (Assistant Professor) working in CSE Department, submitting following report of guest lecture conduction.

Name of the Guest Faculty : Mr. Ramesh Adavi (Member of Multinational groups)

Class : L.Y. B.Tech Div A (SEM_II)

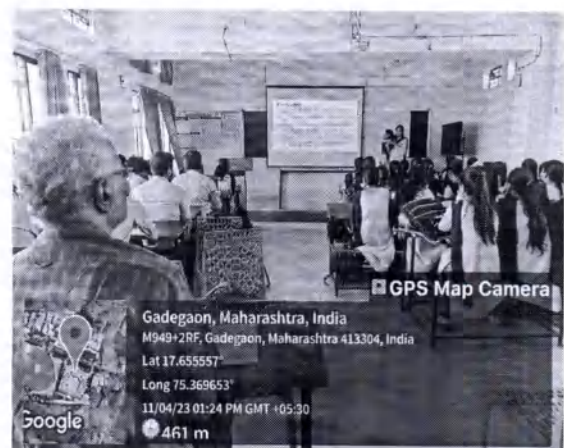
Topic of Guest Lecture : Product Development

Total No. of Hours : 2.00 Hrs

Total No. of Students : 65

Date of Guest Lecture Conducted : 11/04/2023

Snapshots:-



Thanking You,
Hajare
Subject Teacher

S. P. Pawar
HOD CSE

HOD,
Department of Computer Science & Engg
SVERI's C.O.E Pandharpur

Bank Details

Particulars	Details
Beneficiary Name & Address ,Mobile No	RAMESH HANUMANT ADAVI, PUNE Mobile: 9673010222
Beneficiary Bank Name	HDFC BANK LTD.,
Beneficiary Bank Branch Address	ANAND PARK, RAJYOG CREATIONS OFF ITI ROAD, AUNDH, PUNE-411011
Beneficiary Branch IFSC Code	HDFC0000052
Beneficiary Branch MICR Code 9 digit	411240005
Beneficiary Account Number	00521000099483
Amount (in Rs)	
Pin Code Number	
Beneficiary E-Mail Address	ramesh.adavi@gmail.com
PAN NUMBER	ABWPA9469Q

Ramesh Adavi

Seal & Signature



SHRI VITHAL EDUCATION & RESEARCH INSTITUTE'S

COLLEGE OF ENGINEERING, PANDHARPUR



P.B. No. 54, Gopalpur -Ranjani Road, Gopalpur, Tal.- Pandharpur- 413 304,Dist.- Solapur (Maharashtra)

Tel.: 02186-216063, 9503103757, E-mail : coe@sveri.ac.in, Website: www.sveri.ac.in

(Approved by A.I.C.T.E., New Delhi and affiliated to Solapur University, Solapur)

NBA Accredited all Eligible UG Programmes and , NAAC, Accredited Institute,

Accredited by The Institution of Engineers (India), Kolkata and TCS, Pune ISO 9001-2015 Certified Institute

Department of Computer Science & Engineering

Ref No: COE/CSE/2022-23/


Date: 05/04/2023

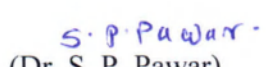
NOTICE

All the LY BTech Students of CSE Department are hereby informed that CSE Department has scheduled an interactive session/Expert talk. Details are as follows

Mentor Name:	Mr. Sudarshan Natu
Designation	Cofounder & Managing Director
Institute Name	NitAI Computers
Session Date & Time	11/04/2021 at 9: 30 am
Session Topic	Product development
Venue/Mode	Offline Mode
Target Audience	Last Year B.Tech B Class

Your intellect participation is expected throughout entire session without fail and absenteeism will charged by fine.


(Mr. M. Y. Shaikh)
IIC Coordinator


(Dr. S. P. Pawar)
HOD CSE

HOD,
Department of Computer Science & Engg.
SVERI's C.O.E. Pandharpur

Last Year B.Tech- B



SHRI VITHAL EDUCATION & RESEARCH INSTITUTE'S

COLLEGE OF ENGINEERING, PANDHARPUR



P.B. No. 54, Gopalpur -Ranjani Road, Gopalpur, Tal.- Pandharpur- 413 304,Dist.- Solapur (Maharashtra)

Tel.: 02186-216063, 9503103757, E-mail : coe@sveri.ac.in, Website: www.sveri.ac.in

(Approved by A.I.C.T.E., New Delhi and affiliated to Solapur University, Solapur)

NBA Accredited all Eligible UG Programmes and , NAAC, Accredited Institute,

Accredited by The Institution of Engineers (India), Kolkata and TCS, Pune ISO 9001-2015 Certified Institute

Department of Computer Science & Engineering

Ref No: COE/CSE/2022-23/

Date: 8/4/2023

To,
Mr. Sudarshan Natu.
Cofounder & Managing Director.
NitAI Computers.

Subject: Invitation for Expert Talk

Respected Sir,

Wishing you greetings for the day!!!

We, on behalf of CSE Department take privilege to invite you as resource person for mentoring our students, on topic "**Product development**" subject arranged for Last Year B. Tech B Class Computer Science and Engineering students on 11/04/2021.

We are hopefully waiting for your presence & valuable time with us.

Thanking You.

Yours faithfully,

S. Pawar
(Dr. S. P. Pawar)
HoD CSE Dept. SVERI's CoE, Pandharpur.

HOD,
Department of Computer Science & Eng.
SVERI's C.O.E. Pandharpur

Received
Natu.



SHRI VITHAL EDUCATION & RESEARCH INSTITUTE'S

COLLEGE OF ENGINEERING, PANDHARPUR



P.B. No. 54, Gopalpur -Ranjani Road, Gopalpur, Tal.- Pandharpur- 413 304,Dist.- Solapur (Maharashtra)

Tel.: 02186-216063, 9503103757, E-mail : coe@sveri.ac.in, Website: www.sveri.ac.in

(Approved by A.I.C.T.E., New Delhi and affiliated to Solapur University, Solapur)

NBA Accredited all Eligible UG Programmes and , NAAC, Accredited Institute,

Accredited by The Institution of Engineers (India), Kolkata and TCS, Pune ISO 9001-2015 Certified Institute

Department of Computer Science & Engineering

RefNo: COE/CSE/2022-23/

Date: 11/04/2023

Thanks letter

To,
Mr. Sudarshan Natu.
Cofounder & Managing Director.
NitAI Computers.

Respected Sir,

This is expressing our heartfelt gratitude towards you for accepting our invitation and gave us expert talk on "**Product development**".

It was really very valuable and useful session for our students.

We expect same kind of cooperation in future also.

Thanking You.

Yours faithfully,

S. P. Pawar
(Dr. S. P. Pawar)
HoD CSE Dept. SVERI's CoE, Pandharpur.

HOD,
Department of Computer Science & Engg
SVERI's C.O.E. Pandharpur

Received
Natu



**SHRI VITHAL EDUCATION & RESEARCH INSTITUTE'S
COLLEGE OF ENGINEERING, PANDHARPUR.**

ISO 9001-2015 Certified Institute & Accredited by Institute of Engineers, India,
NAAC and NBA Accredited.
Gopalpur-Ranjani Road, Gopalpur, P.B. No. 54, Tal-Pandharpur-413 304
Dist. Solapur (Maharashtra) Ph.: (02186)225083, Fax: (02186)225082
(Approved by AICTE, New Delhi and affiliated to Solapur University, Solapur)
E-mail :- coe_pan@rediffmail.com

Date: 11/04/2023

Department of Computer Science and Engineering

To,
The Principal,
SVERI's COE,
Pandharpur

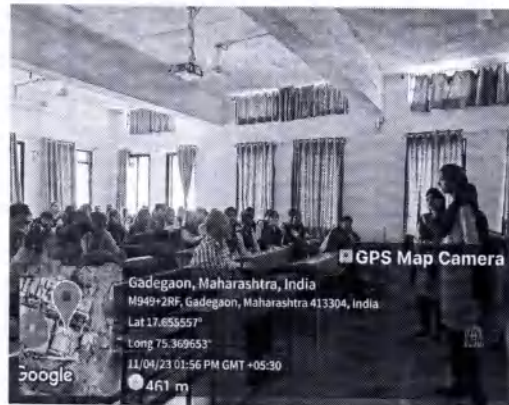
Subject: Report Regarding Guest Lecture

Respected Sir,

I, the undersigned Ms. S. A. Hajare (Assistant Professor) working in CSE Department, submitting following report of guest lecture conduction.

Name of the Guest Faculty : Mr. Sudarshan Natu (Co-Founder & Managing Director @ NitAI Computers)
Class : L.Y. B.Tech Div B (SEM_II)
Topic of Guest Lecture : Product Development
Total No. of Hours : 2.00 Hrs
Total No. of Students : 50
Date of Guest Lecture Conducted : 11/04/2023

Snapshots:-



Thanking You,
[Signature]
Subject Teacher

S.P. Pawar
HOD CSE
HOD,
Department of Computer Science & Engg
SVERI's C.O.E. Pandharpur

Bank Details

Sr.No.	Particulars	Details
	Beneficiary Name & Address ,Mobile No	Sudarshan Vitthalrao Natu B607 om Avishkar sneh paradise Rambaug Colony Paud Road kotwad Pune 9822068430
	Beneficiary Bank Name	ICICI Bank Ltd.
	Beneficiary Bank Branch Address	Ramchandra Sabha mandap Shivajinagar Pune 411005
	Beneficiary Branch IFSC Code	ICIC0000039
	Beneficiary Branch MICR Code 9 digit	411229003
	Beneficiary Account Number	003901012916
	Amount (in Rs)	
	Pin Code Number	411038
	Beneficiary E-Mail Address	SUNATU@GMAIL.COM
	PAN NUMBER	AAJPN4233H

Nate

Seal & Signature



SHRI VITHAL EDUCATION & RESEARCH INSTITUTE'S

COLLEGE OF ENGINEERING, PANDHARPUR



P.B. No. 54, Gopalpur -Ranjani Road, Gopalpur, Tal.- Pandharpur- 413 304,Dist.- Solapur (Maharashtra)

Tel.: 02186-216063, 9503103757, E-mail : coe@sveri.ac.in, Website: www.sveri.ac.in

(Approved by A.I.C.T.E., New Delhi and affiliated to Solapur University, Solapur)

NBA Accredited all Eligible UG Programmes and , NAAC, Accredited Institute,

Accredited by The Institution of Engineers (India), Kolkata and TCS, Pune ISO 9001-2015 Certified Institute

Department of Computer Science & Engineering

Ref No: COE/CSE/2022-23/


Date: 05/04/2023

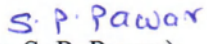
NOTICE

All the TY BTech Students of CSE Department are hereby informed that CSE Department has scheduled an interactive session/Expert talk. Details are as follows

Mentor Name:	Mr. Atul Marathe
Designation	Ex Vice President.
Institute Name	Persistent.
Session Date & Time	10/04/2023 at 02.30 pm
Session Topic	Project to Product
Venue/Mode	Offline Mode
Target Audience	Third Year B.Tech Class

Your intellect participation is expected throughout entire session without fail and absenteeism will charged by fine.


(Mr. M. Y. Shaikh)
IIC Coordinator


(Dr. S. P. Pawar)
HOD CSE

Third Year B.Tech- A
Third Year B.Tech- B

HOD,
Department of Computer Science & Engg.
SVERI's C.O.E. Pandharpur

SHRI VITHAL EDUCATION & RESEARCH INSTITUTE'S

COLLEGE OF ENGINEERING, PANDHARPUR



P.B. No. 54, Gopalpur -Ranjani Road, Gopalpur, Tal.- Pandharpur- 413 304,Dist.- Solapur (Maharashtra)

Tel.: 02186-216063, 9503103757, E-mail : coe@sveri.ac.in, Website: www.sveri.ac.in

(Approved by A.I.C.T.E., New Delhi and affiliated to Solapur University, Solapur)

NBA Accredited all Eligible UG Programmes and , NAAC, Accredited Institute,

Accredited by The Institution of Engineers (India), Kolkata and TCS, Pune ISO 9001-2015 Certified Institute

Department of Computer Science & Engineering

Ref No: COE/CSE/2022-23/

Date: 8/4/2023

To,
Mr. Atul Marathe
Ex Vice President.
Persistent.

Subject: Invitation for Expert Talk

Respected Sir,

Wishing you greetings for the day!!!

We, on behalf of CSE Department take privilege to invite you as resource person for mentoring our students, on topic "**Project to Product**" subject arranged for Third Year B. Tech Computer Science and Engineering students on 10/04/2023.

We are hopefully waiting for your presence & valuable time with us.

Thanking You.

Yours faithfully,

S.P. Pawar
(Dr. S. P. Pawar)
HoD CSE Dept. SVERI's CoE, Pandharpur.

*Received.
Atul Marathe*

HOD,
Department of Computer Science & Engg
SVERI's C.O.E. Pandharpur



SHRI VITHAL EDUCATION & RESEARCH INSTITUTE'S

COLLEGE OF ENGINEERING, PANDHARPUR



P.B. No. 54, Gopalpur -Ranjani Road, Gopalpur, Tal.- Pandharpur- 413 304,Dist.- Solapur (Maharashtra)

Tel.: 02186-216063, 9503103757, E-mail : coe@sveri.ac.in, Website: www.sveri.ac.in

(Approved by A.I.C.T.E., New Delhi and affiliated to Solapur University, Solapur)

NBA Accredited all Eligible UG Programmes and , NAAC, Accredited Institute,

Accredited by The Institution of Engineers (India), Kolkata and TCS, Pune ISO 9001-2015 Certified Institute

Department of Computer Science & Engineering

RefNo: COE/CSE/2022-23/

Date: 10/04/2023

Thanks letter

To,
Mr. Atul Marathe
Ex Vice President.
Persistent.

Respected Sir,

This is expressing our heartfelt gratitude towards you for accepting our invitation and gave us expert talk on "**Project to Product**".

It was really very valuable and useful session for our students.

We expect same kind of cooperation in future also.

Thanking You.

Yours faithfully,

S. P. Pawar
(Dr. S. P. Pawar)
HoD CSE Dept. SVERI's CoE, Pandharpur.

*Received
At Marathe*

HOD,
Department of Computer Science & Engg
SVERI's C.O.E. Pandharpur

Bank Details

Particulars	Details
Beneficiary Name & Address ,Mobile No	ATUL M MARATHE 3 ANAND APTS. CTS 103/13 ERANDWAI PUNE - 411004
Beneficiary Bank Name	BANK OF INDIA 98900150
Beneficiary Bank Branch Address	F.C. ROAD PUNE - 411004
Beneficiary Branch IFSC Code	BKID0000514
Beneficiary Branch MICR Code 9 digit	411013014
Beneficiary Account Number	051410100008004
Amount (in Rs)	
Pin Code Number	411004
Beneficiary E-Mail Address	atulmarathe@outlook.com
PAN NUMBER	ABEPM6308E

Atul Marathe

Seal & Signature



SHRI VITHAL EDUCATION & RESEARCH INSTITUTE'S

COLLEGE OF ENGINEERING, PANDHARPUR



P.B. No. 54, Gopalpur -Ranjani Road, Gopalpur, Tal.- Pandharpur- 413 304,Dist.- Solapur (Maharashtra)
Tel.: 02186-216063, 9503103757, E-mail : coe@sveri.ac.in, Website: www.sveri.ac.in
(Approved by A.I.C.T.E., New Delhi and affiliated to P.A.H.Solapur University, Solapur)
NBA Accredited all Eligible UG Programmes and , NAACA+, Accredited Institute,
Accredited by The Institution of Engineers (India), Kolkata and TCS, Pune ISO 9001-2015 Certified
Institute



INSTITUTION'S
INNOVATION
COUNCIL
(Ministry of Education Initiative)



End to End Product Development Which Covers Ideation to Product Launch

Theme: Expert Session

Mode: Offline

Date of Session: 10 April 2023

Name of Speaker: Mr. Sudarshan Natu

**Organizer: SVERI's IIC with Collaboration of Electronics & Telecommunication
Engineering Department**

Organized for: Students

Flyer:

Shri Vithal Education & Research Institute's
College of Engineering,
Pandharpur

Institution's Innovation Council (IIC), Institute of Electrical and
Electronics (IEEE) & Department of Electronics and
Telecommunication Engineering Organizes
An Expert Session on-

End to End Product Development Which Covers Ideation To Product Launch

Day: Monday,
Date: 10th April, 2023
Timing: 12:30 pm To
1:30pm

Mr. Sudarshan Natu
M.Tech From IITx, Vice President of Harman
Connected Services, Co-founder and
Managing Director of NAI Computers, Pune



SHRI VITHAL EDUCATION & RESEARCH INSTITUTE'S

COLLEGE OF ENGINEERING, PANDHARPUR



P.B. No. 54, Gopalpur -Ranjani Road, Gopalpur, Tal.- Pandharpur- 413 304, Dist.- Solapur (Maharashtra)

Tel.: 02186-216063, 9503103757, E-mail : coe@sveri.ac.in, Website: www.sveri.ac.in

(Approved by A.I.C.T.E., New Delhi and affiliated to P.A.H.Solapur University, Solapur)

NBA Accredited all Eligible UG Programmes and , NAACA+, Accredited Institute,

Accredited by The Institution of Engineers (India), Kolkata and TCS, Pune ISO 9001-2015 Certified Institute

Description:

A Expert Session on “**End to End Product Development Which Covers Ideation to Product Launch**” was conducted on 10th April 2023, by the Department of Electrical Engineering Department and SVERI's Institution Innovation Council, Pandharpur. The speaker for this Expert Talk was Mr. Sudarshan Natu, who had completed his M.Tech. from IIT, and had a total Industrial experience of 35 plus years, The title End to End Product Development Which Covers Ideation to Product Launch, identifies the importance for students which refers to every step of a product's development from start to finish. The phrase can be used to mean a product is ready for launch, i.e. that the roadmap has been achieved, from end-to-end.

Objectives:

1. To facilitate the student understands of the concept of End to End Product Development Which Covers Ideation to Product Launch.
2. To recognize the importance of every step of a product's development.
3. To identify when the product can launch.
4. To make the students familiar with roadmap of product's development from start to finish.

Outcome:

1. Students are aware about the concept of End to End Product Development Which Covers Ideation to Product Launch.
2. Students are able to develop their thinking level to develop a product and how launch it.
3. The Session is aimed to build entrepreneurship skills in students.

Recorded Link: https://youtu.be/_48EnPKOcgU



SHRI VITHAL EDUCATION & RESEARCH INSTITUTE'S
COLLEGE OF ENGINEERING, PANDHARPUR



P.B. No. 54, Gopalpur -Ranjani Road, Gopalpur, Tal.- Pandharpur- 413 304,Dist.- Solapur (Maharashtra)
Tel.: 02186-216063, 9503103757, E-mail : coe@sveri.ac.in, Website: www.sveri.ac.in
(Approved by A.I.C.T.E., New Delhi and affiliated to P.A.H.Solapur University, Solapur)
NBA Accredited all Eligible UG Programmes and , **NAACA+**, Accredited Institute,
Accredited by The Institution of Engineers (India), Kolkata and TCS, Pune ISO 9001-2015 Certified
Institute



Entrepreneurship And Experience Sharing

Theme: Expert Session

Mode: Offline

Date of Session: 10 April 2023

Name of Speaker: Mr. Sudarshan Natu

Organizer:SVERI's IIC with Collaboration of Electronics and Telecommunication Engineering Department

Organized for: Students

Flyer:



Shri Vithal Education & Research Institute's
College of Engineering, Pandharpur



Institution's Innovation Council (IIC)
Organizes
An Expert Session on

Entrepreneurship And Experience Sharing

by



Mr. Sudarshan Natu

M.Tech From IIT, Ex Vice President of Harman Connected Services;
Cofounder and Managing Director of NitAI Computers, pune

Day & Date: Monday, 10th April, 2023



SHRI VITHAL EDUCATION & RESEARCH INSTITUTE'S

COLLEGE OF ENGINEERING, PANDHARPUR



P.B. No. 54, Gopalpur -Ranjani Road, Gopalpur, Tal.- Pandharpur- 413 304, Dist.- Solapur (Maharashtra)
Tel.: 02186-216063, 9503103757, E-mail : coe@sveri.ac.in, Website: www.sveri.ac.in
(Approved by A.I.C.T.E., New Delhi and affiliated to P.A.H.Solapur University, Solapur)
NBA Accredited all Eligible UG Programmes and , **NAACA+**, Accredited Institute,
Accredited by The Institution of Engineers (India), Kolkata and TCS, Pune ISO 9001-2015 Certified Institute

Description:

Mr. Sudarshan Natu Sir conducted Expert Session on Entrepreneurship And Experience Sharing. Entrepreneurship is the skill and behavior of an entrepreneur. On the other hand, entrepreneurship is the study of taking calculated risks when starting new businesses and when managing those businesses well. Sir also explained Entrepreneurship has been defined as the "capacity and willingness to develop, organize, and manage a business venture along with any risks in order to make a profit." It is the process of creating, launching, and operating a new firm. The topic of entrepreneurship is currently up for discussion. From this Expert session, students understood startups related information and also how to start our own company using different technology.

Objectives:

1. To recognize the steps and processes involved in establishing small units.
2. To Learn about the resources for assistance and support available to launch a small business.
3. To obtain the managerial expertise required to manage the industrial unit.
4. To understand the benefits and drawbacks of entrepreneurship.
5. TO Assisting the individual in comprehending opportunities and changes in the environment.
6. TO learn and respect the necessary entrepreneurial/social responsibility principles.

Outcome: By achieving the following outcomes, students will be able to successfully establish and manage small business units, understand the entrepreneurial landscape, and fulfill their social responsibility:



SHRI VITHAL EDUCATION & RESEARCH INSTITUTE'S
COLLEGE OF ENGINEERING, PANDHARPUR



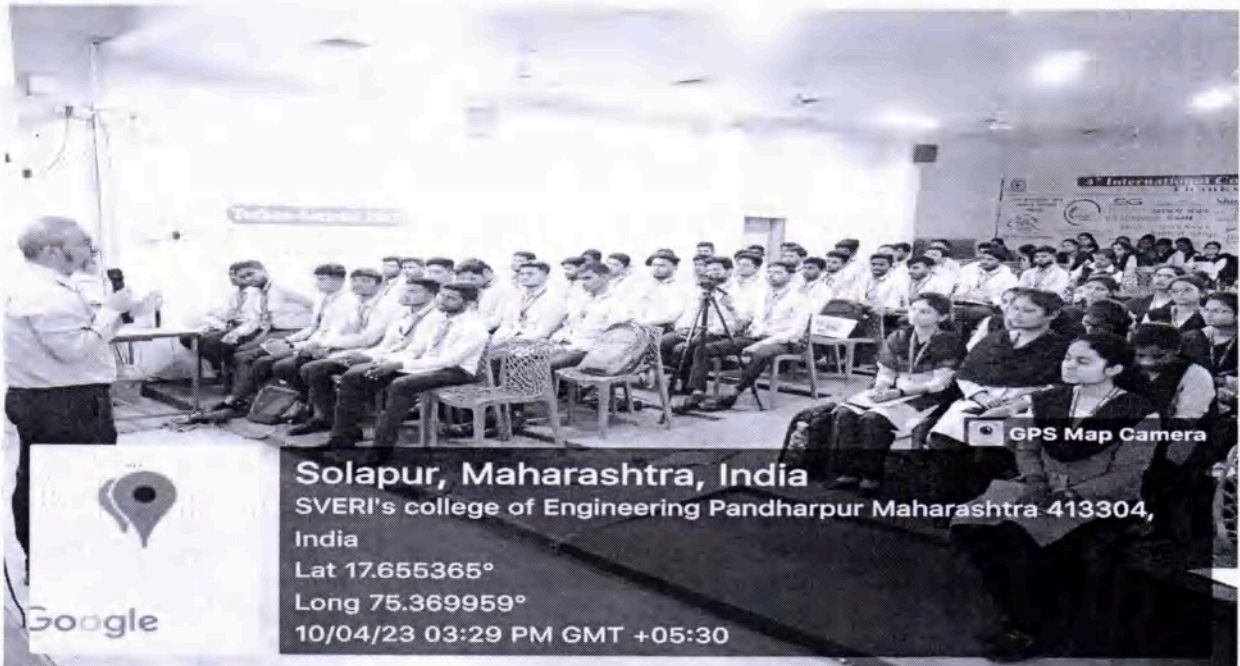
P.B. No. 54, Gopalpur -Ranjani Road, Gopalpur, Tal.- Pandharpur- 413 304,Dist.- Solapur (Maharashtra)
Tel.: 02186-216063, 9503103757, E-mail : coe@sveri.ac.in, Website: www.sveri.ac.in
(Approved by A.I.C.T.E., New Delhi and affiliated to P.A.H.Solapur University, Solapur)
NBA Accredited all Eligible UG Programmes and , NAACA+, Accredited Institute,
Accredited by The Institution of Engineers (India), Kolkata and TCS, Pune ISO 9001-2015 Certified
Institute

1. Recognize the steps and processes involved in establishing small units.
2. Gain knowledge about the resources available for assistance and support in launching a small business.
3. Acquire the necessary managerial expertise to effectively manage an industrial unit.
4. Understand the benefits and drawbacks of entrepreneurship.
5. Develop an understanding of opportunities and changes in the business environment.
6. Learn and embrace the necessary principles of entrepreneurial and social responsibility.

Recorded Link: <https://youtu.be/as93HyofnYI>

Facebook/Twitter/Insta link: <https://www.facebook.com/100081964986786/posts/202273165848182/?app=fbl>

Glimpses:

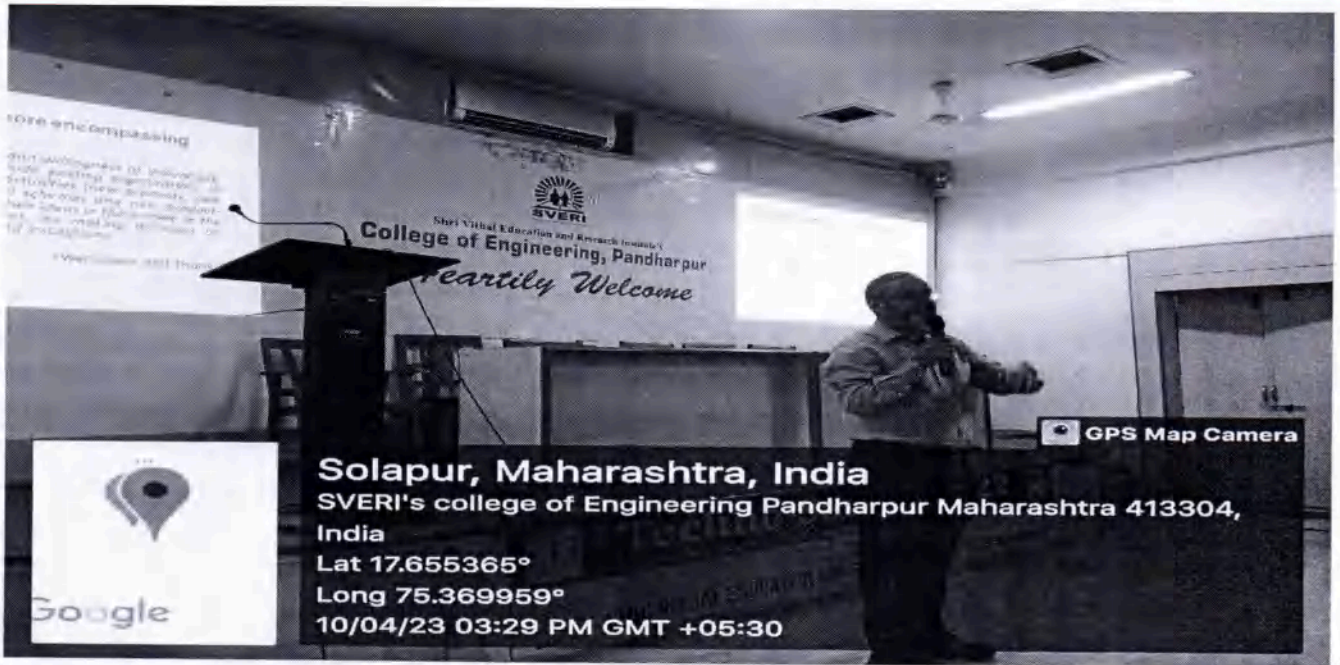




SHRI VITHAL EDUCATION & RESEARCH INSTITUTE'S
COLLEGE OF ENGINEERING, PANDHARPUR



P.B. No. 54, Gopalpur -Ranjani Road, Gopalpur, Tal.- Pandharpur- 413 304,Dist.- Solapur (Maharashtra)
Tel.: 02186-216063, 9503103757, E-mail : coe@sveri.ac.in, Website: www.sveri.ac.in
(Approved by A.I.C.T.E., New Delhi and affiliated to P.A.H.Solapur University, Solapur)
NBA Accredited all Eligible UG Programmes and , **NAACA+**, Accredited Institute,
Accredited by The Institution of Engineers (India), Kolkata and TCS, Pune ISO 9001-2015 Certified
Institute

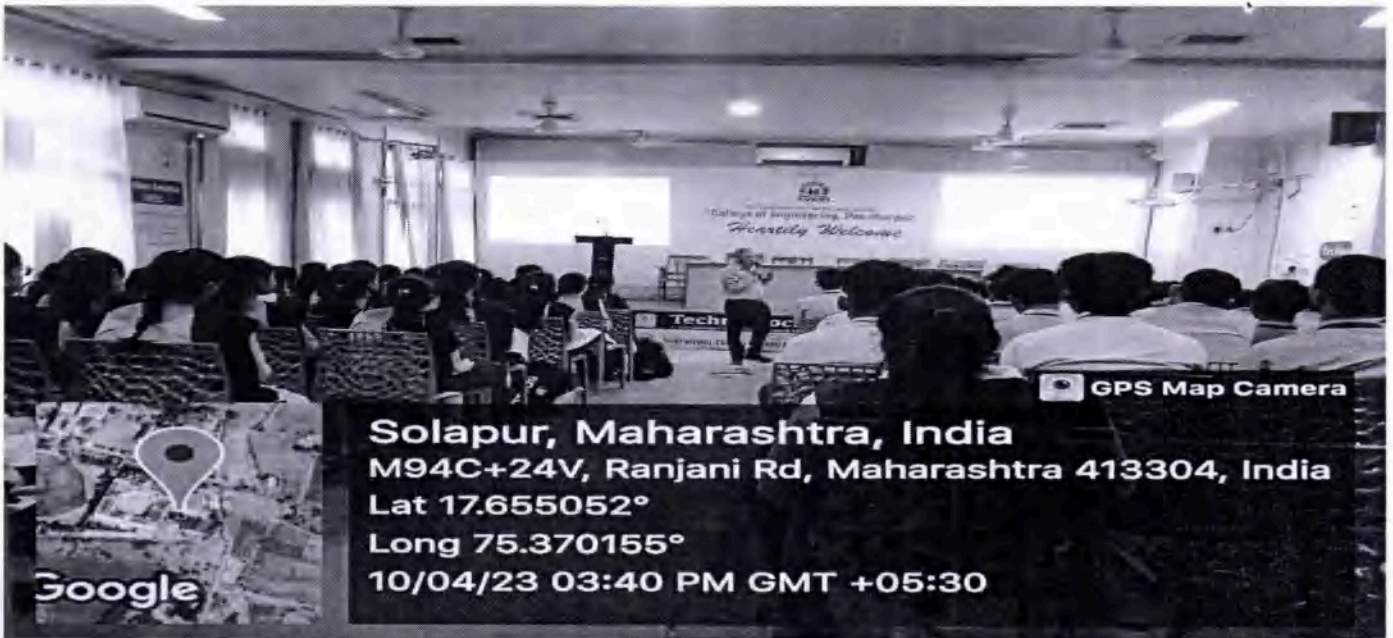




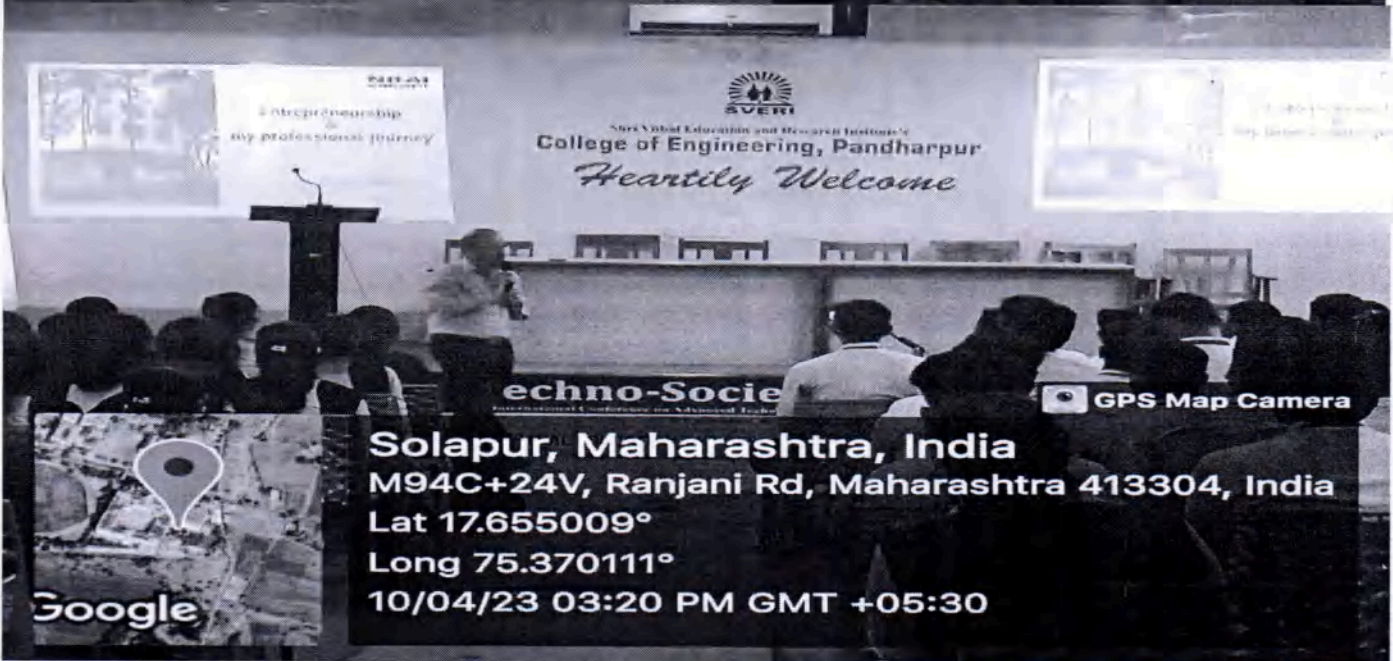
SHRI VITHAL EDUCATION & RESEARCH INSTITUTE'S
COLLEGE OF ENGINEERING, PANDHARPUR



P.B. No. 54, Gopalpur -Ranjani Road, Gopalpur, Tal.- Pandharpur- 413 304,Dist.- Solapur (Maharashtra)
Tel.: 02186-216063, 9503103757, E-mail : coe@sveri.ac.in, Website: www.sveri.ac.in
(Approved by A.I.C.T.E., New Delhi and affiliated to P.A.H.Solapur University, Solapur)
NBA Accredited all Eligible UG Programmes and , **NAACA+**, Accredited Institute,
Accredited by The Institution of Engineers (India), Kolkata and TCS, Pune ISO 9001-2015 Certified Institute



Solapur, Maharashtra, India
M94C+24V, Ranjani Rd, Maharashtra 413304, India
Lat 17.655052°
Long 75.370155°
10/04/23 03:40 PM GMT +05:30



Solapur, Maharashtra, India
M94C+24V, Ranjani Rd, Maharashtra 413304, India
Lat 17.655009°
Long 75.370111°
10/04/23 03:20 PM GMT +05:30

Attendance:



SHRI VITHAL EDUCATION & RESEARCH INSTITUTE'S

COLLEGE OF ENGINEERING, PANDHARPUR

P.B. No. 54, Gopalpur -Ranjani Road, Gopalpur, Tal.- Pandharpur- 413 304,Dist.- Solapur (Maharashtra)

Tel.: 02186-216063, 9503103757, E-mail : coe@sveri.ac.in, Website: www.sveri.ac.in

(Approved by A.I.C.T.E., New Delhi and affiliated to P. A. H. Solapur University, Solapur)

NBA Accredited all Eligible UG Programmes and NAAC A+, Accredited Institute,

Accredited by the Institute of Engineers (India), Kolkata and TCS, Pune ISO 9001-2015 Certified Institute



ISO 9001:2015



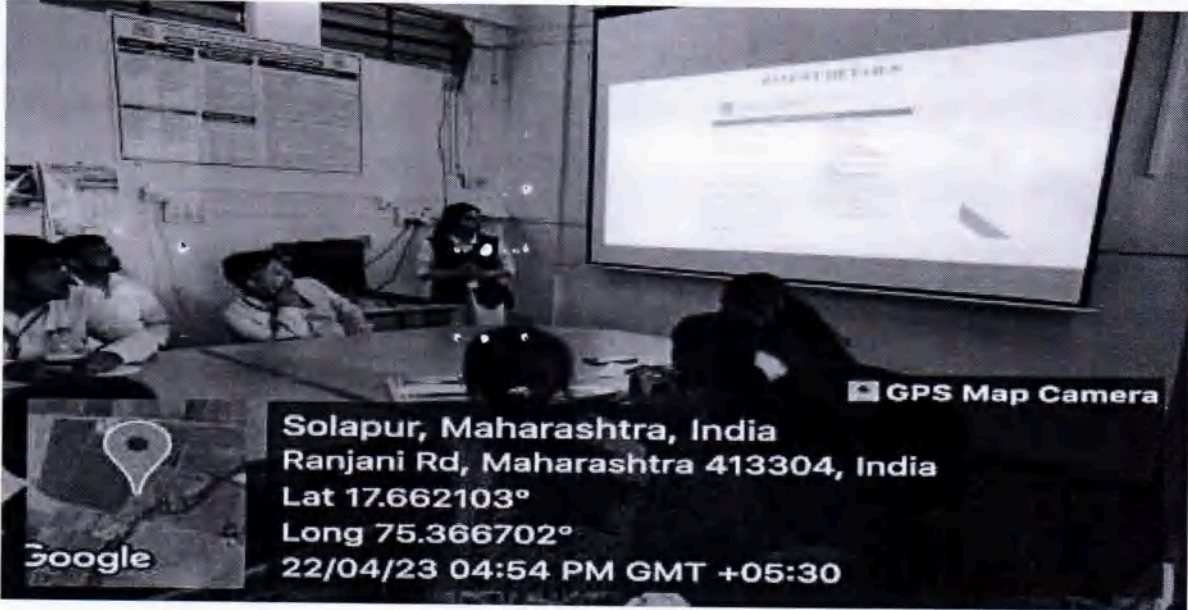
www.iso.org

IIC Report

Date:22/04/2023

Sr. No.	Event : IIC Expert Talk
1.	Name of Programme : Automatic Dust Cleaning Smart Fan
2.	Faculty Name-Ms. Ms. Mohua Biswas
3.	Objectives: <ol style="list-style-type: none">1. To provide an automatic dust-cleaning smart fan for cleaning the dust accumulate on the edge of the fan leaves.2. To provide the camera to capture the image of the fan leaves to detect whether dust is accumulated on the edge of the fan leaves.3. To provide a controller to turn on/off the DC motor to clean the edge of the smart fan leaves.
4.	Working: The camera is embedded within the bottom canopy of the motor unit of the smart fan to capture the image of leaves and pass the captured image to the image processing unit. The image processing detects whether dust particles are accumulated on the leaves or not. The detected information will be passed to the controller. The controller is embedded within the smart leaf to turn on or off the DC motor based on the received information from the image processing unit. If dust particles accumulate on the edge of the leaves and reach a particular range, then the controller turns on the DC motor to clean the dust. The smart dust cleaner comprises of DC motor, belt pulley and dust cleaner holder. When the DC motor turns on, it rotates the belt pulley so that the belt connected with each pulley can also rotate and clean dust present on the edge of the smart leaf.
5.	Outcome: From this session, Faculty can easily comprehend how to draft a patent, how to make a claim in a patent, and how the patenting process works after listening to this expert talk.
6.	Videolink: https://drive.google.com/file/d/14wo4O9dQr2tJLhjbXtZVCU6MMR0dmVsc/view?usp=drive link

Glimpses:



Attendance:

ST NO	Name	Sign	ST NO	Name	Sign
1.	MS. Bhirde	<i>[Signature]</i>	14	Mr. J.L. Musale	<i>[Signature]</i>
2.	MS. M.A. Sawant	<i>[Signature]</i>	15	Dr. Meenakshi Bhat	<i>[Signature]</i>
3.	MS. S. B. Jagtap	<i>[Signature]</i>	16	MS. S. S. Pawar	<i>[Signature]</i>
4.	MS. S. A. Apte	<i>[Signature]</i>	17	MS. S. S. Gaurav	<i>[Signature]</i>
5.	MS. S. D. Pujari	<i>[Signature]</i>			
6.	Ms. Sanghvi Indhu	<i>[Signature]</i>			
7.	MS. Nirmala P. Pujari	<i>[Signature]</i>			
8.	J.N.P. Kulkarni	<i>[Signature]</i>			
9.	MS. S. D. Indulkar	<i>[Signature]</i>			
10.	ST. N.K. Mishra	<i>[Signature]</i>			
11.	Mr. A.A. Gatale	<i>[Signature]</i>			
12.	Mr. R.B. Pawar	<i>[Signature]</i>			
13.	Mr. P.S. Dastmalkar	<i>[Signature]</i>			

HOD

(Dr. Mrs. M.M. Pawar)

Head

Dept. of Electronics & Telecomm.
 Engg. SVERI'S C.O.E. Pandharpur



SHRI VITHAL EDUCATION & RESEARCH INSTITUTE's

COLLEGE OF ENGINEERING, PANDHARPUR



ISO 9001:2015



P.B. No. 54, Gopalpur -Ranjani Road, Gopalpur, Tal.- Pandharpur- 413 304, Dist.- Solapur (Maharashtra)

Tel.: 02186-216063, 9503103757, E-mail : coe@sveri.ac.in, Website: www.sveri.ac.in

(Approved by A.I.C.T.E., New Delhi and affiliated to P. A. H. Solapur University, Solapur)

NBA Accredited all Eligible UG Programmes and , NAAC A+, Accredited Institute,

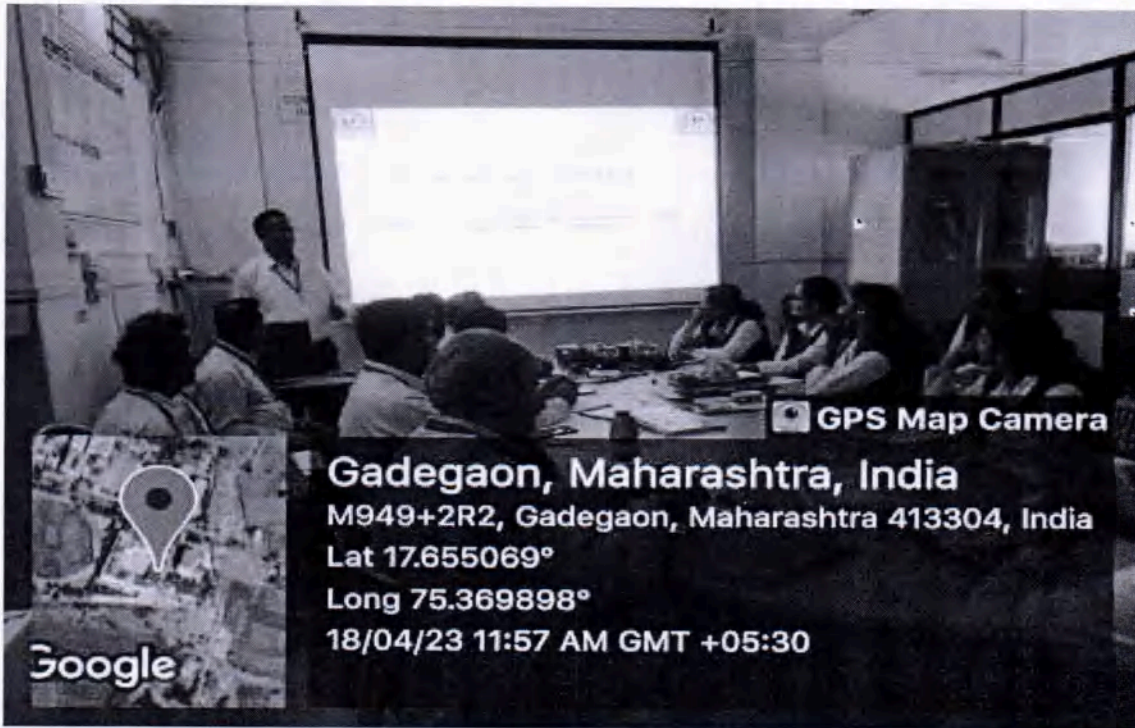
Accredited by the Institute of Engineers (India), Kolkata and TCS, Pune ISO 9001-2015 Certified Institute

IIC Report

Date:18/04/2023

Sr. No.	Event : IIC Expert Talk
1.	Name of Programme: How to write a Patent
2.	Faculty Name-Dr. M.S. Mathapati
3.	Objectives: <ol style="list-style-type: none">1. How to write patent2. Facilitate technology transfer from academia3. Use patents to advance and recognize innovative research
4.	Working: A patent is a type of intellectual property that gives its owner the legal right to exclude others from making, using, or selling an invention for a limited period of time in exchange for publishing an enabling disclosure of the invention. utility patents, design patents, and plant patents. Each type has its own eligibility requirements and protects a specific type of invention, useful process, or discovery. However, it's possible for one invention or discovery to have more than one type of patent available for it.
5.	Outcome: for this expert session faculty can understand how to write patent and types of patents ,for our new innovation and research paper etc.
6.	Videolink: https://drive.google.com/file/d/1dAKU876PMZXX2BBZRFTX4PrUPYiiLY59/view?usp=drive_link

Glimpses:



Attendance:

Sl. No.	Name	Sign	Sl. No.	Name	Sign
1)	Mr. S. K. Jadhav	[Signature]	15	Pr. Chaudhary	[Signature]
2)	Mr. S. B. Jadhav	[Signature]			
3)	Mr. N. P. Kulkarni	[Signature]			
4)	Mr. S. S. Gokhale	[Signature]			
5)	Mr. S. R. Waghmare	[Signature]			
6)	Mr. S. D. Jadhav	[Signature]			
7)	Mr. S. A. Inamdar	[Signature]			
8)	Mr. T. J. Hollari	[Signature]			
9)	Mr. A. A. Gargal	[Signature]			
10)	Mr. N. K. Mishra	[Signature]			
11)	Mr. J. L. Munde	[Signature]			
12)	Mr. B. S. Dastmalkar	[Signature]			
13)	Mr. Sang. S. Jadhav	[Signature]			
14)	Mr. M. A. Jadhav	[Signature]			
15)					

[Handwritten Signature]
HOD

(Dr. Mrs. M. M Pawar)

Head

Dept. of Electronics & Telecomm.
Engg. SVERI'S C.O.E. Pandharpur

SVERI's College of Engineering, Pandharpur



REPORT

Expert Session

On

**“Accelerators/Incubation-Opportunities for
Students & Faculties-Early Stage
Entrepreneurs (ESE)”**

(Date: 03/08/2022)

Organized by

**Institution's Innovation Council (IIC),
Institute of Electrical and
Electronics(IEEE)**

**Department of Electronics and Telecommunication
Engineering**

AY: 2022-2023



Shri Vithal Education & Research Institute's

COLLEGE OF ENGINEERING, PANDHARPUR



ISO 9001:2015



P.B. No. 54, Gopalpur -Ranjani Road, Gopalpur, Pandharpur- 413 304, District: Solapur (Maharashtra)
Tel.: 02186-216063, 9503103757, Toll Free No.: 1800-3000-4131, E-mail: coe@sveri.ac.in, Web: www.sveri.ac.in

Approved by A.I.C.T.E., New Delhi and Affiliated to P.A.H. Solapur University, Solapur)

NBA Accredited all eligible UG Programmes, NAAC A+ Accredited Institute, Accredited by The Institution of Engineers (India), Kolkata and TCS, Pune. ISO 9001-2015 Certified Institute

Report of Expert Session

Topic of Session : "Accelerators/Incubation-Opportunities for Students & Faculties-Early Stage Entrepreneurs (ESE)"

Date: Wednesday, 3rd August, 2022

Time: 2:30pm Onwards

Mode of Conduct: Online through Zoom link

<https://zoom.us/j/98644489861?pwd=NWlZWlVPbGIYSm1KRENpS2ovcmtuUT>

Organizing Department: Institution's Innovation Council (IIC), Institute of Electrical and Electronics (IEEE) & Department of Electronics and Telecommunication Engineering

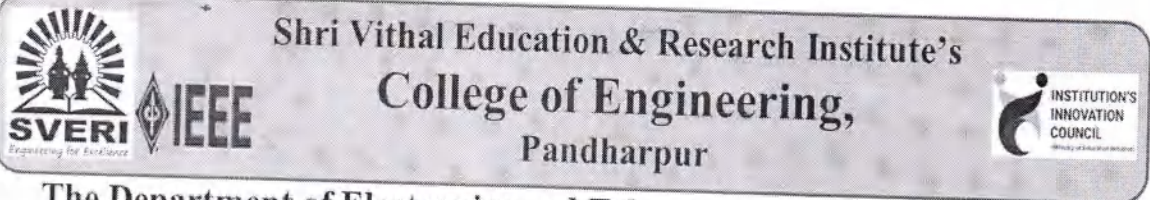
Brief Details about the Programme:

The department of Electronics and Telecommunication Engineering, SVERI's College of Engineering, Pandharpur had organized an expert session on "Accelerators/Incubation-Opportunities for Students & Faculties-Early Stage Entrepreneurs (ESE)" on Wednesday, 3rd August, 2022.

The aim of this online session is to provide Knowledge regarding Early Stage Entrepreneurs (ESE) and details regarding Accelerators/Incubation. An incubator helps entrepreneurs flesh out business ideas while accelerators expedite growth of existing companies with a minimum viable product (MVP). Incubators operate on a flexible time frame ending when a business has an idea or product to pitch to investors or consumers. So Session was arranged for all* students of the electronics and communication department on "Accelerators/Incubation-Opportunities for Students & Faculties-Early Stage Entrepreneurs (ESE)".

The session was conducted By Mr.Girish Sampath, Manager, Community, And Programs, Sobus Insight Forum. He explained regarding Accelerators/Incubation. Ms.S.S.Gawade gave a brief introduction about the resource person and regarding the session and also proposed a Vote of thanks. More than 100 students and 20 faculties participated in this session.

Brochure of FDP:



Shri Vithal Education & Research Institute's
College of Engineering,
Pandharpur

The Department of Electronics and Telecommunication Engineering in
Collaboration with Institution's Innovation Council (IIC) and Institute of
Electrical and Electronics (IEEE)

Organizes Expert Session on:

Accelerators/Incubation-Opportunities for Students & Faculties-Early
Stage Entrepreneurs

Platform : 



Mr. Girish Sampath

Day & Date: Wednesday,
3rd August, 2022
Time: 2:30 pm Onwards

Manager, Community and Programs, Sobus
Insight Forum

Schedule of FDP:

Date: Wednesday, 3rd August, 2022

Time: 2:30pm Onwards

Mode of Conduct: Online through Zoom link:

<https://zoom.us/j/98644489861?pwd=NWlzWlVpPbGIYSm1KRENpS2ovcmtuUT09>

Resource Person of FDP:

Mr. Girish Sampath Manager, (Community, And Programs, Sobus Insight Forum)



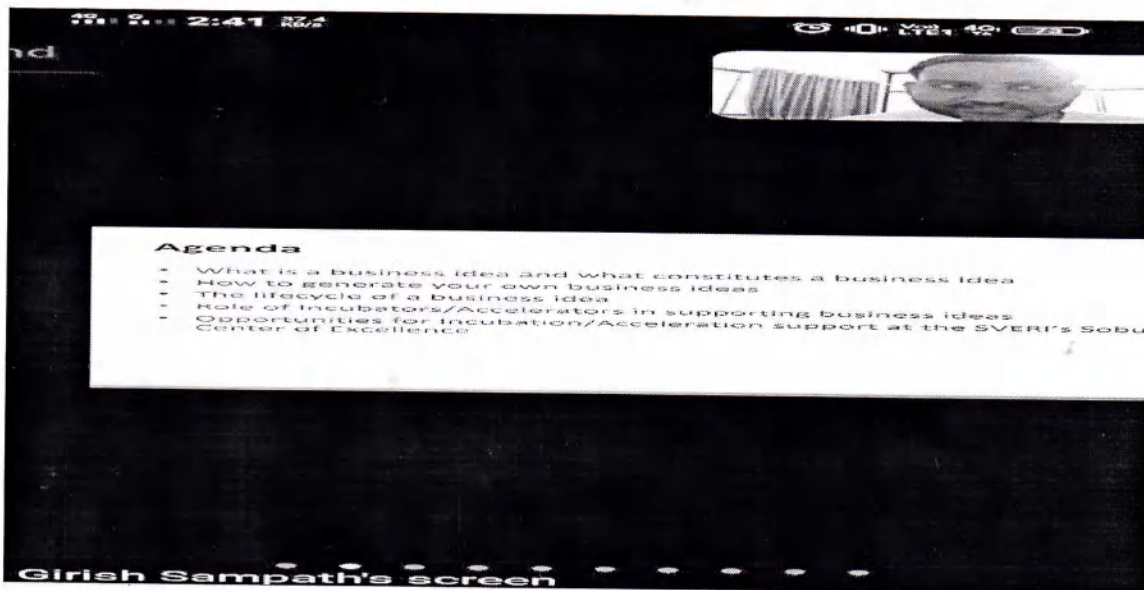
Qualification:

- **MBA**– (Marketing and Finance) from Dept.of Management Studies, Anna University.
- **B.E.** (Electrical and Electronics Engineering), St. Josephs College of Engineering (2004-2008).

Experience:

- **Community Builder:** Sobus Insight Forum In Bengaluru.
- **Manager Partnership:** Omnicuris, Mumbai Area.
- **Deputy Manager Partnerships:** Mylan In Bengaluru.
- **Project Co-ordinator-** The shola Trust
- **India Fellow :** India Fellow Social Leadership Program, Delhi
- **Intern:** L&T Ltd, ECC Division, Chennai area
- **Intern:** TVS motors
- **System Engineer:** Infosys

Glimpses of FDP Sessions:



Initials	Name of Faculty	Username	Official Email-id
Ms.	Mohua Biswas	msbiswas@coe.sveri.ac.in	msbiswas@coe.sveri.ac.in
Mr.	Rahul Bandopant Pawar	rbpawar@coe.sveri.ac.in	rbpawar@coe.sveri.ac.in
Ms.	Smita Suresh Gawade	ssgawade@coe.sveri.ac.in	ssgawade@coe.sveri.ac.in
Mr.	Amol Achyutrao Kadam	aakadam@coe.sveri.ac.in	aakadam@coe.sveri.ac.in
Ms.	N.T.Pujari	ntpujari@coe.sveri.ac.in	ntpujari@coe.sveri.ac.in
Ms.	Seema Ashok Atole	saatole@coe.sveri.ac.in	saatole@coe.sveri.ac.in
Ms.	Jyoti Sahadev Shinde	jakendule@coe.sveri.ac.in	jakendule@coe.sveri.ac.in
Ms.	Sangeeta jadhav	sjadhav@coe.sveri.ac.in	sjadhav@coe.sveri.ac.in
Mr.	M A Deshmukh	madeshmukh@coe.sveri.ac.in	madeshmukh@coe.sveri.ac.in



Life stages of a startup and its activities at each stage

Stage 1: Newborn Phase (0-3 months)	Infancy Phase (3-12 months)	Toddler Phase (12-24 months)	Stand up Phase (18-24 months)	Walk Ahead Phase (24-36 months)
<ul style="list-style-type: none"> Idea formation Idea Validation Core team setup Entity creation Proof of concept creation 	<ul style="list-style-type: none"> Office setup Proof of concept validation Seed Funding Initial or early customer sign up 	<ul style="list-style-type: none"> Creation of business value proof points Reframing of value proposition and product features based on initial feedback Team Expansion Partnerships creation Initiation of angel or institutional round 	<ul style="list-style-type: none"> Revenue scaling by increasing customer base Product hardening for robustness Setup of organizational processes and functions 	<ul style="list-style-type: none"> Raising of series A funds Creation of new product variants for scaling the footprint Geographical expansion

Source: The manual for Indian startups

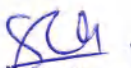


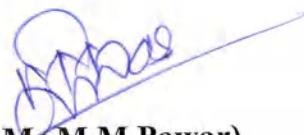
Outcomes of FDP:

In this session students learnt about the life stages of a startup and its activities at each stage. Students get the knowledge about Accelerators/Incubation and also Students get opportunities for Incubation/Acceleration support at the SVERI's Sobus Center of Excellence platform of Early Stage Entrepreneurs.

You-tube Link of Session:

<https://youtube.com/playlist?list=PLF2Tj6hbnH7hIBJKi7xqSHAvC2JWVlpAJ>


(Ms.S.S.Gawade)
IEEE Coordinator


(Dr. Ms.M.M.Pawar)
HOD E&TC Department
Head
Dept. of Electronics & Telecomm.
Engg. SVERI'S C.O.E. Pandharpur



SHRI VITHAL EDUCATION & RESEARCH INSTITUTE'S
COLLEGE OF ENGINEERING, PANDHARPUR



P.B. No. 54, Gopalpur -Ranjani Road, Gopalpur, Tal.- Pandharpur- 413 304, Dist.- Solapur (Maharashtra)
Tel.: 02186-216063, 9503103757, E-mail : coe@sveri.ac.in, Website: www.sveri.ac.in
(Approved by A.I.C.T.E., New Delhi and affiliated to P.A.H.Solapur University, Solapur)
NBA Accredited all Eligible UG Programmes and , NAACA+, Accredited Institute,
Accredited by The Institution of Engineers (India), Kolkata and TCS, Pune ISO 9001-2015 Certified
Institute



Theme: Exhibition Day

Mode: Offline

Date of Session: 21 April 2023

Name of Speaker: Er. Mohan S. Deshpande, Hon. Secretary, IEI, Solapur Chapter.

Organizer: SVERI's IIC with Collaboration of Electronics And Telecommunication Engineering Department

Organized for: Students



SHRI VITHAL EDUCATION & RESEARCH INSTITUTE'S
COLLEGE OF ENGINEERING, PANDHARPUR



P.B. No. 54, Gopalpur -Ranjani Road, Gopalpur, Tal.- Pandharpur- 413 304,Dist.- Solapur (Maharashtra)
Tel.: 02186-216063, 9503103757, E-mail : coe@sveri.ac.in, Website: www.sveri.ac.in
(Approved by A.I.C.T.E., New Delhi and affiliated to P.A.H.Solapur University, Solapur)
NBA Accredited all Eligible UG Programmes and , NAACA+, Accredited Institute,
Accredited by The Institution of Engineers (India), Kolkata and TCS, Pune ISO 9001-2015 Certified
Institute

Flyer:



**Shri Vithal Education & Research Institute's
College of Engineering,
Pandharpur**



Institution's Innovation Council (IIC), All India Council for Technical Education(AICTE), Institute of Electrical and Electronics Engineers (IEEE) Student Chapter & Department of E&TC Engineering Organized

Exhibition Day

Description: Electronic & Telecommunication Engineering Department coordination with SVERI's IIC organized an Event Exhibition Day.



SHRI VITHAL EDUCATION & RESEARCH INSTITUTE'S
COLLEGE OF ENGINEERING, PANDHARPUR



P.B. No. 54, Gopalpur -Ranjani Road, Gopalpur, Tal.- Pandharpur- 413 304,Dist.- Solapur (Maharashtra)
Tel.: 02186-216063, 9503103757, E-mail : coe@sveri.ac.in, Website: www.sveri.ac.in
(Approved by A.I.C.T.E., New Delhi and affiliated to P.A.H.Solapur University, Solapur)
NBA Accredited all Eligible UG Programmes and , NAACA+, Accredited Institute,
Accredited by The Institution of Engineers (India), Kolkata and TCS, Pune ISO 9001-2015 Certified
Institute

Objectives:

1. To facilitate the students explore their practical knowledge.
2. To make students interactive other than academic.
3. To facilitate students about the new innovative concepts.
4. To facilitate students about the importance of implementing the idea into a prototype.

Outcomes:

The students will be able to:

- 1 Explore their practical knowledge.
- 2 Make students interactive other than academic.
- 3 Facilitate students about the new innovative concepts.
- 4 Facilitate students about the importance of implementing the idea into a prototype.

RecordedLink:https://drive.google.com/drive/folders/1YHPDyPGq-BSDNYUhPeUQW5nttAweCPVw?usp=share_link

Facebook/Twitter/Insta link: <https://www.facebook.com/100081964986786/posts/277503271658504/>



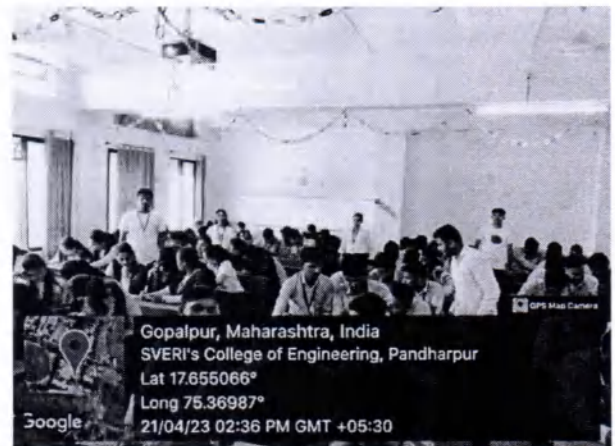
SHRI VITHAL EDUCATION & RESEARCH INSTITUTE'S
COLLEGE OF ENGINEERING, PANDHARPUR



P.B. No. 54, Gopalpur -Ranjani Road, Gopalpur, Tal.- Pandharpur- 413 304,Dist.- Solapur (Maharashtra)
Tel.: 02186-216063, 9503103757, E-mail : coe@sveri.ac.in, Website: www.sveri.ac.in
(Approved by A.I.C.T.E., New Delhi and affiliated to P.A.H.Solapur University, Solapur)
NBA Accredited all Eligible UG Programmes and , NAACA+, Accredited Institute,
Accredited by The Institution of Engineers (India), Kolkata and TCS, Pune ISO 9001-2015 Certified
Institute

Glimpses:

1

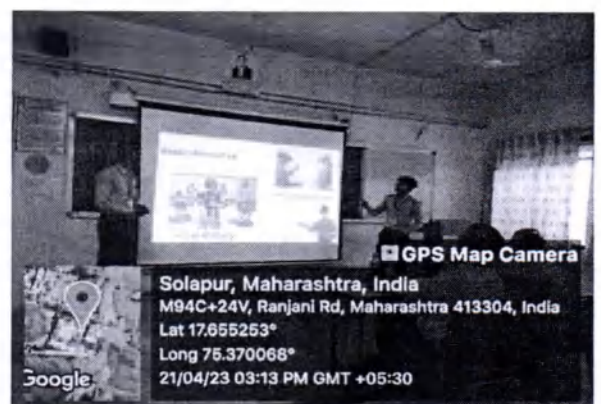
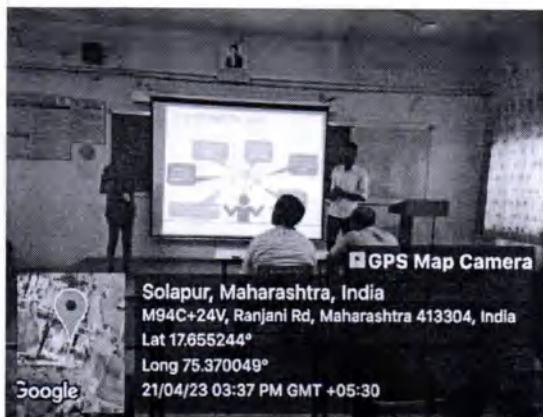
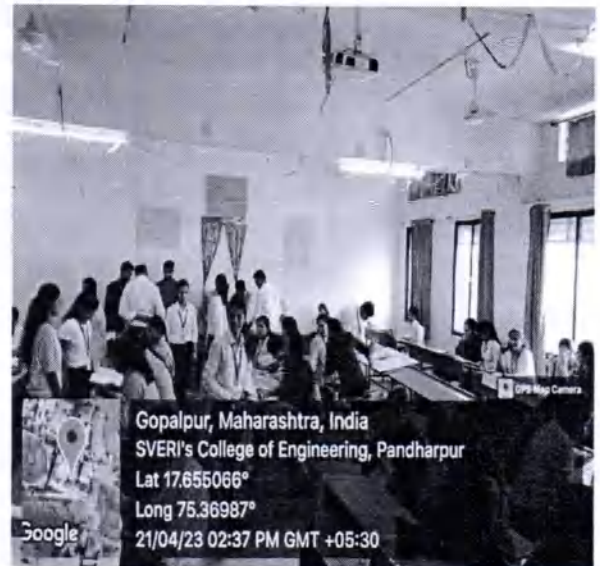


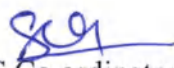


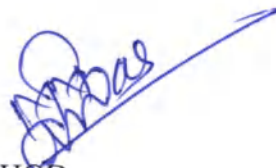
SHRI VITHAL EDUCATION & RESEARCH INSTITUTE'S
COLLEGE OF ENGINEERING, PANDHARPUR



P.B. No. 54, Gopalpur -Ranjani Road, Gopalpur, Tal.- Pandharpur- 413 304, Dist.- Solapur (Maharashtra)
Tel.: 02186-216063, 9503103757, E-mail : coe@sveri.ac.in, Website: www.sveri.ac.in
(Approved by A.I.C.T.E., New Delhi and affiliated to P.A.H.Solapur University, Solapur)
NBA Accredited all Eligible UG Programmes and , NAACA+, Accredited Institute,
Accredited by The Institution of Engineers (India), Kolkata and TCS, Pune ISO 9001-2015 Certified
Institute




IIC Co ordinator


HOD

Head
Dept. of Electronics & Telecomm.,
Engg. SVERI'S C.O.E. Pandharpur

Sponsored Project

Sunshine Powertronics Pvt Ltd

Reg.Off- B403, Karan Bella Vista, Sr.No 75/1,75/2 , Pune-Solapur Road, Manjari, Pune-412307

To,

Date: 22.08.22

The Principal,
SVERI's College of Engineering, Pandharpur

Subject: Regarding sponsored project

Respected Sir,

With reference to above cited subject, Sunshine Power Electronics Pvt. Ltd. Pune conducted a meeting for sponsored projects with final year students on 24.08.2022. The following projects listed below are sponsored under MOU activity of SVERI's COE Pandharpur and Sunshine Power Electronics Pvt. Ltd. Pune for the academic year 2022-23.

Sr.No	Project	Student Name
1	Development of Fish Monitoring System using IoT for Aquaculture.	Ms. Walke Vaishnavi Digambar
		Ms. Shelke Rutuja Sanjay
		Ms. Devkule Aishwarya Appa
2	Water Quality Analysis and Smart water meter using IoT.	Ms. Bharna Sakshitai Shivsharan
		Ms. Gaddam Shefali Ajay
		Ms. Lokare Amruta Rajabhau

Thanking you.



Regards,

(Mr. Ashwin Tayade)

Technical Director

Sunshine Powertronics Pvt. Ltd. Pune



Caainos Technologies

H-302, La Vida Loca , Pimple Saudagar, Pune- 411027

Email : Caainos@gmail.com, Phone : +917674066055

To,

Date: 20.08.22

The Principal,
SVERI's College of Engineering, Pandharpur

Subject: Regarding sponsored project

Respected Sir,

With reference to above cited subject, Caainos Technologies. Pune conducted a meeting for sponsored projects with final year students on 22.08.2022. The following projects listed below are sponsored under MOU activity of SVERI's COE Pandharpur and Caainos Technologies. Pune for the academic year 2022-23.

Sr.No	Project	Student Name
1	IoT Based Health Monitoring Device.	Ms. Deshmukh Vaishnavi Shardkar
		Ms. Jadhav Akansha Anil
		Ms. Sonar Trupti Govind
2	Power Generation from Foot Steps using Piezo Sensor.	Ms. Atkale Shivani Ramdas
		Ms. Bansode Ankita Annasaheb
		Ms. Chavan Vaishnavi Sudhir

Thanking you.

Regards,

Rajesh Bhalerao
Caainos Technologies,
Pune-411027





Shri Vithal Education & Research Institute's
COLLEGE OF ENGINEERING, PANDHARPUR



ISO 9001:2015



P.B. No. 54, Gopalpur - Ranjani Road, Gopalpur, Tal.: Pandharpur- 413304, Dist.: Solapur (MH)
Contact No.: 9545553888, 9545553757, E-mail : coe@sveri.ac.in, Website: www.sveri.ac.in
Approved by A.I.C.T.E., New Delhi and affiliated to Panyashlok Ahilyadevi Holkar Solapur University,
Solapur NAAC A+ with 3.46 CGPA out of 4.00, An ISO 9001-2015 Certified Institute, Accredited by the
Institution of Engineers, Kolkata and TCS, Pune.

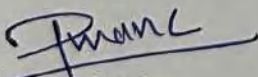
Date:-

SVRI's College of Engineering, Pandharpur
Department of Computer Science & Engineering

Sponsored Project List
A. Y. 2022-23

Sr. No	Name of Student	Title of the Project	Name of Industry
1	Vishakha Vijaykumar Savalkar	An Eminent Visual Model for Deaf and Mute People using Machine Learning	Shrinivas Medical and General Stores, Pandharpur
	Prerana Raju Limbole		
	Trupti Sunil Katkamwar		
	Vaishnavi M. Abhangrao		
2	Pratik Gorakh Mali	Social Media Platform Based on Blockchain	Namrata Computers, Pandharpur
	Onkar Bhimrao Babar		
	Arbaj Jalaluddin Mujawar		
	Harshad Bharat Bad		
3	Shailesh Ravikant Bhosale	File Integrity Monitoring	IIT Computers, Pandharpur
	Jadhav Abhishek Ashok		
	Sathe Omkar Ghansham		
	Lingade Vishal Anil		
4	Jagdale Pavanraj Balasaheb	Skin Disease Prediction Using Dynamic Testing In Machine Learning	Shanti Clinic, Pandharpur
	Nagane Ananda Rajendra		
	Sakshi Vikas Shivsharan		
	Aparna Baliram Vasmale		
5	Pallavi Aba jadhav	Scan An Pay	VSD Mart, Chale, Pandharpur
	Shruti pandurang Adat		
	Anushka Santosh Chavan		
	Swarupa Kolle		
	Anisha Kamble		
5	Yogeshree Pawar	Scan An Pay	VSD Mart, Chale, Pandharpur
	Dipali Mungase		
	Pradnya Ingale		

6	Raviraj Kudal	RG Legal Associates	R. G. Legal Associates, Pandharpur
	Aditya Keskar		
	Omkar Kale		
	Rushikesh Ghogardare		
7	Vaishnvi vikram jathar	Online courier management	Techno Scripts, Pune
	Lazina sadik devale		
	Mayeshwari shrikrishna more		
	Sakshi ganesh bhosale		
	Shaina ismile shaikh		
8	Dnyaneshwar sanjivan Lohar	Multiple Crop Disease Prediction Web App	TechnoWings IT Solutions, Solapur
	Swapnil Bharat More		
	Umesh Vijay madane		
	Rahul kisan Devkate		
	Shubham Gorakh Shende		
9	Pranav Santoshkumar Dongare	Smart Timetable System using AI and ML	TechnoWings IT Solutions, Solapur
	Suraj Suryakant Nagtilak		
	Anand Dattatraya Salave		
	Ganesh Bandu Yeole		
	Nivrutee Dnyaneshwar Dongare		
10	Vaishnavi Gurupadappa Nanna	MedCare-Android Based Medical Services Application	Techno Scripts, Pune
	Vaibhavi Vivekanand Patil		
	Vibhuti Ananda Pawar		
	Poonam Dattatray Bhandare		
	Aarti Ashok Mali		


(Mr. P. D. Mane)
Project Coordinator

S. P. Pawar
(Dr. S. P. Pawar)

HOD
HOD,

Department of Computer Science & Engg
SVRI's C.O.E. Pandharpur.



Shri Vithal Education & Research Institute's
COLLEGE OF ENGINEERING, PANDHARPUR



P.B. No. 54, Gopalpur - Ranjani Road, Gopalpur, Tal.: Pandharpur- 413304, Dist.: Solapur (MH)
Contact No.: 9545553888, 9545553757, E-mail : coe@sveri.ac.in, Website: www.sveri.ac.in
Approved by A.I.C.T.E., New Delhi and affiliated to Punyashlok Ahilyadevi Holkar Solapur University,
Solapur NAAC A+ with 3.46 CGPA out of 4.00, An ISO 9001-2015 Certified Institute, Accredited by the
Institution of Engineers, Kolkata and TCS, Pune.

Ref. No.

Date: 07/12/2022

To,
Mr. Nitin Asabe,
IIT Computers,
Pandharpur

Subject: About getting Sponsored Project.

Respected Sir,

Hope this letter finds you in good health and pleasant mood.

It gives me immense pleasure to put before you few words about our institute, Shri Vithal Education and Research Institute (SVERI), a Charitable Trust formed by devoted technocrats, established its first project, College of Engineering, Pandharpur in 1998 with approval from AICTE, New Delhi and Government of Maharashtra. All eligible UG courses of our college are accredited by NBA. The Engineering College is accredited by NAAC A+, TCS, The Institution of Engineers (India), Kolkata and is also ISO 9001:2015 Certified. The college administration is striving hard to provide the best facilities to the students along with the quality education. Every year our students are grabbing 10-12 University ranks. Campus placement rate of our college is also very high.

As per our Final Year B. Tech. (Computer Science and Engineering) syllabus, students/project groups are expected to complete a project sponsored by the same industry. They should observe various activities/processes/functions those are happening in industry for getting exposure & knowledge. Based on this, they should prepare a project report, which will be submitted to college.

Following mentioned our students are interested to do their project work with your esteemed organization. We request to provide necessary support to them. We assure you that student will complete the project in time without disturbing your scheduled work. The names of the students are as follows:

Name of Student:

- | | |
|---------------------------|-------------------------------|
| 1. Jadhav Abhishek Ashok | 2. Sathe Omkar Ghansham |
| 3. Lingade Vishal Anil | 4. Jagdale Pavanraj Balasaheb |
| 5. Nagane Ananda Rajendra | |

Name of Project Guide: Prof. P.D.Mane

Such activity will really bridge the gap between industry & institute for further strengthening the relations resulting in powerful academic environment.

We will be grateful to you always.

Thanking you
Yours truly,

S. P. Pawar
(Dr. Mrs. S. P. Pawar)
HOD CSE

HOD,

Department of Computer Science & Engg
SVERI's C.O.E. Pandharpur



Address: - 4002, Arbuji Mension, Station Road,
Bhosale Nagar, Pandharpur - 413304

Date: - 04/01/2023

**The Head,
Department of Computer Science and Engineering,
SVETI's C.O.E. Pandharpur.**

Subject: About approving Sponsored Project.

Respected Madam,

I received your letter and I am glad to inform you that, we are allowing your students for undergoing the internship in our company.

During this period, following mentioned students will work on Sponsored Project titled "**File Integrity Monitoring**" We hope that students will complete the project in time. The names of the students are as follows:

Names of students:

- | | |
|---------------------------|-------------------------------|
| 1. Jadhav Abhishek Ashok | 2. Sathe Omkar Ghansham |
| 3. Lingade Vishal Anil | 4. Jagdale Pavanraj Balasaheb |
| 5. Nagane Ananda Rajendra | |

Name of project guide: Prof. P.D.Mane

Such activity will really bridge the gap between industry and institute for further strengthening the relations resulting in powerful academic environment.

Regards.


Nitin Asube




Address: - 4002, Arbuj Mension, Station Road,
Bhosale Nagar, Pandharpur - 413304

Date: 05/06/2023

This is to certify that the student of Computer Science and Engineering Department from SVERI's College of Engineering, Pandharpur are allowed to develop software module for our IIT Computer Center, under the title of,
"File Integrity Monitoring"

The Details of operation will be provided as per the requirements.

The students are as follows:

Abhishek A. Jadhav

Pavanraj B. Jagdale

Vishal A. Lingade

Omkar G. Sathe

Ananda R. Nagane.

Regards.


Nitin Asabe




Shri Vitthal Education & Research Institute's
COLLEGE OF ENGINEERING, PANDHARPUR



P.B. No. 54, Gopalpur - Ranjani Road, Gopalpur, Tal.: Pandharpur- 413304, Dist.: Solapur (MH)
Contact No.: 9545553888, 9545553757, E-mail : coe@sveri.ac.in, Website: www.sveri.ac.in
Approved by A.I.C.T.E., New Delhi and affiliated to Punyashlok Ahilyadevi Holkar Solapur University,
Solapur NAAC A+ with 3.46 CGPA out of 4.00, An ISO 9001-2015 Certified Institute, Accredited by the
Institution of Engineers, Kolkata and TCS, Pune.

Ref. No.

Date: 05/11/2022

To,
Mr. Sachin Kole,
Pharmacist,
Shrinivas Medical and General Stores,
Pandharpur

Subject: About getting Sponsored Project.
Respected Sir,

Hope this letter finds you in good health and pleasant mood.

It gives me immense pleasure to put before you few words about our institute, Shri Vitthal Education and Research Institute (SVERI), a Charitable Trust formed by devoted technocrats, established its first project, College of Engineering, Pandharpur in 1998 with approval from AICTE, New Delhi and Government of Maharashtra. All eligible UG courses of our college are accredited by NBA. The Engineering College is accredited by NAAC A+, TCS, The Institution of Engineers (India), Kolkata and is also ISO 9001:2015 Certified. The college administration is striving hard to provide the best facilities to the students along with the quality education. Every year our students are grabbing 10-12 University ranks. Campus placement rate of our college is also very high.

As per our Final Year B. Tech. (Computer Science and Engineering) syllabus, students/project groups are expected to complete a project sponsored by the same industry. They should observe various activities/processes/functions those are happening in industry for getting exposure & knowledge. Based on this, they should prepare a project report, which will be submitted to college.

Following mentioned our students are interested to do their project work with your esteemed organization. We request to provide necessary support to them. We assure you that student will complete the project in time without disturbing your scheduled work. The names of the students are as follows:

Name of Student:

- | | |
|---------------------------|------------------------|
| 1. Vaishnavi M. Abhangrao | 2. Prerana R. Limbole |
| 3. Vishakha V. Savalkar | 4. Trupti S. Katkamwar |

Name of Project Guide: Prof. T. A. Dhumal

Such activity will really bridge the gap between industry & institute for further strengthening the relations resulting in powerful academic environment.
We will be grateful to you always.

Thanking you
Yours truly,

S.P. Pawar
(Dr. Mrs. S. P. Pawar)
HOD CSE

HOD,
Department of Computer Science & Engg
SVERI's C.O.E. Pandharpur.

SHRINIVAS MEDICAL AND GENERAL STORES

4726/41, Manisha Nagar, Near Vitthal Mandir, Opposite Ujani Colony
Pandharpur 413304, Maharashtra India

Date: - 11/02/2023

**The Head,
Department of Computer Science and Engineering,
SVERI's C.O.E. Pandharpur.**

Subject: About approving Sponsored Project.

Respected Madam,

I received your letter and I am glad to inform you that, we are allowing your students for undergoing the internship in our company.

During this period, following mentioned students will work on Sponsored Project titled “**An Eminent Visual Model for Deaf and Mute People using Machine Learning**” We hope that students will complete the project in time. The names of the students are as follows:

Names of students:

- | | |
|---------------------------|------------------------|
| 1. Vaishnavi M. Abhangrao | 2. Prerana R. Limbole |
| 3. Vishakha V. Savalkar | 4. Trupti S. Katkamwar |

Name of project guide: Prof. T. A. Dhumal

Such activity will really bridge the gap between industry and institute for further strengthening the relations resulting in powerful academic environment.



Mr. Sachin Kole
(Pharmacist)

**Shrinivas Medical
& General Stores**
4726/41, Manisha Nagar Pandharpur
Mob. 9423328961

Contact Details

Mob: +919423328961
Email ID: sachinkole1978@gmail.com

SHRINIVAS MEDICAL AND GENERAL STORES

4726/41, Manisha Nagar, Near Vitthal Mandir, Opposite Ujani Colony
Pandharpur 413304, Maharashtra India

Date: 05/07/2023

To Whomsoever It May Concern

This is to certify that the student of Computer Science and Engineering Department from SVERI's College of Engineering, Pandharpur are allowed to develop software module for our Shrinivas Medical, under the title of **"An Eminent Visual Model for Deaf and Mute People using Machine Learning"**

The Details of operation will be provided as per the requirements.

The students are as follows:

Vaishnavi M. Abhangrao

Vishakha V. Savalkar

Prerana R. Limbole

Trupti S. Katkamwar

Name of the Guide: **Prof. T. A. Dhumal**



Mr. Sachin Kole

(Pharmacist)

**Shrinivas Medical
& General Stores**
4726/41, Manisha Nagar Pandharpur
Mob. 9423328961

Contact Details

Mob: +919423328961

Email ID: sachinkole1978@gmail.com

SHANTI CLINIC

Chatrapati Shivaji maharaj chowk, pandharpur
dis-solapur, pin-413304 mob-7972077462

Date:30/04/2023

To Whomsoever It May Concern

This is to certify that the student of computer science and Engineering Department from SVERI's College of Engineering, Pandharpur are allowed to develop software module for our Shanti Clinic, under title of "Skin Disease Prediction Dynamic Testing in Machine Learning"

As per the discussion made, we are ready to pay the amount of Rs. 25000 for the research development and implementation of this model, our contribution will be utilized for prototyping testing software development hardware integration and marketing efforts associated with the project.

The Details of operation will be provided as per the requirements.

The students are as follows;

Sakshi V. Shivkaran

Pallavi A. Jadhav

Aparna B. Vasmale

Shruti P. Adat

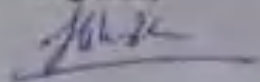
Anushka S. Chavan

Guide Name: Prof. T.A. Dhumal

Mob-7972077462

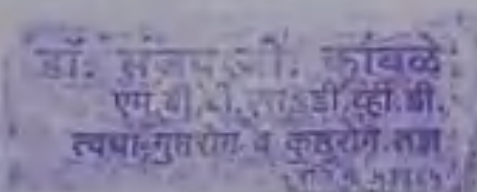
Regards,

shanticlinic@gmail.com



Sanjay G. Kamble

(MBBS & V.D)



SHANTI CLINIC

Chatrapati Shivaji maharaj chowk, pandharpur,
dis-solapur, pin-413304 mob-7972077462

Date: 10/05/2023

To Whomsoever It May Concern

This is to certify that the student of computer science and Engineering Department from SVRI's College of Engineering, Pandharpur are allowed to develop software module for our Shanti Clinic, under title of "Skin Disease Prediction Dynamic Testing in Machine Learning"

As per the discussion made, we have paid a certain amount for this model the student in the following installment:

1st Installment = Rs. 5000

2nd Installment = Rs. 8000

And we will pay the remaining amount in further installments.

The Details of operation will be provided as per the requirements.

The students are as follows:

Sakshi V. Shivsharan

Poojavi A. Jadhav

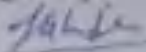
Aparna B. Vamrale

Shruti P. Adat

Anushka S. Chavan

Guide Name: Prof. T.A. Dhumal

Regards,



Sanjay G. Kambale

(MBBS P.C.D)

Mob-7972077462

shanticlinic@gmail.com

डॉ. संजय जी. कांबळे
एन.टी.सी.एन. डी.एच.डी.
स्वचा, गुनरोग व कुष्ठरोग तज्ञ
पिन-४१३३०४

SHANTI CLINIC

Chatrapati Shivaji maharaj chowk, pandharpur
dis-solapur, pin-413304 **mob-7972077462**

Date:31/05/2023

To Whomsoever It May Concern

This is to certify that the student of computer science and Engineering Department from SVERI's College of Engineering ,Pandharpur are allowed to develop software module for our Shanti Clinic ,under title of "Skin Disease Prediction Dynamic Testing in Machine Learning"

The Details of operation will be provided as per the requirments.

The students are as follows;

Sakshi V. Shivsharan

Pallavi A. Jadhav

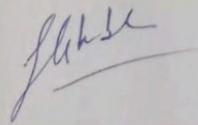
Aparna B. Vasmale

Shruti P. Adat

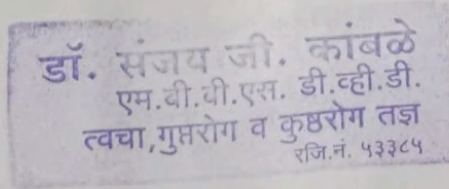
Anushka S. Chavan

Guide Name: Prof. T.A. Dhumal

Regards,



Dr.Sanjay Kambale
(MBBS P.C.D)



Mob-+917972077462

Shanticlinic@gmail.com



+91 8668659319

pratikghogardare45@gmail.com

Sawarkar chowk, Station road,
Pandharpur, 413304.

Date : / / 2023

To Whomsoever It May Concern

This is to certify that the student of Computer Science and Engineering Department from SVERI's College of Engineering, Pandharpur are allowed to develop software module for our R. G. Legel Associates, under the title of "R. G. Legel Associates".

The Details of operation will be provided as per the requirements.

The students are as follows:

1. Mr. Pardeshi Siddhesh Shivsingh.
2. Mr. Kudal Raviraj Dhondappa.
3. Mr. Ghogardare Rushikesh Mahendra.
4. Mr. Keskar Aditya Bhagwat.
5. Mr. Kale Omkar Ajitkumar.

Regards,

Rajesh Ghogardare,

R. B. Ghogardare
B.C. 118 D.L. 118 Advocate
407 Sarve 3, Sanyal Road, Pandharpur.
Reg. No. MAH-1255-1993
Mob. 9822392593

VSD Mart

Chale, Near to Maharashtra Bank Chale

Shri Sitaram Dandage

Date: 7/2020

To,

Head of Computer Science Engineering Department,
SVERT's College of Engineering,
Pandharpur

Subject: Approval sponsorship for your following mentioned students for their last year project work.

Respected Sir,

We are approving sponsorship of the below mentioned students for final year project work of below mentioned students on subject "Scan An Pay" under the guidance of Prof. V. M. Sale.

We will be in the role for them. It is expected that they focus on project and complete the same within stipulated time frame.

1. Ms. Anisha Kamble
2. Dipali Murgase
3. Swarupa Kollé
4. Yogeshree Pawar
5. Pradnya Ingale

Thanking You

For

SVERT's College of Engineering (Poly.), Pandharpur.

VSD MART CHALE
(Signature)
Proprietor

Sincerely

Mr. Sitaram Dandage

VSD Mall Chale

NAMRATA COMPUTERS

SHOP NO- 55JIJAMATA SHOPPING CENTER, NAVI PETH, PANDHARPUR
DIST- SOLAPUR CONTACTS -9921283008

DATE:- 12/06/2023

To,

This is to certify that the student of Computer Science and Engineering Department from SVERI's College of Engineering, Pandharpur are allowed to develop software module for our NAMARATA COMPUTERS, under the title of, "Social Media Platform Based on blockchain" The details of operation will be provided as per the requirements.

The students are as follows:


Pratik G Mali

Onkar B Babar

Arbaj J Mujawar

Harshad B Bad

Shailesh R Bhosale.

NAMRATA COMPUTERS

[SOHAM SHITAL SHAHA]
PROPRIETOR
[NAMRATA COMPUTERS]